NASA/CR—2016-219411

Uncertainty Analysis of the NASA Glenn 8×6 Supersonic Wind Tunnel

Julia Stephens
HX5 Sierra, LLC, Cleveland, Ohio

Erin Hubbard
Jacobs Technology Inc., Cleveland, Ohio

Joel Walter
Jacobs Technology Inc., Bingham Farms, Michigan

Tyler McElroy
Jacobs Technology Inc., Tullahoma, Tennessee

November 2016

NASA STI Program . . . in Profile

Since its founding, NASA has been dedicated to the advancement of aeronautics and space science. The NASA Scientific and Technical Information (STI) Program plays a key part in helping NASA maintain this important role.

The NASA STI Program operates under the auspices of the Agency Chief Information Officer. It collects, organizes, provides for archiving, and disseminates NASA's STI. The NASA STI Program provides access to the NASA Technical Report Server—Registered (NTRS Reg) and NASA Technical Report Server—Public (NTRS) thus providing one of the largest collections of aeronautical and space science STI in the world. Results are published in both non-NASA channels and by NASA in the NASA STI Report Series, which includes the following report types:

- TECHNICAL PUBLICATION. Reports of completed research or a major significant phase of research that present the results of NASA programs and include extensive data or theoretical analysis. Includes compilations of significant scientific and technical data and information deemed to be of continuing reference value. NASA counter-part of peer-reviewed formal professional papers, but has less stringent limitations on manuscript length and extent of graphic presentations.

- TECHNICAL MEMORANDUM. Scientific and technical findings that are preliminary or of specialized interest, e.g., "quick-release" reports, working papers, and bibliographies that contain minimal annotation. Does not contain extensive analysis.

- CONTRACTOR REPORT. Scientific and technical findings by NASA-sponsored contractors and grantees.

- CONFERENCE PUBLICATION. Collected papers from scientific and technical conferences, symposia, seminars, or other meetings sponsored or co-sponsored by NASA.

- SPECIAL PUBLICATION. Scientific, technical, or historical information from NASA programs, projects, and missions, often concerned with subjects having substantial public interest.

- TECHNICAL TRANSLATION. English-language translations of foreign scientific and technical material pertinent to NASA's mission.

For more information about the NASA STI program, see the following:

- Access the NASA STI program home page at http://www.sti.nasa.gov

- E-mail your question to help@sti.nasa.gov

- Fax your question to the NASA STI Information Desk at 757-864-6500

- Telephone the NASA STI Information Desk at 757-864-9658

- Write to:
  NASA STI Program
  Mail Stop 148
  NASA Langley Research Center
  Hampton, VA 23681-2199

NASA/CR—2016-219411

Uncertainty Analysis of the NASA Glenn 8×6 Supersonic Wind Tunnel

Julia Stephens
HX5 Sierra, LLC, Cleveland, Ohio

Erin Hubbard
Jacobs Technology Inc., Cleveland, Ohio

Joel Walter
Jacobs Technology Inc., Bingham Farms, Michigan

Tyler McElroy
Jacobs Technology Inc., Tullahoma, Tennessee

Prepared under Contract NNC15BA02B

National Aeronautics and
Space Administration

Glenn Research Center
Cleveland, Ohio 44135

November 2016

Level of Review: This material has been technically reviewed by NASA technical management OR expert reviewer(s).

Available from

NASA STI Program
Mail Stop 148
NASA Langley Research Center
Hampton, VA 23681-2199

National Technical Information Service
5285 Port Royal Road
Springfield, VA 22161
703-605-6000

This report is available in electronic form at http://www.sti.nasa.gov/ and http://ntrs.nasa.gov/

Contents

List of Figures

List of Tables

1 Abstract

This paper presents methods and results of a detailed measurement uncertainty analysis that was performed for the 8- by 6-foot Supersonic Wind Tunnel located at the NASA Glenn Research Center. The statistical methods and engineering judgments used to estimate elemental uncertainties are described. The Monte Carlo method of propagating uncertainty was selected to determine the uncertainty of calculated variables of interest. A detailed description of the Monte Carlo method as applied for this analysis is provided.

The primary variable of interest for this facility is free stream Mach number. In addition to determining the uncertainty in Mach number, the uncertainty in free stream values of static pressure, total pressure, dynamic pressure, total temperature, static temperature, Reynolds number, and velocity were also calculated. Uncertainty results are presented as random (variation in observed values about a true value), systematic (potential offset between observed and true value), and total (random and systematic combined) uncertainty. Individual uncertainty sources are presented both dimensionally and as percent contributions to uncertainty in all variables of interest, to aid in the identification of primary uncertainty sources. Using these results, potential improvement opportunities for the facility are investigated.

Approaches to commonly faced obstacles in wind tunnel uncertainty analysis, such as limited data sets and measurement error correlations, are discussed. The practicality and detail provided in this report should equip the reader to replicate the methods presented for similar facilities.

A summary of random and systematic uncertainty results for all free stream variables are shown in Tables 1 and 2, respectively, for commonly used tunnel configurations. Uncertainties in free stream values generally vary through the Mach number range and by tunnel configuration. This report details all of these results, and provides estimates and estimation methods used for elemental uncertainties that propagate to free stream uncertainties.

	Subsonic, k = 2	Supersonic, k = 2
Mach Number	0.0001-0.0004	0.001-0.004
Static Pressure, psia	0.0004-0.004	0.01-0.03
Total Pressure, psia	0.0003-0.0007	0.001-0.03
Dynamic Pressure, psia	0.001-0.003	0.002-0.02
Static Temperature, °R	0.1-0.5	0.2-0.7
Total Temperature, °R	0.1-0.5	0.1-0.3
Reynolds Number, x 10^6 ft^{-1}	0.001-0.003	0.002-0.009
Free Stream Air Speed, ft/s	0.1-0.4	0.5-2.5

Table 1: Summary of random uncertainties of calibrated free stream conditions with 95% level of confidence for commonly used tunnel configurations.

	Subsonic, k = 2	Supersonic, k = 2
Mach Number	0.002-0.004	0.002-0.014
Static Pressure, psia	0.025	0.025-0.04
Total Pressure, psia	0.009	0.04-0.3
Dynamic Pressure, psia	0.01-0.02	0.02-0.05
Static Temperature, °R	2.3-2.8	2.1-2.8
Total Temperature, °R	2.8	2.8
Reynolds Number, x 10^6 ft^{-1}	0.02-0.03	0.03-0.05
Free Stream Air Speed, ft/s	2.9-4.8	3.3-8.4

Table 2: Summary of systematic uncertainties of calibrated free stream conditions with 95% level of confidence for commonly used tunnel configurations.

Nomenclature

$\bar{X}$	Mean of the sample population of variable X
β	An error due to systematic uncertainty
ϵ	An error due to random uncertainty
γ	Ratio of specific heats
μ	Air viscosity, slugs/(ft $\cdot$ sec)
Φ	Ratio between balance chamber static pressure and bellmouth total pressure
ρ	Air density, slugs/ft^3
σ_x	Estimated standard deviation of a sample population of variable x
$A_0 - A_2$	Total pressure calibration coefficients, subsonic range
$AS_0 - AS_6$	Total pressure calibration coefficients, supersonic range
$B_0 - B_6$	Static pressure calibration coefficients
b_x	Systematic standard uncertainty of variable x
$C_0 - C_3$	Total temperature calibration coefficients
$d_2(n)$	Statistical weighting factor for small samples; value is based on sample size, n
k	Coverage factor; $k = 2$ corresponds to approximately 95% level of confidence
M	Mach number
P_S	Static pressure
P_T	Total pressure
$P_{T,2}$	Total pressure measured downstream of a normal shock
q	Dynamic pressure, psia
Re	Reynolds number, ft^{-1}
s_f	Standard error of forecast; used to quantify regression uncertainty
s_x	Random standard uncertainty of variable x
s_{yx}	Standard error of estimate; used to quantify regression uncertainty

T_S	Static temperature
T_T	Total temperature
U	Free stream air speed, ft/s
u_x	Standard uncertainty of a measurement of variable x
v	Degrees of freedom
UPC	Uncertainty Percent Contribution

Subscripts

$_{arr}$	Designates transonic array (calibration hardware) as location of measurement
$_{bal}$	Designates balance chamber as location of measurement
$_{bar}$	Designates barometric (pressure)
$_{bm}$	Designates bellmouth (entry to contraction) as location of measurement
$_{corr}$	Designates correlated errors or uncertainties
$_{cyl}$	Designates cone-cylinder (calibration hardware) as location of measurement
$_{Inst}$	Designates combined effect of instrumentation of parameter
$_{PSCAL}$	Designates static pressure calibration
$_{PTCAL}$	Designates total pressure calibration
$_{reg}$	Designates regression of parameter
$_{ts}$	Designates 8- by 6-ft test section as location of calculated variable of interest
$_{TTCAL}$	Designates total temperature calibration
$_{unif}$	Designates spatial uniformity of parameter

2 Introduction

As advancements in science and engineering continue, the measurable desired improvements to technology become smaller. For example, an aircraft engine company may hope to achieve a 1% increase in efficiency with design changes. To measure such improvements, it is critical that the actual value of measurements are known to within these small boundaries.

Researchers continue to inquire about the uncertainties of measurements and calculations provided by facilities in which they perform tests. Depending on the type of test being performed, different aspects of uncertainty may be of interest. For example, researchers wishing to compare test results with CFD results will care about facility bias, while researchers looking for small measurement changes corresponding to design modifications may be more concerned with facility repeatability. Due to this desire by researchers to understand facility uncertainties, an effort is underway at the NASA Glenn Research Center to quantify and characterize the uncertainties of variables of interest at facilities within the testing division.

Uncertainty analysis is a continually evolving field. As interest in the analysis process grows and computational processing improves, the practice continues to be refined. Recommended practices for uncertainty analysis include ASME's Test Uncertainty Standard [1], AIAA's Standard for Wind Tunnel Test Uncertainty [2], ISO's Guide to the Expression of Uncertainty in Measurement [3], and NASA's Measurement Uncertainty Analysis Principles and Methods Handbook [4]. These are all useful resources when exploring uncertainty and were used heavily to develop this analysis.

This paper details the measurement uncertainty analysis performed for the NASA Glenn 8- by 6-foot Supersonic Wind Tunnel (SWT). Data used for this analysis was obtained during a calibration in 1996-1997 [5]. The uncertainty analysis was performed in 2014-2015. The objective was to determine the uncertainty in the free stream Mach number, as well as uncertainties in other free stream variables of interest (static pressure, total pressure, dynamic pressure, static temperature, total temperature, Reynolds number, and velocity). In addition to determining the overall uncertainties, the elemental contributors that drive these uncertainties were also identified. These broken down results were ultimately used to develop scenarios to improve the free stream Mach number uncertainty.

The document begins by providing background information on the facility. This includes a brief description of the facility and how it operates, as well as the calibration procedure used to define the free stream conditions. Next, the uncertainty sources considered in this analysis are defined, and a description of the ways in which these uncertainties propagate is given. A summary of the results is presented and discussed, followed by a detailed description of the analysis process. A discussion of the findings and ways to improve the uncertainties is then presented before conclusions are summarized. More details on the analysis process and results are provided in the appendices for interested readers.

3 Background Information

3.1 Description of 8- by 6-foot Supersonic Wind Tunnel

The 8- by 6-foot Supersonic Wind Tunnel (SWT) is an atmospheric, continuous flow wind tunnel. A schematic of the facility is shown in Figure 1. During standard operations, airflow is driven by a 7-stage compressor with three 29,000-hp motors located in the drive motor building. A side view of the 23 foot long test section is shown in Figure 2. The test section is 8 feet tall and 6 feet wide, with no divergence over the test section length. The test section is divided in to two testing sections: a solid wall supersonic flow region 9 feet 1 inch in length, and a porous wall transonic region 14 feet 5 inches in length. The Mach number range for the transonic test section is 0.25 to 2.0. Six configurations for the transonic test section are defined based on the length of the porous area used and porosity of the test section surfaces. These configurations are:

Configuration	Description
1	14 feet, 5.8-percent-porosity
2	8 feet, 6.2-percent-porosity
3	8 feet, 3.1-percent-porosity
4	8 feet, 6.2-percent-porosity modified
5	8 feet, 3.1-percent-porosity modified
6	14 feet, Schlieren windows installed

Table 3: Test section configuration descriptions.

The facility operating conditions are set by controlling compressor speed, flexible wall position, balance chamber pressure (test section bleed), and shock door position. The set point is determined predominantly by the ratio of the static pressure in the balance chamber to the total pressure in the bellmouth (the contraction directly upstream of the flex wall). To obtain these measurements, four static pressure measurements are taken at various locations in the balance chamber and are averaged to give $P_{S,bal}$. Two wall-mounted rakes near the exit of the bellmouth on the north and south tunnel walls acquire four total pressures and two total temperatures each, and are averaged to give $P_{T,bm}$ and $T_{T,bm}$. All pressures measured are differential and are added to measured barometric pressure P_{bar} to give absolute pressures. Unless otherwise noted, pressures are quoted in psia and temperature is degrees Rankine. More details on the facility operation can be found in the facility manual [6]. A schematic of the bellmouth rakes is shown in Figure 3.

3.2 Calibration Procedure

The purpose of any wind tunnel calibration is to relate free stream behavior (no model installed) to facility measurements that can be taken with or without a model present in the test section. Data is taken in both the facility and test section during a calibration, and a curve-fit relating the two is created. During a test, when customers are obtaining data from their model, test section conditions are determined by the facility data and calibration coefficients.

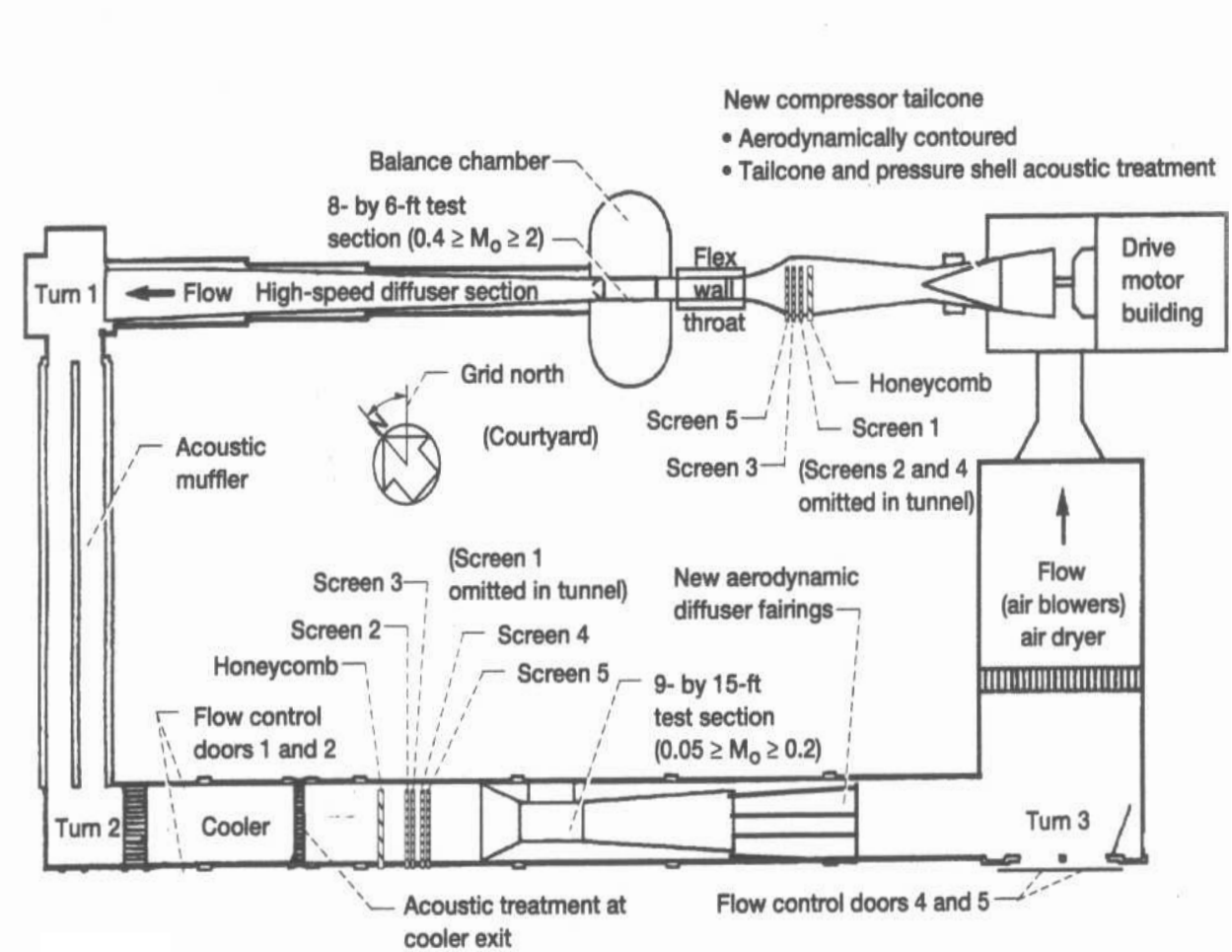

Figure 1: Overview of 8- by 6-foot Supersonic Wind Tunnel.

The facility was calibrated in 1997 [5] to provide facility-to-test-section relationships for static pressure ($P_{S,ts}$), total pressure ($P_{T,ts}$), total pressure downstream of a normal shock ($P_{T,2,ts}$), and total temperature ($T_{T,ts}$).

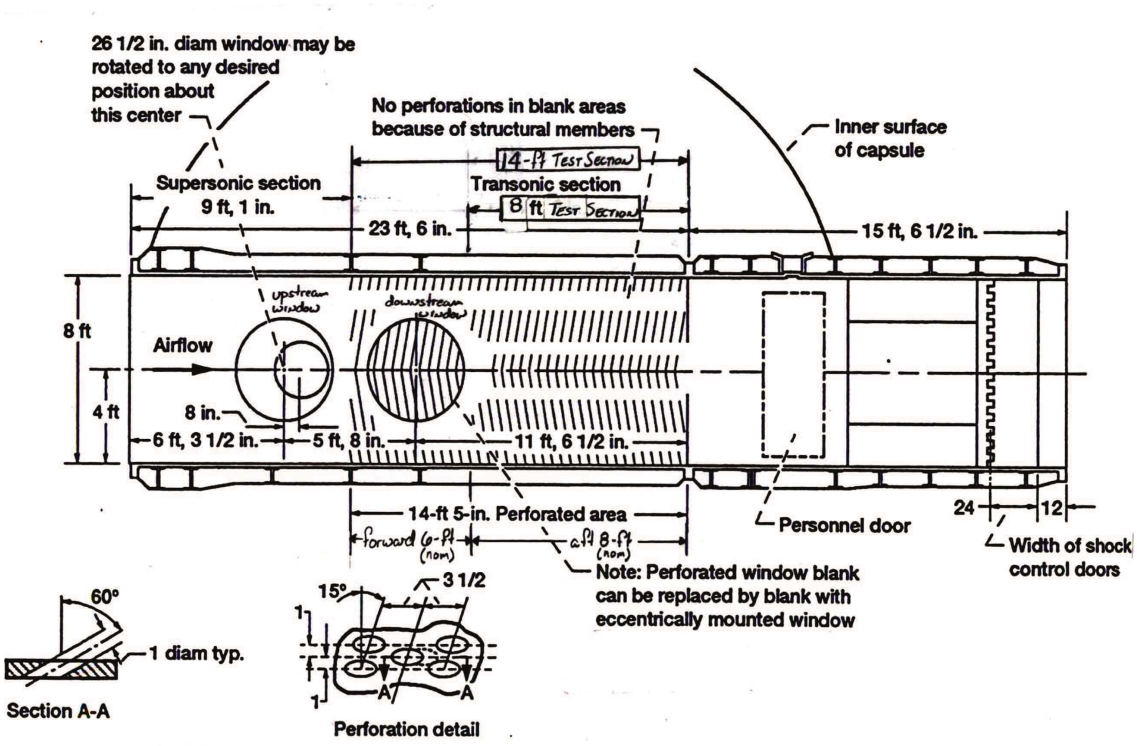

Figure 2: Schematic 8- by 6-foot test section.

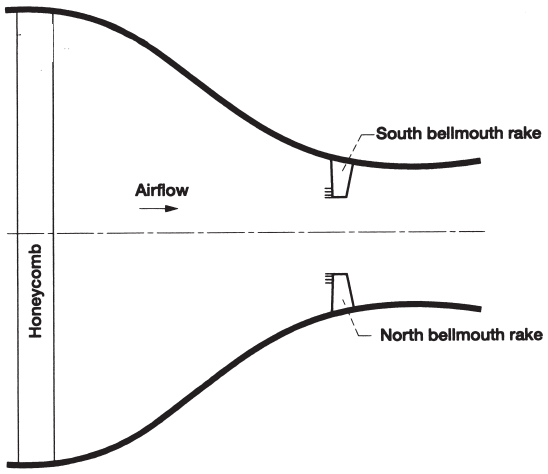

Figure 3: Rakes as installed in the bellmouth.

3.2.1 Calibration Instrumentation

The calibration instrumentation used to collect test section data consisted of a cone-cylinder and a transonic probe array. The 4-inch diameter, 86-inch long cone-cylinder shown in Figure 4 has four rows of static pressure taps: rows 1 and 2 have 51 static taps each, rows 3 and 4 have 15 static taps each.

The instrumentation on the transonic probe array includes 5 five-hole flow angularity probes, 6 Pitot-static probes and 11 thermocouples. A schematic of the instrumentation on the array is shown in Figure 5. The array is sting-mounted to a transonic strut in the facility and has wall plates at both ends for additional support, as shown in Figure 6. The vertical height of the array can be set to 5 different heights, from 24 to 72 inches in 12-inch increments as shown, with 48 inches being the tunnel centerline. The axial position of the array is also variable, as shown in Figure 7. For configurations 1 and 6, the 138.4-inch station is used, placing the centerline of the flow angularity probes approximately at the centerline of the Schlieren window blanks. All other configurations place the array at the 171.4-inch axial station so that the probe measurement plane is at the inlet of the 8-foot test section. There is a third axial position used for tunnel characterization at the 246-inch station, which is not used for calibration.

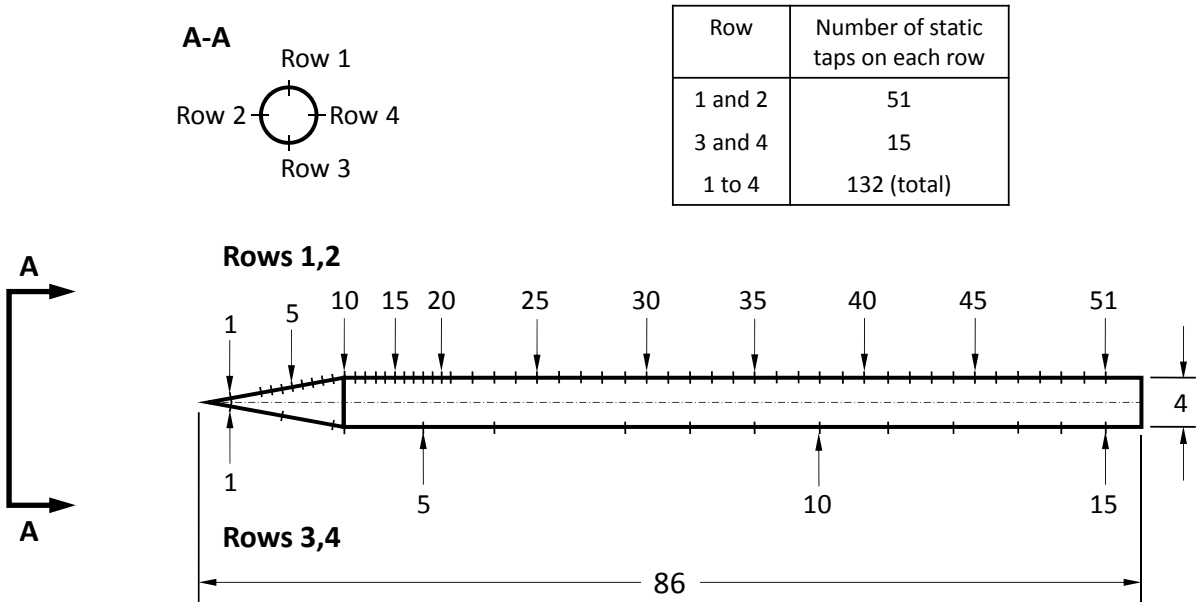

Figure 4: Instrumentation for the 4-inch cone-cylinder used during calibration. All dimensions in inches.

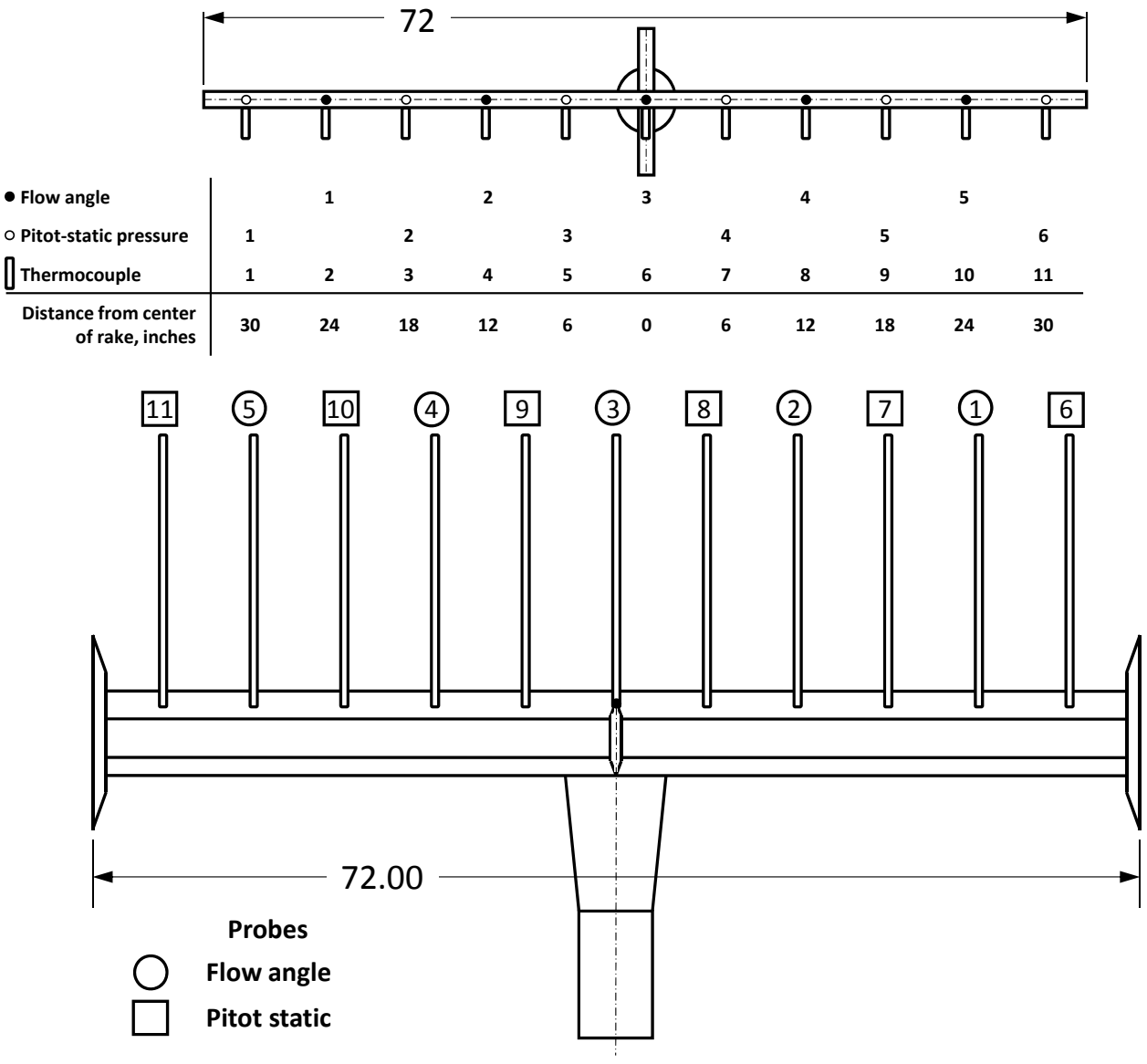

Figure 5: Instrumentation on the transonic array used during calibration. All dimensions are in inches.

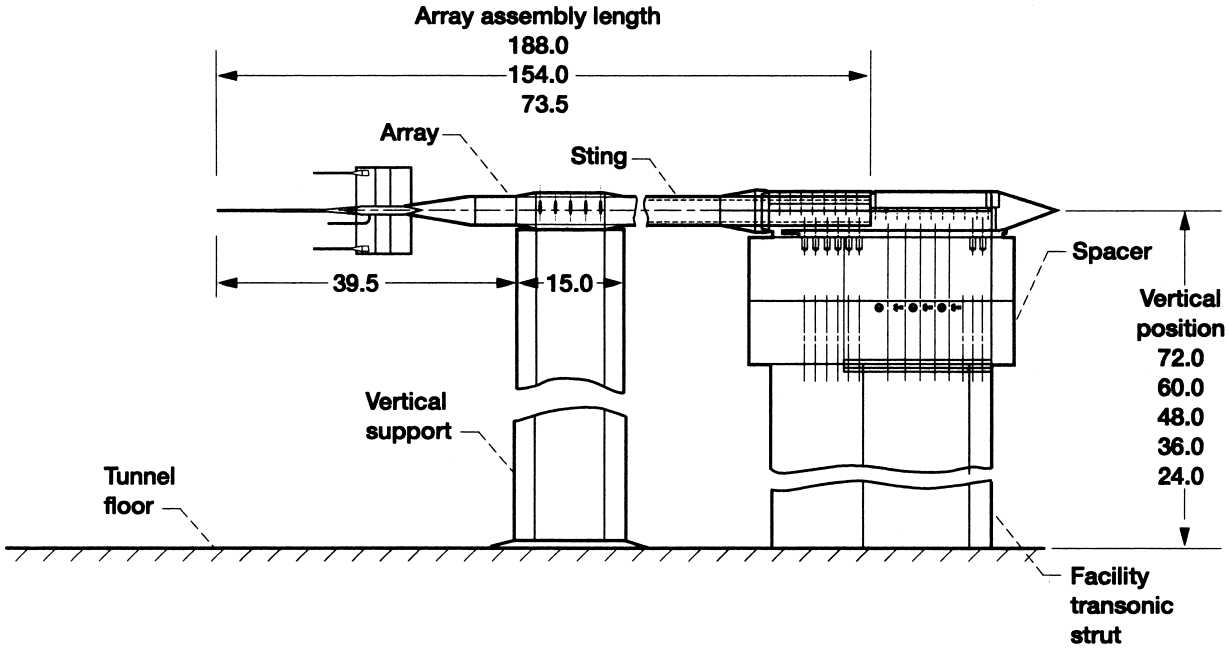

Figure 6: Schematic of transonic array as sting-mounted in the test section for calibration. All dimensions are in inches.

Nominal axial station (x) location of the measurement planes in the 8x6 SWT.		
Model	14-ft TS	8-ft TS
Array	138.4 in.	171.4 in.
Cone Cylinders	144.2 in.	178.4 in.

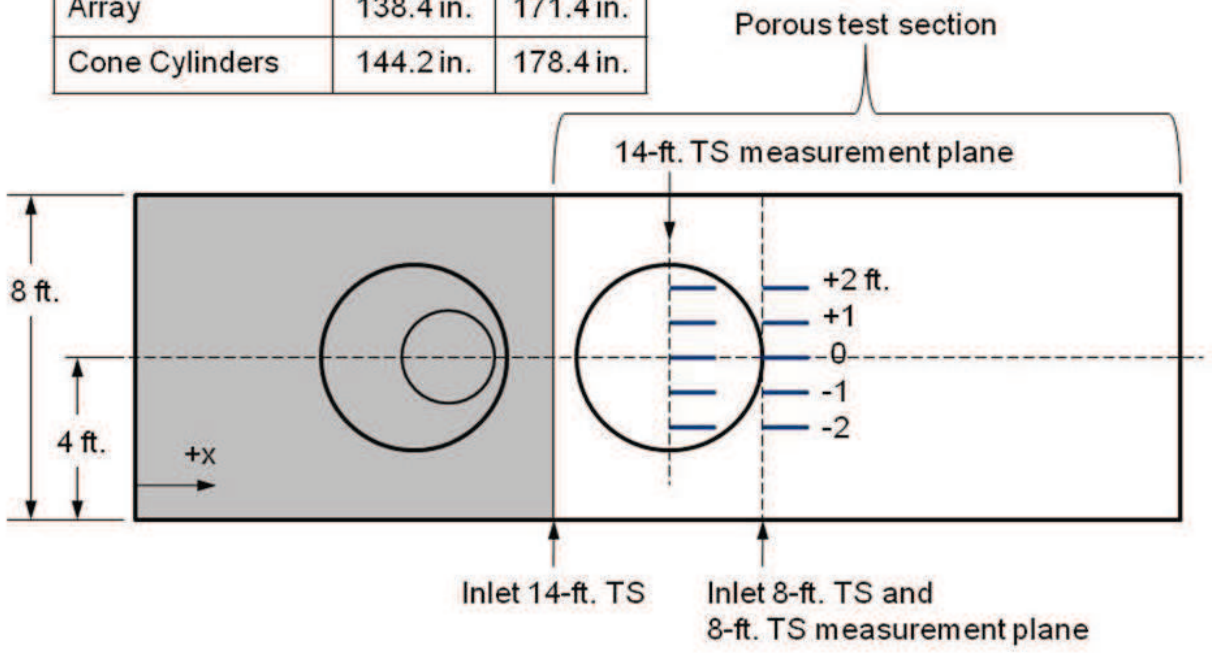

Figure 7: Side view of the tunnel indicating placement of the transonic array in the 8- by 6-foot test section for calibration. All dimensions are in inches.

3.2.2 Calibration Curves

When operating the tunnel, nominal conditions for compressor speed, flexible wall position, and shock door positions are set. The ratio of the balance chamber static to bellmouth total pressures is also set to a nominal value based on the tables in the facility operations manual [6]. This ratio is defined as

$$\Phi = \frac{P_{S,bal}}{P_{T,bm}}, \tag{1}$$

which is achieved and maintained via active control of a bleed valve in the balance chamber.

The static pressure calibration relates the facility ratio Φ to test section static pressure. To develop this relationship, the average of the 54 static pressures measured over the aft half of the cone-cylinder (see Figure 4), defined as $P_{S,cyl}$, was used to represent the mean test section static pressure $P_{S,ts}$ during calibration. The equation for test section static pressure is given by

$$P_{S,ts} = P_{T,bm} \cdot (B_0 + B_1 \cdot \Phi + B_2 \cdot \Phi^2 + B_3 \cdot \Phi^3 + B_4 \cdot \Phi^4 + B_5 \cdot \Phi^5 + B_6 \cdot \Phi^6). \tag{2}$$

These coefficients are used to define test section conditions for the entire operating range of the tunnel.

The total pressure calibration relates facility parameters $P_{T,bm}$ and Φ to test section total pressure for subsonic and supersonic flow ranges, respectively. The average of the innermost seven total pressure readings taken at the centerline vertical array height by the transonic array (see Figure 5), defined as $P_{T,arr}$, was used to represent test section total pressure $P_{T,ts}$ during calibration. Note that in supersonic flow, the measurement observed by a probe is the total pressure downstream of the normal shock produced by the probe, denoted by $P_{T,2}$.

The equation for the calibrated total pressure in the subsonic operating range ($\Phi > 0.533$) is given by

$$P_{T,ts} = A_0 + A_1 \cdot P_{T,bm} + A_2 \cdot P_{T,bm}^2, \tag{3}$$

and for the supersonic operating range ($\Phi \leq 0.533$) is given by

$$P_{T,2,ts} = P_{T,bm} \cdot (AS_0 + AS_1 \cdot \Phi + AS_2 \cdot \Phi^2 + AS_3 \cdot \Phi^3 + AS_4 \cdot \Phi^4 + AS_5 \cdot \Phi^5 + AS_6 \cdot \Phi^6). \tag{4}$$

Likewise, the total temperature calibration relates facility temperature $T_{T,bm}$ to test section temperature. An average of the seven innermost total temperature readings taken at the centerline vertical array height, defined as $T_{T,arr}$, was used to represent test section total temperature $T_{T,ts}$. The equation for test section total temperature is

$$T_{T,ts} = (C_0 + C_1 \cdot T_{T,bm} + C_2 \cdot T_{T,bm}^2 + C_3 \cdot T_{T,bm}^4) + 459.6, \tag{5}$$

where $T_{T,bm}$ is in °F and $T_{T,ts}$ is in °R.

All coefficients determined by these calibrations for all tunnel configurations as well as additional calibration information can be found in Reference [5].

3.3 Data Reduction

Using test-time facility measurements and the calibrated values for $P_{S,ts}$, $P_{T,ts}$, and $P_{T,2,ts}$ as well as γ (the ratio of specific heats, assumed here to be a constant 1.4), the test section Mach number is calculated in the subsonic range by

$$M_{ts} = \sqrt{\frac{2}{\gamma - 1}\left[\left(\frac{P_{S,ts}}{P_{T,ts}}\right)^{-\frac{\gamma-1}{\gamma}} - 1\right]}, \tag{6}$$

and is solved for iteratively in the supersonic range using the Rayleigh Pitot formula (Equation 100 from Reference [7])

$$\frac{P_{T,2,ts}}{P_{S,ts}} = \left[\frac{(\gamma+1)M_{ts}^2}{2}\right]^{\frac{\gamma}{\gamma-1}} \left[\frac{\gamma+1}{2\gamma M_{ts}^2 - (\gamma-1)}\right]^{\frac{1}{\gamma-1}}. \tag{7}$$

The data flow from measured values to Mach number is presented in Figure 8 for subsonic flow, and in Figure 9 for supersonic flow. The supersonic test section total pressure can then be calculated using Equation 99 from Reference [7]

$$\frac{P_{T,2,ts}}{P_{T,ts}} = \left[\frac{(\gamma+1)M_{ts}^2}{(\gamma-1)M_{ts}^2 + 2}\right]^{\frac{\gamma}{\gamma-1}} \left[\frac{\gamma+1}{2\gamma M_{ts}^2 - (\gamma-1)}\right]^{\frac{1}{\gamma-1}}. \tag{8}$$

Test section static temperature is defined as

$$T_{S,ts} = \frac{T_{T,ts}}{1 + \frac{\gamma-1}{2}M_{ts}^2}. \tag{9}$$

Test section free stream airspeed is defined as

$$U_{ts} = M_{ts}\sqrt{\gamma \cdot R \cdot T_{S,ts}}. \tag{10}$$

Test section air density is calculated as

$$\rho_{ts} = \frac{P_{S,ts}}{R \cdot T_{S,ts}}, \tag{11}$$

and test section air viscosity (slugs/(ft $\cdot$ sec)) is

$$\mu_{ts} = 2.270\frac{T_{S,ts}^{1.5}}{T_{S,ts} + 198.6} \cdot 10^{-8} \tag{12}$$

for $T_{S,ts}$ in $^\circ R$. Test section Reynolds number per unit length is calculated as

$$Re_{ts} = \frac{\rho_{ts} U_{ts}}{\mu_{ts}}, \tag{13}$$

and the test section dynamic pressure is

$$q_{ts} = P_{T,ts} \cdot \frac{\gamma}{2}M_{ts}^2\left(1 + \frac{\gamma-1}{2}M_{ts}^2\right)^{-\frac{\gamma}{\gamma-1}}. \tag{14}$$

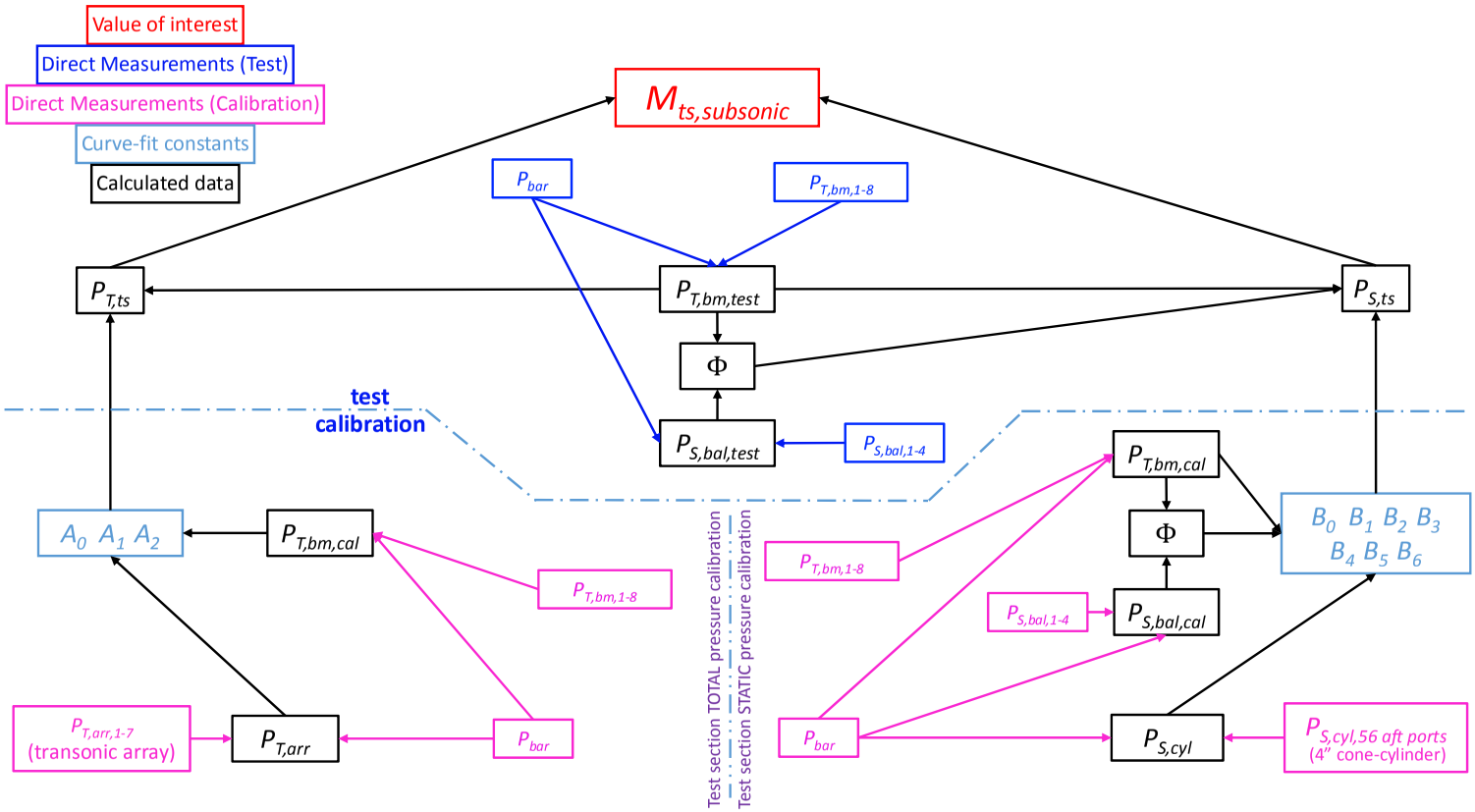

Figure 8: Data flow from measured value to calculated Mach number for subsonic flow.

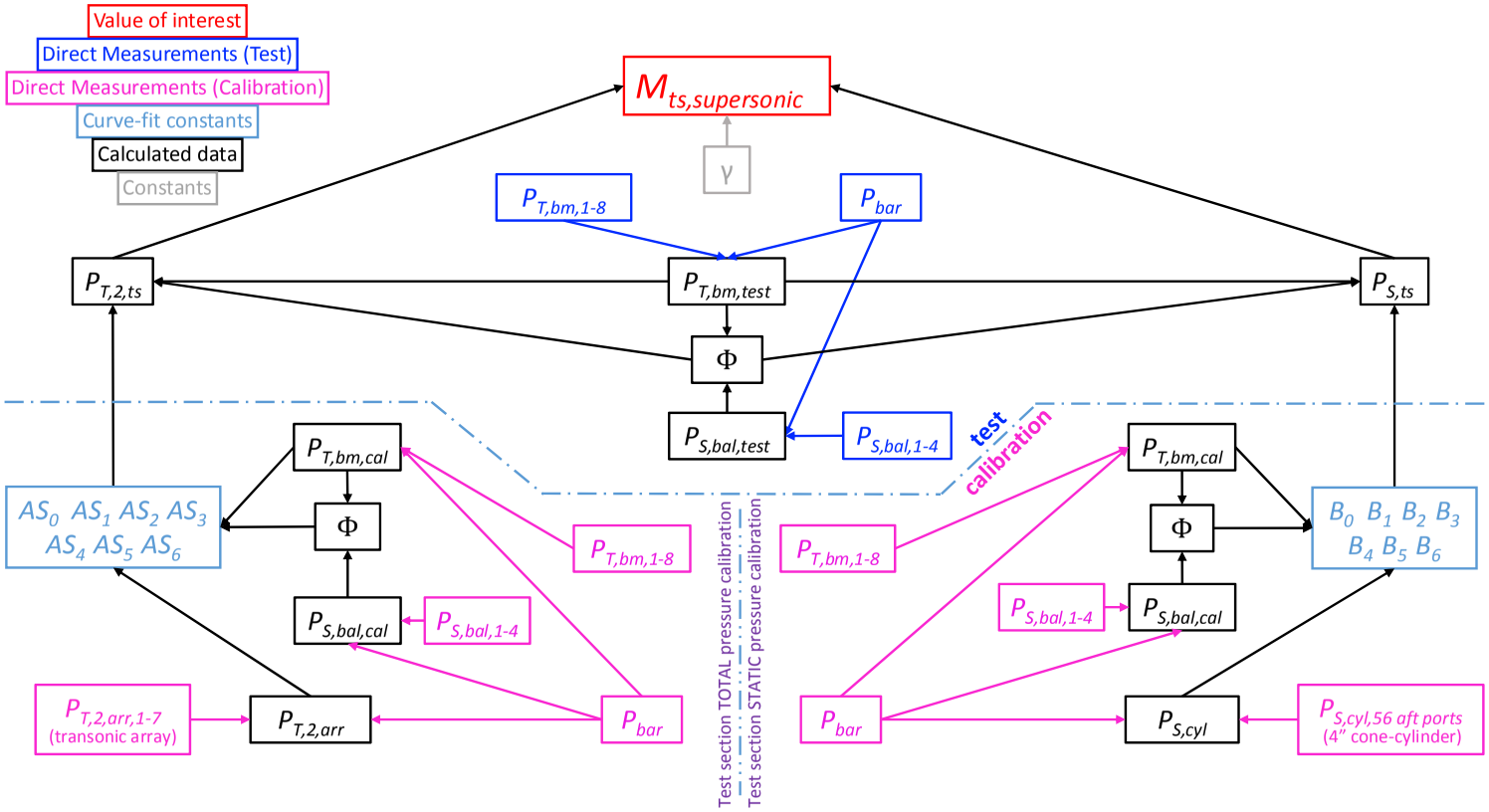

Figure 9: Data flow from measured value to calculated Mach number for supersonic flow.

4 Measurement Uncertainty Analysis Overview

This section briefly describes measurement uncertainty and the general approach followed for this analysis. The objective is to highlight the overall process, as well as the general procedure followed, for all elemental error sources considered. For more detail and quantified elemental uncertainty estimates, refer to Section 6.

4.1 Random and Systematic Errors

The most basic error sources are called elemental errors. All uncertainty texts begin by defining these elemental error types, and grouping them for ease of investigation. The ISO Guide to the Expression of Uncertainty in Measurement [3] classifies uncertainties as Type A and Type B. Type A estimates are based on direct observation and statistical analysis, while Type B estimates are based on operator experience, manufacturer documentation, or other means.

Other texts (References [1], [2], [4], [8]) classify uncertainties as random and systematic. Systematic errors create an offset from the actual value (X_{true}) to the nominal value (X_{nom}), while random errors cause a random variation, typically following a Gaussian distribution, about the nominal value. Figure 10 shows the effect each of these error types has on a measured value.

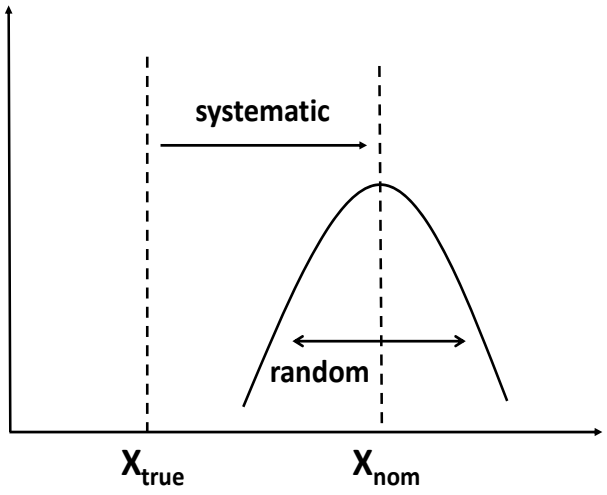

Figure 10: Comparison of the effects of systematic and random errors on a measurement.

The uncertainty of a measurement is defined by Coleman and Steele [8] as an estimate of the range within which the actual value of an unknown error is believed to fall. They further define the standard uncertainty of a measurement, u, as "an estimate of the standard deviation of the parent population from which a particular elemental error originates."

Random uncertainty characterizes the inability to exactly replicate a measurement of variable x. A population of random errors of measurement x with a Gaussian distribution has a standard deviation of s_x, known as the random standard uncertainty. This non-repeatability is a result of many unquantifiable factors and, depending on the time scale between repeated data points, can include random AND systematic errors which contribute to observed random variation. Due to the nature of random errors, increasing sampling time and/or number of discrete repeats in the test matrix reduces the effect of random uncertainty on test data.

Systematic standard uncertainty, b_x, characterizes the potential for bias in the measurement of variable x. Examples of systematic error sources can include instrumentation calibration and installation, operator interaction, facility behavior such as spatial non-uniformity,

and math models. Tunnel calibrations, comprised of both random and systematic uncertainties when calibration tests are performed, become fossilized [9] as a systematic uncertainty when a customer uses the resultant calibration curves for test-time analysis.

Correlated errors can occur when there is some type of link between two or more measurements. One example of a random correlated error would be two total pressure probes in close proximity taking measurements in a slightly unsteady flow, where test section conditions may change on a time basis; that variability would appear in all probes experiencing the same phenomena, and would be present in any simultaneous measurements of the probes. An example of systematic correlated errors would be measurements from multiple instruments that are calibrated by the same process and instrumentation; any offset due to calibration would appear in all measurements from these instruments within a given calibration cycle.

While the ISO *Guide* [3] generally recommends against it because "such categorization of components of uncertainty can be ambiguous when generally applied," distinguishing between uncertainty sources as random and systematic can be useful in determining which changes have the potential to reduce a facility's uncertainty. Additionally, categorizing uncertainties in this manner may help researchers understand how the uncertainties will affect their data. For example, a researcher conducting a test to compare observed results with CFD models requires low systematic uncertainty but may not be bothered by high random uncertainty, while a researcher examining small changes in results due to model modification requires low random uncertainty but may not be concerned with an offset in his or her data.

4.2 Uncertainty Propagation

Mach number is considered the primary variable of interest in the 8- by 6-foot SWT. This section uses Mach number to illustrate how uncertainties propagate through from measurement uncertainty to the calculated result. The same approach can be used for any selected variable of interest.

Variables from the data reduction that determine the free stream Mach number in this facility are the calibrated test section static pressure, $P_{S,ts}$, total pressure in the subsonic range, $P_{T,ts}$, and total pressure downstream of a normal shock in the supersonic range, $P_{T,2,ts}$ (see Equations 6 and 7). These calibrated values are calculated during a customer test using facility measurements of average total pressure in the bellmouth, $P_{T,bm}$, average static pressure in the balance chamber, $P_{S,bal}$, and total and static pressure calibration regression coefficients, as shown in Figures 8 and 9 and Equations 2, 3, and 4. All measured pressures are differential and referenced to barometric pressure, P_{bar}, to produce absolute pressures.

Contributors to uncertainty in the test section Mach number are, therefore, random and systematic uncertainties in the measured pressures $P_{T,bm}$ and $P_{S,bal}$, systematic uncertainty in the reference pressure P_{bar} (random uncertainty is assumed to be negligible), and fossilized systematic uncertainty from the calibration curves used to determine values of $P_{S,ts}$, $P_{T,ts}$, and $P_{T,2,ts}$. This fossilized uncertainty includes a regression uncertainty, s_{reg}, that accounts for the uncertainty due to the math model used to define the calibration relationship curves.

Figures 11-13 depict the uncertainty propagation through the data reduction for subsonic total pressure, supersonic total pressure, and static pressure calibrations. The uncertainties in the test-time measured values and calibrations propagate through to the Mach number

calculation as shown in Figures 14 and 15. Each of the elemental uncertainties shown in these figures must be quantified with an estimate to gain an understanding of the combined uncertainty in the calculated Mach number.

It should also be noted from Figures 14 and 15 that the calibrations of $P_{S,ts}$, $P_{T,ts}$ and $P_{T,2,ts}$ contribute only systematic errors to the Mach number uncertainty, since random and systematic uncertainty introduced during the calibration tests are fossilized into the calibration regressions as combined systematic uncertainties u_{PSCAL} and u_{PTCAL}.

Using the same general approach, uncertainty analyses are also performed for free stream static and total pressure, Reynolds number, total and static temperature, air speed, and dynamic pressure by propagating the uncertainties through each variable's respective data reduction. The combined uncertainty of these variables includes the elemental pressure uncertainties discussed above, and some variables additionally include random and systematic uncertainty contributions from the bellmouth total temperature measurement, $T_{T,bm}$, and fossilized systematic uncertainty from the calibration curve used to determine values of $T_{T,ts}$ (see Figure 16). Data and uncertainty flow charts for all variables of interest can be found in their respective appendices.

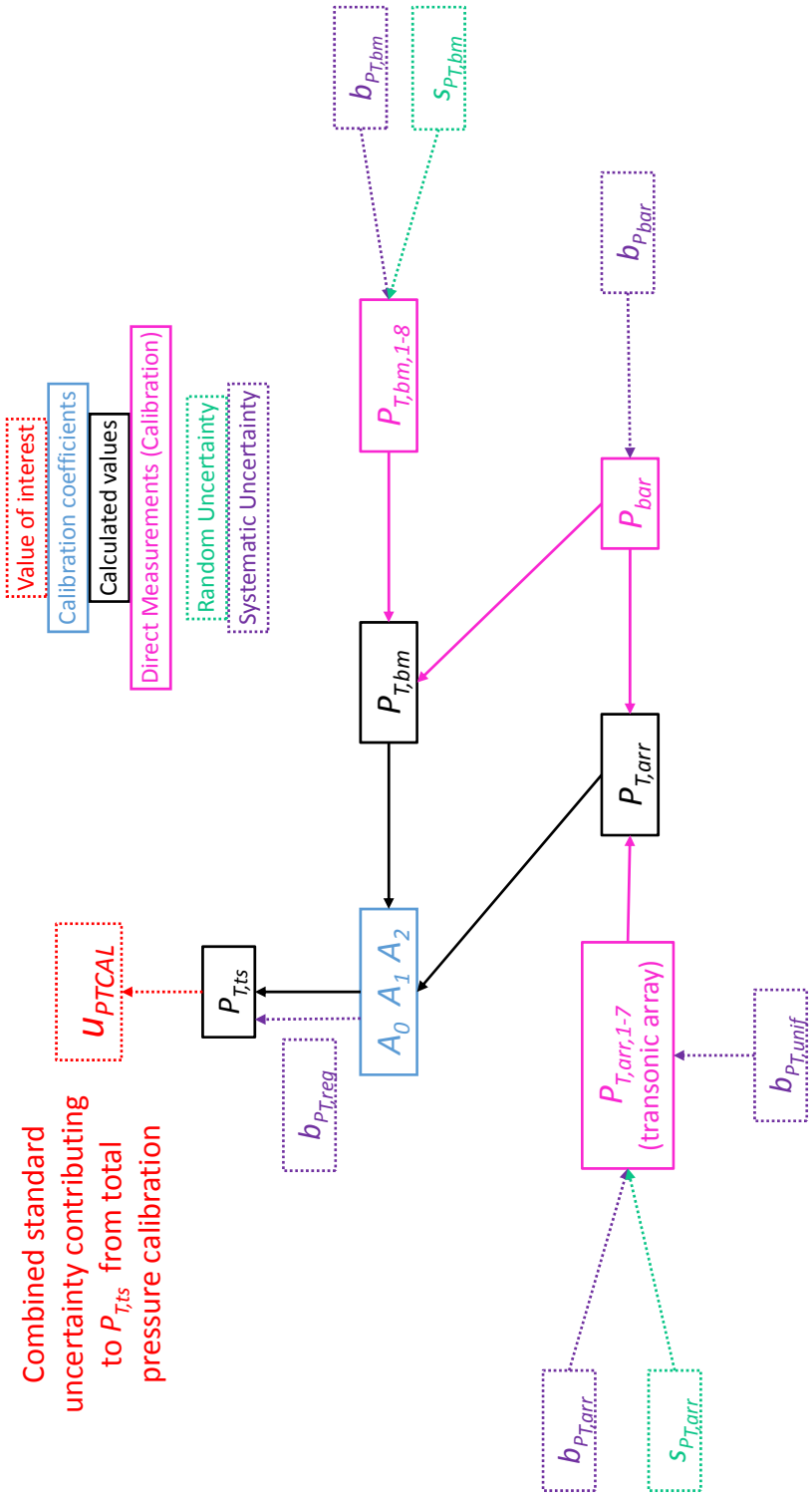

Figure 11: Flow chart depicting the flow of uncertainty for total pressure calibration: subsonic flow range

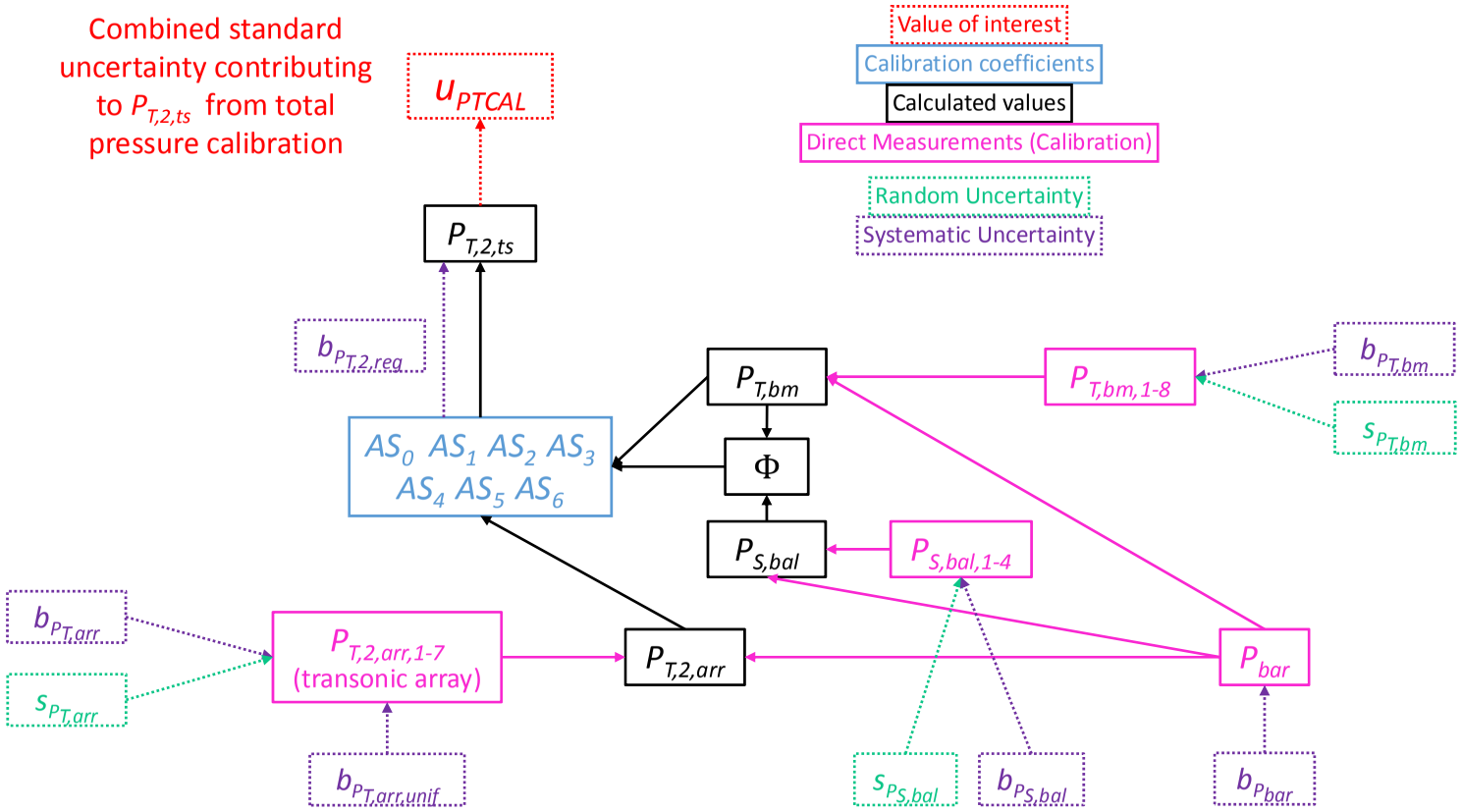

Figure 12: Flow chart depicting the flow of uncertainty for total pressure calibration: supersonic flow range

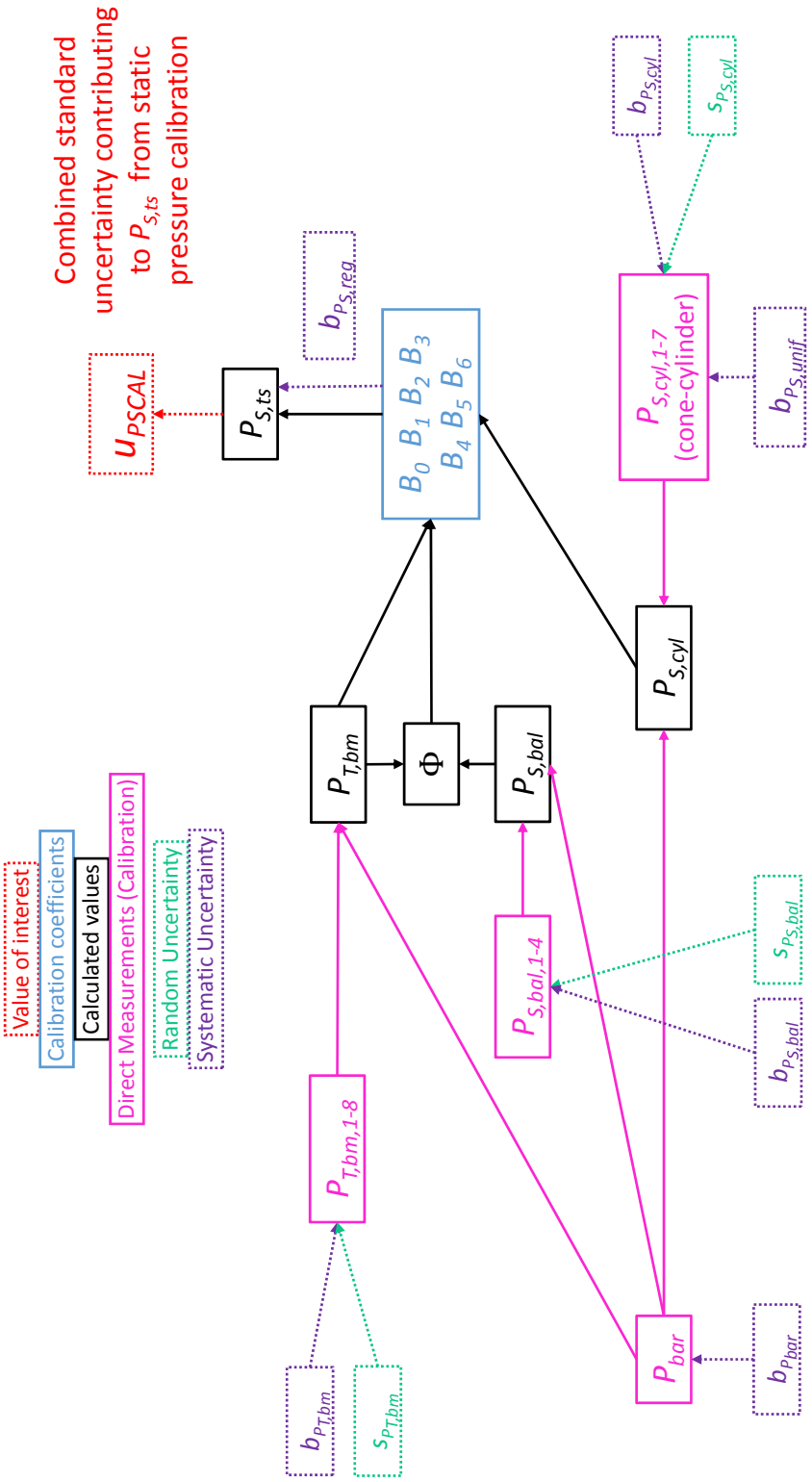

Figure 13: Flow chart depicting the flow of uncertainty for static pressure calibration

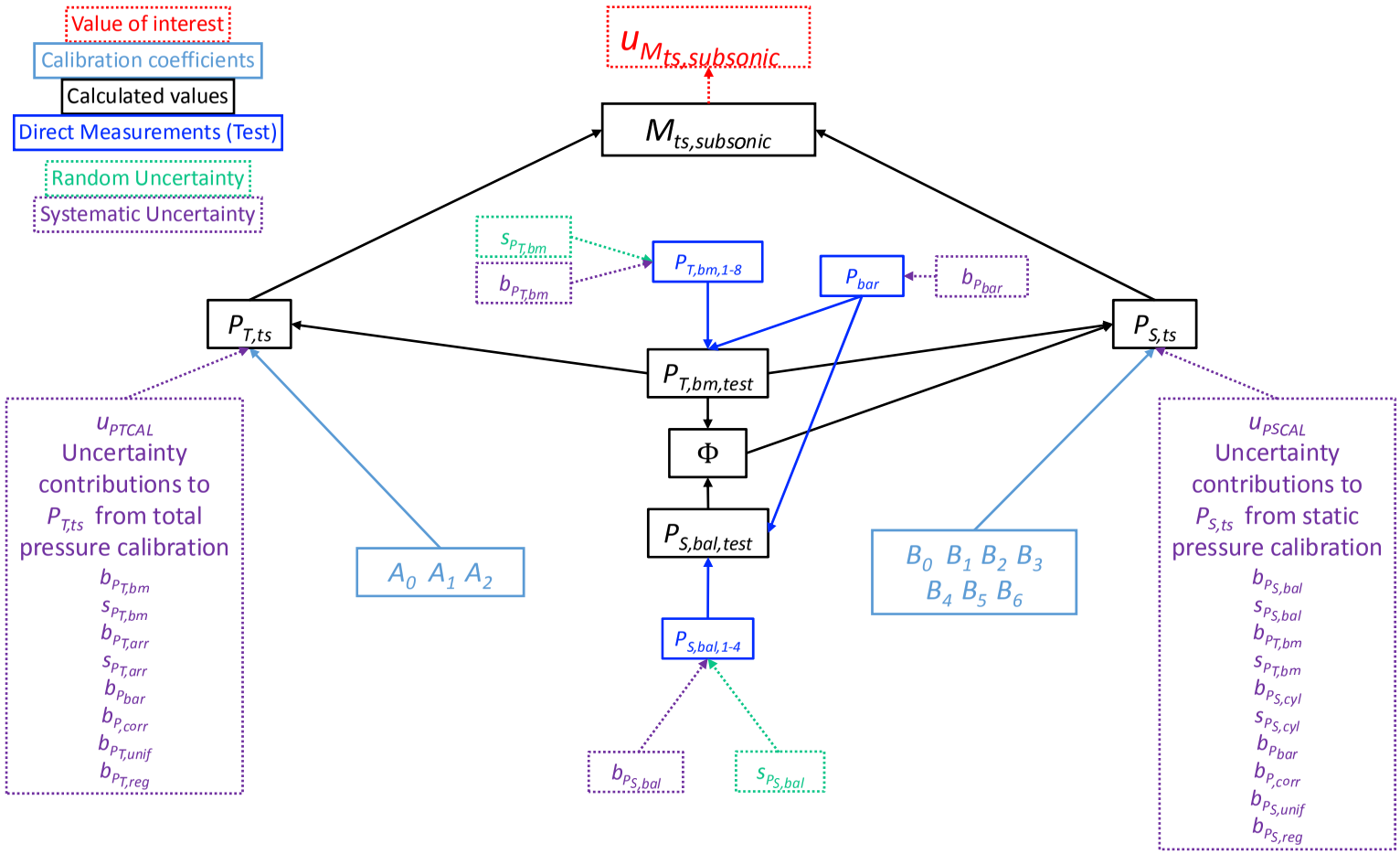

Figure 14: Flow chart depicting the propagation of uncertainties in Mach number calculation: subsonic flow range

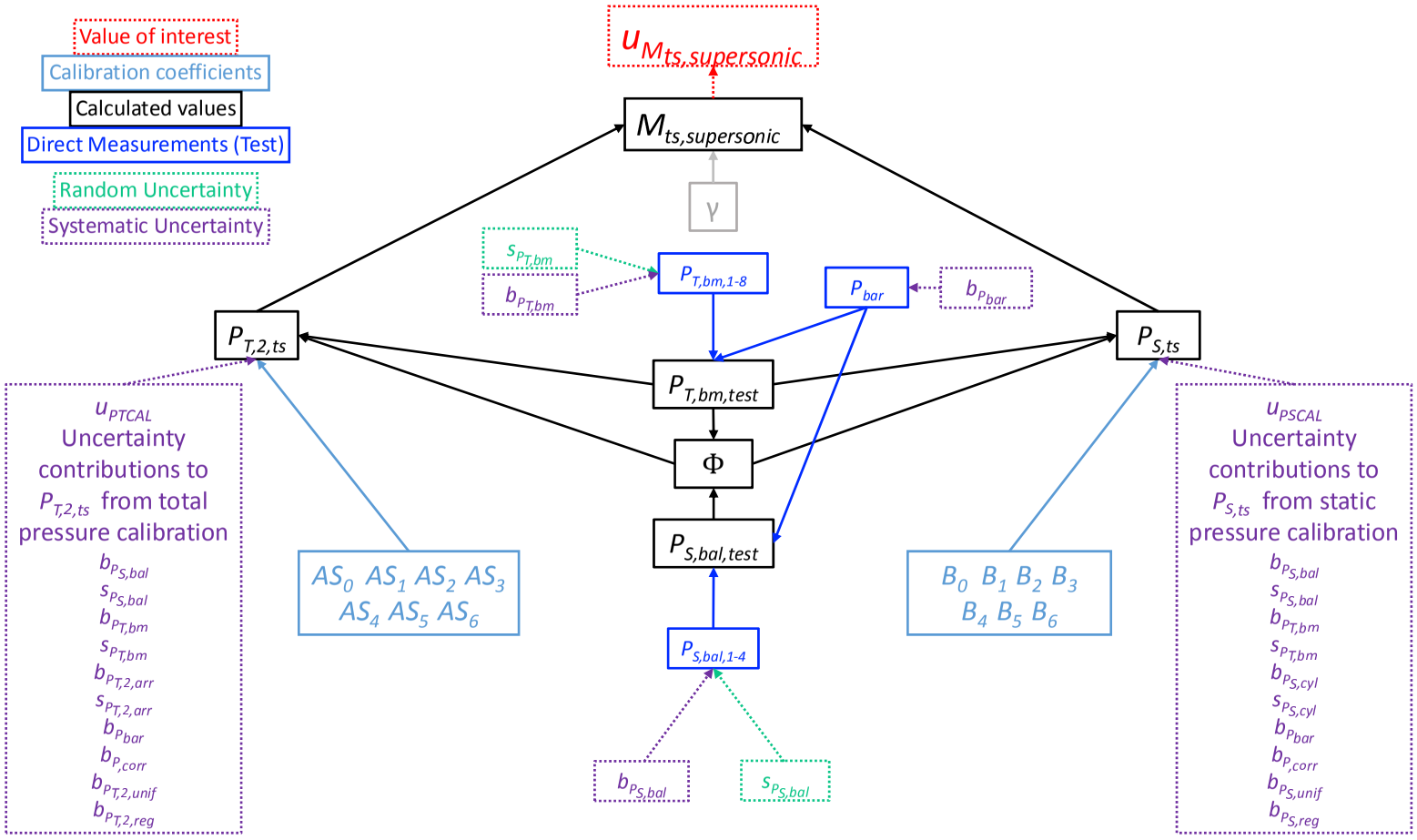

Figure 15: Flow chart depicting the propagation of uncertainties in Mach number calculation: supersonic flow range

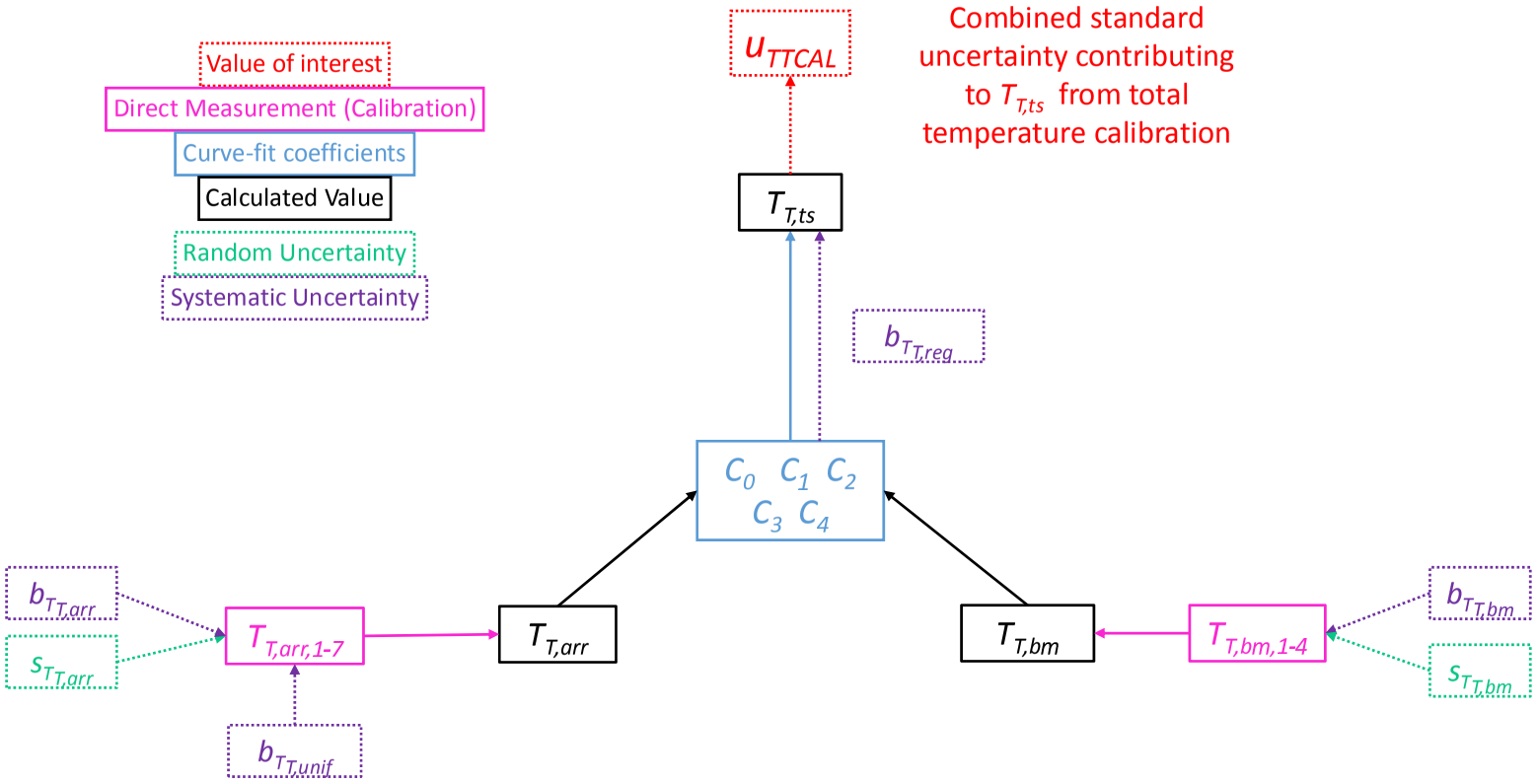

Figure 16: Flow chart depicting the propagation of uncertainties for total temperature calibration.

4.3 Uncertainty Models

To properly propagate the elemental uncertainties to the uncertainty of the calculated value of interest, an error model is necessary. The traditional model for propagating uncertainty is the Taylor Series Method (TSM), which is derived as a linearized Taylor series expansion about the true result from the data reduction equation. The true (but unknowable) result is then replaced by its estimate, i.e. the sum of the measured result and the error estimates (uncertainties). The complete derivation of the model is provided in Reference [8], leading to an expression for the combined standard uncertainty u_c of result $y = f(x_1, x_2, ..., x_n)$ (following the ISO *Guide* [3] notation):

$$u_c^2(y) = \sum_{i=1}^{n} \sum_{j=1}^{n} \frac{\partial f}{\partial x_i} \frac{\partial f}{\partial x_j} u^2(x_i, x_j), \tag{15}$$

or

$$u_c(y) = \sqrt{\sum_{i=1}^{n} (\frac{\partial f}{\partial x_i})^2 u^2(x_i) + 2 \sum_{i=1}^{n-1} \sum_{j=i+1}^{n} \frac{\partial f}{\partial x_i} \frac{\partial f}{\partial x_j} u(x_i, x_j)}, \tag{16}$$

where $u(x_i)$ is the combined standard uncertainty of measurement x_i, and $u(x_i, x_j)$ is the estimated covariance between x_i and x_j and accounts for correlations in the pair of measurements. Further, the degree of correlation is estimated using the correlation coefficient,

$$r(x_i, x_j) = \frac{u(x_i, x_j)}{u(x_i) u(x_j)} \tag{17}$$

where $-1 \leq r(x_i, x_j) \leq 1$. Complete lack of correlation between the two measurements results in $r(x_i, x_j) = 0$.

The simple example below illustrates this method for finding the uncertainty in the calculated volume of a cylinder. Volume V is a function of measurements of cylinder length, l, and diameter, D by the equation:

$$V = \pi l (\frac{D}{2})^2. \tag{18}$$

Combining equations 16 and 17 this example reduces to

$$\begin{aligned} u_{c,V} &= \sqrt{(u_l \frac{\partial V}{\partial l})^2 + (u_D \frac{\partial V}{\partial D})^2 + 2 \frac{\partial V}{\partial l} \frac{\partial V}{\partial D} u_{l,D}} \\ &= \sqrt{[u_l \pi (\frac{D}{2})^2]^2 + (u_D \pi l \frac{D}{2})^2 + 2 u_l u_D [\pi^2 l (\frac{D}{2})^3] r(l, D)}. \end{aligned} \tag{19}$$

The correlation term in the equation above would be non-zero if, for example, the same device was used to measure both length and diameter of the cylinder. If measurements of the two parameters were completely independent, the correlation term would become 0.

Due to the nature of complex or highly non-linear equations, the Taylor Series Method can become cumbersome to implement or may require assumptions to simplify equations, ultimately increasing the uncertainty in the final result. In such instances, the Monte Carlo

Method (MCM) is very useful as an uncertainty propagation technique. Standards for using the MCM are detailed by Coleman and Steele [8], and the method is included in the ISO *Guide's* supplement [10].

A Monte Carlo simulation begins with a data set representative of a typical test. A population of i synthetic data sets are produced by perturbing each representative measurement in the data set by errors that are populated based on elemental uncertainty estimates and assumed error distrubtions for each uncertainty source considered, and for each measurement [11]. Each of the i perturbed data sets are sent through the data reduction sequence, producing i calculations of any values of interest. Finally, the standard uncertainty of the calculated values are determined by taking the standard deviation of the perturbed results.

A simplified example of pseudo-code for a Monte Carlo error propagation simulation calculating uncertainty in the volume of a cylinder V as a function of length L and diameter D (as described in Section 4.3) is shown in Figure 17. The code provides examples of how to populate the random, systematic, and correlated systematic errors as described in this section.

Given the iterative calculations required to obtain the free stream Mach number in this facility, the MCM of uncertainty propagation was selected for this analysis. Further details on the method as implemented in this analysis can be found in Section 6.2.

```
%% Monte Carlo Code Example
% Determine the uncertainty of a cylinder volume
% D = diameter of cylinder
% L = cylinder length
% V = cylinder volume, pi*l*(D/2)^2.

% Number of Monte Carlo iterations to perform:
numIts = 10000;

%% CASE 1:
% L is measured twice using a ruler by one user.  D is measured twice using a
% micrometer by a second user.  Two readings are averaged to give L and D for
calculation. Assume no correlations are present between parameters L and D.

% Measured values, assumed to reasonably represent "true" unknowable values
% used as inputs, or starting points, for the Monte Carlo
L1 = 5.07;  L2 = 4.98;
D1 = 2.02;  D2 = 2.00;

% Estimate the standard uncertainties
% a: Random Uncertainties
RanUnc_L = 0.1;   RanUnc_D = 0.05;
% b: Systematic Uncertainties
SysUnc_L = 0.1;   SysUnc_D = 0.02;

% Populate Random Errors:
% Note:  randn( 1, x ) creates a population of x random numbers with a normal
% distribution, a mean of 0, and a standard deviation of 1.  It can be scaled by
% the standard uncertainty to create a desired population of errors.
L1_RanErrors = RanUnc_L * randn( 1, numIts );
L2_RanErrors = RanUnc_L * randn( 1, numIts );
D1_RanErrors = RanUnc_D * randn( 1, numIts );
D2_RanErrors = RanUnc_D * randn( 1, numIts );

% Populate Systematic errors
% Note: Unique random numbers are generated once for each measurement
% parameter and applied to all measurements of that parameter in the for-loop
L_SysErrors = SysUnc_L * randn( 1, numIts );
D_SysErrors = SysUnc_D * randn( 1, numIts );

% Monte Carlo Iterations:
for i = 1:numIts
    L1_perturbed(i) = L1 + L1_RanErrors(i) + L_SysErrors(i);
    L2_perturbed(i) = L2 + L2_RanErrors(i) + L_SysErrors(i);
    D1_perturbed(i) = D1 + D1_RanErrors(i) + D_SysErrors(i);
    D2_perturbed(i) = D2 + D2_RanErrors(i) + D_SysErrors(i);

    %  Average the two measurements for L and the two measurements for D as
    %  part of the data reduction.
    L_perturbed(i) = mean([L1_perturbed(i),L2_perturbed(i)]);
    D_perturbed(i) = mean([D1_perturbed(i),D2_perturbed(i)]);

    %  Calculate V for each iteration
    V_perturbed(i) = pi * L_perturbed(i) * (D_perturbed(i)/2)^2;
end

% Evaluate the standard uncertainty of the result, V.
% std(x) takes the standard deviation of the array x.
stdUnc_V = std(V_perturbed);
```

```
%% CASE 2:
% Same as Case 1, except that the micrometer is used for both measurements,
% and L and D are measured by the same user.  As a result, the systematic
% measurement errors for L1, L2, D1 and D2 are treated as completely
% correlated.

% Estimate the standard uncertainties
% a: Random Uncertainties
RanUnc = 0.05;

% b: Systematic Uncertainties
SysUnc = 0.02;

% Populate Random Errors:
% Note:  Same as for Case 1
L1_RanErrors = RanUnc * randn( 1, numIts );
L2_RanErrors = RanUnc * randn( 1, numIts );
D1_RanErrors = RanUnc * randn( 1, numIts );
D2_RanErrors = RanUnc * randn( 1, numIts );

% Populate Systematic errors
% Note:  The unique random numbers generated once for each iteration and
% applied to all measurements
SysErrors = SysUnc * randn( 1, numIts );

% Monte Carlo Iterations:
for i = 1:numIts
    L1_perturbed(i) = L1 + L1_RanErrors(i) + SysErrors(i);
    L2_perturbed(i) = L2 + L2_RanErrors(i) + SysErrors(i);
    D1_perturbed(i) = D1 + D1_RanErrors(i) + SysErrors(i);
    D2_perturbed(i) = D2 + D2_RanErrors(i) + SysErrors(i);

    %  Average the two measurements for L and the two measurements for D as
    %  part of the data reduction
    L_perturbed(i) = mean([L1_perturbed(i),L2_perturbed(i)]);
    D_perturbed(i) = mean([D1_perturbed(i),D2_perturbed(i)]);

    %  Calculate V for each iteration
    V_perturbed(i) = pi * L_perturbed(i) * (D_perturbed(i)/2)^2;
end

% Evaluate the standard uncertainty of the result, V.
% std(x) takes the standard deviation of the array x.
stdUnc_V = std(V_perturbed);
```

Figure 17: Monte Carlo simulation pseudo-code showing error population and propagation

5 Results

The results of the uncertainty analysis for tunnel configuration 1 are presented in this section. Details on the analysis process (including descriptions of the elemental uncertainties, estimation methods, and how various obstacles in the analysis were handled) are discussed in Section 6. All results are presented in this section with an appropriate coverage factor to obtain a 95% level of confidence in the quoted uncertainty[1]. For each variable of interest the random, systematic and total uncertainties are presented with a break down of how each elemental uncertainty described in Section 4.2 contributes as an uncertainty percent contribution (UPC) to each variables of interest. UPC results are determined by:

$$\mathrm{UPC}_i = \frac{u_i^2}{u_{total}^2} \times 100, \tag{20}$$

where u_i is the uncertainty contribution to the variable of interest due to elemental uncertainty i, and u_{total} is the total uncertainty of the variable of interest.

Dimensional and UPC results are presented separately for random and systematic uncertainty, then are presented as total uncertainty (simply a root sum square of the random and systematic results). Random and systematic uncertainty results in isolation are frequently of more interest to test customers than the overall combined uncertainty. Separating results also allows researchers to focus on the uncertainties that pertain to their test type, and allows facility personnel to determine the best use of time and money for facility improvements.

UPC results are presented such that all contributors add to 100% of the total of the uncertainty type being considered. Take random uncertainty for example; all random uncertainty sources add up to 100% of the total random uncertainty, modifying Equation 20 with $u_i = u_{i,random}$ and $u_{total} = u_{total,random}$. The same is done for systematic and total uncertainty.

All quoted uncertainties for each variable of interest should be considered calibration point uncertainties, centered on the tunnel's x and y axes and axially defined by the configuration's nominal axial station (see Table 3 and Section 3.1 and the table in Figure 7). Results do not include uncertainties due to test time factors such as blockage effects or spatial non-uniformity, since those can change significantly model-to-model. (Note that spatial uniformity uncertainty is, however, considered for its impact on the calibration of each parameter.)

The uncertainty results determined for each variable of interest for tunnel configuration 1 are discussed in this section. Results for other configurations can be found in Appendices B - I.

[1]There are limited data points resulting in very low degrees of freedom in random uncertainty estimates. Use of the d_2 statistic to un-bias the data results in a large enough effective degree of freedom from the small sample size such that once all the uncertainties combine through data reduction, the effective degrees of freedom of the system is adequate for $k = 2$ to obtain the 95% confidence level [2].

5.1 Random Uncertainty Results

As described in Section 4.2, random uncertainty characterizes the variation of a measurement about its mean. This type of uncertainty may be of interest to researchers looking for small changes due to model modifications. These results provide an understanding of the facility's test-to-test variation.

5.1.1 Mach Number

The expanded random uncertainty in M_{ts} for configuration 1 is shown in Figure 18. The values are below 0.0003 through the subsonic range, then increase through the transonic regime to about 0.004 at supersonic Mach numbers.

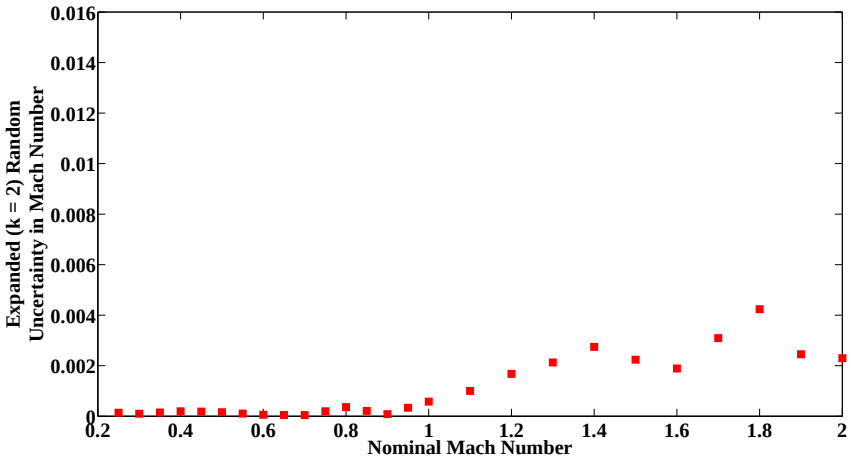

Figure 18: Random uncertainty in M_{ts} as a function of nominal Mach number for configuration 1.

Equations 6 and 7 as well as Figures 8 and 9 show that the elemental random uncertainties in $P_{T,bm}$ and $P_{S,bal}$ contribute to random uncertainty in Mach number. The UPC of these elemental uncertainties to the total random uncertainty in M_{ts} is shown in Figure 19. Random variation of the static pressure in the balance chamber overwhelmingly drives the random uncertainty in M_{ts} across most of the range. Similar results were observed in the National Transonic Facility [11].

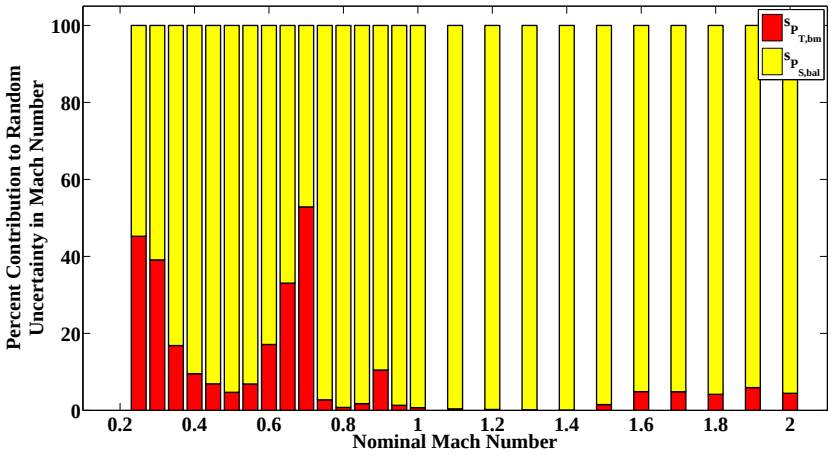

Figure 19: Random UPC of M_{ts} as a function of nominal Mach number for configuration 1. Red is the random uncertainty of the total pressure in the bellmouth, yellow is the random uncertainty of the static pressure in the balance chamber.

The random uncertainty of the calculated test section Mach number is shown for every nominal Mach number set point in Table 4. This table also shows how each of the measurement parameters in the facility contribute to the combined random uncertainty.

Nominal Mach	**Typical** M_{ts}	$s_{M_{ts}}$ **k = 2**	$s_{M_{ts}}$ **due to** $s_{P_{T,bm}}$ **k = 2**	$s_{M_{ts}}$ **due to** $s_{P_{S,bal}}$ **k = 2**	$s_{M_{ts}}$ **UPC due to** $s_{P_{T,bm}}$	$s_{M_{ts}}$ **UPC due to** $s_{P_{S,bal}}$
0.25	0.25	0.0001	0.0001	0.0001	45.2	54.8
0.40	0.41	0.0002	0.0001	0.0002	9.5	90.5
0.60	0.60	0.0001	0.0000	0.0001	17.1	82.9
0.80	0.81	0.0004	0.0000	0.0004	0.8	99.2
1.00	1.00	0.0006	0.0000	0.0006	0.7	99.3
1.20	1.18	0.0017	0.0001	0.0017	0.2	99.8
1.40	1.35	0.0027	0.0001	0.0027	0.1	99.9
1.60	1.56	0.0019	0.0004	0.0018	4.9	95.1
1.80	1.78	0.0042	0.0009	0.0041	4.2	95.8
2.00	1.99	0.0023	0.0005	0.0022	4.4	95.6

Table 4: Summary of calculated Mach Number random uncertainty with 95% level of confidence for configuration 1.

5.1.2 Static Pressure

The random uncertainty in $P_{S,ts}$ is a result of random uncertainty in the measured pressures $P_{T,bm}$ and $P_{S,bal}$ (see Equation 2 and Figure 13). The combined random uncertainty for configuration 1 is shown in Figure 20. The total uncertainty in static pressure calculation due to random uncertainty sources is below 0.002 psia subsonically, increases in the transonic region, and bounces between 0.03 psia and 0.01 psia supersonically. A bar plot of the elemental

random uncertainty UPCs to $P_{S,ts}$ is shown in Figure 21. While $P_{T,bm}$ contributes very small amounts, the only notable random contributor to static pressure calculation uncertainty is the static pressure measurement in the balance chamber.

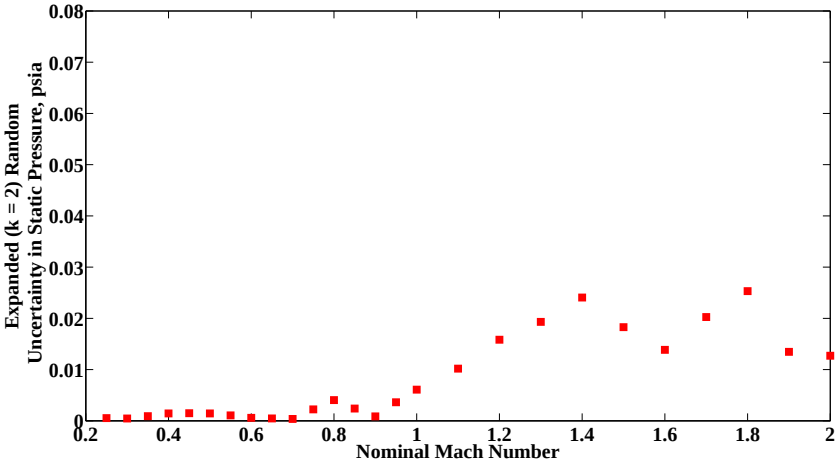

Figure 20: Random uncertainty in $P_{S,ts}$ as a function of nominal Mach number for configuration 1.

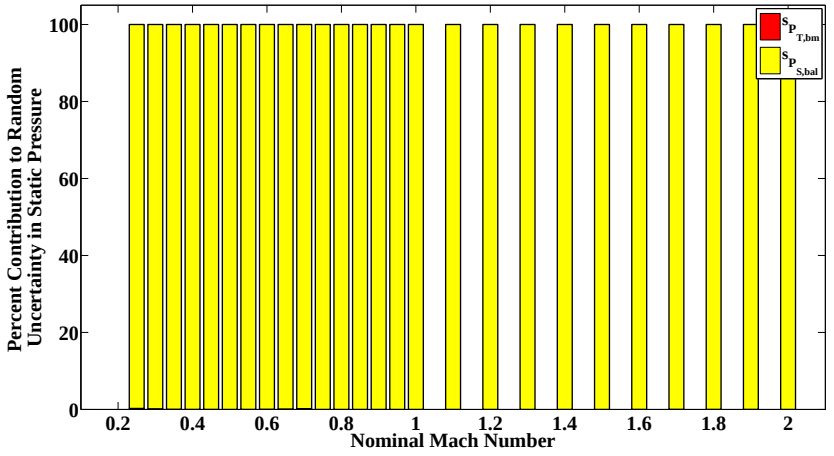

Figure 21: Random UPCs of $P_{S,ts}$ as a function of nominal Mach number for configuration 1. Red is the random uncertainty of the total pressure in the bellmouth, yellow is the random uncertainty of the static pressure in the balance chamber.

The random uncertainty of the calculated test section static pressure is shown for every nominal Mach number set point in Table 5. This table also shows how each of the measurements in the facility contribute to the random uncertainty.

Nominal Mach	**Typical** $P_{S,ts}$ **psia**	$s_{P_{S,ts}}$ **psia k = 2**	$s_{P_{S,ts}}$ **due to** $s_{P_{T,bm}}$ **psia k = 2**	$s_{P_{S,ts}}$ **due to** $s_{P_{S,bal}}$ **psia k = 2**	$s_{P_{S,ts}}$ **UPC due to** $s_{P_{T,bm}}$	$s_{P_{S,ts}}$ **UPC due to** $s_{P_{S,bal}}$
0.25	14.85	0.0005	0.0000	0.0005	0.3	99.7
0.40	13.86	0.0014	0.0000	0.0014	0.0	100.0
0.60	13.86	0.0006	0.0000	0.0006	0.0	100.0
0.80	11.29	0.0040	0.0000	0.0040	0.0	100.0
1.00	9.05	0.0061	0.0000	0.0061	0.0	100.0
1.20	7.34	0.0158	0.0000	0.0158	0.0	100.0
1.40	6.18	0.0241	0.0000	0.0241	0.0	100.0
1.60	5.16	0.0139	0.0002	0.0139	0.0	100.0
1.80	4.24	0.0253	0.0004	0.0253	0.0	100.0
2.00	3.25	0.0127	0.0000	0.0127	0.0	100.0

Table 5: Summary of calculated Static Pressure random uncertainty with 95% level of confidence for configuration 1.

5.1.3 Total Pressure

The random uncertainty in $P_{T,ts}$ is due to the random uncertainties in measured pressures in the balance chamber and bellmouth, as defined in Equations 3 and 8 and shown in Figures 11 and 12. The total random uncertainty for configuration 1 is shown in Figure 22. The values are steady below 0.0005 psia subsonically, then increase gradually to about 0.02 psia supersonically. A bar plot of the UPC of the elemental random uncertainties to total uncertainty of $P_{T,ts}$ is shown in Figure 23. The primary contributor is the random variation in the measured total pressure in the bellmouth.

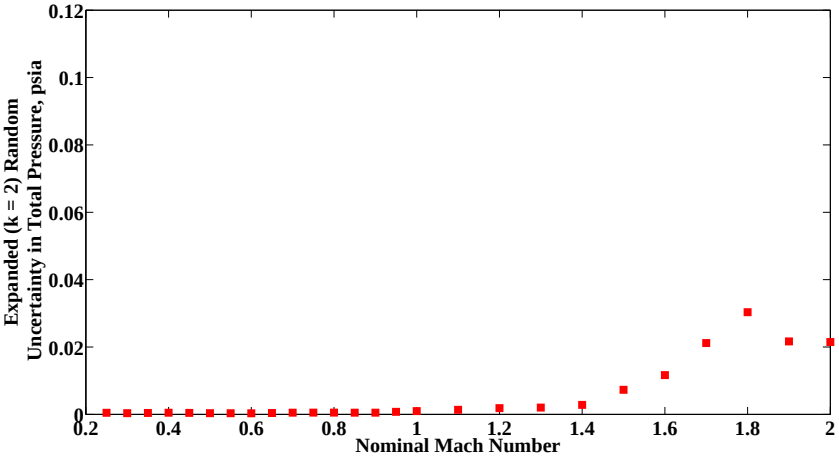

Figure 22: Random uncertainty of $P_{T,ts}$ as a function of nominal Mach number for configuration 1.

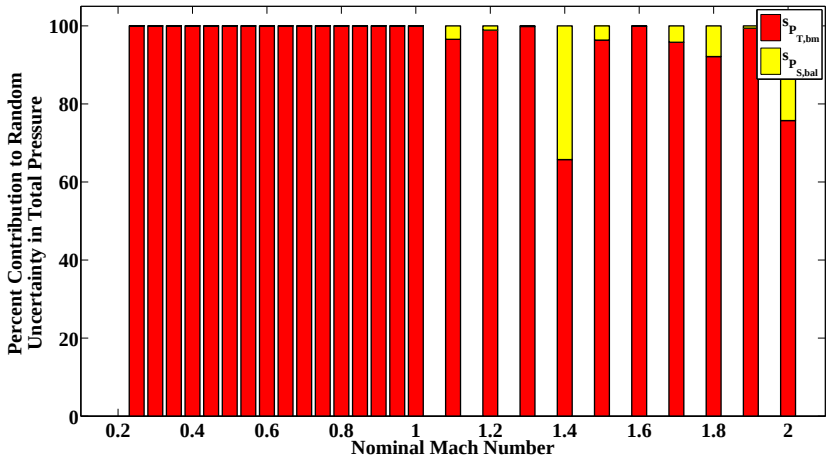

Figure 23: Random UPC for $P_{T,ts}$ as a function of nominal Mach number for configuration 1. Red is the random uncertainty of the total pressure in the bellmouth, and yellow is the random uncertainty of the static pressure in the balance chamber.

The random uncertainty of the calculated test section total pressure for configuration 1 is shown for every nominal Mach number set point in Table 6. This table also shows how each of the measurements in the facility contribute to the random uncertainty.

Nominal Mach	**Typical $P_{T,ts}$ psia**	$s_{P_{T,ts}}$ **psia k = 2**	$s_{P_{T,ts}}$ **due to** $s_{P_{T,bm}}$ **psia k = 2**	$s_{P_{T,ts}}$ **due to** $s_{P_{S,bal}}$ **psia k = 2**	$s_{P_{T,ts}}$ **UPC due to** $s_{P_{T,bm}}$	$s_{P_{T,ts}}$ **UPC due to** $s_{P_{S,bal}}$
0.25	15.51	0.0005	0.0005	0.0000	100.0	0.0
0.40	15.54	0.0005	0.0005	0.0000	100.0	0.0
0.60	17.74	0.0003	0.0003	0.0000	100.0	0.0
0.80	17.31	0.0005	0.0005	0.0000	100.0	0.0
1.00	17.15	0.0010	0.0010	0.0000	100.0	0.0
1.20	17.43	0.0019	0.0018	0.0002	98.9	1.1
1.40	18.43	0.0028	0.0023	0.0016	65.7	34.3
1.60	20.54	0.0117	0.0117	0.0004	99.9	0.1
1.80	23.69	0.0303	0.0291	0.0085	92.1	7.9
2.00	25.01	0.0215	0.0187	0.0106	75.7	24.3

Table 6: Summary of calculated Total Pressure random uncertainty with 95% level of confidence for configuration 1.

5.1.4 Dynamic Pressure

Dynamic pressure, q_{ts}, is a function of Mach number (see Equation 14), which is also a calculation and is therefore subject to random uncertainties in the measured pressures $P_{T,bm}$ and $P_{S,bal}$. Dynamic pressure random uncertainty results are shown in Figure 24. Values are relatively steady below 0.003 psia subsonically, then gradually increase supersonically to about 0.015 psia. A breakdown of the random uncertainties as UPCs to the total random uncertainty in dynamic pressure is shown in Figure 25. Both pressure measurements are significant contributors to the random uncertainty of dynamic pressure.

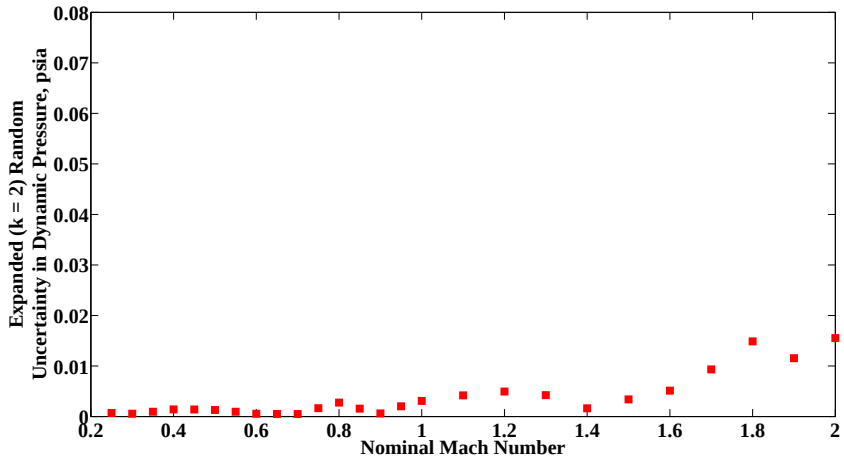

Figure 24: Random uncertainty of q_{ts} as a function of nominal Mach number for configuration 1.

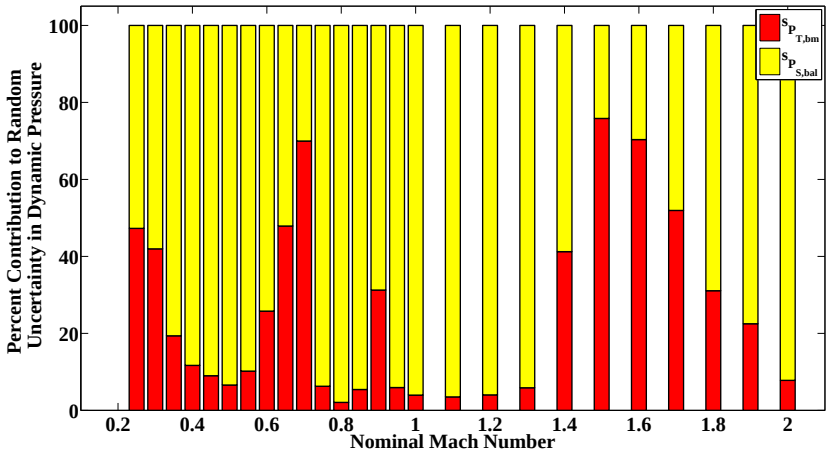

Figure 25: Random UPCs of q_{ts} as a function of nominal Mach number for configuration 1. Red is the random uncertainty of the total pressure in the bellmouth, and yellow is the random uncertainty of the static pressure in the balance chamber.

The random uncertainty of the calculated test section dynamic pressure is shown for configuration 1 for every nominal Mach number set point in Table 7. This table also shows how each of the measurements in the facility contribute to the random uncertainty.

Nominal Mach	**Typical q_{ts} psia**	$s_{q_{ts}}$ **psia k = 2**	$s_{q_{ts}}$ **due to** $s_{P_{T,bm}}$ **psia k = 2**	$s_{q_{ts}}$ **due to** $s_{P_{S,bal}}$ **psia k = 2**	$s_{q_{ts}}$ **UPC due to** $s_{P_{T,bm}}$	$s_{q_{ts}}$ **UPC due to** $s_{P_{S,bal}}$
0.25	0.64	0.001	0.000	0.001	47.3	52.7
0.40	1.61	0.001	0.000	0.001	11.7	88.3
0.60	3.54	0.001	0.000	0.000	25.8	74.2
0.80	5.13	0.003	0.000	0.003	2.1	97.9
1.00	6.35	0.003	0.001	0.003	4.0	96.0
1.20	7.20	0.005	0.001	0.005	4.0	96.0
1.40	7.93	0.002	0.001	0.001	41.2	58.8
1.60	8.74	0.005	0.004	0.003	70.4	29.6
1.80	9.42	0.015	0.008	0.012	31.1	68.9
2.00	9.00	0.016	0.004	0.015	7.8	92.2

Table 7: Summary of calculated Dynamic Pressure random uncertainty with 95% level of confidence for configuration 1.

5.1.5 Total Temperature

The random uncertainty in $T_{T,ts}$ is due to the random uncertainty in the measured temperature $T_{T,bm}$ (Equation 5). This result is shown for configuration 1 in Figure 26. The random uncertainty in $T_{T,ts}$ for configuration 1 is about 0.5 °R at the lowest Mach numbers,

then holds steady around 0.25 °R for the remaining Mach numbers. The UPC of the elemental random uncertainty to total random uncertainty is shown for completeness in Figure 27, although the only contributor is random uncertainty in the total temperature in the bellmouth.

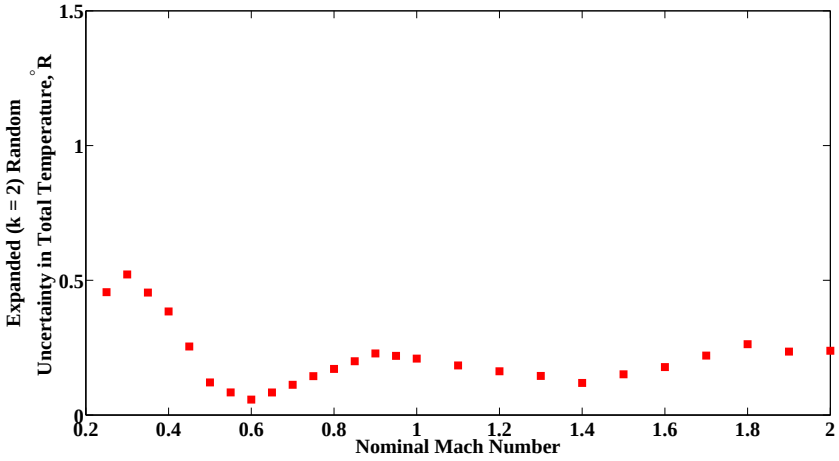

Figure 26: Random uncertainty in $T_{T,ts}$ as a function of nominal Mach number for configuration 1.

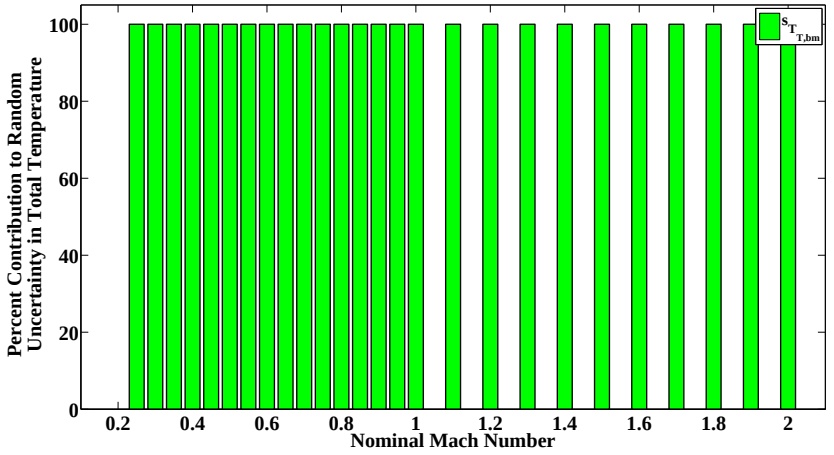

Figure 27: Random UPCs of $T_{T,ts}$ as a function of nominal Mach number for configuration 1. The only contributor is the total temperature in the bellmouth.

The random uncertainty of the calculated test section total temperature is shown for every nominal Mach number set point for configuration 1 in Table 8. This table also shows how each of the measurements in the facility contribute to the random uncertainty.

Nominal Mach	**Typical** $T_{T,ts}$ **°R**	$s_{T_{T,ts}}$ **°R k = 2**	$s_{T_{T,ts}}$ **due to** $s_{T_{T,bm}}$ **°R k = 2**	$s_{T_{T,ts}}$ **UPC due to** $s_{T_{T,bm}}$
0.25	520	0.46	0.46	100.0
0.40	525	0.38	0.38	100.0
0.60	557	0.06	0.06	100.0
0.80	565	0.17	0.17	100.0
1.00	559	0.21	0.21	100.0
1.20	576	0.16	0.16	100.0
1.40	585	0.12	0.12	100.0
1.60	604	0.18	0.18	100.0
1.80	630	0.26	0.26	100.0
2.00	649	0.24	0.24	100.0

Table 8: Summary of calculated Total Temperature random uncertainty with 95% level of confidence for configuration 1.

5.1.6 Static Temperature

$T_{S,ts}$ is calculated using the calculated values of $T_{T,ts}$ and M_{ts} (Equation 9). The random uncertainty in $T_{S,ts}$ is, therefore, due to random uncertainties in the measured pressures and temperatures $P_{T,bm}$, $P_{S,bal}$ and $T_{T,bm}$. The result is shown for configuration 1 in Figure 28. The uncertainty is about 0.5 °R subsonically then increases supersonically to about 0.7 °R. UPCs of elemental random uncertainties to total random uncertainty of $T_{S,ts}$ for configuration 1 are shown in Figure 29. The random uncertainty is dominated subsonically by the random variation of the total temperature in the bellmouth, contributing over 90% of the total random uncertainty in $T_{S,ts}$. Supersonically, however, the static pressure in the balance chamber drives the random uncertainty, contributing over 80% of the random uncertainty in $T_{S,ts}$.

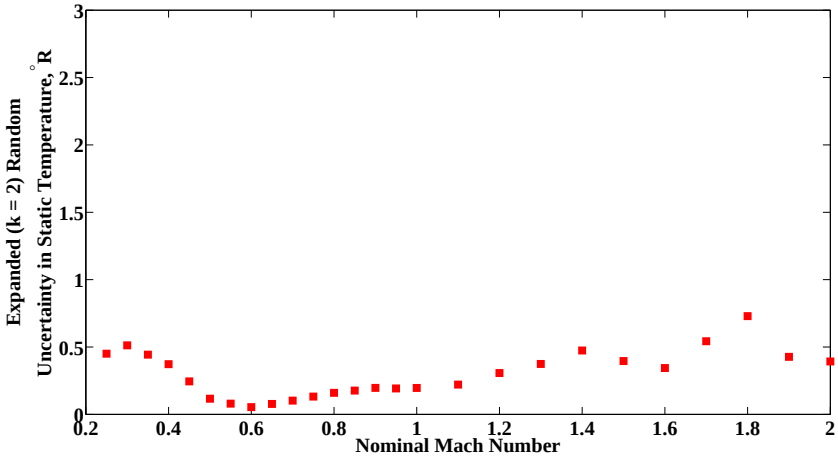

Figure 28: Random uncertainty in $T_{S,ts}$ as a function of nominal Mach number for configuration 1.

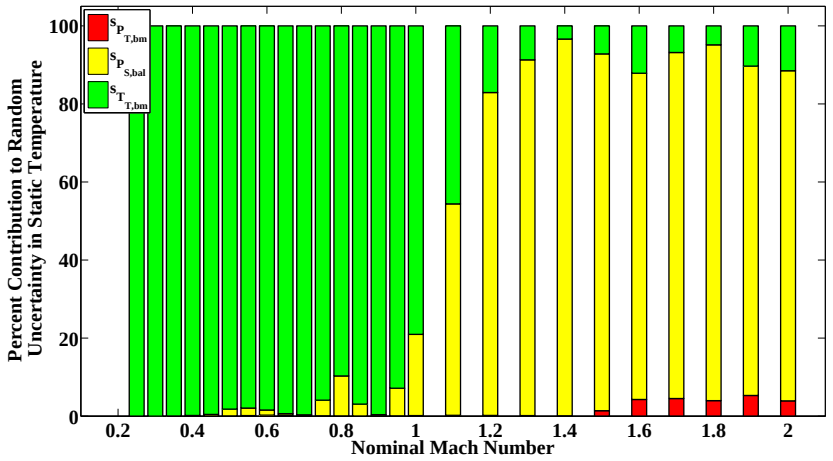

Figure 29: Random UPCs of $T_{S,ts}$ as a function of nominal Mach number for configuration 1. Red is the random uncertainty of the total pressure in the bellmouth, yellow is the random uncertainty of the static pressure in the balance chamber, and green is the random uncertainty of the total temperature in the bellmouth.

The random uncertainty of the calculated test section static temperature is shown for every nominal Mach number set point for configuration 1 in Table 9. This table also shows how each of the measurements in the facility contribute to the random uncertainty.

Nominal Mach	**Typical** $T_{S,ts}$ **°R**	$s_{T_{S,ts}}$ **°R k = 2**	$s_{T_{S,ts}}$ **due to** $s_{P_{T,bm}}$ **°R k = 2**	$s_{T_{S,ts}}$ **due to** $s_{P_{S,bal}}$ **°R k = 2**	$s_{T_{S,ts}}$ **due to** $s_{T_{T,bm}}$ **°R k = 2**	$s_{T_{S,ts}}$ **UPC due to** $s_{P_{T,bm}}$	$s_{T_{S,ts}}$ **UPC due to** $s_{P_{S,bal}}$	$s_{T_{S,ts}}$ **UPC due to** $s_{T_{T,bm}}$
0.25	513	0.45	0.00	0.01	0.45	0.0	0.0	100.0
0.40	508	0.37	0.00	0.02	0.37	0.0	0.2	99.8
0.60	519	0.05	0.00	0.01	0.05	0.3	1.3	98.4
0.80	500	0.16	0.00	0.05	0.15	0.1	10.2	89.7
1.00	466	0.20	0.01	0.09	0.17	0.1	20.8	79.0
1.20	450	0.31	0.01	0.28	0.13	0.2	82.7	17.1
1.40	428	0.47	0.02	0.47	0.09	0.1	96.5	3.4
1.60	407	0.34	0.07	0.31	0.12	4.3	83.6	12.1
1.80	385	0.73	0.15	0.70	0.16	4.0	91.2	4.9
2.00	362	0.39	0.08	0.36	0.13	3.9	84.6	11.5

Table 9: Summary of calculated Static Temperature random uncertainty with 95% level of confidence for configuration 1.

5.1.7 Reynolds Number

Re_{ts} is calculated using Equation 13. It is dependent on the calculated values of U_{ts} and μ_{ts}. The random uncertainty in Re_{ts} is due,then, to the random uncertainties in the measured pressures and temperatures $P_{T,bm}$, $P_{S,bal}$ and $T_{T,bm}$. The result is shown in Figure 30. Random uncertainty in Re_{ts} for configuration 1 is below about 0.003 x 10^6 ft^{-1} subsonically, then increases supersonically to about 0.01 x 10^6 ft^{-1}.

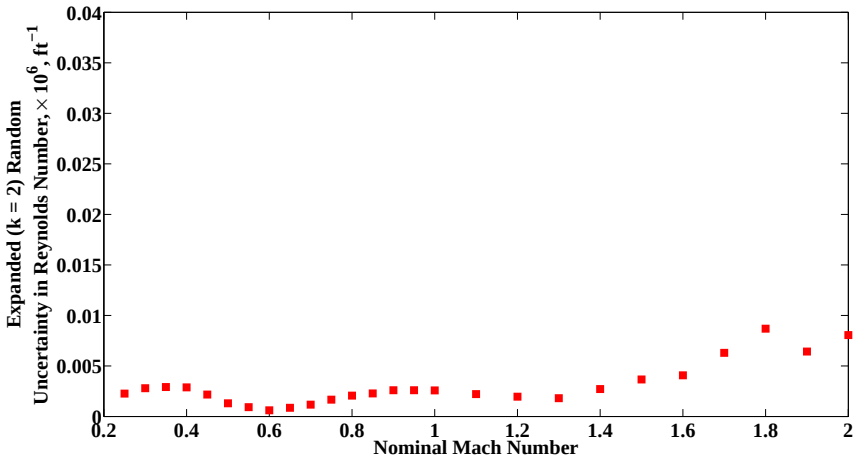

Figure 30: Random uncertainty in Re_{ts} as a function of nominal Mach number for configuration 1.

A bar chart depicting the UPC of the elemental random uncertainties to the total random uncertainty in Re_{ts} for configuration 1 is shown in Figure 31. Subsonically, random uncertainty in Reynolds number is driven by the total temperature variation in the bellmouth. Supersonically, it is driven by the static pressure variation in the balance chamber.

The random uncertainty of the calculated test section Reynolds number is shown for every nominal Mach number set point for configuration 1 in Table 10. This table also shows how each of the measurements in the facility contribute to the random uncertainty.

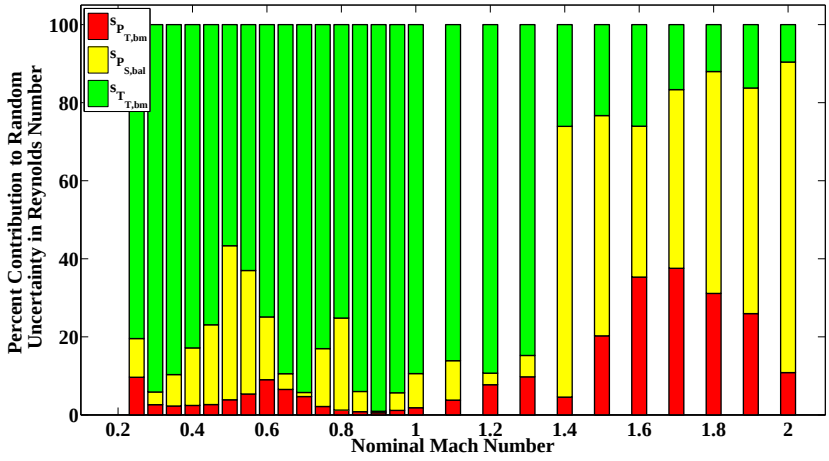

Figure 31: Random UPCs of Re_{ts} as a function of nominal Mach number for configuration 1. Red is the random uncertainty of the total pressure in the bellmouth, yellow is the random uncertainty of the static pressure in the balance chamber, and green is the random uncertainty of the total temperature in the bellmouth.

Nominal Mach	**Typical Re_{ts} $\times 10^6$ ft^{-1}**	**$s_{Re_{ts}}$, $\times 10^6$ ft^{-1} k = 2**	**$s_{Re_{ts}}$, due to $s_{P_{T,bm}}$, $\times 10^6$ ft^{-1} k = 2**	**$s_{Re_{ts}}$ due to $s_{P_{S,bal}}$, $\times 10^6$ ft^{-1} k = 2**	**$s_{Re_{ts}}$ due to $s_{T_{T,bm}}$, $\times 10^6$ ft^{-1} k = 2**	**$s_{Re_{ts}}$ UPC due to $s_{P_{T,bm}}$**	**$s_{Re_{ts}}$ UPC due to $s_{P_{S,bal}}$**	**$s_{Re_{ts}}$ UPC due to $s_{T_{T,bm}}$**
0.25	1.81	0.0023	0.0007	0.0007	0.0020	9.6	9.9	80.4
0.40	2.80	0.0029	0.0004	0.0011	0.0026	2.4	14.7	82.8
0.60	4.04	0.0006	0.0002	0.0002	0.0005	9.0	16.1	74.9
0.80	4.60	0.0021	0.0002	0.0010	0.0018	1.2	23.6	75.2
1.00	5.02	0.0026	0.0004	0.0008	0.0024	1.8	8.7	89.4
1.20	5.04	0.0020	0.0005	0.0003	0.0019	7.7	3.0	89.3
1.40	5.18	0.0027	0.0006	0.0023	0.0014	4.6	69.4	26.1
1.60	5.32	0.0041	0.0024	0.0025	0.0021	35.3	38.7	26.0
1.80	5.39	0.0087	0.0048	0.0066	0.0030	31.1	56.8	12.0
2.00	5.01	0.0081	0.0027	0.0072	0.0025	10.8	79.6	9.6

Table 10: Summary of calculated Reynolds Number random uncertainty with 95% level of confidence for configuration 1.

5.1.8 Air Speed

U_{ts} is calculated using Equation 10. It is determined based on M_{ts} and T_{ts}. The random uncertainty in U_{ts} is due to the random uncertainties in the measured pressures and temperatures $P_{T,bm}$, $P_{S,bal}$ and $T_{T,bm}$. The result is shown in Figure 32. Subsonically the random

uncertainty in U_{ts} for configuration 1 is less than 0.4 ft/s. Supersonically it increases to between 1 and 3 ft/s. UPCs of elemental random uncertainties to the total random uncertainty of U_{ts} are shown in Figure 33. The primary contributor is the random variation of the static pressure in the bellmouth, though subsonically the total temperature in the bellmouth contributes significantly as well.

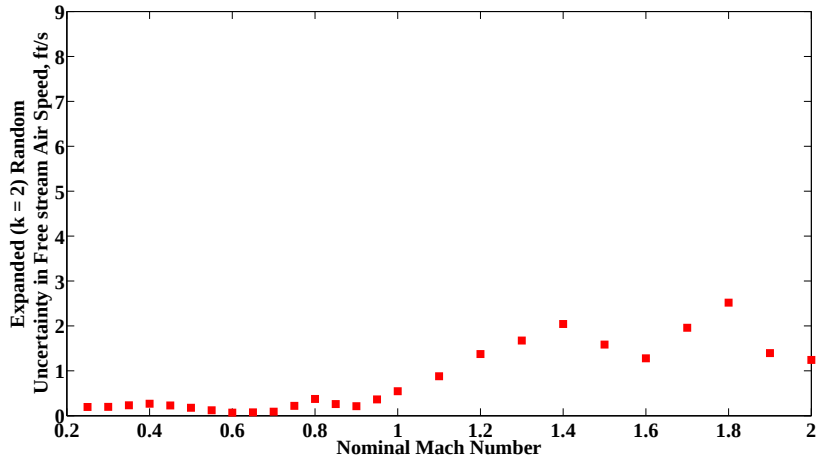

Figure 32: Random uncertainty of U_{ts} as a function of nominal Mach number for configuration 1.

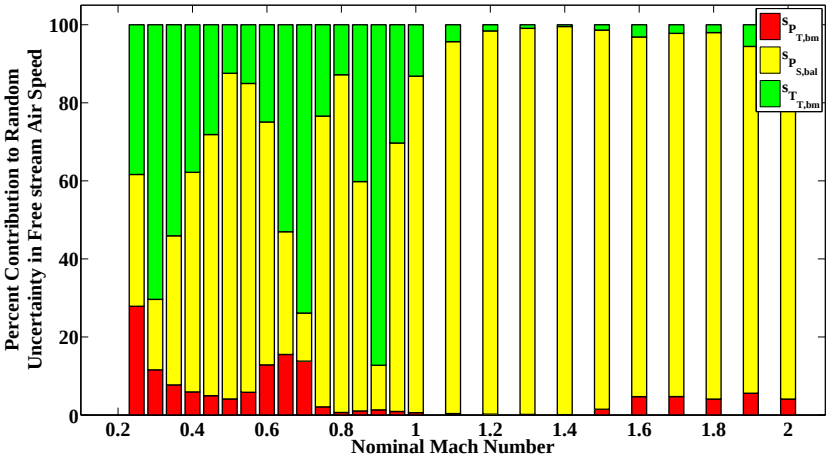

Figure 33: Random uncertainty of U_{ts} as a function of nominal Mach number for configuration 1. Red is the random uncertainty of the total pressure in the bellmouth, yellow is the random uncertainty of the static pressure in the balance chamber, and green is the random uncertainty of the total temperature in the bellmouth.

The random uncertainty of the calculated test section free stream air speed is shown for every nominal Mach number set point for configuration 1 in Table 11. This table also shows how each of the measurements in the facility contribute to the random uncertainty.

Nominal Mach	**Typical** U_{ts} **ft/s**	$s_{U_{ts}}$ **ft/s k = 2**	$s_{U_{ts}}$ **due to** $s_{P_{T,bm}}$ **ft/s k = 2**	$s_{U_{ts}}$ **due to** $s_{P_{S,bal}}$ **ft/s k = 2**	$s_{U_{ts}}$ **due to** $s_{T_{T,bm}}$ **ft/s k = 2**	$s_{U_{ts}}$ **UPC due to** $s_{P_{T,bm}}$	$s_{U_{ts}}$ **UPC due to** $s_{P_{S,bal}}$	$s_{U_{ts}}$ **UPC due to** $s_{T_{T,bm}}$
0.25	280	0.20	0.10	0.11	0.12	27.9	33.8	38.4
0.40	450	0.27	0.07	0.20	0.16	5.9	56.2	37.8
0.60	670	0.07	0.02	0.05	0.03	12.8	62.2	24.9
0.80	880	0.37	0.03	0.35	0.13	0.7	86.5	12.8
1.00	1060	0.55	0.04	0.51	0.20	0.6	86.2	13.2
1.20	1230	1.37	0.07	1.36	0.17	0.2	98.2	1.6
1.40	1370	2.04	0.07	2.04	0.14	0.1	99.4	0.5
1.60	1540	1.28	0.28	1.23	0.23	4.7	92.1	3.1
1.80	1710	2.52	0.51	2.44	0.36	4.1	93.9	2.0
2.00	1860	1.24	0.25	1.17	0.34	4.1	88.4	7.5

Table 11: Summary of calculated Free stream Air Speed random uncertainty with 95% level of confidence for configuration 1.

5.2 Systematic Uncertainty Results

As described in Section 4.2, systematic uncertainty characterizes the potential offset of a value from its true value due to manufacturing, calibration, flow quality, installation, or other sources. This type of uncertainty may be of interest to researchers trying to compare results either with tests in other facilities or CFD models. In this analysis, the systematic uncertainties considered include instrumentation calibration and fossilized uncertainties due to tunnel calibrations. This type of uncertainty characterizes the potential for bias in the measurements and calculations, but does not impact the short term repeatability of variables of interest.

5.2.1 Mach Number

Mach number is calculated by Equations 6 and 7. The combined systematic uncertainty in M_{ts} is, therefore, due to the uncertainty in total and static pressure calibrations (b_{PTCAL} and b_{PSCAL}), and instrumentation uncertainties in test-time total pressure in the bellmouth and static pressure in the balance chamber measurements (combined as $b_{P,Inst}$). The result is shown in Figure 34. The systematic uncertainty is below 0.005 subsonically, increasing to about 0.014 in the supersonic range.

A bar plot of the UPCs of the elemental systematic uncertainties contributing to M_{ts} are shown in Figure 35. Uncertainty due to instrumentation contributes very little, while the primary contributor to systematic uncertainty in Mach number is the static pressure calibration.

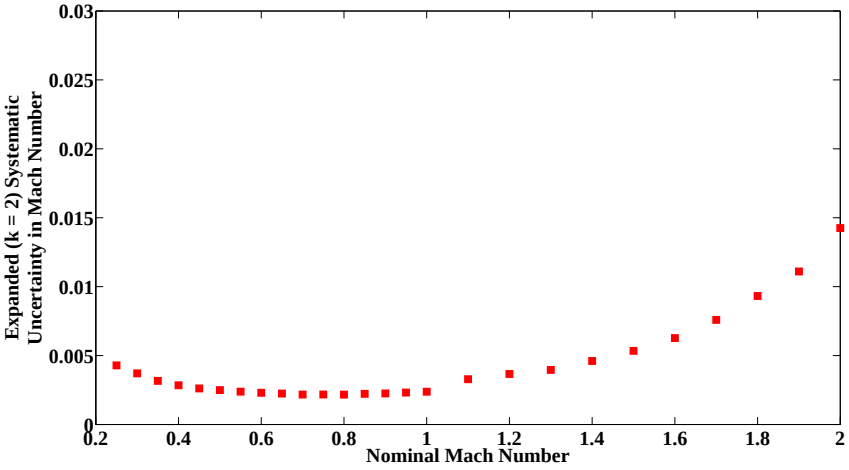

Figure 34: Systematic uncertainty of M_{ts} as a function of nominal Mach number for configuration 1.

The systematic uncertainty of the calculated test section Mach number is shown for every nominal Mach number set point for configuration 1 in Table 12. This table also shows how each of the parameters considered contributes to the systematic uncertainty.

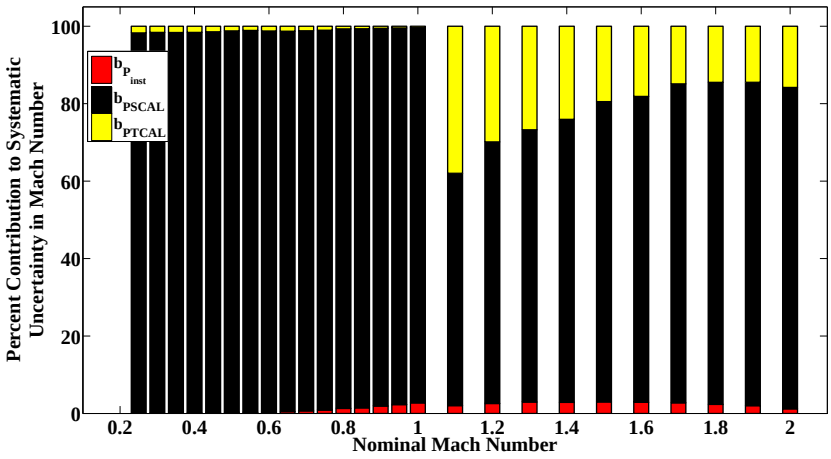

Figure 35: Systematic UPC for M_{ts} as a function of nominal Mach number for configuration 1. Red is the systematic uncertainty due to pressure instrumentation, yellow is the systematic uncertainty due to total pressure calibration, and black is the systematic uncertainty due to static pressure calibration.

Nominal Mach	**Typical** M_{ts}	$b_{M_{ts}}$ **k = 2**	$b_{M_{ts}}$ **due to** $b_{P_{Inst}}$ **k = 2**	$b_{M_{ts}}$ b_{PSCAL} **k = 2**	$b_{M_{ts}}$ b_{PTCAL} **k = 2**	$b_{M_{ts}}$ **UPC due to** $b_{P_{Inst}}$	$b_{M_{ts}}$ **UPC due to** b_{PSCAL}	$b_{M_{ts}}$ **UPC due to** b_{PTCAL}
0.25	0.25	0.0043	0.0001	0.0043	0.0006	0.0	98.3	1.7
0.40	0.41	0.0028	0.0001	0.0028	0.0004	0.1	98.3	1.6
0.60	0.60	0.0023	0.0001	0.0023	0.0003	0.4	98.4	1.2
0.80	0.81	0.0022	0.0002	0.0021	0.0002	1.3	98.0	0.7
1.00	1.00	0.0024	0.0004	0.0023	0.0001	2.7	96.9	0.4
1.20	1.18	0.0037	0.0006	0.0030	0.0020	2.6	67.6	29.9
1.40	1.35	0.0046	0.0008	0.0039	0.0023	2.9	73.1	24.0
1.60	1.56	0.0063	0.0011	0.0056	0.0027	2.9	79.0	18.1
1.80	1.78	0.0093	0.0014	0.0085	0.0036	2.3	83.2	14.5
2.00	1.99	0.0143	0.0016	0.0130	0.0057	1.2	83.0	15.8

Table 12: Summary of calculated Mach Number systematic uncertainty with 95% level of confidence for configuration 1.

5.2.2 Static Pressure

Static pressure is calculated using Equation 2. Systematic uncertainty in $P_{S,ts}$ is due to test section total and static pressure calibrations (b_{PTCAL} and b_{PSCAL}), and instrumentation uncertainties in test-time total pressure in the bellmouth and static pressure in the balance chamber measurements (combined as $b_{P,Inst}$). The result is shown for configuration 1 in Figure 36. The systematic uncertainty is generally around 0.025 psia subsonically, then increases to about 0.04 psia supersonically. The UPCs of elemental systematic uncertainties to the total systematic uncertainty of $P_{S,ts}$ are shown in Figure 37. The primary contributor is uncertainty in the static pressure calibration. Instrumentation uncertainty contributes up to 12.5%.

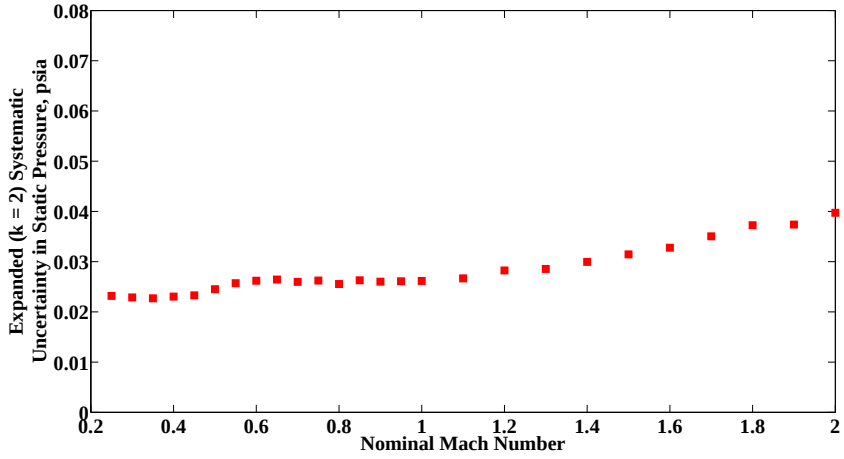

Figure 36: Systematic uncertainty of $P_{S,ts}$ as a function of nominal Mach number for configuration 1.

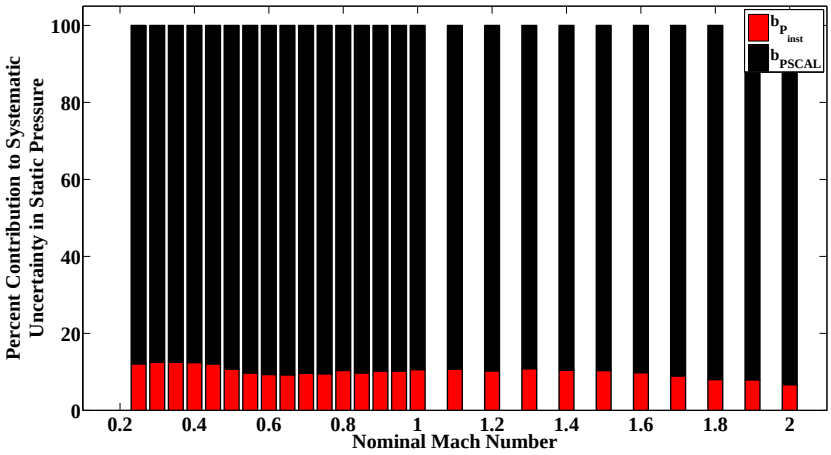

Figure 37: Systematic UPCs of $P_{S,ts}$ as a function of nominal Mach number for configuration 1. Red is the systematic uncertainty due to pressure instrumentation and black is the systematic uncertainty due to static pressure calibration.

The systematic uncertainty of the calculated test section static pressure is shown for every nominal Mach number set point for configuration 1 in Table 13. This table also shows how each of the parameters considered contributes to the systematic uncertainty.

Nominal Mach	**Typical $P_{S,ts}$ psia**	$b_{P_{S,ts}}$ **psia k = 2**	$b_{P_{S,ts}}$ **due to** $b_{P_{Inst}}$ **psia k = 2**	$b_{P_{S,ts}}$ **due to** b_{PSCAL} **psia k = 2**	$b_{P_{S,ts}}$ **UPC due to** $b_{P_{Inst}}$	$b_{P_{S,ts}}$ **UPC due to** b_{PSCAL}
0.25	14.85	0.0232	0.0081	0.0217	12.1	87.9
0.40	13.86	0.0230	0.0081	0.0216	12.4	87.6
0.60	13.86	0.0262	0.0080	0.0250	9.3	90.7
0.80	11.29	0.0255	0.0082	0.0242	10.4	89.6
1.00	9.05	0.0262	0.0085	0.0247	10.6	89.4
1.20	7.34	0.0282	0.0091	0.0268	10.3	89.7
1.40	6.18	0.0300	0.0097	0.0284	10.4	89.6
1.60	5.16	0.0328	0.0103	0.0311	9.8	90.2
1.80	4.24	0.0373	0.0105	0.0357	8.0	92.0
2.00	3.25	0.0397	0.0103	0.0384	6.7	93.3

Table 13: Summary of calculated Static Pressure systematic uncertainty with 95% level of confidence for configuration 1.

5.2.3 Total Pressure

$P_{T,ts}$ is calculated using Equations 3 and 8. The systematic uncertainty in $P_{T,ts}$ is due to test section total and static pressure calibrations (b_{PTCAL} and b_{PSCAL}), and instrumentation uncertainties in test-time total pressure in the bellmouth and static pressure in the balance chamber measurements (combined as $b_{P,Inst}$). The result is shown in Figure 38. Subsonically, the uncertainty is relatively steady around 0.009 psia. Supersonically, the systematic

uncertainty gradually increases to 0.3 psia at Mach 2.0.

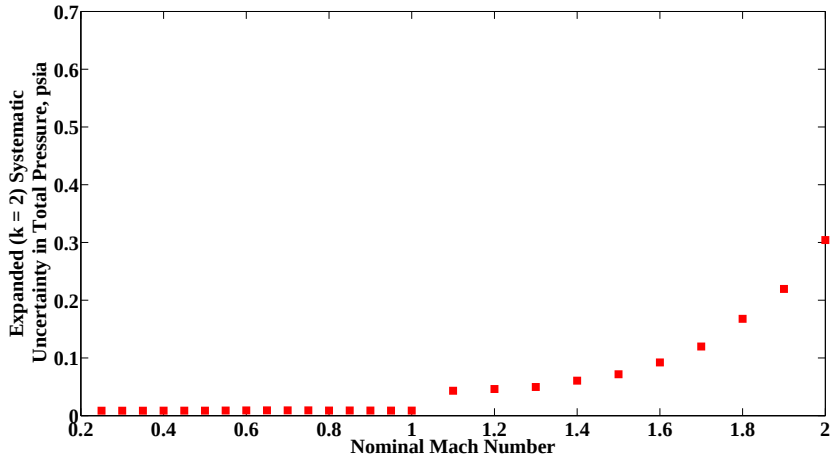

Figure 38: Systematic uncertainty of $P_{T,ts}$ as a function of nominal Mach number for configuration 1.

A bar plot of the UPCs of the elemental systematic uncertainties in $P_{T,ts}$ is shown in Figure 39. Subsonically, total pressure calibration contributes between 10 and 15% of the systematic uncertainty, with instrumentation making the rest of it. Supersonically, the static pressure calibration contributes increasing amounts (up to 50%), and the instrumentation becomes less influential (less than 1%).

The systematic uncertainty of the calculated test section total pressure is shown for every nominal Mach number set point for configuration 1 in Table 14. This table also shows how each of the parameters considered contribute to the systematic uncertainty.

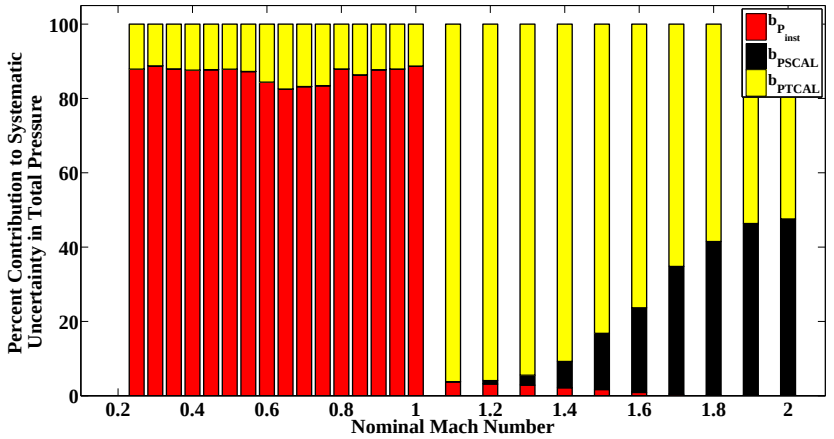

Figure 39: Systematic UPC for $P_{T,ts}$ as a function of nominal Mach number for configuration 1. Red is the systematic uncertainty due to pressure instrumentation, yellow is the systematic uncertainty due to total pressure calibration, and black is the systematic uncertainty due to static pressure calibration.

Nominal Mach	**Typical $P_{T,ts}$ psia**	**$b_{P_{T,ts}}$, psia k = 2**	**$b_{P_{T,ts}}$ due to $b_{P_{Inst}}$, psia k = 2**	**$b_{P_{T,ts}}$ due to b_{PSCAL}, psia k = 2**	**$b_{P_{T,ts}}$ due to b_{PTCAL}, psia k = 2**	**$b_{P_{T,ts}}$ UPC due to $b_{P_{Inst}}$**	**$b_{P_{T,ts}}$ UPC due to b_{PSCAL}**	**$b_{P_{T,ts}}$ UPC due to b_{PTCAL}**
0.25	15.51	0.0086	0.0081	0.0000	0.0030	87.9	0.0	12.1
0.40	15.54	0.0087	0.0082	0.0000	0.0031	87.6	0.0	12.4
0.60	17.74	0.0090	0.0083	0.0000	0.0036	84.4	0.0	15.6
0.80	17.31	0.0089	0.0083	0.0000	0.0031	87.9	0.0	12.1
1.00	17.15	0.0088	0.0083	0.0000	0.0029	88.7	0.0	11.3
1.20	17.43	0.0461	0.0082	0.0044	0.0452	3.2	0.9	95.9
1.40	18.43	0.0606	0.0089	0.0161	0.0578	2.2	7.1	90.8
1.60	20.54	0.0921	0.0087	0.0440	0.0805	0.9	22.8	76.3
1.80	23.69	0.1678	0.0073	0.1078	0.1283	0.2	41.3	58.5
2.00	25.01	0.3041	0.0182	0.2090	0.2202	0.4	47.2	52.4

Table 14: Summary of calculated Total Pressure systematic uncertainty with 95% level of confidence for configuration 1.

5.2.4 Dynamic Pressure

Dynamic pressure, q_{ts} is calculated using Equation 14. The equation uses M_{ts}, which is itself calculated using the total and static pressures. The systematic uncertainty in q_{ts}, then, is due to test section total and static pressure calibrations (b_{PTCAL} and b_{PSCAL}), and instrumentation uncertainties in test-time total pressure in the bellmouth and static pressure in the balance chamber measurements (combined as $b_{P,Inst}$). This result is shown for configuration 1 in Figure 40. The systematic uncertainty is steady around 0.02 psia subsonically, then gradually increases to about 0.05 psia at Mach 2.0.

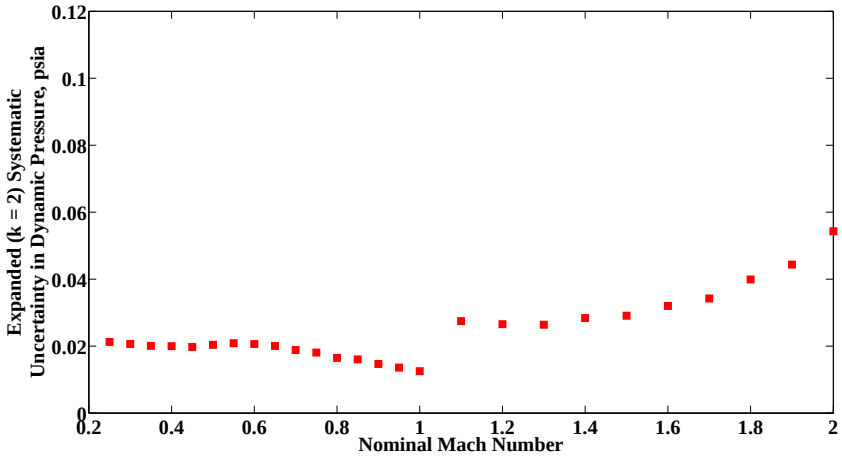

Figure 40: Systematic uncertainty of q_{ts} as a function of nominal Mach number for configuration 1.

A bar plot of the UPCs of elemental systematic uncertainties to the total systematic uncertainty in the calculated dynamic pressure is shown in Figure 41. Subsonically, the

systematic uncertainty is driven by the static pressure calibration, while supersonically the total pressure calibration drives uncertainty.

The systematic uncertainty of the calculated test section dynamic pressure is shown for every nominal Mach number set point for configuration 1 in Table 15. This table also shows how each of the parameters considered contributes to the systematic uncertainty.

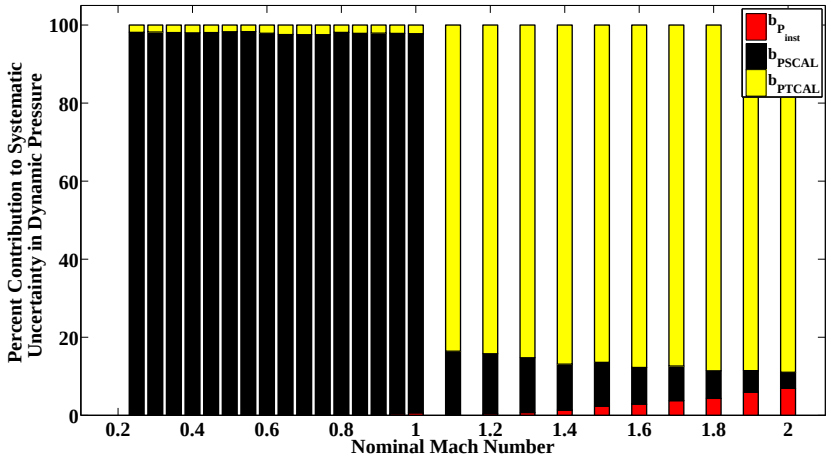

Figure 41: Systematic UPCs of q_{ts} as a function of nominal Mach number for configuration 1. Red is the systematic uncertainty due to pressure instrumentation, yellow is the systematic uncertainty due to total pressure calibration, and black is the systematic uncertainty due to static pressure calibration.

Nominal Mach	**Typical q_{ts} psia**	$b_{q_{ts}}$ **psia k = 2**	$b_{q_{ts}}$ **due to** $b_{P_{Inst}}$ **psia k = 2**	$b_{q_{ts}}$ **due to** b_{PSCAL} **psia k = 2**	$b_{q_{ts}}$ **due to** b_{PTCAL} **psia k = 2**	$b_{q_{ts}}$ **UPC due to** $b_{P_{Inst}}$	$b_{q_{ts}}$ **UPC due to** b_{PSCAL}	$b_{q_{ts}}$ **UPC due to** b_{PTCAL}
0.25	0.64	0.021	0.000	0.021	0.003	0.0	98.1	1.9
0.40	1.61	0.020	0.000	0.020	0.003	0.0	98.0	2.0
0.60	3.54	0.021	0.000	0.020	0.003	0.0	97.8	2.1
0.80	5.13	0.017	0.001	0.016	0.002	0.1	98.0	1.9
1.00	6.35	0.013	0.001	0.012	0.002	0.6	97.1	2.2
1.20	7.20	0.027	0.002	0.010	0.024	0.4	15.3	84.2
1.40	7.93	0.028	0.003	0.010	0.026	1.3	11.8	86.9
1.60	8.74	0.032	0.005	0.010	0.030	2.9	9.4	87.7
1.80	9.42	0.040	0.008	0.011	0.038	4.3	7.1	88.6
2.00	9.00	0.054	0.014	0.011	0.051	6.9	4.1	89.0

Table 15: Summary of calculated Dynamic Pressure systematic uncertainty with 95% level of confidence for configuration 1.

5.2.5 Total Temperature

The systematic uncertainty in $T_{T,ts}$ is due to the test section total temperature calibration (b_{TTCAL}). The result is shown for configuration 1 in Figure 42. The systematic uncertainty is relatively steady about 2.75 °R. The UPC of elemental systematic uncertainties to the total systematic uncertainty are shown in Figure 43, although only the total temperature calibration contributes.

It is noted that, just as it was for $T_{S,ts}$, temperature instrumentation does not appear in the contributing systematic uncertainties. Since facility thermocouples ($T_{T,bm}$) do not undergo calibration, systematic errors present during calibration are also present during testing. The facility instrumentation is considered fully correlated from calibration to test-time analysis. This effectively negates the impact of systematic bias from these instruments [8].

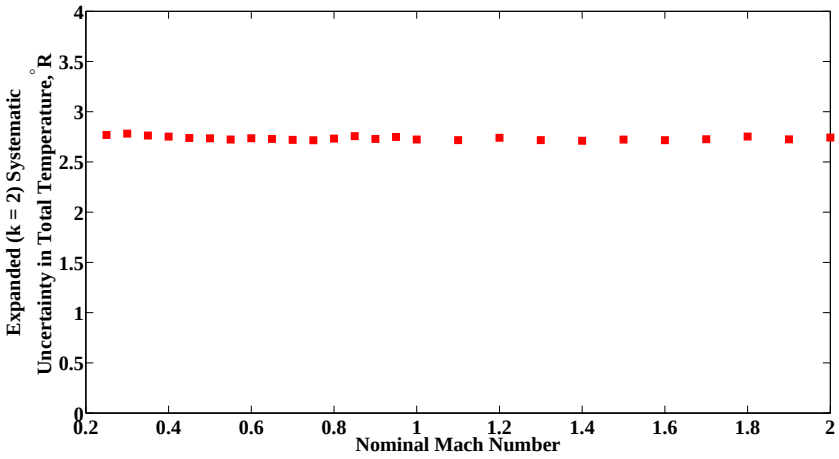

Figure 42: Systematic uncertainty in $T_{T,ts}$ as a function of nominal Mach number for configuration 1.

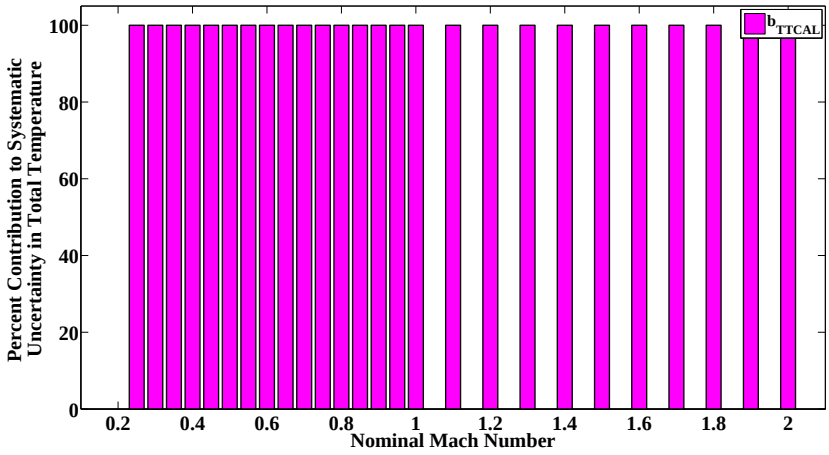

Figure 43: Systematic UPCs of $T_{T,ts}$ as a function of Mach number for configuration 1. Purple is the systematic uncertainty due to total temperature calibration.

The systematic uncertainty of the calculated test section total temperature is shown for every nominal Mach number set point for configuration 1 in Table 16. This table also shows how each of the parameters considered contributes to the systematic uncertainty.

Nominal Mach	**Typical** $T_{T,ts}$ **°R**	$b_{T_{T,ts}}$ **°R k = 2**	$b_{T_{T,ts}}$ **due to** b_{TTCAL} **°R k = 2**	$b_{T_{T,ts}}$ **UPC due to** b_{TTCAL}
0.25	520	2.77	2.77	100.0
0.40	525	2.75	2.75	100.0
0.60	557	2.74	2.74	100.0
0.80	565	2.73	2.73	100.0
1.00	559	2.72	2.72	100.0
1.20	576	2.74	2.74	100.0
1.40	585	2.71	2.71	100.0
1.60	604	2.72	2.72	100.0
1.80	630	2.75	2.75	100.0
2.00	649	2.74	2.74	100.0

Table 16: Summary of calculated Total Temperature systematic uncertainty with 95% level of confidence for configuration 1.

5.2.6 Static Temperature

$T_{S,ts}$ is calculated using the calculated values of $T_{T,ts}$ and M_{ts} (Equation 9). The systematic uncertainty in $T_{S,ts}$ is due to all test section calibrations (b_{PTCAL}, b_{PSCAL}, and b_{TTCAL}), and instrumentation uncertainties in test-time total bellmouth pressure, balance chamber static pressure ($b_{P,Inst}$). The result is shown for configuration 1 in Figure 44. The systematic

uncertainty is generally higher in the low Mach range, starting at about 2.8 °R at Mach 0.25 and decreasing to about 2.1 °R at Mach 1.6 before increasing again through the high Mach range. UPCs of the elemental systematic uncertainties to the total systematic uncertainty of $T_{S,ts}$ are shown in Figure 45. Temperature calibrations clearly dominate subsonically. Supersonically, the static pressure calibration has increasing influence, contributing over 50% of the systematic uncertainty at Mach 2.0.

It is noted that temperature instrumentation does not appear in the contributing systematic uncertainties. Since facility thermocouples ($T_{T,bm}$) do not undergo calibration, systematic errors present during calibration are also present during testing. The facility instrumentation is considered fully correlated from calibration to test-time analysis. This effectively negates the impact of systematic bias from these instruments [8].

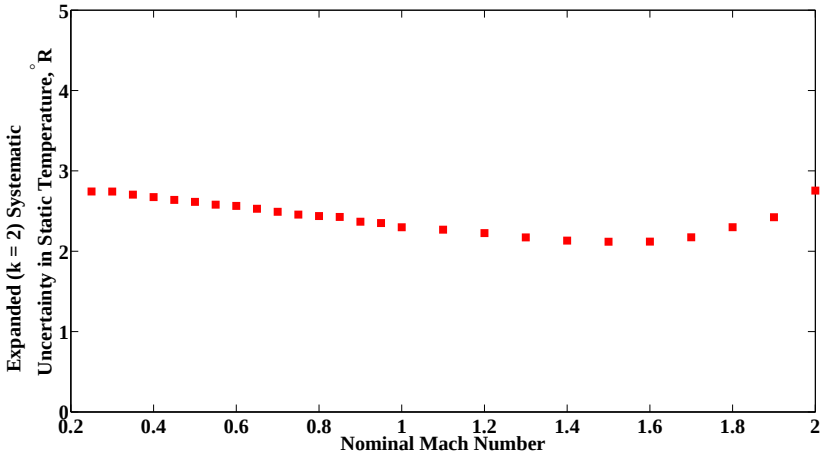

Figure 44: Systematic uncertainty in $T_{S,ts}$ as a function of nominal Mach number for configuration 1.

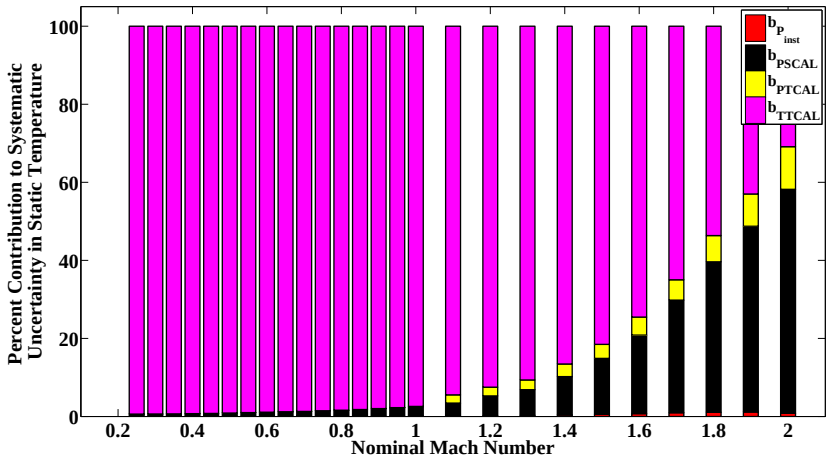

Figure 45: Systematic UPCs of $T_{S,ts}$ as a function of nominal Mach number for configuration 1. Red is the systematic uncertainty due to pressure instrumentation, yellow is the systematic uncertainty due to total pressure calibration, black is the systematic uncertainty due to static pressure calibration, and purple is the systematic uncertainty due to total temperature calibration.

The systematic uncertainty of the calculated test section static temperature is shown for every nominal Mach number set point for configuration 1 in Table 17. This table also shows how each of the parameters considered contributes to the systematic uncertainty.

Nominal Mach	**Typical** $T_{S,ts}$ **°R**	$b_{T_{S,ts}}$ **°R k = 2**	$b_{T_{S,ts}}$ **due to** $b_{P_{Inst}}$ **°R k = 2**	$b_{T_{S,ts}}$ **due to** b_{PSCAL} **°R k = 2**	$b_{T_{S,ts}}$ **due to** b_{PTCAL} **°R k = 2**	$b_{T_{S,ts}}$ **due to** b_{TTCAL} **°R k = 2**	$b_{T_{S,ts}}$ **UPC due to** $b_{P_{Inst}}$	$b_{T_{S,ts}}$ **UPC due to** b_{PSCAL}	$b_{T_{S,ts}}$ **UPC due to** b_{PTCAL}	$b_{T_{S,ts}}$ **UPC due to** b_{TTCAL}
0.25	513	2.74	0.00	0.21	0.03	2.73	0.0	0.6	0.0	99.4
0.40	508	2.67	0.01	0.23	0.03	2.66	0.0	0.7	0.0	99.3
0.60	519	2.56	0.02	0.27	0.03	2.55	0.0	1.1	0.0	98.9
0.80	500	2.44	0.04	0.31	0.03	2.42	0.0	1.6	0.0	98.4
1.00	466	2.30	0.06	0.36	0.02	2.27	0.1	2.5	0.0	97.4
1.20	450	2.23	0.10	0.50	0.33	2.14	0.2	5.1	2.2	92.5
1.40	428	2.13	0.13	0.67	0.38	1.98	0.4	9.8	3.2	86.5
1.60	407	2.12	0.18	0.95	0.46	1.83	0.7	20.1	4.6	74.5
1.80	385	2.30	0.24	1.43	0.60	1.68	1.1	38.5	6.7	53.6
2.00	362	2.75	0.25	2.09	0.91	1.53	0.8	57.4	10.9	30.9

Table 17: Summary of calculated Static Temperature systematic uncertainty with 95% level of confidence for configuration 1.

5.2.7 Reynolds Number

Re_{ts} is calculated using Equation 13. It is dependent on the calculated values of U_{ts} and μ_{ts}. The systematic uncertainty in Re_{ts} is due to all test section calibrations (b_{PTCAL}, b_{PSCAL}, and b_{TTCAL}), and instrumentation uncertainties in test-time total bellmouth pressure, and balance chamber static pressure ($b_{P,Inst}$). The result for configuration 1 is shown in Figure 46. The systematic uncertainty is 0.032 x 10^6 ft^{-1} at Mach 0.25, dips slightly then rises steadily until Mach 2 where it reaches 0.045 x 10^6 ft^{-1}.

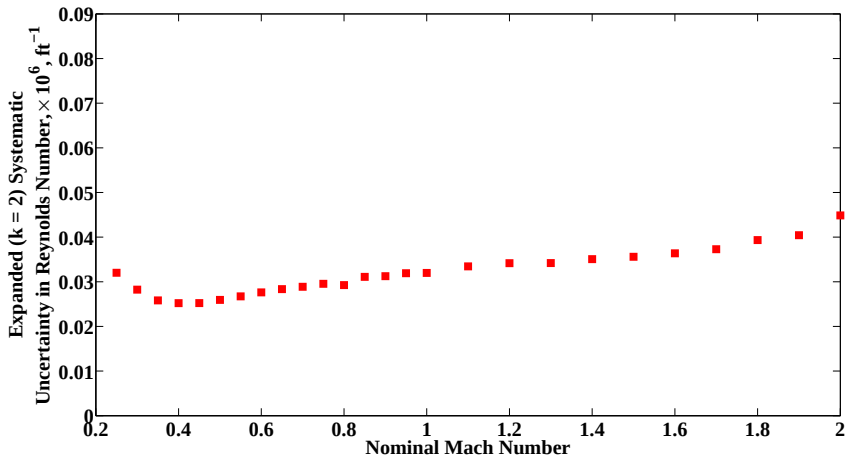

Figure 46: Systematic uncertainty of Re_{ts} as a function of nominal Mach number for configuration 1.

The UPCs of elemental systematic uncertainties to the total systematic uncertainty of the calculated Reynolds number are shown in Figure 47. Static pressure calibration is dominant at Mach 0.25, but has decreasing importance compared to total pressure calibration. In the supersonic regime, total pressure calibration uncertainties have increases affect.

The systematic uncertainty of the calculated test section Reynolds number is shown for every nominal Mach number set point for configuration 1 in Table 18. This table also shows how each of the parameters considered contributes to the systematic uncertainty.

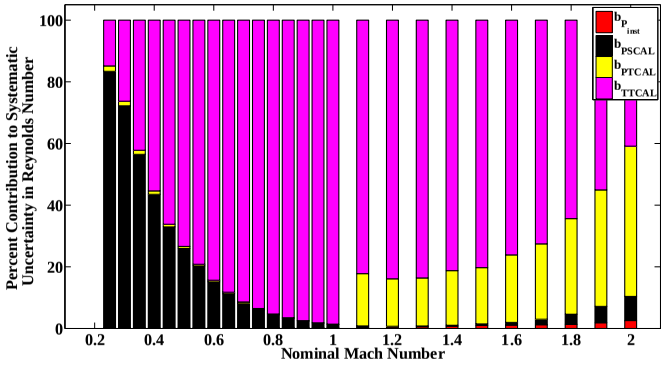

Figure 47: Systematic UPCs of Re_{ts} as a function of nominal Mach number for configuration 1. Red is the systematic uncertainty due to pressure instrumentation, yellow is the systematic uncertainty due to total pressure calibration, black is the systematic uncertainty due to static pressure calibration, and purple is the systematic uncertainty due to total temperature calibration.

Nominal Mach	**Typical** Re_{ts} $\times 10^6$ **ft^{-1}**	$b_{Re_{ts}}$ $\times 10^6$ **ft^{-1} k = 2**	$b_{Re_{ts}}$ **due to** $b_{P_{Inst}}$ $\times 10^6$ **ft^{-1} k = 2**	$b_{Re_{ts}}$ **due to** b_{PSCAL}, $\times 10^6$ **ft^{-1} k = 2**	$b_{Re_{ts}}$ **due to** b_{PTCAL}, $\times 10^6$ **ft^{-1} k = 2**	$b_{Re_{ts}}$ **due to** b_{TTCAL}, $\times 10^6$ **ft^{-1} k = 2**	$b_{Re_{ts}}$ **UPC due to** $b_{P_{Inst}}$	$b_{Re_{ts}}$ **UPC due to** b_{PSCAL}	$b_{Re_{ts}}$ **UPC due to** b_{PTCAL}	$b_{Re_{ts}}$ **UPC due to** b_{TTCAL}
0.25	1.81	0.0320	0.0005	0.0292	0.0042	0.0123	0.0	83.4	1.7	14.9
0.40	2.80	0.0252	0.0008	0.0166	0.0027	0.0188	0.1	43.4	1.1	55.4
0.60	4.04	0.0276	0.0013	0.0107	0.0020	0.0254	0.2	14.9	0.5	84.4
0.80	4.60	0.0293	0.0015	0.0060	0.0013	0.0286	0.3	4.2	0.2	95.3
1.00	5.02	0.0320	0.0019	0.0031	0.0011	0.0317	0.4	0.9	0.1	98.6
1.20	5.04	0.0342	0.0023	0.0018	0.0134	0.0313	0.4	0.3	15.4	83.9
1.40	5.18	0.0351	0.0030	0.0019	0.0148	0.0316	0.7	0.3	17.7	81.2
1.60	5.32	0.0364	0.0038	0.0034	0.0170	0.0317	1.1	0.9	21.9	76.1
1.80	5.39	0.0393	0.0046	0.0071	0.0219	0.0316	1.4	3.3	31.0	64.4
2.00	5.01	0.0449	0.0072	0.0126	0.0313	0.0287	2.6	7.8	48.7	40.9

Table 18: Summary of calculated Reynolds Number systematic uncertainty with 95% level of confidence for configuration 1.

5.2.8 Air Speed

U_{ts} is calculated using Equation 10. It is determined based on M_{ts} and T_{ts}. The systematic uncertainty in U_{ts} is due to all test section calibrations (b_{PTCAL}, b_{PSCAL}, and b_{TTCAL}), and instrumentation uncertainties in test-time total bellmouth pressure, and balance chamber static pressure ($b_{P,Inst}$). The result is shown for configuration 1 in Figure 48. The systematic uncertainty is about 4.75 ft/s at Mach 0.25, dips slightly then rises steadily to about 8.4 ft/s at Mach 2.

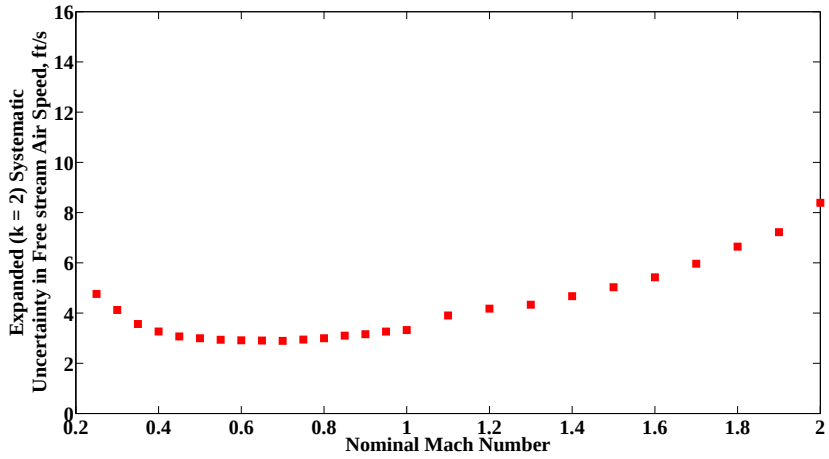

Figure 48: Systematic uncertainty of U_{ts} as a function of nominal Mach number for configuration 1.

A bar plot of the systematic uncertainty UPCs from all of the elemental systematic uncertainties to the combined systematic uncertainty in U_{ts} is shown in Figure 49. Static pressure calibration drives the uncertainty, although total temperature has increasing importance around Mach 1.

The systematic uncertainty of the calculated test section free stream air speed is shown for every nominal Mach number set point for configuration 1 in Table 19. This table also shows how each of the parameters considered contribute to the systematic uncertainty.

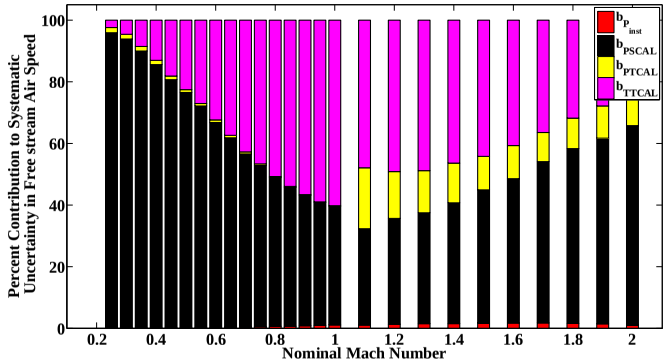

Figure 49: Systematic UPCs of U_{ts} as a function of nominal Mach number for configuration 1. Red is the systematic uncertainty due to pressure instrumentation, yellow is the systematic uncertainty due to total pressure calibration, black is the systematic uncertainty due to static pressure calibration, and purple is the systematic uncertainty due to total temperature calibration.

Nominal Mach	**Typical** U_{ts} **ft/s**	$b_{U_{ts}}$ **ft/s k = 2**	$b_{U_{ts}}$ **due to** $b_{P_{Inst}}$ **ft/s k = 2**	$b_{U_{ts}}$ **due to** b_{PSCAL} **ft/s k = 2**	$b_{U_{ts}}$ **due to** b_{PTCAL} **ft/s k = 2**	$b_{U_{ts}}$ **due to** b_{TTCAL} **ft/s k = 2**	$b_{U_{ts}}$ **UPC due to** $b_{P_{Inst}}$	$b_{U_{ts}}$ **UPC due to** b_{PSCAL}	$b_{U_{ts}}$ **UPC due to** b_{PTCAL}	$b_{U_{ts}}$ **UPC due to** b_{TTCAL}
0.25	280	4.76	0.07	4.66	0.62	0.74	0.0	95.9	1.7	2.4
0.40	450	3.26	0.12	3.02	0.38	1.18	0.1	85.4	1.4	13.0
0.60	670	2.91	0.14	2.38	0.27	1.66	0.2	66.6	0.8	32.4
0.80	880	3.00	0.24	2.08	0.17	2.14	0.6	48.3	0.3	50.7
1.00	1060	3.32	0.35	2.06	0.13	2.58	1.1	38.5	0.2	60.2
1.20	1230	4.18	0.48	2.45	1.63	2.93	1.3	34.4	15.2	49.1
1.40	1370	4.67	0.58	2.92	1.68	3.18	1.5	39.2	12.9	46.4
1.60	1540	5.42	0.71	3.71	1.78	3.46	1.7	46.8	10.7	40.7
1.80	1710	6.64	0.84	5.00	2.09	3.75	1.6	56.7	9.9	31.8
2.00	1860	8.39	0.82	6.75	2.95	3.92	0.9	64.8	12.4	21.9

Table 19: Summary of calculated Free stream Air Speed systematic uncertainty with 95% level of confidence for configuration 1.

5.3 Total Uncertainty Results

Combining the random and systematic uncertainties as root-sum-squares provides the total uncertainty of the variables of interest. This provides the same values as running the Monte Carlo code with all error sources flagged "on," indicating the data reduction equations taken as a whole are fairly linear. The total results are discussed in this section.

5.3.1 Mach Number

The total uncertainty in M_{ts} is shown for configuration 1 in Figure 50, with the random and systematic contributions included for reference. The total uncertainty in M_{ts} is generally below 0.005 subsonically, increases transonically, and reaches about 0.015 at Mach 2.0. The total uncertainty in Mach number is driven almost entirely by the systematic uncertainty as seen in Figure 51. In this case, overall Mach uncertainty is therefore driven by the static pressure calibration (see Figure 35). A table detailing the systematic, random, and total uncertainty in M_{ts} for configuration 1 is shown in Table 20.

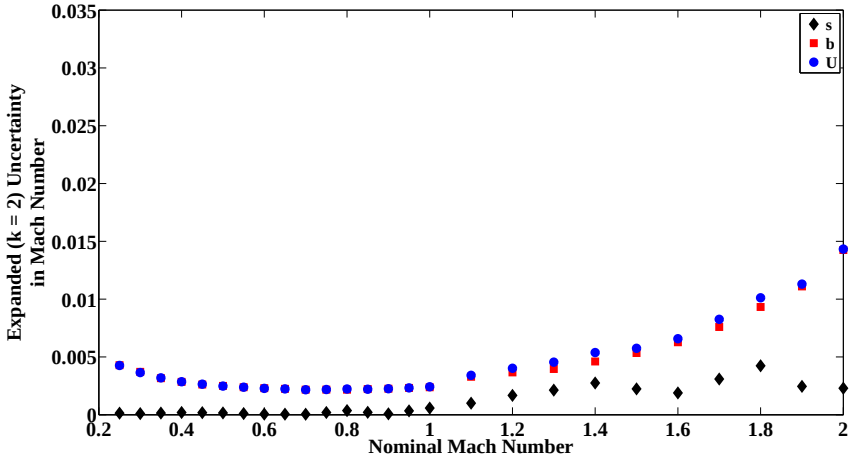

Figure 50: Total uncertainty in M_{ts} as a function of nominal Mach number for configuration 1.

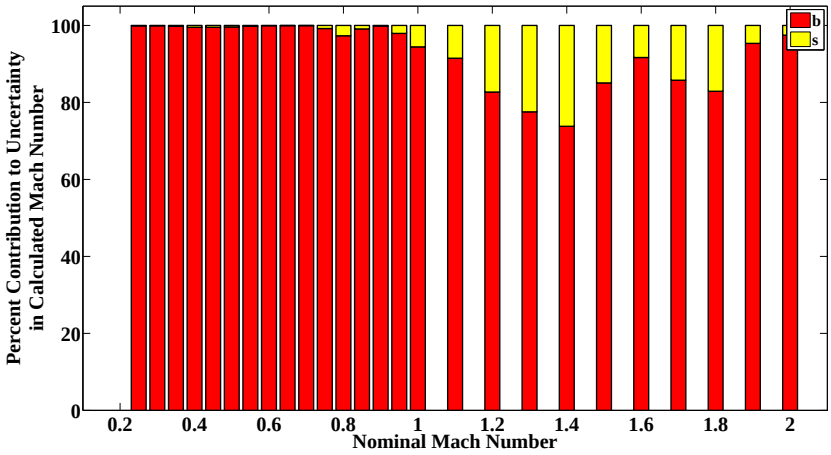

Figure 51: UPCs contributing to total uncertainty in M_{ts} as a function of nominal Mach number for configuration 1.

Nominal Mach	**Typical** M_{ts}	$s_{M_{ts}}$ **k = 2**	$b_{M_{ts}}$ **k = 2**	$u_{M_{ts}}$ **k = 2**	$s_{M_{ts}}$ **UPC**	$b_{M_{ts}}$ **UPC**
0.25	0.25	0.0001	0.0043	0.0043	0.1	99.9
0.40	0.41	0.0002	0.0028	0.0029	0.5	99.5
0.60	0.60	0.0001	0.0023	0.0023	0.1	99.9
0.80	0.81	0.0004	0.0022	0.0022	2.7	97.3
1.00	1.00	0.0006	0.0024	0.0024	5.6	94.4
1.20	1.18	0.0017	0.0037	0.0040	17.3	82.7
1.40	1.35	0.0027	0.0046	0.0054	26.2	73.8
1.60	1.56	0.0019	0.0063	0.0066	8.3	91.7
1.80	1.78	0.0042	0.0093	0.0101	17.1	82.9
2.00	1.99	0.0023	0.0143	0.0143	2.5	97.5

Table 20: Summary of calculated Mach Number uncertainty with 95% level of confidence for configuration 1.

5.3.2 Static Pressure

The combined uncertainty in $P_{S,ts}$ for configuration 1 is shown in Figure 52 with the random and systematic contributions included for reference. The total uncertainty in $P_{S,ts}$ is relatively stable around 0.025 psia subsonically. It increases transonically, peaks around 0.045 psia at Mach 1.8. The total uncertainty is driven by the systematic uncertainty, as confirmed by the bar plot of UPCs in Figure 53. Random, systematic and total uncertainty are detailed in table 21.

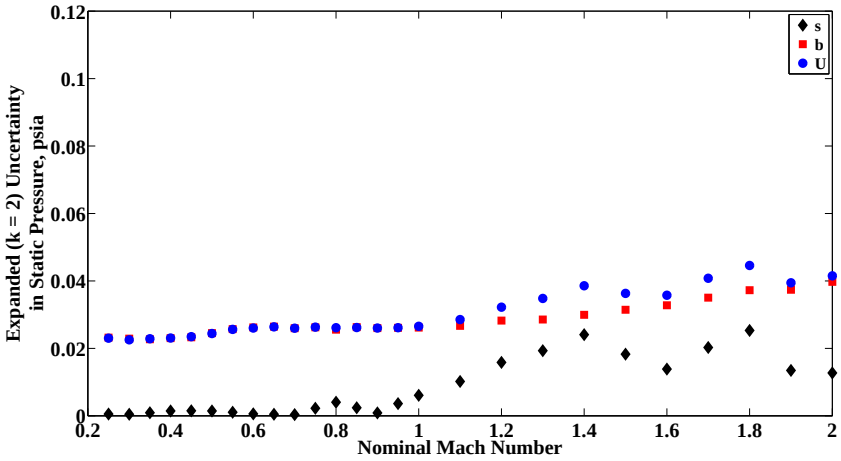

Figure 52: Total uncertainty of $P_{S,ts}$ as a function of nominal Mach number for configuration 1.

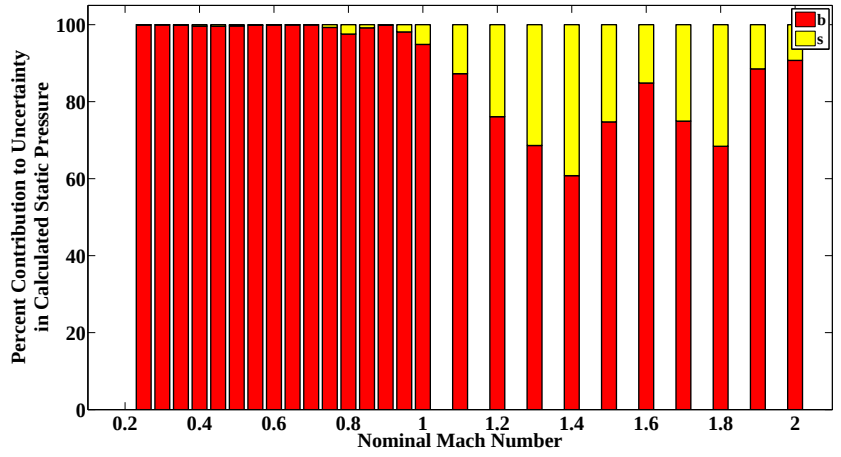

Figure 53: UPCs contributing to total uncertainty in $P_{S,ts}$ as a function of nominal Mach number for configuration 1.

Nominal Mach	**Typical $P_{S,ts}$, psia**	$s_{P_{S,ts}}$ **psia** **k = 2**	$b_{P_{S,ts}}$ **psia** **k = 2**	$u_{P_{S,ts}}$ **psia** **k = 2**	$s_{P_{S,ts}}$ **UPC**	$b_{P_{S,ts}}$ **UPC**
0.25	14.85	0.0005	0.0232	0.0230	0.1	99.9
0.40	13.86	0.0014	0.0230	0.0231	0.4	99.6
0.60	13.86	0.0006	0.0262	0.0260	0.0	100.0
0.80	11.29	0.0040	0.0255	0.0261	2.4	97.6
1.00	9.05	0.0061	0.0262	0.0265	5.1	94.9
1.20	7.34	0.0158	0.0282	0.0322	23.9	76.1
1.40	6.18	0.0241	0.0300	0.0386	39.2	60.8
1.60	5.16	0.0139	0.0328	0.0358	15.2	84.8
1.80	4.24	0.0253	0.0373	0.0446	31.6	68.4
2.00	3.25	0.0127	0.0397	0.0415	9.3	90.7

Table 21: Summary of calculated Static Pressure uncertainty with 95% level of confidence for configuration 1.

5.3.3 Total Pressure

The total uncertainty in $P_{T,ts}$ is shown in Figure 54 with the random and systematic contributions included for reference. The total uncertainty in test section total pressure is relatively steady around 0.009 psia at subsonic Mach numbers. It then gradually increases throughout the supersonic regime to about 0.30 psia at Mach 2.0. The total uncertainty is driven almost entirely by the systematic uncertainty. This is confirmed by the UPCs, shown in Figure 55. A table detailing the random, systematic, and overall uncertainty of $P_{T,ts}$ for configuration 1 is shown in Table 22.

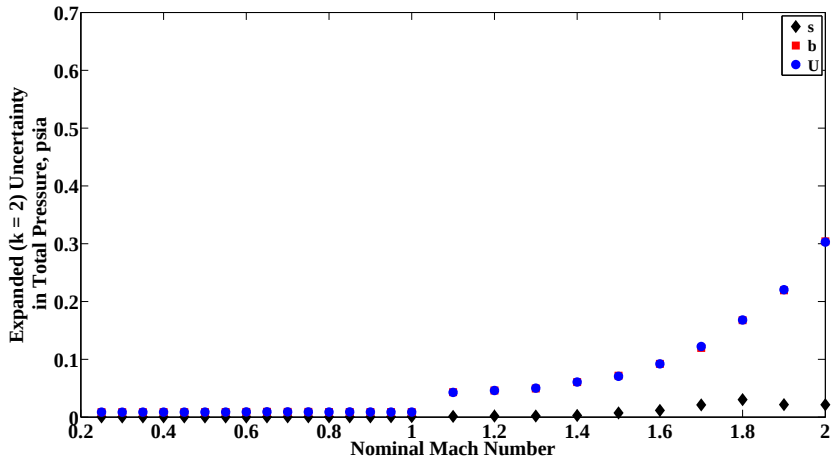

Figure 54: Total uncertainty of $P_{T,ts}$ as a function of nominal Mach number for configuration 1.

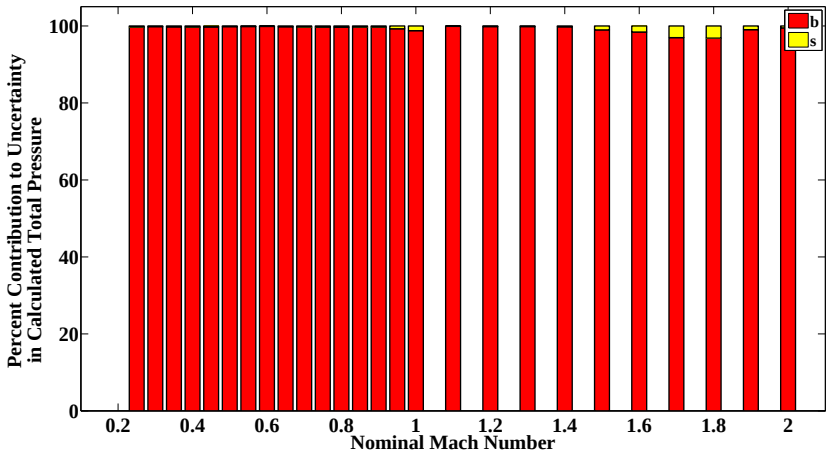

Figure 55: UPCs contributing to total uncertainty in $P_{T,ts}$ as a function of nominal Mach number for configuration 1.

Nominal Mach	Typical $P_{T,ts}$, psia	$s_{P_{T,ts}}$ psia k = 2	$b_{P_{T,ts}}$ psia k = 2	$u_{P_{T,ts}}$ psia k = 2	$s_{P_{T,ts}}$ UPC	$b_{P_{T,ts}}$ UPC
0.25	15.51	0.0005	0.0086	0.0087	0.3	99.7
0.40	15.54	0.0005	0.0087	0.0087	0.3	99.7
0.60	17.74	0.0003	0.0090	0.0091	0.1	99.9
0.80	17.31	0.0005	0.0089	0.0089	0.4	99.6
1.00	17.15	0.0010	0.0088	0.0088	1.2	98.8
1.20	17.43	0.0019	0.0461	0.0461	0.2	99.8
1.40	18.43	0.0028	0.0606	0.0607	0.2	99.8
1.60	20.54	0.0117	0.0921	0.0922	1.6	98.4
1.80	23.69	0.0303	0.1678	0.1681	3.2	96.8
2.00	25.01	0.0215	0.3041	0.3028	0.5	99.5

Table 22: Summary of calculated Total Pressure uncertainty with 95% level of confidence for configuration 1.

5.3.4 Dynamic Pressure

The total uncertainty in q_{ts} is shown in Figure 56 with the random and systematic contributions included for reference. The total uncertainty is around 0.02 psia subsonically, increasing to about 0.03 psia supersonically, and then up to about 0.06 psia at Mach 2.0. The uncertainty in the dynamic pressure is driven almost entirely by the systematic uncertainty. This is confirmed by the bar plot of the UPCs shown in Figure 57. The random, systematic, and total uncertainty of q_{ts} for configuration 1 are shown in Table 23.

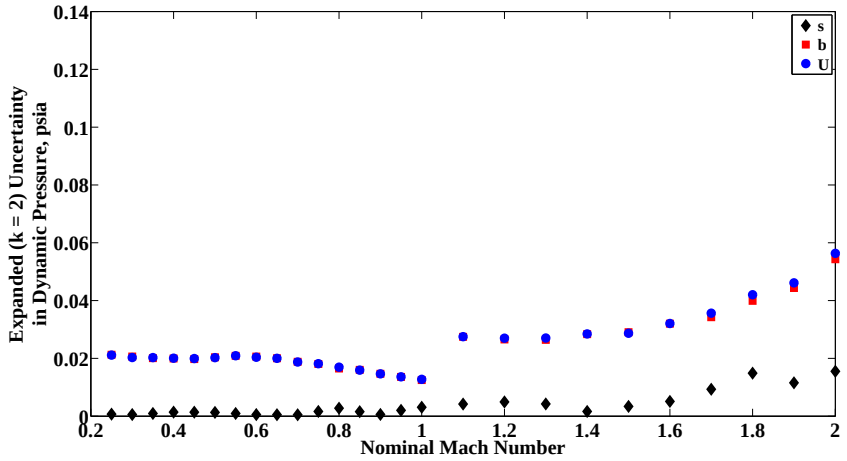

Figure 56: Total uncertainty in q_{ts} as a function of nominal Mach number for configuration 1.

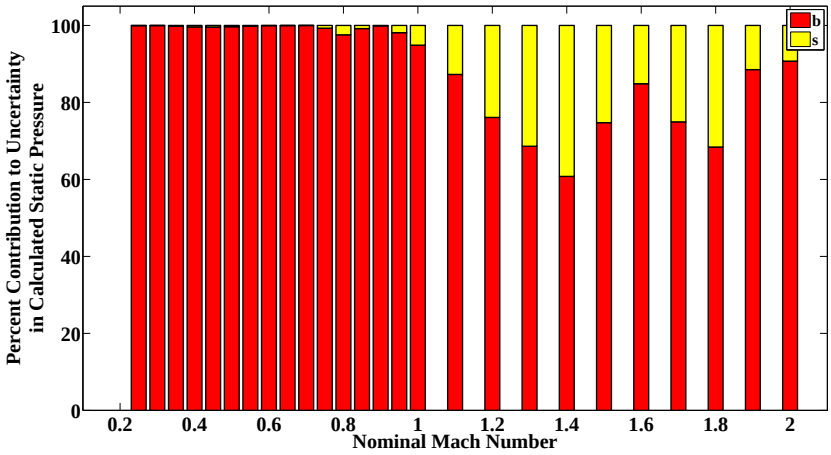

Figure 57: UPCs contributing to total uncertainty in q_{ts} as a function of nominal Mach number for configuration 1.

Nominal Mach	**Typical q_{ts}, psia**	$s_{q_{ts}}$ **psia k = 2**	$b_{q_{ts}}$ **psia k = 2**	$u_{q_{ts}}$ **psia k = 2**	$s_{q_{ts}}$ **UPC**	$b_{q_{ts}}$ **UPC**
0.25	0.64	0.001	0.021	0.021	0.1	99.9
0.40	1.61	0.001	0.020	0.020	0.5	99.5
0.60	3.54	0.001	0.021	0.020	0.1	99.9
0.80	5.13	0.003	0.017	0.017	2.7	97.3
1.00	6.35	0.003	0.013	0.013	5.8	94.2
1.20	7.20	0.005	0.027	0.027	3.4	96.6
1.40	7.93	0.002	0.028	0.028	0.3	99.7
1.60	8.74	0.005	0.032	0.032	2.5	97.5
1.80	9.42	0.015	0.040	0.042	12.2	87.8
2.00	9.00	0.016	0.054	0.056	7.6	92.4

Table 23: Summary of calculated Dynamic Pressure uncertainty with 95% level of confidence for configuration 1.

5.3.5 Static Temperature

The total uncertainty in $T_{S,ts}$ is shown in Figure 58 with the random and systematic contributions included for reference. The total uncertainty is about 2.7 °R at Mach 0.25, decreasing to just about 2.15 °R at Mach 1.6 before increasing again at the highest Mach numbers. Total uncertainty is driven by the systematic uncertainty. This is confirmed by the bar chart of UPCs in Figure 59. The uncertainties of $T_{S,ts}$ for configuration 1 are summarized in Table 24.

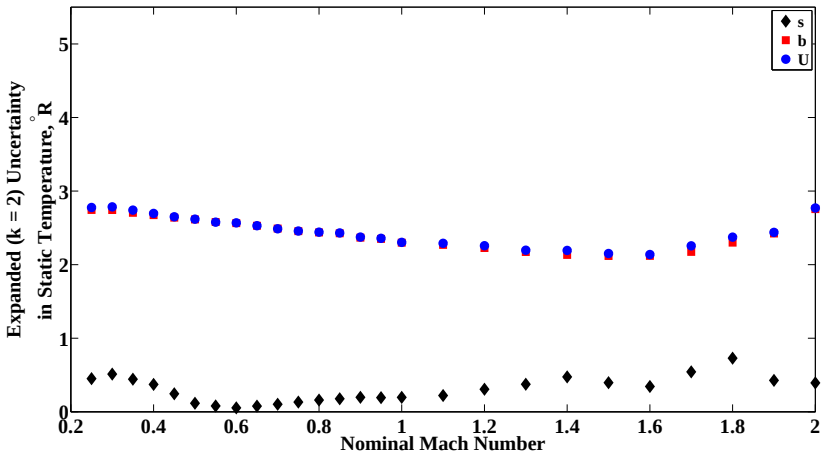

Figure 58: Total uncertainty in $T_{S,ts}$ as a function of nominal Mach number for configuration 1.

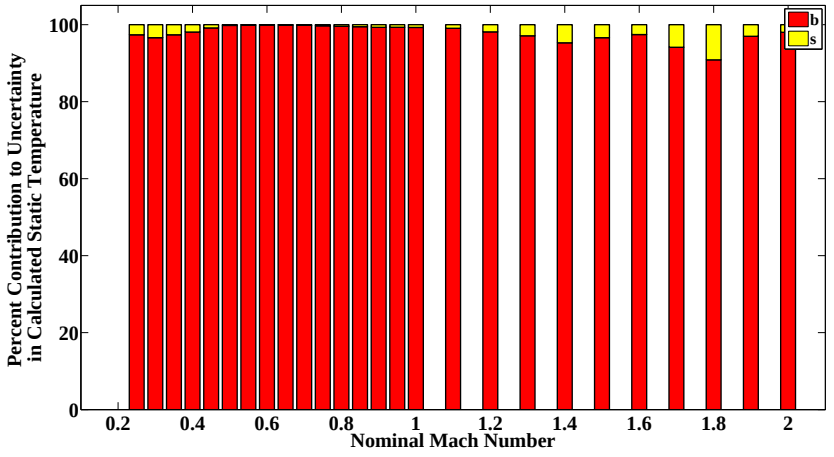

Figure 59: UPCs contributing to total uncertainty in $T_{S,ts}$ as a function of nominal Mach number for configuration 1.

Nominal Mach	**Typical** $T_{S,ts}$**, °R**	$s_{T_{S,ts}}$ **°R** **k = 2**	$b_{T_{S,ts}}$ **°R** **k = 2**	$u_{T_{S,ts}}$ **°R** **k = 2**	$s_{T_{S,ts}}$ **UPC**	$b_{T_{S,ts}}$ **UPC**
0.25	513	0.45	2.74	2.78	2.6	97.4
0.40	508	0.37	2.67	2.70	1.9	98.1
0.60	519	0.05	2.56	2.57	0.0	100.0
0.80	500	0.16	2.44	2.44	0.4	99.6
1.00	466	0.20	2.30	2.30	0.7	99.3
1.20	450	0.31	2.23	2.26	1.9	98.1
1.40	428	0.47	2.13	2.19	4.7	95.3
1.60	407	0.34	2.12	2.14	2.6	97.4
1.80	385	0.73	2.30	2.37	9.1	90.9
2.00	362	0.39	2.75	2.77	2.0	98.0

Table 24: Summary of calculated Static Temperature uncertainty with 95% level of confidence for configuration 1.

5.3.6 Total Temperature

The total uncertainty is shown in Figure 60 with the random and systematic contributions included for reference. The total uncertainty in $T_{T,ts}$ is about 2.8 °R over the entire Mach range. It is driven almost entirely by the systematic uncertainty, as shown by the bar chart of UPCs in Figure 61. Results for configuration 1 are summarized in Table 25.

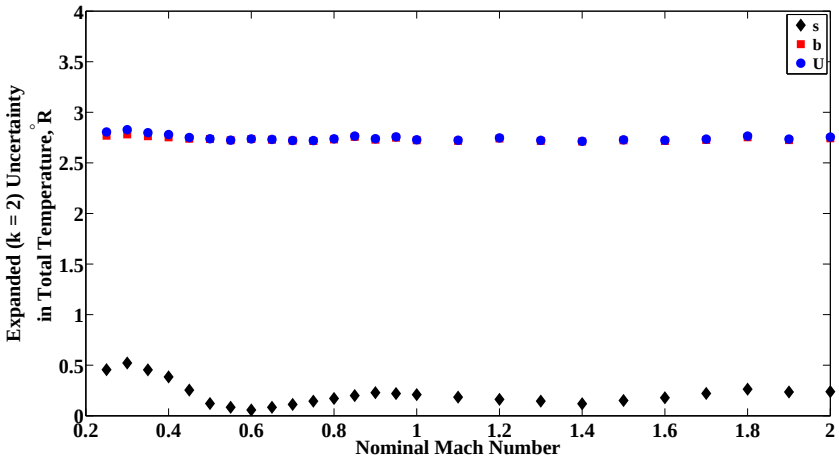

Figure 60: Total uncertainty of $T_{T,ts}$ as a function of nominal Mach number for configuration 1.

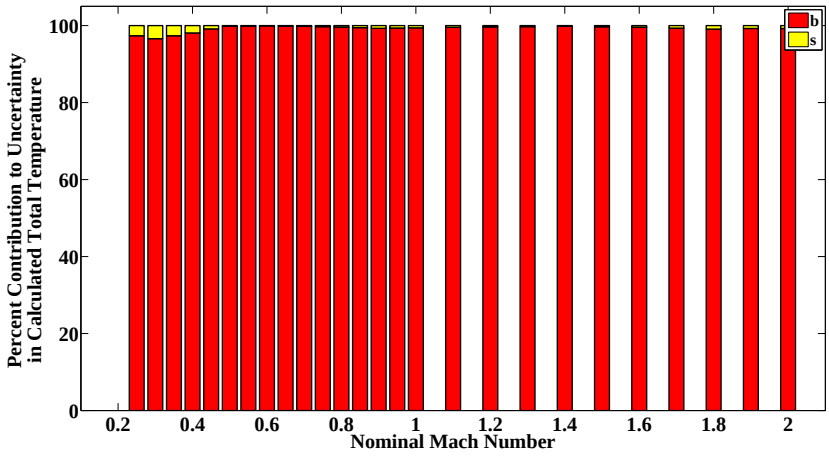

Figure 61: UPCs contributing to total uncertainty in $T_{T,ts}$ as a function of nominal Mach number for configuration 1.

Nominal Mach	**Typical $T_{T,ts}$, °R**	$s_{T_{T,ts}}$ **°R k = 2**	$b_{T_{T,ts}}$ **°R k = 2**	$u_{T_{T,ts}}$ **°R k = 2**	$s_{T_{T,ts}}$ **UPC**	$b_{T_{T,ts}}$ **UPC**
0.25	520	0.46	2.77	2.81	2.6	97.4
0.40	525	0.38	2.75	2.78	1.9	98.1
0.60	557	0.06	2.74	2.74	0.0	100.0
0.80	565	0.17	2.73	2.74	0.4	99.6
1.00	559	0.21	2.72	2.73	0.6	99.4
1.20	576	0.16	2.74	2.75	0.3	99.7
1.40	585	0.12	2.71	2.71	0.2	99.8
1.60	604	0.18	2.72	2.72	0.4	99.6
1.80	630	0.26	2.75	2.76	0.9	99.1
2.00	649	0.24	2.74	2.76	0.8	99.2

Table 25: Summary of calculated Total Temperature uncertainty with 95% level of confidence for configuration 1.

5.3.7 Reynolds Number

The total uncertainty in Re_{ts} is shown in Figure 62 with the random and systematic contributions included for reference. The total uncertainty is about 0.03 x 10^6 ft^{-1} at Mach 0.25, decreasing to 0.025 x 10^6 ft^{-1} at Mach 0.45, then increasing to 0.046 x 10^6 ft^{-1} by Mach 2. The total uncertainty is driven by the systematic uncertainty, as confirmed by Figure 63. The random, systematic and total uncertainties of Re_{ts} for configuration 1 are shown in Table 26

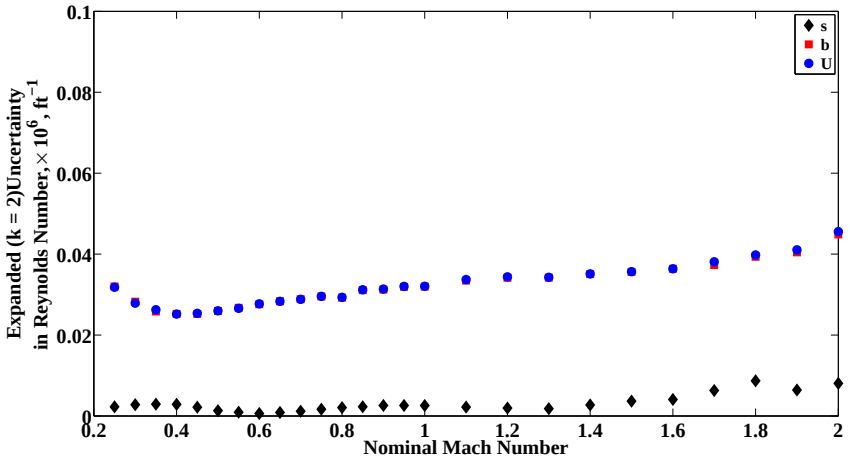

Figure 62: Total uncertainty in Re_{ts} as a function of nominal Mach number for configuration 1.

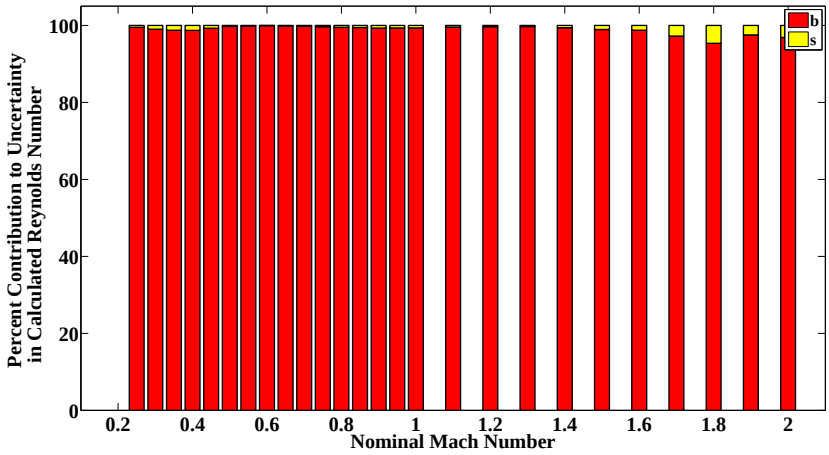

Figure 63: UPCs contributing to total uncertainty in R_{ts} as a function of nominal Mach number for configuration 1.

Nominal Mach	**Typical** Re_{ts} $\times 10^6$ **ft^{-1}**	$s_{Re_{ts}}$ $\times 10^6$ **ft^{-1}** **k = 2**	$b_{Re_{ts}}$ $\times 10^6$ **ft^{-1}** **k = 2**	$u_{Re_{ts}}$ $\times 10^6$ **ft^{-1}** **k = 2**	$s_{Re_{ts}}$ **UPC**	$b_{Re_{ts}}$ **UPC**
0.25	1.81	0.0023	0.0320	0.0318	0.5	99.5
0.40	2.80	0.0029	0.0252	0.0252	1.3	98.7
0.60	4.04	0.0006	0.0276	0.0277	0.0	100.0
0.80	4.60	0.0021	0.0293	0.0293	0.5	99.5
1.00	5.02	0.0026	0.0320	0.0320	0.6	99.4
1.20	5.04	0.0020	0.0342	0.0344	0.3	99.7
1.40	5.18	0.0027	0.0351	0.0351	0.6	99.4
1.60	5.32	0.0041	0.0364	0.0364	1.2	98.8
1.80	5.39	0.0087	0.0393	0.0398	4.7	95.3
2.00	5.01	0.0081	0.0449	0.0456	3.1	96.9

Table 26: Summary of calculated Reynolds Number uncertainty with 95% level of confidence for configuration 1.

5.3.8 Air Speed

The total uncertainty in U_{ts} for configuration 1 is shown in Figure 64 with the random and systematic contributions included for reference. The total uncertainty is about 4.75 ft/s at Mach 0.25, decreases to 2.9 at Mach 0.65, then increases to about 8.5 ft/s at Mach 2.0. The primary contributor to the total uncertainty is the systematic uncertainty. This is confirmed in Figure 65, which shows the UPC of random and systematic uncertainties to overall uncertainty. The random, systematic and total uncertainties are tabulated in Table 27 for configuration 1.

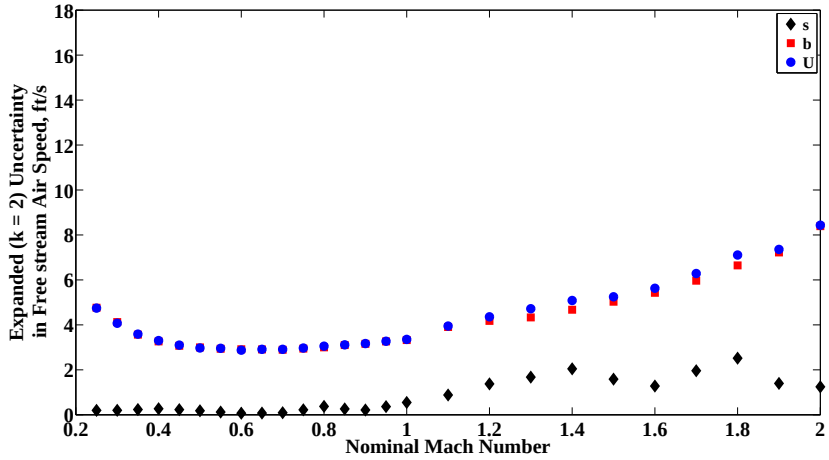

Figure 64: Total uncertainty in U_{ts} as a function of nominal Mach number for configuration 1.

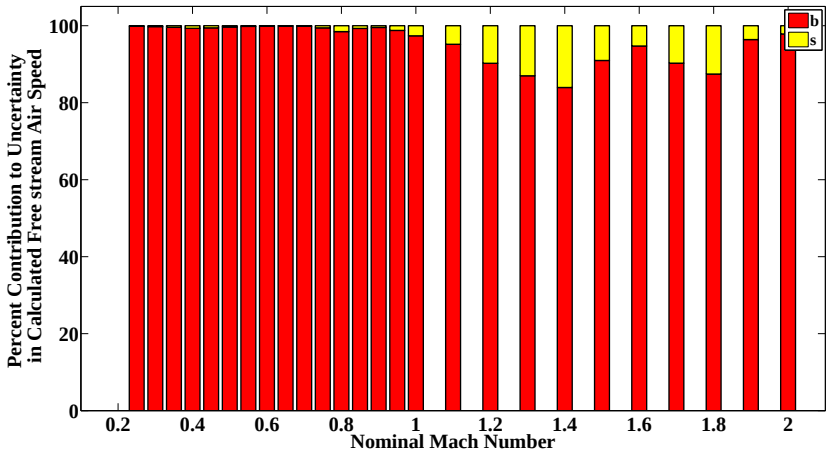

Figure 65: UPCs contributing to total uncertainty in U_{ts} as a function of nominal Mach number for configuration 1.

Nominal Mach	**Typical** U_{ts}**, ft/s**	$s_{U_{ts}}$ **ft/s** **k = 2**	$b_{U_{ts}}$ **ft/s** **k = 2**	$u_{U_{ts}}$ **ft/s** **k = 2**	$s_{U_{ts}}$ **UPC**	$b_{U_{ts}}$ **UPC**
0.25	280	0.20	4.76	4.74	0.2	99.8
0.40	450	0.27	3.26	3.30	0.7	99.3
0.60	670	0.07	2.91	2.87	0.1	99.9
0.80	880	0.37	3.00	3.05	1.5	98.5
1.00	1060	0.55	3.32	3.35	2.6	97.4
1.20	1230	1.37	4.18	4.36	9.8	90.2
1.40	1370	2.04	4.67	5.08	16.1	83.9
1.60	1540	1.28	5.42	5.63	5.3	94.7
1.80	1710	2.52	6.64	7.11	12.6	87.4
2.00	1860	1.24	8.39	8.43	2.1	97.9

Table 27: Summary of calculated Free stream Air Speed uncertainty with 95% level of confidence for configuration 1.

6 Analysis

This uncertainty analysis uses a "ground-up" approach, propagating the elemental uncertainties from the point of measurement to calculated variables of interest, as depicted for Mach number uncertainty in Figures 14 and 15. The analysis begins by determining elemental uncertainty estimates of the instrumentation used for pressure and temperature measurements, and other random and systematic uncertainties associated with the measurements and the facility. As calibrations and calculations (or assumptions) are made, associated uncertainties are also determined, and all uncertainties are propagated to obtain the final result. This section details the methods used in estimating all elemental uncertainties considered in this analysis, and describes how the Monte Carlo program propagates those uncertainties through to the calculated variables of interest. A coverage factor is not added until the final results are obtained; therefore, this section presents the elemental uncertainty estimates as standard uncertainties with no coverage factor.

6.1 Elemental Uncertainty Estimates

6.1.1 Instrumentation Level Uncertainty

The uncertainty of a system begins with the instrumentation used to obtain the measured values. This analysis uses the Measurement Analysis Tool for Uncertainty in Systems (MANTUS), an Excel® based tool which allows the user to break down the overall measurement into component parts, or "modules", to easily handle the analysis of multi-level instrumentation systems. A module can be configured to represent a specific function of a single component, or multiple components can be summarized into one module. The overall system is then assembled from multiple modules within MANTUS, allowing for propagation of uncertainties using the TSM to ultimately produce the final systematic uncertainty of the measurement. This process is depicted in Figure 66.

For this analysis, MANTUS is used to quantify the systematic uncertainties of pressure and temperature measurement instrumentation. Pressure measurements in the 8- by 6-foot SWT are obtained by ±15-psid pressure units within the S3200 Electronic Scanning Pressure (ESP) system. Temperature measurements are obtained using bi-metal Type E and Type K thermocouples. Using the methodology outlined in the NASA Measurement Uncertainty Analysis Handbook [4], MANTUS breaks down temperature and pressure systems into modules such as the sensor, signal conditioner, analog to digital convertor, and data processor. The cumulative uncertainty effects of the different modules on the measurements being taken are determined. This output accounts for multiple variables present in each measurement subsystem, producing a mathematically verifiable instrumentation model. More details on MANTUS can be found in the MANTUS CR [12].

The systematic standard uncertainty for the pressure scanning system determined by MANTUS is shown in Figure 67. All pressures considered in this analysis share a common ±15-psid pressure calibration unit and were calibrated to the same reference pressure. As a result, the instrumentation calibration errors are considered fully correlated between all pressure measurements within a calibration cycle. Details concerning how to apply correlated and uncorrelated uncertainties are discussed in Section 6.2. Throughout this analysis, corre-

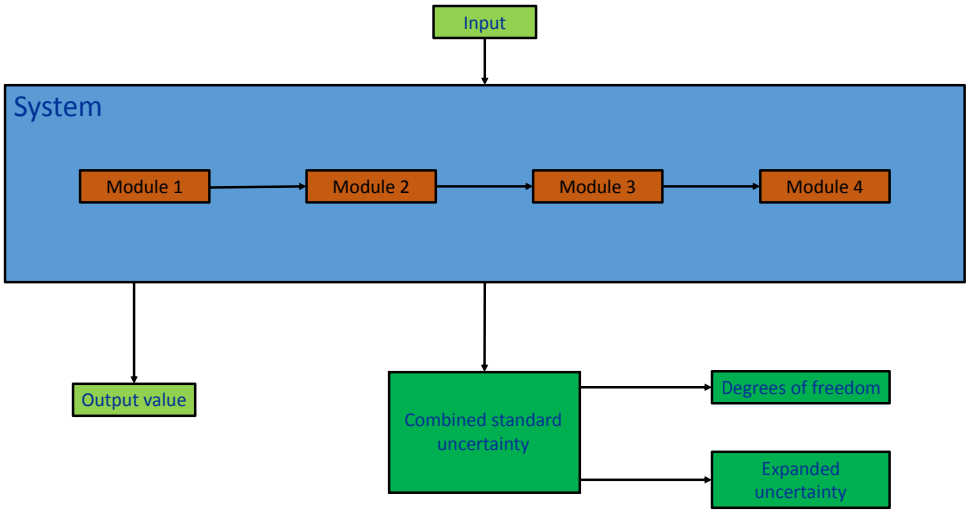

Figure 66: Instrumentation level uncertainty analysis flow.

lated uncertainties from pressure and temperature instrumentation are considered as a unit ($b_{P,corr}$ or $b_{T,corr}$), rather than separated into each specific variable's correlated contribution (i.e. $b_{P_{S,bal,corr}}$ or $b_{T_{T,bm,corr}}$).

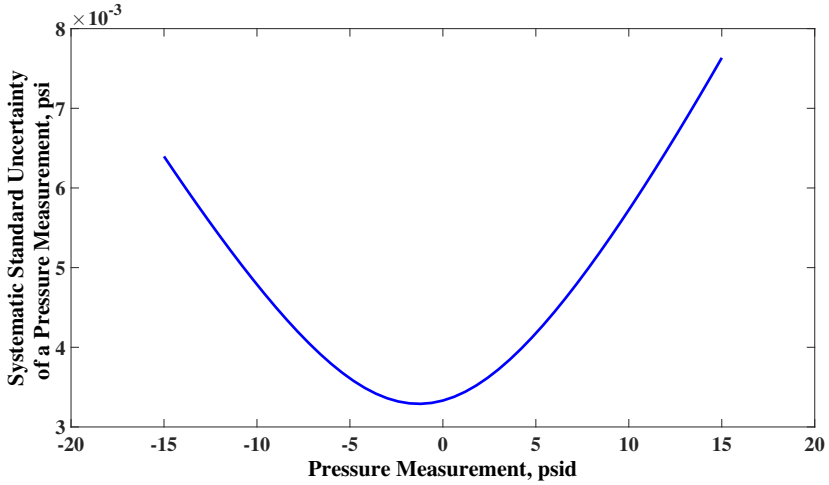

Figure 67: Systematic standard uncertainty of a pressure measurement taken by ±15-psid pressure scanning module.

Although the barometric pressure is not directly shown in any of the calculations for the variables of interest (see Section 3.3), it is present in the data reduction and chain of uncertainty propagation since it is added to the measured differential pressures to produce absolute pressures. The barometric pressure is measured by a high accuracy transducer that is part of the pressure calibration unit for the ESP system. Uncertainty results from MANTUS for P_{bar} as measured by the ESP are shown in Figure 68.

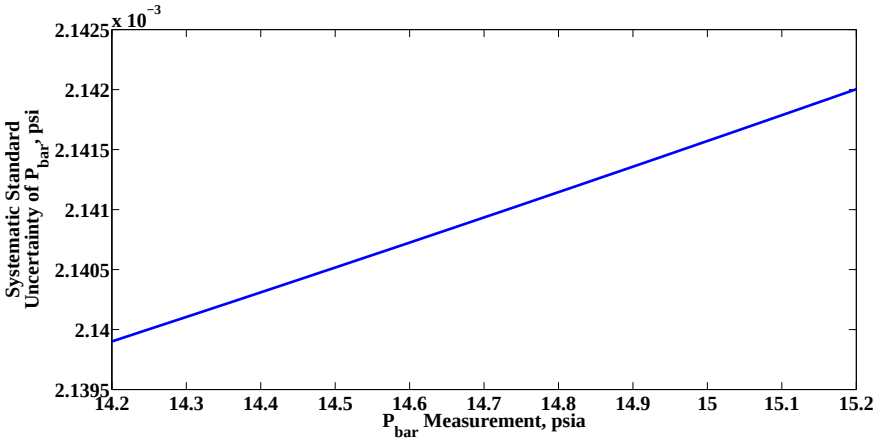

Figure 68: Systematic standard uncertainty of P_{bar} measurement.

Correlated and uncorrelated systematic uncertainties contribute to the temperature measurement errors for both Type E and Type K thermocouples. Figures 69 and 70 show the MANTUS results for Type E thermocouple uncertainties, and results for Type K thermocouples are shown in Figures 71 and 72. The correlated portion of thermocouple uncertainty is a result of the use of a common reference junction, while the uncorrelated portion is mainly due to instrumentation specifications. Details concerning application of correlated and uncorrelated uncertainties are discussed in detail in Section 6.2.

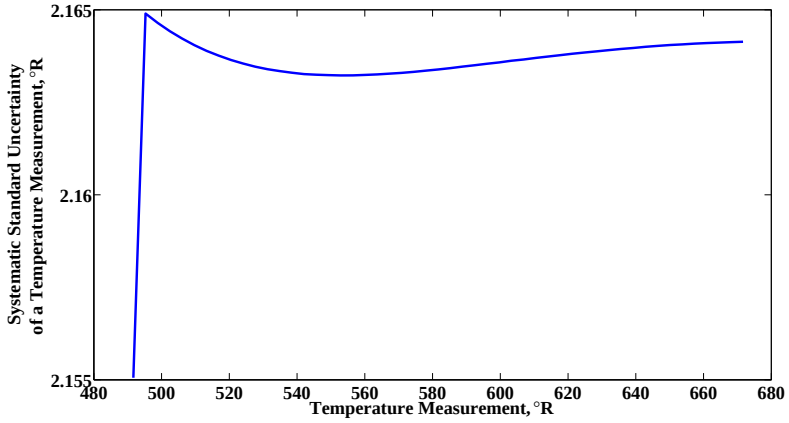

Figure 69: Systematic standard uncertainty of a temperature measurement from a Type E thermocouple.

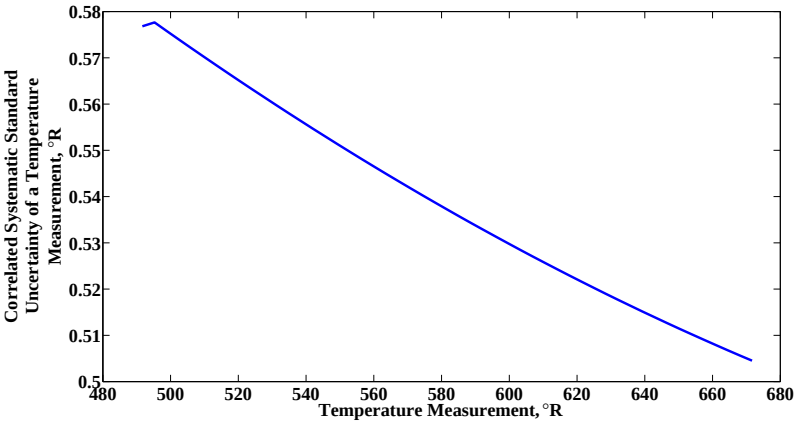

Figure 70: Correlated systematic standard uncertainty of a temperature measurement from a Type E thermocouple.

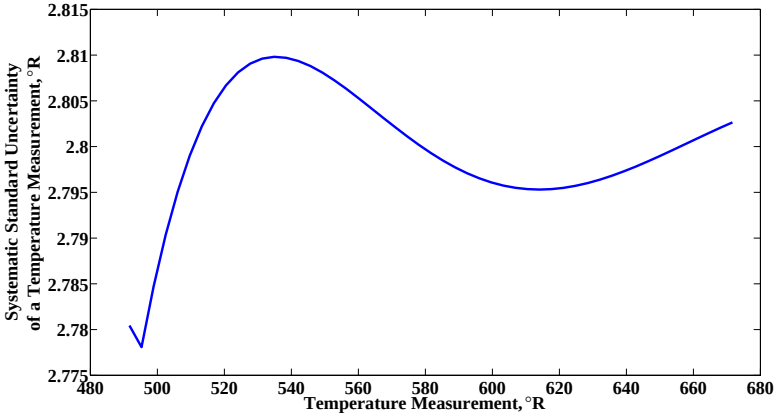

Figure 71: Systematic standard uncertainty of a temperature measurement from a Type K thermocouple.

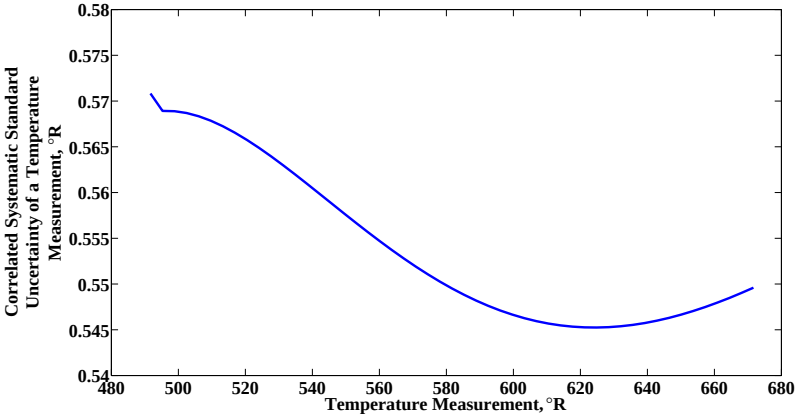

Figure 72: Correlated systematic standard uncertainty of a temperature measurement from a Type K thermocouple.

6.1.2 Uncertainty due to Calibrations of Free Stream Quantities

Any time a calibration is performed, the errors that were present at the time of the calibration test are "fossilized" into the calibration curve. All uncertainties contributing to the calibration form a combined systematic uncertainty and apply to any value calculated by the calibration curve, as depicted in Figure 14. Therefore, the calibration tests for this facility to determine average free stream conditions each require an uncertainty propagation to determine their contributions to live uncertainty.

For each calibration test, contributing uncertainties considered include systematic uncertainties in all instrumentation (facility and calibration hardware), random uncertainties in all measured variables (facility and calibration measurements), systematic uncertainty due to the calibration test (including regression model), and systematic uncertainty due to spatial non-uniformity. A visual example of how these uncertainties apply to calibration measurements is shown for the static pressure calibration in Figure 13.

Measurements used in the calibrations include facility measurements ($P_{T,bm}$, $P_{S,bal}$, P_{bar}, and $T_{T,bm}$) and test section measurements (cone-cylinder: $P_{S,cyl}$, transonic array: $P_{T,arr}$, $P_{T,2,arr}$, $T_{T,arr}$). The instrumentation level uncertainties for all measurements are estimated using MANTUS, and are shown above in Figures 67-72. Random uncertainty estimates are discussed in the following sections.

6.1.3 Random Uncertainty in Test Section Calibration Measurements

Each measurement has a random uncertainty due to the inability to obtain the exact same measurement twice. This can be a result of effects such as noise, dynamic behavior, or unidentified systematic uncertainties that present as random uncertainties. Generally, the random uncertainty of a measured variable can be estimated using the mean and standard deviation of a sample population of measurements at a given tunnel condition. The mean of a sample population is determined by

$$\bar{X} = \frac{1}{N}\sum_{i=1}^{N} X_i, \tag{21}$$

where N is the number of individual measurements i of variable X. The population standard deviation is determined by

$$s_X = \sigma_X = \sqrt{\frac{1}{N-1}\sum_{i=1}^{N}(X_i - \bar{X})^2}. \tag{22}$$

In an ideal world, enough data is available to use Equation 22 to obtain a valid uncertainty estimate for a given variable's data set for each nominal tunnel set point (about ten data points per configuration according to [8]). In some tunnels, where statistical process control is implemented or where calibrations are regularly performed, this may be a good option. Unfortunately, a plethora of repeat data is not a luxury many wind tunnel data analysts enjoy. Understandably, data sets are often small due to high costs of running facilities, leaving few repeat readings available for analysis. The data set for this analysis is limited to data collected during the calibration in 1997 [5]. The calibration test matrix consisted of

only one or occasionally two Mach range sweeps for any given hardware setup, providing very limited repeat data points at any given tunnel set condition. While two to three back-to-back, time-averaged data points are available for each Mach range sweep, these are averaged and considered a single reading to assure the time scale is representative of factors that have significant influence on random uncertainty in the data. [8]

When an insufficient number of distinct repeat data points are available to use Equation 22, the standard deviation can be estimated by converting the range of the available data from a biased to an unbiased estimator of the standard deviation [13]:

$$s_X = \sigma_X \approx \frac{X_{max} - X_{min}}{d_2(n)}, \tag{23}$$

where X_{max} is the maximum value in the sample, X_{min} is the minimum value, and d_2 can be derived as a function of n, the number of readings in the sample, assuming a normal probability distribution. Values of d_2 for small sample sizes are provided in Table 28.

n	2	3	4	5	6	7	8	9
$d_2(n)$	1.128	1.639	2.059	2.326	2.534	2.704	2.847	2.970

Table 28: Values for statistical estimation factor $d_2(n)$ for n samples

During calibration, the transonic array obtained two distinct repeated data samples for approximately half of the tunnel's set points distributed across the Mach range at different times during the test. When Equation 23 is applied to static and total pressure measurements from the array, the results shown in Figure 73 are obtained. The two results show very similar behavior, likely indicating a random correlation between these variables, particularly in the subsonic range where peaks and valleys of the "random" behavior suspiciously match. The presence of these correlations inflates the uncertainty estimates of these variables. The correlation effect is believed to be a product of setting the tunnel condition to pressure ratio Φ. This naturally (and intentionally!) affects the relationship between static and total pressure within the test section. Total and static pressure may vary upward and downward together, perhaps following changes in barometric pressure, even as Φ remains constant.

To remove the effects of this correlation, random uncertainty in array total and static pressure is estimated by calculating an "expected" test section pressure based on facility measurements and calibration curves for $P_{S,ts}$, $P_{T,ts}$, and $P_{T,2,ts}$ for each of the two available data points. The differences between the measured and expected test section values (the residuals) are evaluated at each tunnel set point. When the d_2 factor is applied to those results, modified estimates of random standard uncertainty for $P_{T,arr}$, $P_{T,2,arr}$, and $P_{S,arr}$ are obtained. These are shown in Figure 74.

The same method described for estimating random uncertainty in static and total array pressure is used to estimate random uncertainty in array total temperature, the results of which are shown in Figure 75. Examining the difference between the expected (calibrated) and measured values assures that variations due to lack of temperature control in the facility does not influence the random uncertainty estimate for $T_{T,arr}$.

Only one sweep through the Mach range was performed with the cone-cylinder in place for each tunnel configuration during the static pressure calibration test. Therefore, no repeat

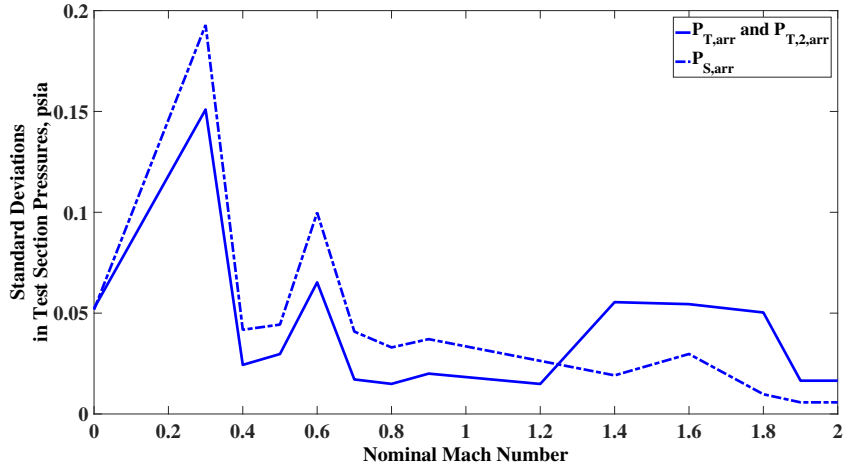

Figure 73: Standard deviations of transonic array pressures, configuration 1

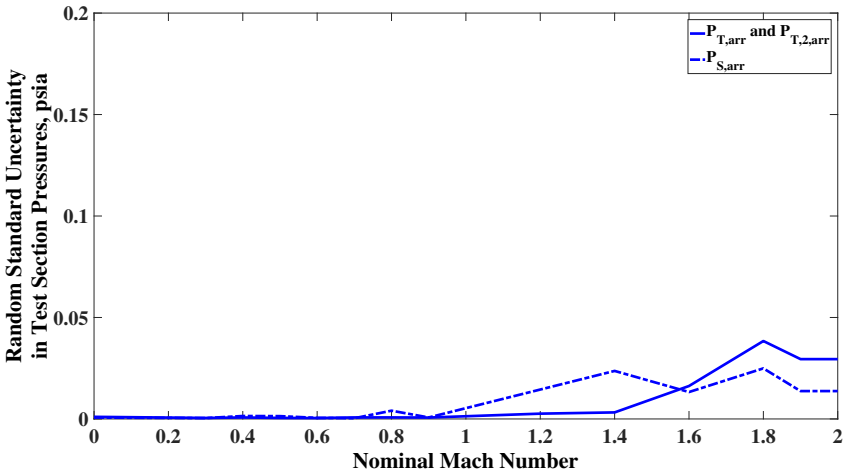

Figure 74: Random standard uncertainty in $P_{T,arr}$, $P_{T,2,arr}$, and $P_{S,arr}$ for configuration 1, with random correlation effect removed

data points were acquired for cylinder static pressure $P_{S,cyl}$. Since static pressure data was acquired by the transonic array with similar pressure probes in similar locations and tunnel conditions, an engineering judgment was made to estimate the random uncertainty in static pressure measured by the cylinder using the available array data, $P_{S,arr}$. If more repeat data is obtained with the cylinder in future tests, the random uncertainty should be estimated using cylinder data.

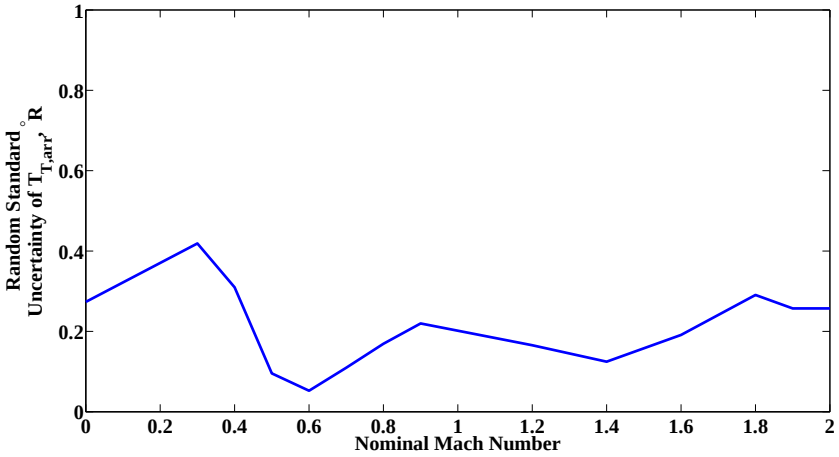

Figure 75: Random standard uncertainty in $T_{T,arr}$ for configuration 1, modified result

6.1.4 Random Uncertainty in Facility Measured Values

Facility measurements in the data reduction chain for variables of interest in the 8- by 6-foot SWT consist of $P_{T,bm}$, $P_{S,bal}$, P_{bar}, and $T_{T,bm}$, as shown in the data reduction charts (Figures 8 and 9). Random uncertainty in P_{bar} is assumed to be negligible for this analysis.

Examining the random uncertainty of $T_{T,bm}$ using Equation 22 results in Figure 76. As an uncertainty estimate, this appears quite high. This variability is indicative not of measurement uncertainty, but rather the general variability of an uncontrolled but measured tunnel condition (temperature) in this facility. For this reason, the result is an inadequate estimate of random uncertainty for $T_{T,bm}$ and another estimate of the random uncertainty in $T_{T,bm}$ must be used.

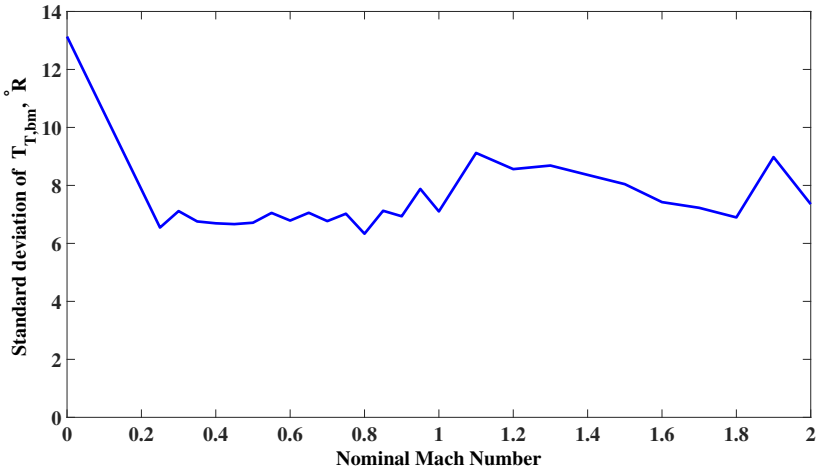

Figure 76: Standard deviation of $T_{T,bm}$, $^{\circ}R$, configuration 1.

Without a suitable way to examine how changes in atmospheric conditions may correlate with measurements in the parameter $T_{T,bm}$, without a reference temperature, and with

no other obvious correlations present, this data set is not conducive to making a random uncertainty estimate for $T_{T,bm}$ based on the direct measurements. Alternatively, based on engineering judgment, the random standard uncertainty estimate for $T_{T,arr}$ is used as an estimate for $T_{T,bm}$. The estimate shown in Figure 77 is likely conservative for $T_{T,bm}$ considering that the test section presumably has slightly more variability due to increased dynamic conditions after convergence at the bellmouth.

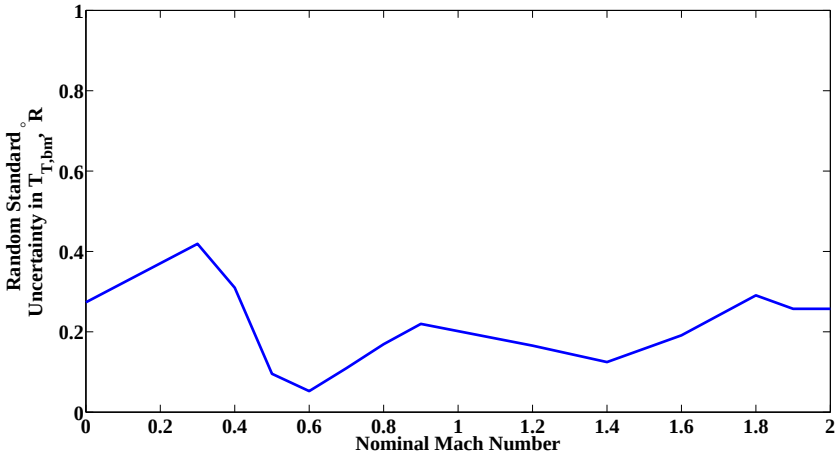

Figure 77: Random standard uncertainty of $T_{T,bm}$ in $^\circ R$ for configuration 1.

As described in Section 3, the operating condition of the facility is determined in part by setting Φ, the ratio of $P_{S,bal}$ to $P_{T,bm}$. As a result, for a given nominal Mach number setting, the two measurements can vary widely even when the same ratio is obtained. This allows values of $P_{T,bm}$ and $P_{S,bal}$ to vary significantly, creating a random correlation effect between the variables. This presents in the analysis as seemingly high uncertainty estimates when straight standard deviations are taken using Equation 23, as shown in Figure 78.

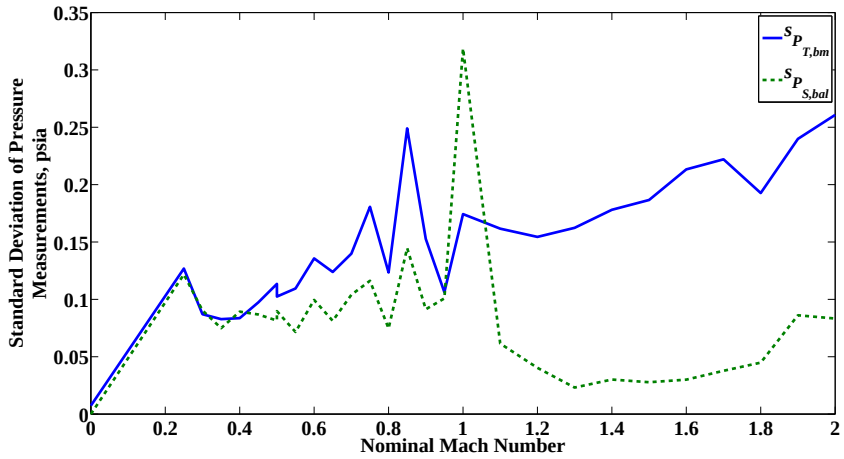

Figure 78: Standard deviations of $P_{T,bm}$ and $P_{S,bal}$ for configuration 1.

Along with being unrealistically high, these uncertainties appear to trend together, veri-

fying the suspected presence of a random correlation between the parameters. As with the correlation between $P_{S,ts}$ and $P_{T,ts}$ described in Section 6.1.3, random correlation between $P_{S,bal}$ and $P_{T,bm}$ is accounted for by finding the difference between an "expected" or "nominal" value and the measured value. To determine the "expected" value, a linear curve-fit is created of the two variables using all available data at a certain tunnel set point and configuration. The standard deviation is estimated from those residuals of the difference between this expected value and the value measured for each variable. An example result using this technique to determine the standard deviation of $P_{S,bal}$ at Mach 0.8 and configuration 1 is shown in Figure 79. It is notable that since facility parameters are not dependent on test section hardware setup, there is more data available for facility measurements than there were for test section measurements.

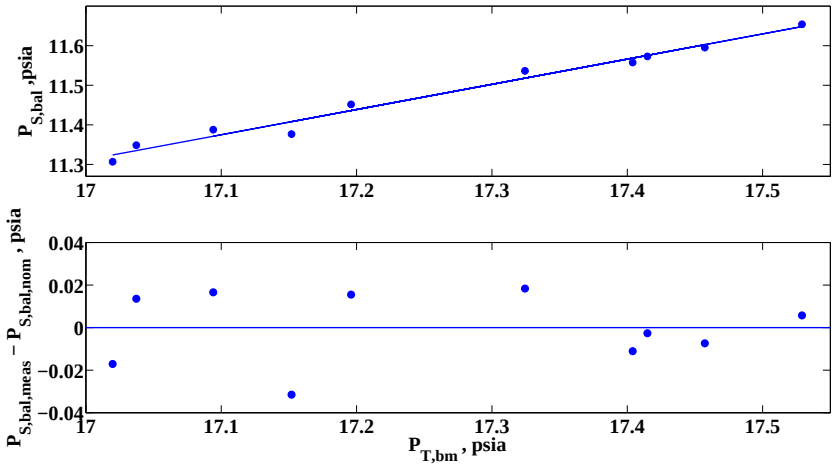

Figure 79: The relationship between $P_{S,bal}$ and $P_{T,bm}$ for configuration 1 at nominal Mach 0.8 tunnel setting. (top) Scatter represents $P_{S,bal}$ vs. $P_{T,bm}$, line represents linear curve-fit and a determined $P_{S,bal,nom}$; (bottom) $P_{S,bal}$ residuals

The resulting random standard uncertainty estimates of $P_{S,bal}$ and $P_{T,bm}$ as a function of nominal Mach number are shown in Figure 80. Despite attempts to account for the correlation due to the ratio Φ described above, there still appears to be a random correlation present in these estimates. Preliminary analysis showed these parameters as driving the overall uncertainty in values of interest, so the correlations need to be addressed for an accurate understanding of the facility uncertainties.

The remaining random correlation effects between $P_{T,bm}$ and $P_{S,bal}$ are likely a result of tunnel operation. Small variations in the primary tunnel set point parameter, Φ, occur when operators attempt to achieve the same tunnel set points repeatedly. While this means that tunnel conditions may not be identical for repeat points, this does not mean conditions are assumed by facility personnel or customers to be the same; Φ is present in data reduction chains leading to $P_{T,ts}$, $P_{S,ts}$ and ultimately Mach number and other free stream quantities. Therefore, while the same precise tunnel condition may not be achieved for repeat measurements, the precise conditions are still known to within measurement uncertainty bounds for each point.

While in this case study it falls outside the scope of true measurement uncertainty,

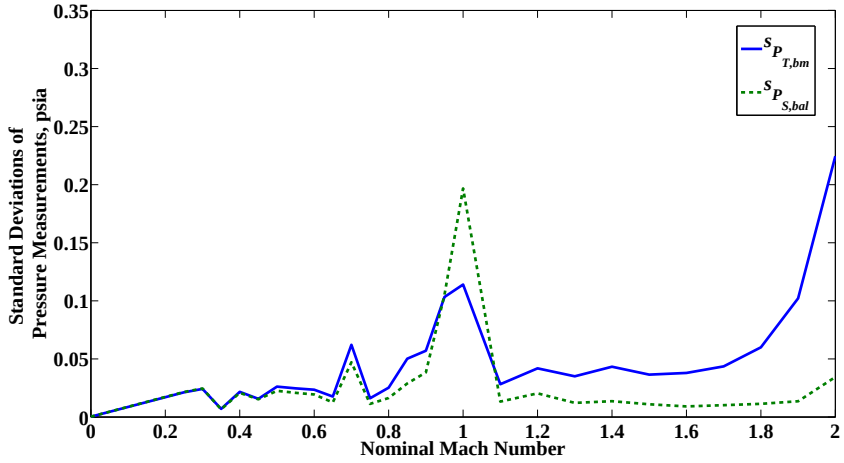

Figure 80: Standard deviations of $P_{T,bm}$ and $P_{S,bal}$, using residuals technique to remove random correlation effect

customers or facility personnel may still be concerned with the ability of the operators to achieve a very specific tunnel condition repeatedly. Further testing could be performed to analyze this capability more closely; with the available data from the calibration tests, the standard deviation of Φ was determined for all nominal tunnel set points and is shown for reference in Figure 81. This uncertainty could easily be propagated as a "set point uncertainty" and its effect on variables of interest could be quantified.

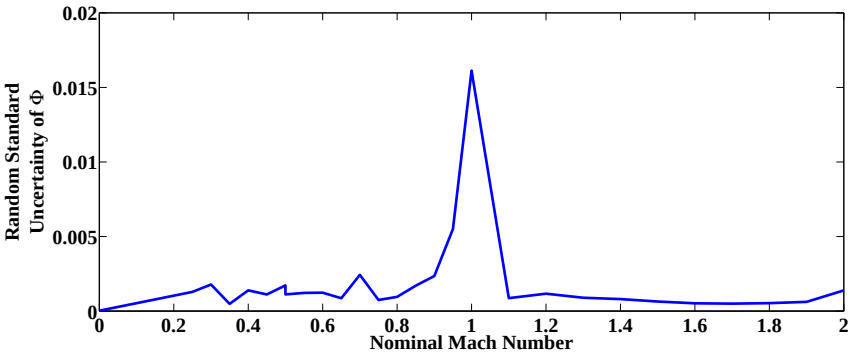

Figure 81: Random standard uncertainty of Φ for configuration 1

Without a way to further refine random uncertainty estimates for $P_{T,bm}$ and $P_{S,bal}$, an engineering judgment was made to use static pressure random standard uncertainty estimates from the array ($s_{P_{S,arr}}$) to estimate random uncertainty of static pressure in the balance chamber ($s_{P_{S,bal}}$). Likewise, total pressure estimates from the array ($s_{P_{T,arr}}$ and $s_{P_{T,2,arr}}$) are used to estimate random uncertainty of total pressure in the bellmouth ($s_{P_{T,bm}}$). As explained previously for $T_{T,bm}$, these estimates are considered conservative since the test section environment where array pressures were measured are presumably more dynamic than the bellmouth and balance chamber probe locations. Final random standard uncertainty estimates for these parameters are shown in Figure 82. These results are used for all

calibration simulations, as well as the test-time simulation.

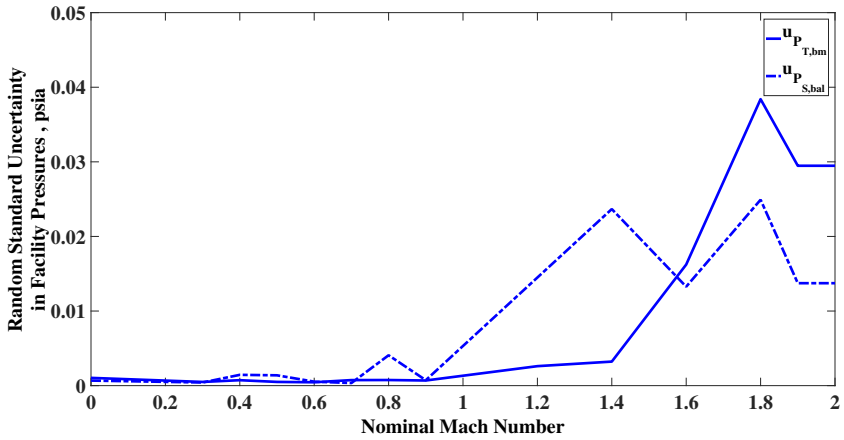

Figure 82: Random standard uncertainty of facility pressures for configuration 1

6.1.5 Spatial Uniformity Uncertainty

During calibration, typically several measurements are taken at different locations within the test section in order to assure a mean value representative of the entire test section is acquired. Spatial non-uniformity characteristics of the facility can become apparent with measurements taken at these different locations. These spatial variations are generally considered systematic facility characteristics, and are not expected to change appreciably for the same tunnel set points unless significant facility modifications are made.

Many practitioners argue that spatial non-uniformity should not contribute to uncertainty in parameters, but should be considered a factor only as it pertains to flow quality. However, unless a flow is perfectly characterized (i.e., measurements are obtained at an infinite number of points in space in the wind tunnel), there is an aspect of uncertainty of the flow that is a factor in uncertainty analysis. For example, if the mean value of total temperature in the test section is to be represented by taking an average of 7 measurements across the test section, as it is for this facility, would a better estimate be obtained by averaging 15 measurements instead of 7? Conversely, would a worse estimate of the mean value be obtained by averaging only 2 measurements? If there is a temperature profile in the flow, is taking an average sufficient, or should a weighted average be considered so a bias is not introduced? These are all questions that relate to spatial issues and can impact the uncertainty of a variable of interest.

Ultimately, uncertainty introduced due to spatial non-uniformity is often ignored in uncertainty analysis because it is somewhat difficult to define and quantify. If a facility has undergone any sort of flow quality characterization, it is possible to attempt to quantify this effect and determine the impact an imperfect flow field has on facility calculations. For this analysis, spatial uniformity uncertainty is defined by the variation in measurements across test section space (cross-section or volume, if available). Application of spatial uniformity uncertainty is limited in this case to its effect on the calibrations, since in Section 5 the uncertainty results are defined at the calibration point, not at any point in space within the

test section. Test-time variations in spatial uniformity are dependent on the model, and are impossible to account for within this analysis.

Uncertainty due to spatial uniformity is initially examined by taking the standard deviation of the measurements across all ports used for the representative average test section measurement during calibration. For the static pressure calibration, this consists of 56 measurements along the aft portion of the cone-cylinder. Variations are found to be very high along the cylinder in the transonic and supersonic regimes, presumably due to the propagation of shocks axially through the test section at these tunnel speeds (see Figure 83). Because these variations are likely induced by the test hardware itself, measurements made by the transonic array are alternatively considered for static pressure uniformity analysis. Array measurements from data obtained at five rake heights in the cross section of the test section entrance are used. Further analysis to isolate spatial effects, detailed in Appendix J, yields a static pressure spatial uniformity estimate shown in Figure 83. The interpolation shown is performed to eliminate the effect of suspected shock interactions introduced by array probes.

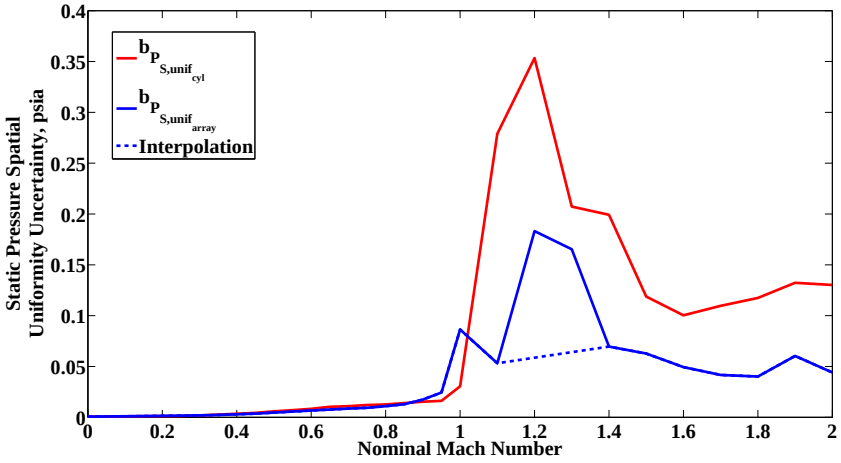

Figure 83: Static pressure spatial uniformity standard uncertainty estimate for configuration 1. The red line indicates the estimate from the cone-cylinder data; the blue line indicates the estimate from the transonic array, with an interpolation performed to reduce shock interactions from calibration instrumentation.

For total pressure and total temperature uniformity, data obtained by the transonic array at five rake heights at the test section entrance is analyzed. Since data was obtained on different days and under different atmospheric conditions (which have a direct impact on temperature and pressure levels in this atmospheric tunnel), a straight standard deviation of these measurements across space is not valid to assess variation of total pressure or total temperature. Attempts to isolate spatial effects of these two variables are detailed in Appendix J. Results for total pressure spatial uniformity are shown in Figure 84.

Generally, when considering uncertainty due to spatial uniformity, it is important to verify that other error sources (instrumentation, random) are not also contributing to the observed results, and that the spatial uniformity errors are isolated. Systematic uncertainty in temperature instrumentation is particular cause for concern, as systematic errors are

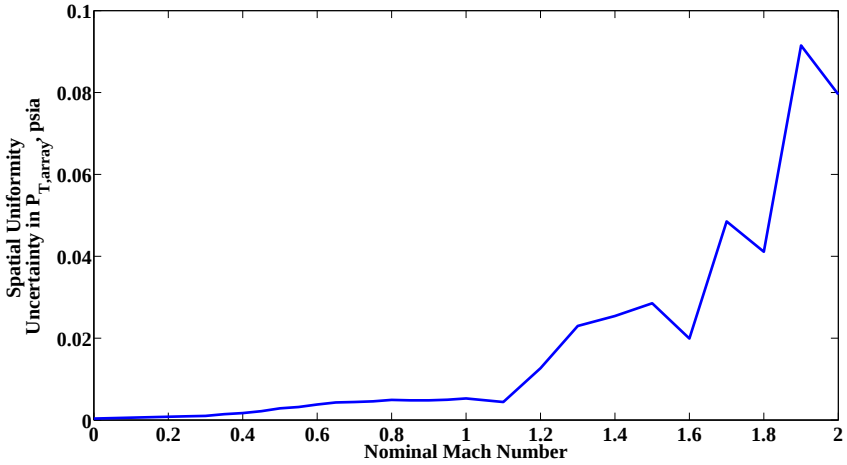

Figure 84: Spatial uniformity standard uncertainty in $P_{T,arr}$ for configuration 1

large and can create offsets in probe measurements, requiring some additional uncertainty accounting. The random uncertainty contribution (Figure 75) to temperature measurements is likely negligible, but will be considered for completeness.

A small Monte Carlo side-analysis is performed to find the contributions of random and uncorrelated systematic uncertainty to the thermocouple probes and subsequent calculation of uniformity, so that a true spatial uniformity uncertainty can be isolated. Note that the correlated portion of uncertainty is not considered, since it would effect all probes equally and thus there would be no impact to the standard deviation calculation. Uncertainty contributions to the spatial uniformity calculation from uncorrelated systematic uncertainty (notated $b_{T_{T,arr,unif_{inst}}}$) and from random uncertainty ($s_{T_{T,arr,unif_{ran}}}$) as deduced from the side-analysis subtract as root-sum-squares from the observed uniformity ($b_{T_{T,arr,unif_{obs}}}$), and are accounted for by

$$b_{T_{T,arr,unif_{true}}} = \sqrt{b^2_{T_{T,arr,unif_{obs}}} - b^2_{T_{T,arr,unif_{inst}}} - s^2_{T_{T,arr,unif_{ran}}}} \tag{24}$$

where $b_{T_{T,arr,unif_{true}}}$ is the isolated systematic uncertainty in array total temperature due to spatial uniformity. Equation 24 simply assumes that the uniformity, instrumentation and random errors are independent, and therefore combine as root-sum-squares. Spatial uniformity of the total temperature after accounting for this can be seen in Figure 85 for configuration 1.

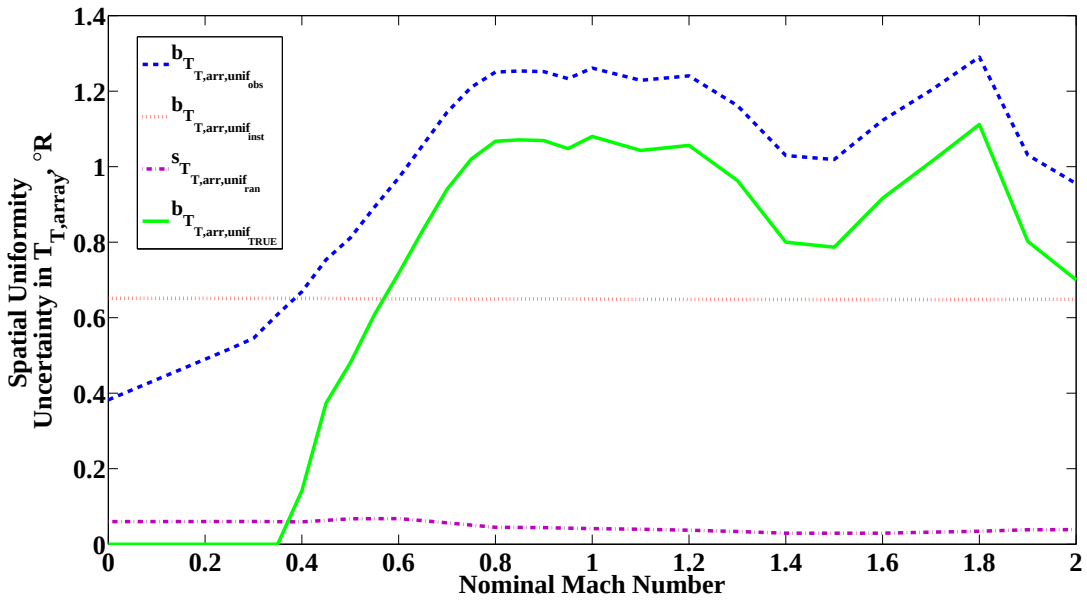

Figure 85: Removing instrumentation and random uncertainty from observed spatial uniformity uncertainty. The dashed blue line represents the observed spatial uniformity uncertainty. The red dotted line represents the uncorrelated instrumentation uncertainty contribution to the spatial uniformity calculation. The purple dash-dot line represents the random uncertainty contribution to the spatial uniformity calculation. The green line is the uncertainty due to spatial uniformity with the instrumentation and random uncertainty effects removed.

6.1.6 Regression Uncertainty

The procedure used for the facility calibration is described in Section 3.2. The calibration curves for $P_{S,ts}$, $P_{T,ts}$, $P_{T,2,ts}$ and T_{ts} (defined by Equations 2 - 4) are math models established to define the test section behavior using data from the calibration test. Each calibration curve has an associated regression uncertainty that is introduced with the math model.

The basis of regression uncertainty is the understanding that math models are not perfect representations of the data used to create them. Regression uncertainty can be thought of as how well the math model fits the data points; the more closely the data fits the chosen model, the lower the regression uncertainty, and vice versa. Therefore, whenever a curve-fit is used to predict a value, there is an associated uncertainty interval bounding the curve that should contain the "true" value of y_i. These bounds can be quantified by the standard error of estimate, s_{yx}, and is determined by

$$s_{yx} = \sqrt{\frac{\sum_{i=1}^{k} (y_i - \hat{y}_i)^2}{v_{s_{yx}}}}, \tag{25}$$

where k is the number of (x_i, y_i) data pairs used to create the curve-fit, v represents the degrees of freedom in s_{yx} (for polynomials of fit order m, $v_{s_{yx}} = k - (m+1)$), and $\hat{y}_i$ is the predicted value at x_i [4]. Since s_{yx} is essentially the standard deviation of the y_i values from the curve-fit [8], the standard uncertainty, s_{reg}, that should be applied to a value predicted from the regression is

$$s_{reg} = s_{yx}. \tag{26}$$

This methodology is applied to quantify regression uncertainty for all four calibration curves in this analysis. Regression uncertainty is applied as stated above whenever a calibration curve is used to calculate a predicted value in the data reduction sequence, based on the determined s_{reg} for each curve.

The standard error of forecast, s_f, is used in some situations to quantify uncertainty that is applied to a regression. On top of the standard uncertainty calculated by s_{yx}, s_f additionally accounts for the dispersion in x_i values present in the calibration data sample. In other words, it can account for high or low areas of data density in x_i collected during calibration; uncertainty in y may be higher in areas of low data density and vice versa. A prediction interval about the curve-fit for a future determination of y as a function of x_0 for a polynomial curve-fit is computed by [14]

$$s_f = s_{yx}\sqrt{1 + x'(X'X)^{-1}x} \tag{27}$$

where s_{yx} is determined from Equation 25, X is determined by

$$X = \begin{bmatrix} 1 & x_1 & x_1^2 & \dots & x_1^k \\ 1 & x_2 & x_2^2 & \dots & x_2^k \\ \vdots & \vdots & \vdots & \ddots & \vdots \\ 1 & x_k & x_k^2 & \dots & x_k^m \end{bmatrix},$$

using x_i values from the total number of calibration data points k, m is the order of fit, and x is determined by

$$x = \begin{bmatrix} 1 \\ x_0 \\ x_0^2 \\ \vdots \\ x_0^m \end{bmatrix}.$$

X' and x' are the transpose of X and x, respectively, and x_0 is the independent variable of interest.

Assumptions of Equation 27 are that no random uncertainty is present in x_i or x_0, random uncertainty in y_i is constant across the calibrated range, and the distribution of y_i data about the curve-fit is purely an artifact of random uncertainty with no uncertainty contribution from the selected math model. If the latter assumption held true, the expectation would be that several repeat data points obtained would show y_i data distributed normally about the calibration curve. The standard error of forecast accounts for the fact that the regression was generated from a select data set, and that if different sets of data were collected (with random errors in y_i present in each), different regression curves would be formed [4].

The assumptions for Equation 27 are almost always violated in actual tests, and this calibration test is no exception. For all four facility calibration curves, random uncertainty *is* present in x, random uncertainty in y is *not* constant across the calibrated range, and according to facility personnel, it is believed that offsets from the curve-fits are primarily

due to math model errors, *not* random uncertainty (repeat readings would be expected to be clustered around the collected (x_i, y_i) data points, not spread about the calibration curves). These violations make it undesirable to use Equation 27 to determine regression uncertainty in this context; doing so would inflate the calculated uncertainty. Additionally, the impact of data density in x on uncertainty in y is inherently accounted for within the Monte Carlo error propagation when appropriate standard uncertainty estimates are applied to x_i and y_i (or to the measured parameters used to calculate these variables).

It should also be noted that the standard error of forecast and standard error of estimate are often quite similar if data is well dispersed across the calibrated range and a large number of data points are included in the regression. In such an instance, if the Monte Carlo method is not being used and the aforementioned assumptions can be made to calculate s_f, it may be simpler to use s_{yx} to approximate the regression standard uncertainty estimate.

6.2 Monte Carlo Simulation

For this uncertainty analysis, an offline data reduction program replicates the actual data reduction script run within the ESCORT data acquisition system. MATLAB is used because of its specialty in performing array calculations, which works well for a Monte Carlo simulation where thousands of iterations are often desired.

After estimating all considered random and systematic uncertainties of all measured values (discussed in Sections 6.1 and 6.1.6), a Monte Carlo simulation is used to propagate those uncertainties through the data reduction to calculate the estimated uncertainty of the calculated values of interest. An overview of this method of uncertainty propagation can be found in Section 4.3 with further details provided by Coleman and Steele [8].

The simulation begins by randomly generating numbers along an appropriate probability distribution and scaling them by the random and systematic uncertainties of each variable. These populations of errors are applied to the measurements in an appropriate manner (discussed below) across all readings, ports, and i synthetic iterations of the test. This analysis uses $i = 10,000$ for the calibrations and "test-time" simulations calculating final uncertainties in all variables of interest.

Once errors are applied to all measured values for each iteration (or synthetic realization) of the test, the variables of interest are calculated using the synthetic data (e.g. Mach and Reynolds number). This results in i calculations of any variable of interest. The standard deviation provides the desired overall uncertainty of the variable of interest. This process is depicted in Figure 86 as it applies to the subsonic total pressure calibration.

When possible, it is preferable to construct a Monte Carlo simulation program that follows an actual test as closely as possible. This approach usually makes it easier to follow the flow of data and introduce elemental errors in the appropriate places. To that end, Monte Carlo simulations are run for each of the calibration tests (static pressure, total pressure, and total temperature). The results of each of these simulations provide the fossilized systematic uncertainties to be applied in the subsequent simulation of a customer test, where all variables of interest and their uncertainties are calculated. Finally, a coverage factor is applied to calculate the expanded uncertainties as presented in Section 5.

The code is written in such a way that elemental uncertainties can be flagged on or off. The flags allow one elemental uncertainty to be propagated at a time so that the effect of

that particular uncertainty on the total uncertainty of a variable can be calculated. These individual contributions sum as root sum squares to the total uncertainty of a variable (which is confirmed by performing the analysis with all uncertainties flagged on). Using these results, the percent contribution of each elemental uncertainty (or group of uncertainties, such as all instrumentation) to the overall uncertainty of the value of interest is observed (see Equation 20 and Section 4.2).

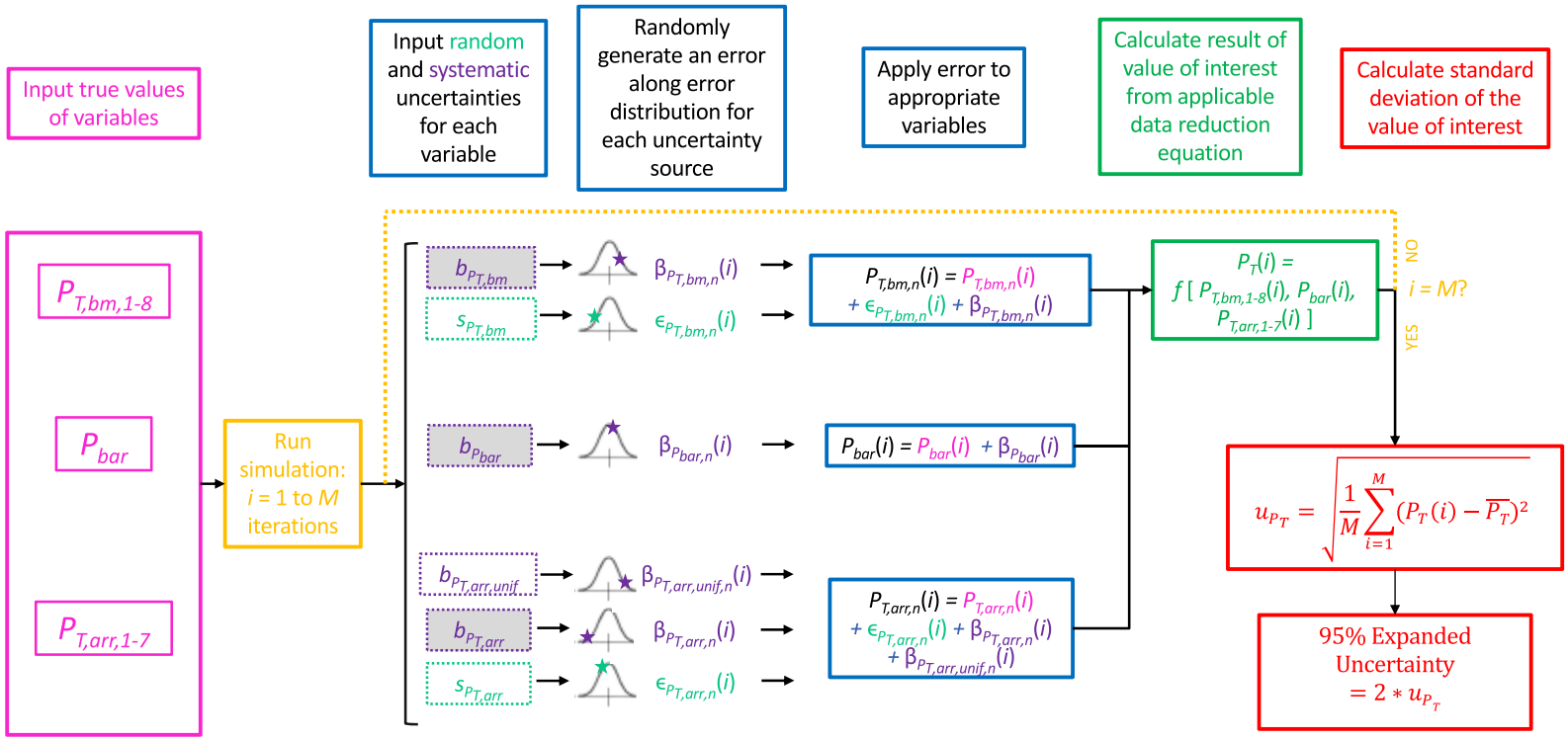

Figure 86: Overview of Monte Carlo Simulation for Uncertainty Analysis: Depicts analysis of total pressure calibration in subsonic range. Based on the method described by Coleman and Steel [8] page 72, Figure 3.4.

6.2.1 Populating Errors due to Random, Systematic, and Correlated Systematic Uncertainty

Error population is a critical component of producing an accurate Monte Carlo test simulation. This can be tricky, as different uncertainty types require different techniques to produce true representations of error populations. Figure 87 shows a general overview of how random number generation is used to populate errors for different uncertainty types. This process is discussed in detail for random, systematic, and correlated systematic error types.

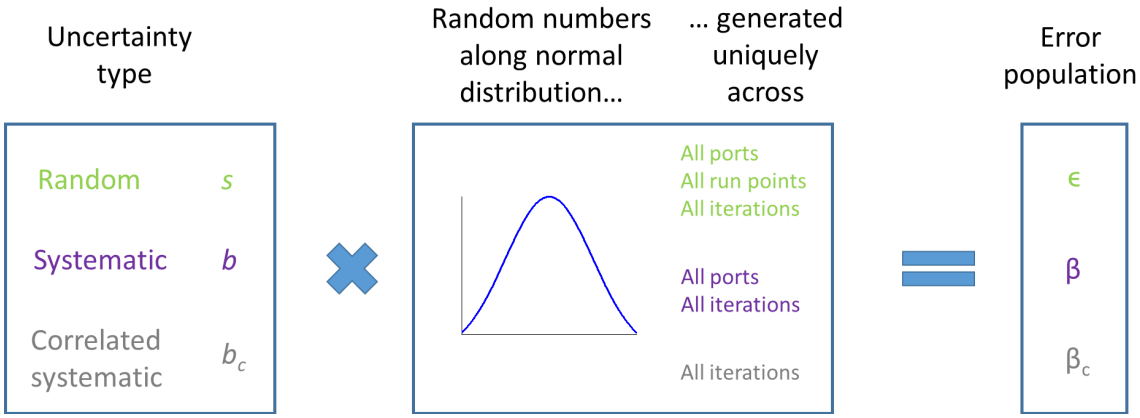

Figure 87: Overview of error population for random, systematic, and correlated systematic uncertainty types

Populating errors due to random uncertainty, ϵ, within the Monte Carlo code is fairly straightforward. By nature the errors are random, so a normal distribution of random numbers with a mean of zero and a variance of one is scaled by the random standard uncertainty of a variable to produce an appropriate population of errors. These errors are then added to the "true" value of the variable that is replicated across the same number of ports, readings and iterations. For example, if errors due to random uncertainty in total pressure array measurements are applied to a test that spans 10 readings, a random number distribution scaled by $s_{P_{T,arr}}$ (Figure 74) across 7 total pressure array ports, 10 readings, and i iterations is constructed to populate these errors (see Table 29).

Populating errors due to systematic uncertainty, β, within the Monte Carlo code is handled differently. Systematic errors (specifically those due to the instrumentation system) are an artifact of the system's calibration, so a single random number scaled by the systematic standard uncertainty is applied to all readings of a given instrument within iteration i for the duration of a calibration cycle. For the same nominal test conditions, this means the errors are identical. For example, if errors due to systematic uncertainty in total temperature bellmouth measurements are applied, a single random number for each thermocouple port is scaled by $b_{T_{T,bm}}$ for all 10 readings within the example calibration cycle (see Table 30). This is shown as it applies to 4 ports for a single iteration. Errors are then added to the true value of the variable $T_{T,bm}$.

			Random Numbers Generated for $P_{T,arr}$						
			Port 1	**Port 2**	**Port 3**	**Port 4**	**Port 5**	**Port 6**	**Port 7**
			0.5377	−1.3499	0.6715	0.8884	−0.1022	−0.8637	−1.0891
			1.8339	3.0349	−1.2075	−1.1471	−0.2414	0.0774	0.0326
			−2.2588	0.7254	0.7172	−1.0689	0.3192	−1.2141	0.5525
			0.8622	−0.0631	1.6302	−0.8095	0.3129	−1.1135	1.1006
			0.3188	0.7147	0.4889	−2.9443	−0.8649	−0.0068	1.5442
			−1.3077	−0.2050	1.0347	1.4384	−0.0301	1.5326	0.0859
			−0.4336	−0.1241	0.7269	0.3252	−0.1649	−0.7697	−1.4916
			0.3426	1.4897	−0.3034	−0.7549	0.6277	0.3714	−0.7423
			3.5784	1.4090	0.2939	1.3703	1.0933	−0.2256	−1.0616
			2.7694	1.4172	−0.7873	−1.7115	1.1093	1.1174	2.3505
			Errors Populated for $P_{T,arr}$, psia						
Rdg	**Nominal Mach**	$s_{P_{T,arr}}$ **psia**	$\epsilon_{P_{T,arr,1}}$	$\epsilon_{P_{T,arr,2}}$	$\epsilon_{P_{T,arr,3}}$	$\epsilon_{P_{T,arr,4}}$	$\epsilon_{P_{T,arr,5}}$	$\epsilon_{P_{T,arr,6}}$	$\epsilon_{P_{T,arr,7}}$
1	1.60	0.0162	0.0087	−0.0219	0.0109	0.0144	−0.0017	−0.0140	−0.0177
2	1.60	0.0162	0.0298	0.0493	−0.0196	−0.0186	−0.0039	0.0013	0.0005
3	1.60	0.0162	−0.0367	0.0118	0.0116	−0.0173	0.0052	−0.0197	0.0090
4	1.60	0.0162	0.0140	−0.0010	0.0265	−0.0131	0.0051	−0.0181	0.0179
5	1.60	0.0162	0.0052	0.0116	0.0079	−0.0478	−0.0140	−0.0001	0.0251
6	1.60	0.0162	−0.0212	−0.0033	0.0168	0.0233	−0.0005	0.0249	0.0014
7	1.60	0.0162	−0.0070	−0.0020	0.0118	0.0053	−0.0027	−0.0125	−0.0242
8	1.60	0.0162	0.0056	0.0242	−0.0049	−0.0123	0.0102	0.0060	−0.0120
9	1.60	0.0162	0.0581	0.0229	0.0048	0.0222	0.0177	−0.0037	−0.0172
10	1.60	0.0162	0.0450	0.023	−0.0128	−0.0278	0.0180	0.0181	0.0382

Table 29: Synthetic error population for random standard uncertainty, as applied to $P_{T,arr}$ measurements for a single Monte Carlo iteration. The errors are different for every port and for every reading.

				Random Numbers Generated for $T_{T,bm}$			
				Port 1	**Port 2**	**Port 3**	**Port 4**
				−0.6156	0.7481	−0.1924	0.8886
				−0.6156	0.7481	−0.1924	0.8886
				−0.6156	0.7481	−0.1924	0.8886
				−0.6156	0.7481	−0.1924	0.8886
				−0.6156	0.7481	−0.1924	0.8886
				−0.6156	0.7481	−0.1924	0.8886
				−0.6156	0.7481	−0.1924	0.8886
				−0.6156	0.7481	−0.1924	0.8886
				−0.6156	0.7481	−0.1924	0.8886
				−0.6156	0.7481	−0.1924	0.8886
				Errors Populated for $T_{T,bm}$, °R			
Rdg	**Nominal Mach**	**Nominal $T_{T,bm}$,°R**	$b_{T_{T,bm}}$ **°R**	$\beta_{T_{T,bm,1}}$	$\beta_{T_{T,bm,2}}$	$\beta_{T_{T,bm,3}}$	$\beta_{T_{T,bm,4}}$
1	0.8	565.1	2.1633	−1.3317	1.6183	−0.4163	1.9223
2	0.8	565.1	2.1633	−1.3317	1.6183	−0.4163	1.9223
3	0.8	565.1	2.1633	−1.3317	1.6183	−0.4163	1.9223
4	0.8	565.1	2.1633	−1.3317	1.6183	−0.4163	1.9223
5	0.8	565.1	2.1633	−1.3317	1.6183	−0.4163	1.9223
6	0.8	565.1	2.1633	−1.3317	1.6183	−0.4163	1.9223
7	0.8	565.1	2.1633	−1.3317	1.6183	−0.4163	1.9223
8	0.8	565.1	2.1633	−1.3317	1.6183	−0.4163	1.9223
9	0.8	565.1	2.1633	−1.3317	1.6183	−0.4163	1.9223
10	0.8	565.1	2.1633	−1.3317	1.6183	−0.4163	1.9223

Table 30: Synthetic error population for systematic standard uncertainty due to instrumentation, as applied to $T_{T,bm}$ measurements for a single Monte Carlo iteration. The error on each port is different, but errors on a specific port are identical through different readings of a test until a new instrument calibration is performed.

Correlated systematic errors are populated in the simulation in a different manner. For this facility, all pressures that share the same Pressure Calibration Unit (PCU) are considered to have correlated systematic errors. Therefore, for any given iteration of the simulation, a single random number scaled by the systematic standard uncertainty applies not only to all readings of a single port, but to all readings of all ports of all correlated measurements within a calibration cycle. For example, since all $P_{T,bm}$ ports are found to be correlated, and errors due to correlated systematic uncertainty in total pressure bellmouth measurements are applied, a single random number is scaled by $b_{P_{corr}}$ as it applies to "true" values of $P_{T,bm}$ for all 10 readings and across all 8 ports (see Table 31). Errors are populated in this manner for each of the i iterations. Furthermore, any pressure measurement obtained that shares the same PCU and is also considered correlated applies the same random number scaled by $b_{P_{corr}}$ as it relates to that variable's "true" value (see Table 32 for how the correlated error also applies to $P_{S,bal}$). Once errors are populated, they are added to the true value of the variable.

				Random Numbers Generated for $P_{T,bm}$							
				Port 1	**Port 2**	**Port 3**	**Port 4**	**Port 5**	**Port 6**	**Port 7**	**Port 8**
				−0.7648	−0.7648	−0.7648	−0.7648	−0.7648	−0.7648	−0.7648	−0.7648
				−0.7648	−0.7648	−0.7648	−0.7648	−0.7648	−0.7648	−0.7648	−0.7648
				−0.7648	−0.7648	−0.7648	−0.7648	−0.7648	−0.7648	−0.7648	−0.7648
				−0.7648	−0.7648	−0.7648	−0.7648	−0.7648	−0.7648	−0.7648	−0.7648
				−0.7648	−0.7648	−0.7648	−0.7648	−0.7648	−0.7648	−0.7648	−0.7648
				−0.7648	−0.7648	−0.7648	−0.7648	−0.7648	−0.7648	−0.7648	−0.7648
				−0.7648	−0.7648	−0.7648	−0.7648	−0.7648	−0.7648	−0.7648	−0.7648
				−0.7648	−0.7648	−0.7648	−0.7648	−0.7648	−0.7648	−0.7648	−0.7648
				−0.7648	−0.7648	−0.7648	−0.7648	−0.7648	−0.7648	−0.7648	−0.7648
				−0.7648	−0.7648	−0.7648	−0.7648	−0.7648	−0.7648	−0.7648	−0.7648
				Errors Populated for $P_{T,bm}$, psia							
Rdg	**Nominal Mach**	**Nominal $P_{T,bm}$, psid**	$b_{P,corr}$ **psia**	$\beta_{P_{T,bm,1}}$	$\beta_{P_{T,bm,2}}$	$\beta_{P_{T,bm,3}}$	$\beta_{P_{T,bm,4}}$	$\beta_{P_{T,bm,5}}$	$\beta_{P_{T,bm,6}}$	$\beta_{P_{T,bm,7}}$	$\beta_{P_{T,bm,8}}$
1	1.6	5.888	0.0044	−0.0034	−0.0034	−0.0034	−0.0034	−0.0034	−0.0034	−0.0034	−0.0034
2	1.6	5.888	0.0044	−0.0034	−0.0034	−0.0034	−0.0034	−0.0034	−0.0034	−0.0034	−0.0034
3	1.6	5.888	0.0044	−0.0034	−0.0034	−0.0034	−0.0034	−0.0034	−0.0034	−0.0034	−0.0034
4	1.6	5.888	0.0044	−0.0034	−0.0034	−0.0034	−0.0034	−0.0034	−0.0034	−0.0034	−0.0034
5	1.6	5.888	0.0044	−0.0034	−0.0034	−0.0034	−0.0034	−0.0034	−0.0034	−0.0034	−0.0034
6	1.6	5.888	0.0044	−0.0034	−0.0034	−0.0034	−0.0034	−0.0034	−0.0034	−0.0034	−0.0034
7	1.6	5.888	0.0044	−0.0034	−0.0034	−0.0034	−0.0034	−0.0034	−0.0034	−0.0034	−0.0034
8	1.6	5.888	0.0044	−0.0034	−0.0034	−0.0034	−0.0034	−0.0034	−0.0034	−0.0034	−0.0034
9	1.6	5.888	0.0044	−0.0034	−0.0034	−0.0034	−0.0034	−0.0034	−0.0034	−0.0034	−0.0034
10	1.6	5.888	0.0044	−0.0034	−0.0034	−0.0034	−0.0034	−0.0034	−0.0034	−0.0034	−0.0034

Table 31: Synthetic error population for correlated systematic standard uncertainty, as applied to $P_{T,bm}$ measurements for the same Monte Carlo iteration as Table 32. The errors on all ports are identical.

Random Numbers Generated for $P_{S,bal}$			
Port 1	**Port 2**	**Port 3**	**Port 4**
−0.7648	−0.7648	−0.7648	−0.7648
−0.7648	−0.7648	−0.7648	−0.7648
−0.7648	−0.7648	−0.7648	−0.7648
−0.7648	−0.7648	−0.7648	−0.7648
−0.7648	−0.7648	−0.7648	−0.7648
−0.7648	−0.7648	−0.7648	−0.7648
−0.7648	−0.7648	−0.7648	−0.7648
−0.7648	−0.7648	−0.7648	−0.7648
−0.7648	−0.7648	−0.7648	−0.7648
−0.7648	−0.7648	−0.7648	−0.7648

				Errors Populated for $P_{S,bal}$, psia			
Rdg	**Nominal Mach**	**Nominal $P_{S,bal}$, psid**	$b_{P,corr}$ **psia**	$\beta_{P_{S,bal,1}}$	$\beta_{P_{S,bal,2}}$	$\beta_{P_{S,bal,3}}$	$\beta_{P_{S,bal,4}}$
1	1.6	-9.048	0.0045	−0.0035	−0.0035	−0.0035	−0.0035
2	1.6	-9.048	0.0045	−0.0035	−0.0035	−0.0035	−0.0035
3	1.6	-9.048	0.0045	−0.0035	−0.0035	−0.0035	−0.0035
4	1.6	-9.048	0.0045	−0.0035	−0.0035	−0.0035	−0.0035
5	1.6	-9.048	0.0045	−0.0035	−0.0035	−0.0035	−0.0035
6	1.6	-9.048	0.0045	−0.0035	−0.0035	−0.0035	−0.0035
7	1.6	-9.048	0.0045	−0.0035	−0.0035	−0.0035	−0.0035
8	1.6	-9.048	0.0045	−0.0035	−0.0035	−0.0035	−0.0035
9	1.6	-9.048	0.0045	−0.0035	−0.0035	−0.0035	−0.0035
10	1.6	-9.048	0.0045	−0.0035	−0.0035	−0.0035	−0.0035

Table 32: Synthetic error population for correlated systematic standard uncertainty, as applied to $P_{S,bal}$ measurements for the same Monte Carlo iteration as Table 31. The errors on all ports are identical. It is the same error source as in Table 31, but is a slightly different magnitude since the nominal pressure reading is different.

In this analysis, Gaussian distributions are used for all variables, including MANTUS produced systematic uncertainties. While elemental inputs to MANTUS for any given instrumentation system's analysis vary and include different error distributions, the combined output is an uncertainty assumed to have a near-Gaussian distribution based on the Central Limit Theorem, since there are multiple error sources (and a high number of degrees of freedom) contributing to the measurement system [3].

6.2.2 Comparing Simulation Results with Direct Calculations

Ideally, there would be a large sample of repeat test section data over representative time periods from which Mach variability (and variability of other variables of interest) could be locally calculated. Such data could provide end-to-end statistical process analysis figures that could be compared to the simulated random uncertainty results, and also could be used to refine random uncertainty estimates. Processes to obtain this data have yet to be designed or implemented in this facility, so there is a limit to verification of the simulated results that can be performed at this time.

6.3 Analysis Limitations

Uncertainty results are only as good as the elemental uncertainty estimates that are propagated. The more pertinent data that is available for random, systematic, and spatial uniformity uncertainty estimates, the better the results of the analysis. This particular analysis is somewhat limited by its data set, which was designed to assess the mean behavior of the facility rather than its dispersive behavior. Random uncertainty estimates are difficult to make due to a lack of repeat data over the appropriate time scales, and correlations between variables during normal operation have been observed but are difficult to account for with the existing data set. Additional runs during a calibration entry or perhaps a specially designed test would be required to refine the random uncertainty estimates.

7 What-If Scenarios

Arguably the greatest value to performing a ground-up analysis of measurement uncertainty is that the parameters that dominate the overall uncertainty can be determined. It is often of interest to find out how changes in data acquisition, hardware, test matrices, or processes might affect uncertainty. Based on the determined main contributors (or out of sheer curiosity), different "What-If" scenarios are developed to assess their potential impact on uncertainty. These proposed scenarios become hypothetical examples using synthetic data sets, which are created based on the existing data set, and are run through the analysis process that is already established. The synthetic scenario results are then compared to the uncertainty results obtained with the original test simulation to assess the value of the scenario.

The scenarios developed in this section primarily focus on Mach number uncertainty, which is the main variable of interest for this facility. Additionally, most scenarios focus on decreasing systematic uncertainty, particularly due to static pressure calibration since UPC results indicate that the systematic uncertainty in Mach number is heavily driven by the fossilized uncertainty from the static pressure calibration (see Figure 35). One scenario considers impact to total temperature, a secondary variable of interest for this facility. Scenarios that are considered in this section include:

1. Splitting the static pressure calibration curve by flow regime (subsonic and supersonic),
2. Obtaining more distinct repeat data during the static pressure calibration or use a look-up table,
3. Using static pressure calibration data from different sources (transonic array vs. cone-cylinder),
4. Replacing current pressure instrumentation with higher accuracy instrumentation, and
5. Replacing current temperature instrumentation with higher accuracy instrumentation.

7.1 Splitting the Static Pressure Calibration Curve by Flow Regime

The static pressure calibration was found to be a driving source of systematic uncertainty in a number of variables of interest. Once this was identified, the calibration test matrix, instrumentation, procedures, math model, and all related uncertainty estimates were under increased scrutiny to ascertain whether there was room for improvement in the result.

Figure 88 shows the calibration curve obtained from the 1997 calibration [5]. Upon further investigation, the residuals indicate the subsonic ($\Phi > 0.533$) and supersonic ($\Phi \leq 0.533$) flow regimes have different variation characteristics from the calibration curve.

The standard error of the estimate, s_{yx}, is the uncertainty which applies to a predicted value due to the math model (see Section 6.1.6). In the instance of the static pressure calibration, where variation from the calibration curve in the subsonic range is much lower than in the supersonic range, it becomes questionable whether the standard error is an appropriate uncertainty estimate. By using this statistic, the regression uncertainty in the

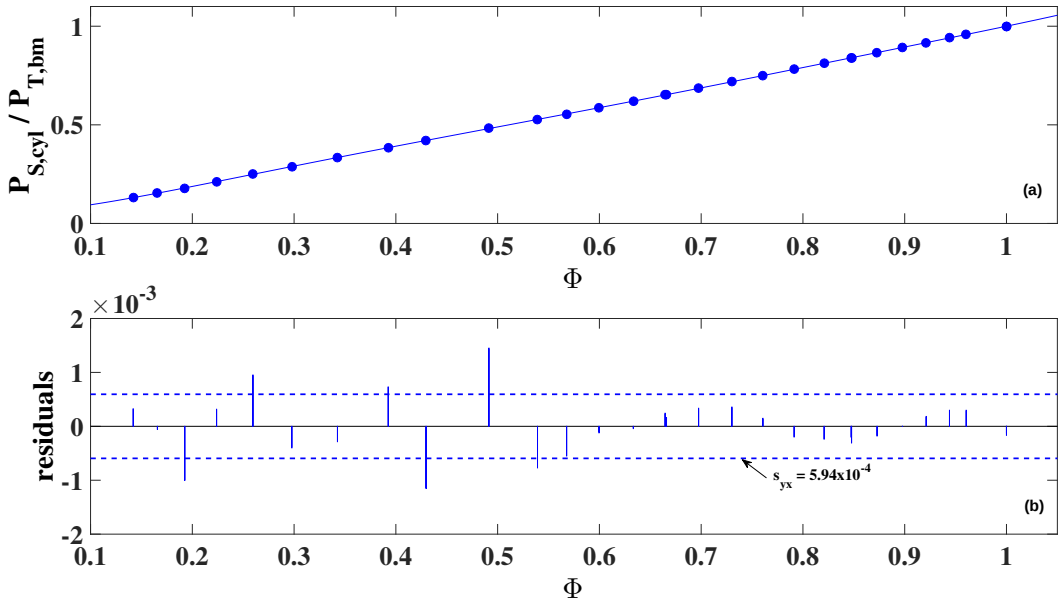

Figure 88: (a) Current 6th order static pressure calibration curve, (b) residuals

subsonic range becomes inflated, while in the supersonic range the regression uncertainty appears lower than what the actual residuals indicate. While the single curve over the entire range is fine for characterizing the overarching static pressure behavior of the tunnel, the difference in variation of the residuals indicates it might be better, for uncertainty purposes, to split the curve by flow regime.

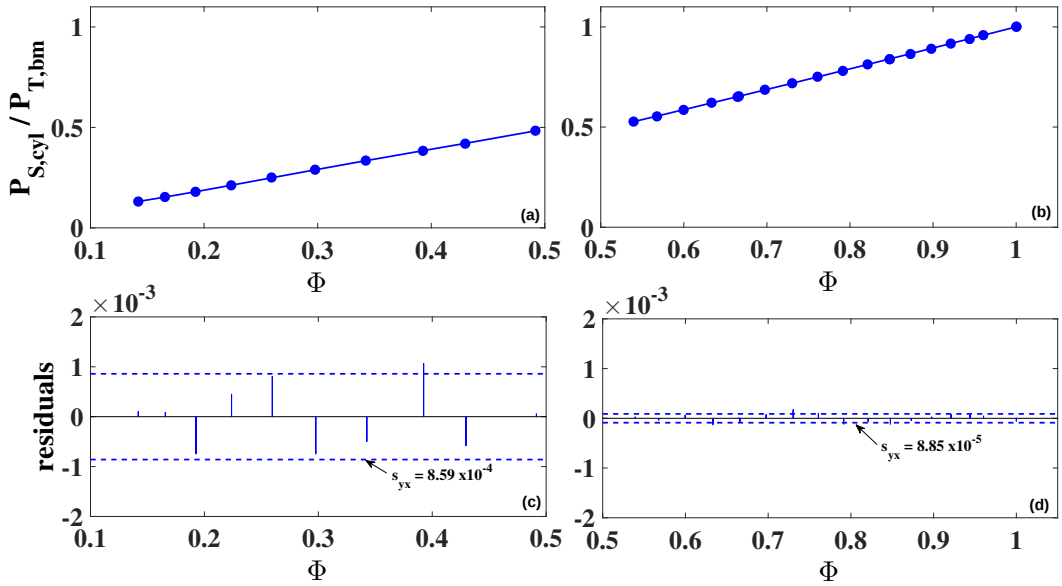

Figure 89: Proposed static pressure calibration curves for the (a) supersonic range and (b) subsonic range, with residuals shown for each (c and d)

Figure 89 shows the result of splitting the single calibration curve into two curves. Lower fit orders are selected for each curve to increase their degrees of freedom, since fewer data points are available for each curve. Analyzing these split curves, the s_{yx} values in the two regimes are observed to differ by a factor of ten. If these split calibration curves and their new regression uncertainty estimates are propagated, the new Mach number uncertainty results are shown in Figure 90. While this scenario appears to increase Mach number uncertainty in the supersonic range and decrease uncertainty in the subsonic range, it is probably more accurate to say that splitting up the calibration curve by flow regime creates a more accurate representation of the math model (regression) uncertainty, and additionally that the initial use of the standard error of estimate to represent the math model uncertainty was probably not sufficient. Splitting the curves allows the standard error of estimate to be used to quantify math model uncertainty for each range.

Based upon this analysis, the recommendation would be to split the static pressure calibration curve by flow regime. This scenario is a good reminder that calibration and uncertainty teams must work closely to ensure that choices made during calibration are beneficial for maintaining calibration integrity, while also being mindful of their impact on evaluating uncertainty.

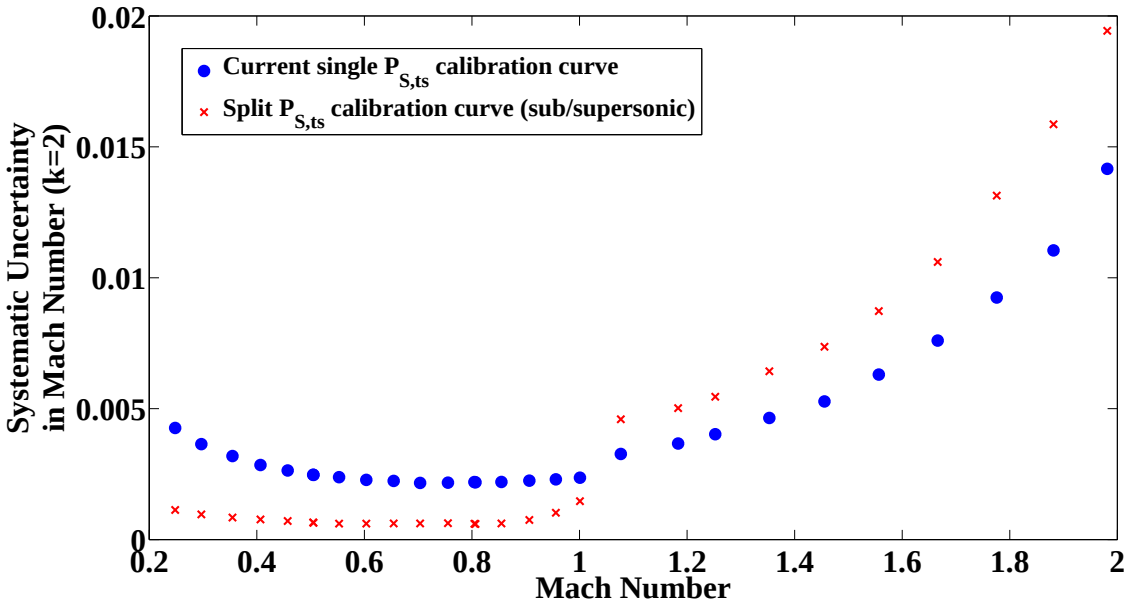

Figure 90: Expanded Systematic Mach Uncertainty (k=2): Effect of splitting up the static pressure calibration curve by flow regime

7.2 Obtaining More Repeat Data During Static Pressure Calibration or Use of a Look-up Table

In theory, random uncertainty from a calibration can be reduced by increasing the distinct (not back-to-back) repeat measurements obtained for each set point used to create a calibration curve. Since the completed analysis includes the full calibration uncertainty analysis,

simulations of the static and total pressure calibrations are already coded and only require slight modifications for this scenario. To simulate this case, synthetic input data for the Monte Carlo simulation of static pressure calibration is changed to include n times more repeat measurements.

The simulation is performed for $n = 1$ (original data set), 3, and 10 repeat measurements, taken at each nominal Mach condition (ranging from Mach 0.25-2.0). Calibration of ESP was assumed to occur halfway through each Mach range sweep. The simulation performs the curve-fit keeping each data point as a discrete point in the fit, as was done for the actual calibration. The results of the scenario's simulation are shown in Figure 91. A small improvement to overall systematic uncertainty in Mach number is observed as n increases, but with diminishing returns; more than three repeat data sweeps have little impact on uncertainty.

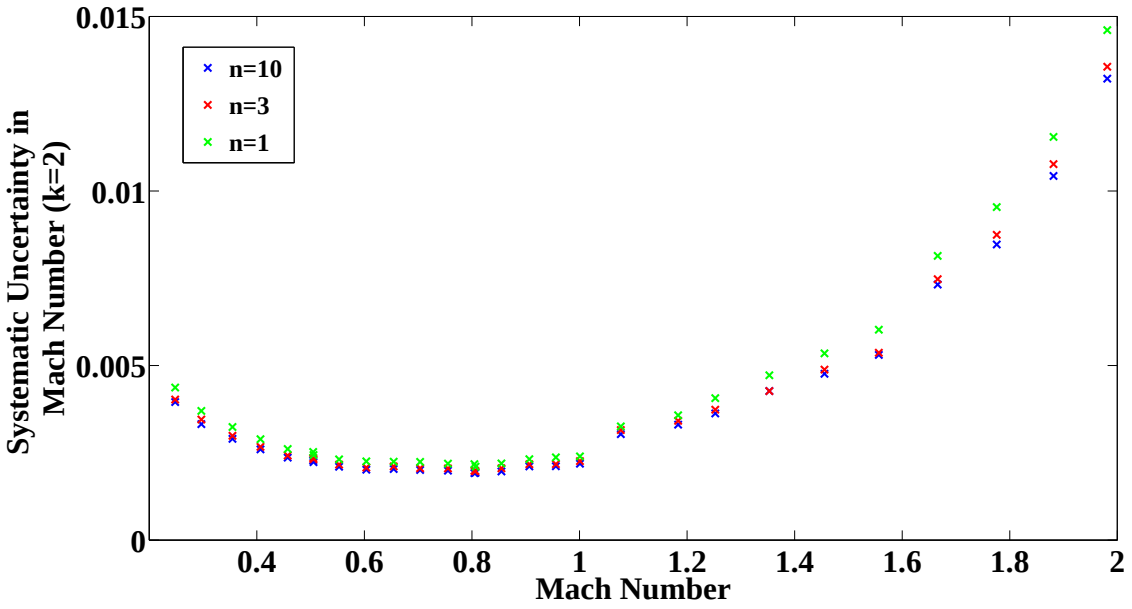

Figure 91: Expanded Systematic Mach Uncertainty (k=2): Effect of n times more repeat data points for static pressure calibration

Since the recommendation for implementing the previous scenario (splitting the static pressure calibration curve by flow regime) is very important for accurate uncertainty quantification in this facility, it is of interest to explore the combined effects of the present scenario with the first. This is done only in the supersonic regime, because the uncertainty in the subsonic regime is already so small that changes would be negligible. The green triangles in Figure 92 show the combined effect of splitting the calibration curve and obtaining additional discrete repeats.

In supersonic operation the facility is only set to explicit Mach numbers (in 0.1 increments). This suggests a third option for the Mach number determination: use of a look-up table relating the facility ratio, Φ, to the ratio $P_{S,ts}/P_{T,bm}$. This method removes the effect of the calibration regression, but maintains other fossilized uncertainties due to the calibration measurements. The result is shown in Figure 92 as the purple stars. Use of a look-up

table is not desirable in the subsonic range because customers are often test in between the calibrated points in this regime.

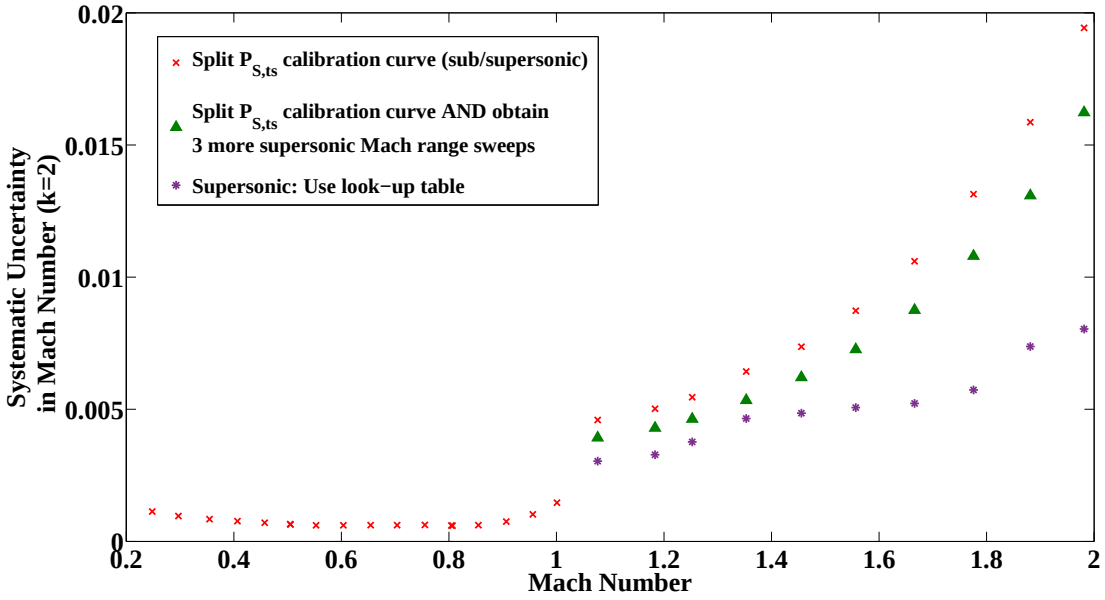

Figure 92: Expanded Systematic Mach Uncertainty (k=2): Effect of 3 times more repeat data points in the supersonic range for static pressure calibration and splitting the calibration curve by flow regime; Effect of using a look-up table

It appears beneficial to strongly consider the use of the look-up table in the supersonic flow range. For example, at Mach 2.0, use of the table may lower uncertainty by approximately 60%. If for some reason a look-up table is not desirable, obtaining more data in that flow regime would decrease uncertainty in Mach number as well.

It should be noted that calibration data can be accumulated over time, creating a collaborative data set, assuming no significant changes have occurred in the facility between calibrations. If calibrations with smaller test matrices could be executed more frequently and designed identically in run sequence, sample size, etc., then the data sets could be smaller but could continue to be combined to increase overall sample size. This would also provide additional data for making better elemental uncertainty estimates and for providing checks on simulation results.

7.3 Using Static Pressure Calibration Data From Different Sources (Transonic Array vs. Cone-Cylinder)

The calibration data obtained during the 1996-1997 calibration test included test section static pressure measured by both the cone-cylinder (currently used for static pressure calibration curve) and from the transonic array. In the calibration's data analysis, the presence of apparent shock interaction effects on the array static pressures made use of the data undesirable. Even though shock effects were also present in the cone-cylinder data, it was

concluded that the cylinder data is a better representation of tunnel static pressure behavior than the array, and that the shock effects average out when data from the aft half of the cylinder is used.

A simulation is performed to analyze use of array static pressures in place of cone-cylinder static pressures. A calibration curve based on array static pressures is created and applied to the calculation of $P_{S,ts}$. The curve-fit and residuals for the currently used cone-cylinder data are shown if Figure 88, while the curve fit and residuals obtained using the transonic array are shown in Figure 93. The array data is analyzed to obtain the array static pressure standard uncertainty estimate in the same manner other uncertainty parameters are determined (see Section 6). A comparison is between the two static pressure calibration methods to determine which provides a more desirable uncertainty outcome. Results of this comparison are shown in Figure 94. Results indicate the current use of cone-cylinder data is far superior to the array data. This is a result of the influence of static pressure regression uncertainty; comparing residuals from Figures 93 and 88, it is obvious that the fit from the cone-cylinder has much better residual characteristics than the fit from the array data.

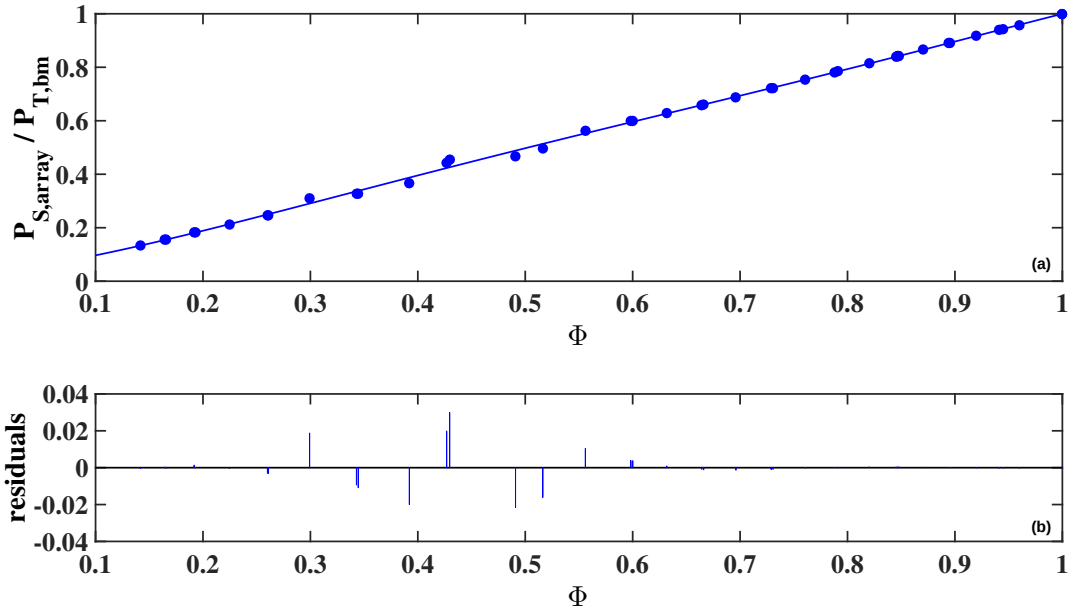

Figure 93: Transonic array static pressure calibration curve (top) and residuals (bottom)

This scenario should not preclude analysis of array static pressure data for use in calibration. By identifying outliers in the data that are suspected to have shock interactions playing a role in inflated variation, these data points could be eliminated from calibration analysis, providing a better outcome of residuals for the calibration curve. Also, combining this scenario with others (splitting the calibration curve by flow regime, etc.) may also help with the uncertainty outcome using the array.

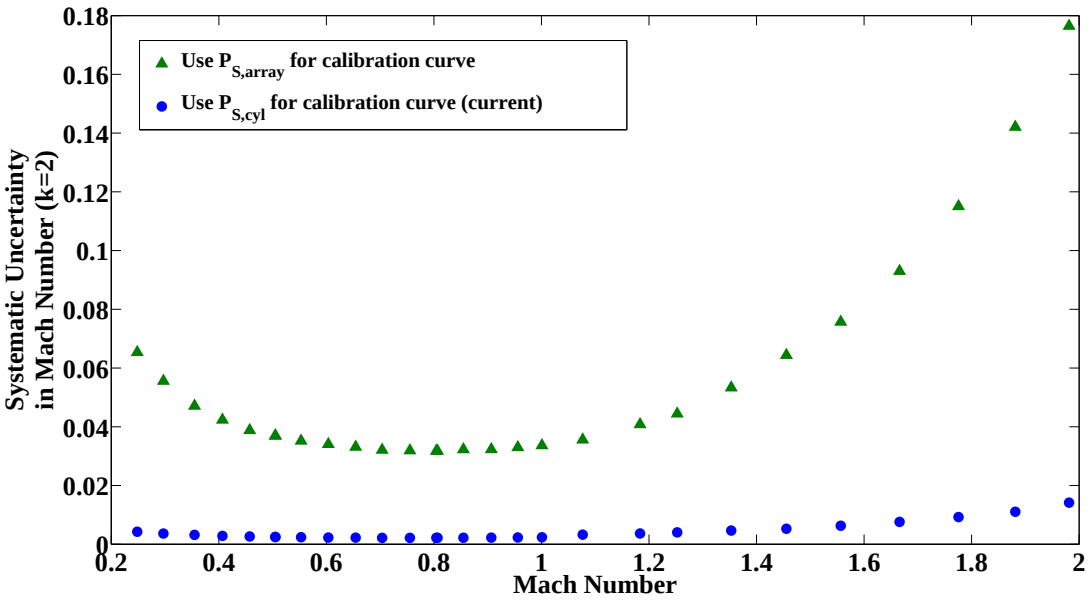

Figure 94: Mach Uncertainty (k=2): Effect of using different data sources for static pressure calibration

7.4 Replacing Current Pressure Instrumentation with Higher Accuracy Instrumentation

A high accuracy instrument is often equated with a low measurement uncertainty. But this often is not the case in complex measurement systems, as the following example shows. A simulation is performed to investigate what the Mach uncertainty impact is if the instrumentation chain for pressure transducers have an accuracy of 0.02% reading. This scenario also assumes re-calibration of the tunnel after hardware changes. Results of this scenario can be seen in Figure 95. It is apparent from the plot that although making the instrumentation change decreases the uncertainty contribution from instrumentation, since the current drivers to systematic uncertainty in Mach number in the supersonic range are primarily due to static pressure spatial uniformity and regression uncertainty from the static pressure calibration, there is no benefit to making such a costly instrumentation change at this time. This result is easily predicted by Figures 35 and A.2. Unless other major systematic uncertainty contributors are addressed first, this instrumentation change would have no effect over systematic uncertainty in the calculated Mach number.

7.5 Replacing Current Temperature Instrumentation with Higher Accuracy Instrumentation

During the analysis process, the authors were approached with the question of upgrading the thermocouple wires in the 8- by 6-foot SWT. It was proposed that the historical extension grade, standard error thermocouple wires for both the bellmouth and array measurements be replaced with new high accuracy, calibrated thermocouple wire and a higher accuracy ref-

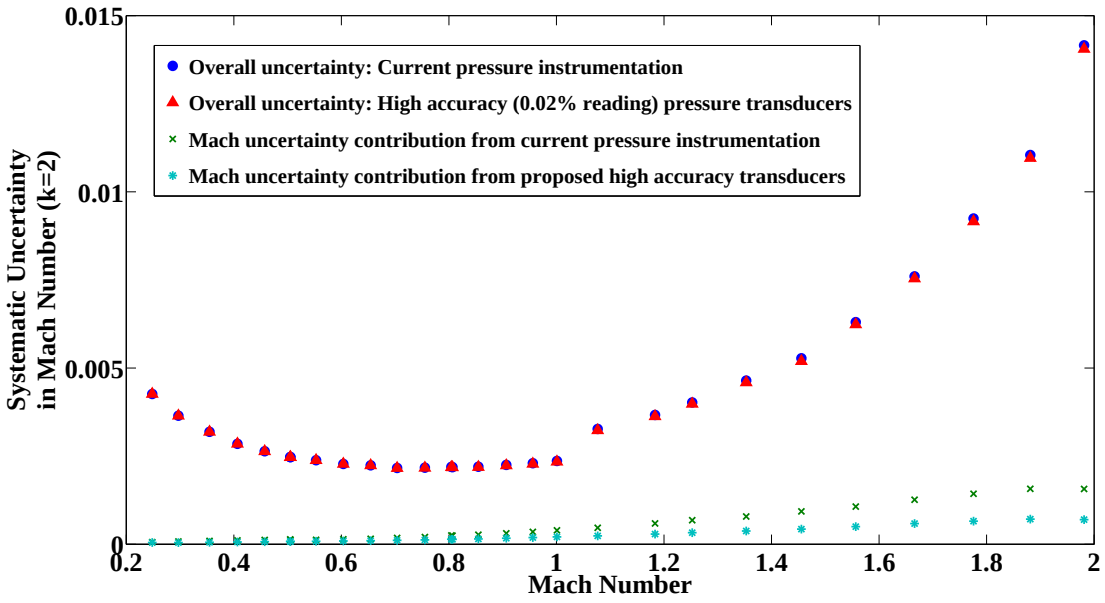

Figure 95: Mach Uncertainty (k=2): Effect of Replacing Current Instrumentation with High Accuracy Instrumentation

erence block. These changes were anticipated to greatly improve the quality of temperature data obtained in the facility.

The systematic standard uncertainty was evaluated by MANTUS with specifications of the new hardware, and the individual temperature measurement uncertainty was on the order of 80% lower than that of the original instrumentation chain. A simulation was then performed using existing data with new temperature instrumentation system uncertainty estimates to get an idea of how much improvement should be expected in the calibrated test section conditions. Results of this simulation are shown in Figure 96, indicating the test section total temperature uncertainty is expected to be cut in half by the improvements. The changes are currently being implemented in the facility.

Improving temperature instrumentation will decrease total temperature uncertainty to a large degree since from Figure 97 it is apparent that uncertainty from instrumentation is the driving factor; however, once that factor is reduced, other uncertainty factors become more influential. Figure 98 shows the UPCs from the improved instrumentation simulation, and it is now the regression uncertainty that drives the calculated total temperature uncertainty.

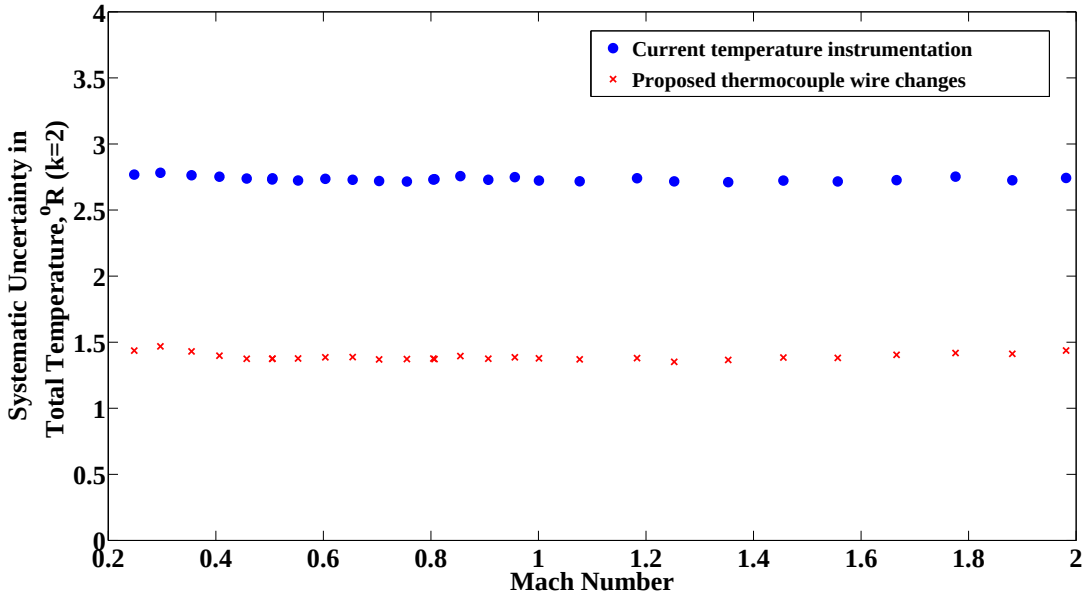

Figure 96: Total Temperature (k=2): Effect of replacing current temperature instrumentation with higher accuracy instrumentation

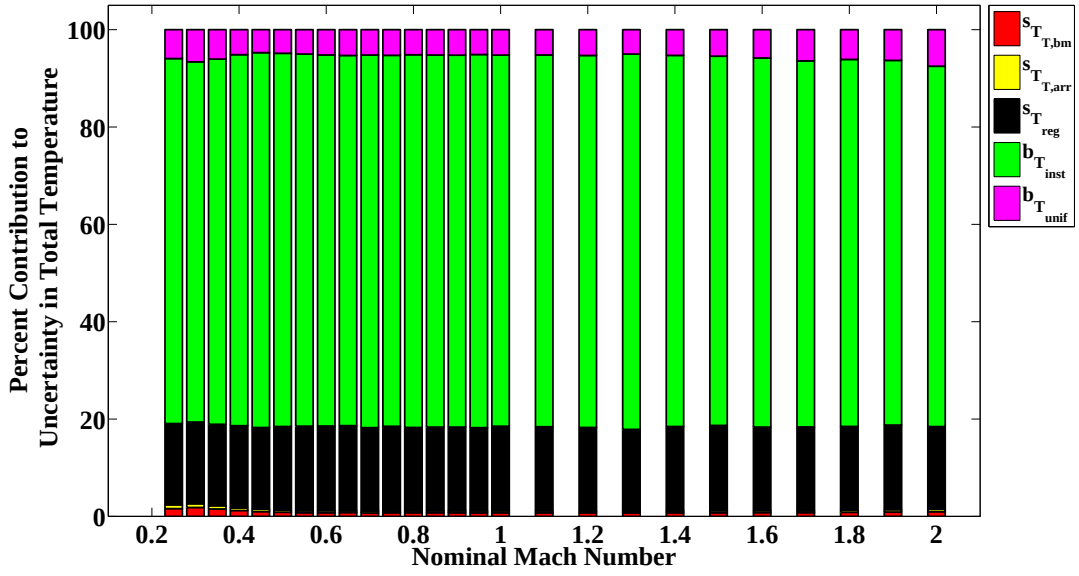

Figure 97: Total Temperature UPC: Original temperature instrumentation

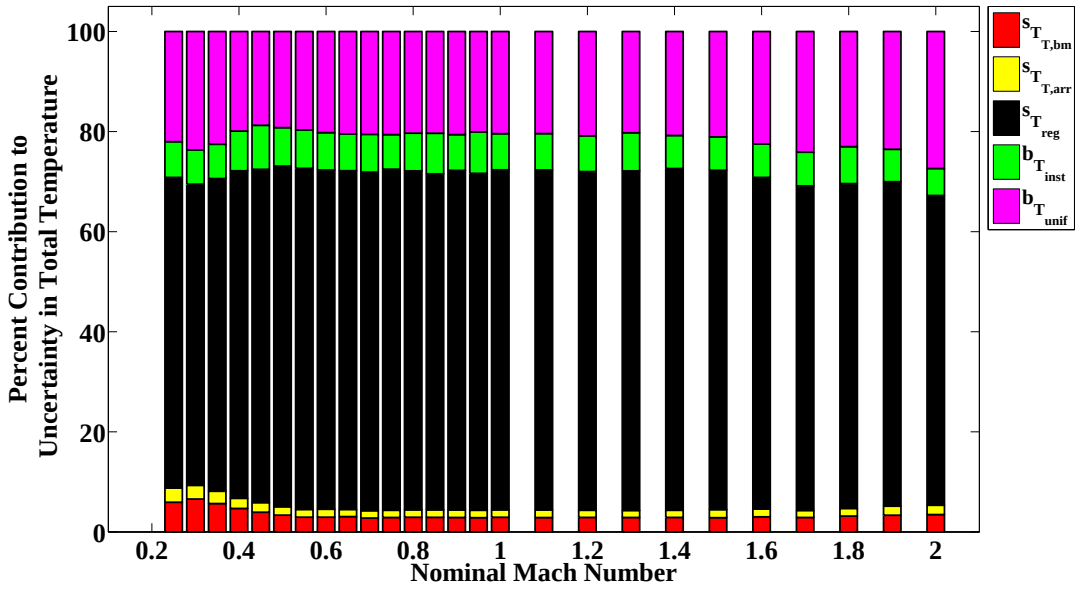

Figure 98: Total Temperature UPC: Determined using higher accuracy temperature instrumentation

8 Conclusions

An uncertainty analysis was performed on the 8- by 6-foot Supersonic Wind Tunnel at NASA Glenn Research Center. The complexity of the data reduction process made a faithful replication of it impractical using traditional Taylor series error propagation techniques. As a result, the Monte Carlo method of propagating uncertainty was selected. The general process for each of these method was described in this document.

Throughout this document, uncertainties were classified as random (variability about the mean value) and systematic (offset of average measured value from the true value) to aid users in determining which uncertainties are of interest for specific tests. Uncertainty sources were determined and elemental uncertainty estimates were made for all considered sources. Instrumentation uncertainties were estimated using MANTUS [12], an Excel® based tool tailored for modularized instrument systems to determine the combined uncertainty of an instrument. Random uncertainties and spatial uniformity uncertainty were estimated using data from the most recent tunnel calibration [5]. All uncertainties considered in the analysis were propagated from the point of measurement through the instrumentation, data system, tunnel calibrations and finally data reduction to arrive at uncertainties for several variables of interest. Results were analyzed and broken down at every step so that a comprehensive understanding of driving uncertainty sources could be determined.

Correlation effects and a small repeat data set were two challenges faced in this analysis. Measurements were correlated due to the instrumentation and/or operation of the facility. For example, the facility set point was based on the ratio of $P_{S,bal}$ to $P_{T,bm}$. As a result, there was a seemingly wide variation in each of these parameters, while the ratio stayed fairly constant at any given set point. This translated to an unrealistically large random uncertainty estimate when the correlation was not properly accounted for. The statistical analyses, engineering judgments made to account for correlations, and other challenges faced were detailed in this document.

A summary of typical uncertainties for subsonic and supersonic regimes for all variables is shown for random uncertainties in Table 33, and for systematic uncertainties in Table 34. The primary contributor to the uncertainty is also shown, although it should be noted that driving contributors sometimes varied through the specified range.

Scenarios were developed and simulated to deduce their potential impact on uncertainty. Table 35 summarizes the notable results of the scenarios explored. These scenarios and conclusions enable facility personnel to make educated improvements such as those presented in Table 36 as they consider facility upgrades and plan future calibration tests.

	Subsonic, k = 2	Supersonic, k = 2	Primary Contributor
Mach Number	0.0001-0.0004	0.001-0.004	$s_{P_{S,bal}}$
Static Pressure, psia	0.0004-0.004	0.01-0.03	$s_{P_{S,bal}}$
Total Pressure, psia	0.0003-0.0007	0.001-0.03	$s_{P_{T,bm}}$
Dynamic Pressure, psia	0.001-0.003	0.002-0.02	$s_{P_{S,bal}}$
Static Temperature, °R	0.1-0.5	0.2-0.7	$s_{T_{T,bm}} \mid s_{P_{S,bal}}$
Total Temperature, °R	0.1-0.5	0.1-0.3	$s_{T_{T,bm}}$
Reynolds Number, x 10^6 ft^{-1}	0.001-0.003	0.002-0.009	$s_{T_{T,bm}} \mid s_{P_{S,bal}}$
Free Stream Air Speed, ft/s	0.1-0.4	0.5-2.5	$s_{P_{S,bal}}$

Table 33: Summary of random uncertainties of average free stream conditions with 95% level of confidence for commonly used tunnel configurations.

	Subsonic, k = 2	Supersonic, k = 2	Primary Contributor
Mach Number	0.002-0.004	0.002-0.014	b_{PSCAL}
Static Pressure, psia	0.025	0.025-0.04	b_{PSCAL}
Total Pressure, psia	0.009	0.04-0.3	$b_{P_{inst}} \mid b_{PTCAL}$
Dynamic Pressure, psia	0.01-0.02	0.02-0.05	$b_{PSCAL} \mid b_{PTCAL}$
Static Temperature, °R	2.3-2.8	2.1-2.8	b_{TTCAL}
Total Temperature, °R	2.8	2.8	b_{TTCAL}
Reynolds Number, x 10^6 ft^{-1}	0.02-0.03	0.03-0.05	b_{TTCAL}
Free Stream Air Speed, ft/s	2.9-4.8	3.3-8.4	b_{PSCAL}

Table 34: Summary of systematic uncertainties of average free stream conditions with 95% level of confidence for commonly used tunnel configurations.

Scenario	Result
Split static pressure calibration curve by flow regime	Subsonic regime: Decrease of systematic uncertainty in Mach number by 50-75%. Supersonic regime: Increase of systematic uncertainty in Mach number by 30%. For each flow range, a more representative uncertainty estimate is achieved.
Obtain additional distinct repeat data points during static pressure calibration	Beneficial (15% decrease in Mach number uncertainty) after calibration curve is split by flow regime.
Use a look-up table instead of supersonic static pressure calibration	Decrease of systematic uncertainty in Mach number by 20-60% (or more, if also considered for total pressure)
Use static pressure measured by the transonic array vs. cone-cylinder for calibration	Current calibration using cone-cylinder data is far superior
Replace pressure instrumentation with higher accuracy instrumentation	No benefit since other sources currently drive systematic uncertainty in Mach number
Replace temperature instrumentation with higher accuracy instrumentation	50% decrease in calculated test section total temperature uncertainty

Table 35: Summary of What-If Scenarios

Sources that drive uncertainty	Actions suggested to mitigate their impact
$s_{P_{S,bal}}, s_{P_{T,bm}}, s_{T_{T,bm}}$	Random uncertainty needs to be understood more fully in this facility before suggestions can be made. A facility study using a test matrix with at least 5-10 repeat Mach sweeps and identical hardware setup for both the transonic array and cone-cylinder should be considered to begin to achieve this understanding. In the meantime, customers desiring better repeatability than quoted should plan repeat data points in their own test matrices.
b_{PSCAL}, b_{PTCAL}	Static pressure calibration curve should be split by flow regime. Calibration test matrices should include at least 3 full Mach range sweeps for critical calibration runs (i.e., tunnel center-line). Use of look-up table for tunnel set points in supersonic range should be strongly considered for both static and total pressure relationships.[2]
b_{TTCAL}	Upgrade thermocouple hardware.[3]

Table 36: Summary of uncertainty mitigation factors

[2]As a result of this analysis, these recommendations were approved by facility personnel and will be implemented for future testing (Spring 2016).

[3]Thermocouple upgrades for both the facility and calibration hardware are in progress (Winter 2016).

9 References

1. American Society of Mechanical Engineers. "Test Uncertainty". Standard ASME PTC 19.1-2013, 2014.

2. American Institute of Aeronautics and Astronautics. "Assessment of Experimental Uncertainty with Application to Wind Tunnel Testing". Standard AIAA S-071A-1999, 1999.

3. Joint Committee for Guides in Metrology. "Evaluation of Measurement Data - Guide to the Expression of Uncertainty in Measurement". Guide JCGM 100:2008, International Organization for Standardization, 2008.

4. S. Castrup and H.T. Castrup. "Measurement Uncertainty Analysis Principles and Methods: NASA Measurement Quality Assurance Handbook - ANNEX 3". Handbook NASA HDBK 8739.19-3, National Aeronautics and Space Administration, 2010.

5. E. A. Arrington. "Calibration of the NASA Glenn 8- by 6-foot Supersonic Wind Tunnel". Calibration Report NASA/CR-2012-217270, National Aeronautics and Space Administration, January 2012.

6. R. H. Soeder. "NASA Glenn 8-by 6-foot Supersonic Wind Tunnel User Manual". Technical Memorandum NASA TM 105771, National Aeronautics and Space Administration, 1993.

7. Ames Research Staff. "Equations, Tables, and Charts for Compressible Flow". Technical Report NACA TR-1135, National Aeronautics and Space Administration, 1953.

8. H. W. Coleman and W. G. Steele. *Experimentation, Validation and Uncertainty Analysis for Engineers*. John Wiley and Sons, Inc., Third edition, 2009.

9. R.J. Moffat. "Describing the Uncertainties in Experimental Results". *Experimental Thermal and Fluid Science*, Vol. 1(No. 1), 1988.

10. Joint Committee for Guides in Metrology. "Evaluation of Measurement Data - Supplement 1 to the "guide to the Expression of Uncertainty in Measurement" - Propagation of Distributions using a Monte Carlo Method". Supplement JCGM 101:2008, International Organization for Standardization, 2008.

11. J. Walter, W. Lawrence, D. Elder, and M. Treece. "Development of an Uncertainty Model for the National Transonic Facility". Technical Report AIAA 2010-4925, American Institute of Aeronautics and Astronautics, 2010.

12. B. Rouse, J. Morales, and T. McElroy. "Measurement Analysis Tool for Uncertainty in Systems Overview". Contractor report, National Aeronautics and Space Administration, In Progress.

13. J.L. Devore. *Probability and Statistics for Engineering and the Sciences*. Brooks/Cole, Fifth edition, 2000.

14. R.A. Wahls, J.B. Adcock, D.P. Witkowski, and F.L. Wright. “A Longitudinal Aerodynamic Data Repeatability Study for a Commercial Transport Model Test in the National Transonic Facility”. Technical Paper NASA TP 3522, National Aeronautics and Space Administration, August 1995.

Appendices

List of Figures in Appendices

List of Tables in Appendices

Appendix A: Uncertainty Contributions to Calibrations

In Section 5, the random, systematic and total uncertainties were presented for every variable of interest. Combined systematic uncertainties of those variables are influenced by the systematic uncertainty from tunnel calibrations (static pressure, total pressure, and total temperature). Random measurement errors, systematic instrumentation errors, and systematic errors due to uniformity of the flow contribute to the uncertainty of these calibrations. While comprised of both random and systematic components, these errors are fossilized and contribute as a combined systematic uncertainty for test-time analysis (b_{PSCAL}, b_{PTCAL}, and b_{TTCAL}). This Appendix breaks down the contributions of elemental uncertainties for each calibration. Details of the calibration procedure are provided in Section 3.

A.1 Static Pressure Calibration

Uncertainties present during the static pressure calibration include the random uncertainties from total pressure in the bellmouth, static pressure in the balance chamber and static pressure on the cylinder ($s_{P_{T,bm}}, s_{P_{s,bal}}$, and $s_{P_{s,cyl}}$), random uncertainty in the calibration regression ($s_{P_{S,reg}}$), systematic uncertainty in pressure measurement instrumentation (combined as $b_{P_{inst}}$), and systematic uncertainty due to static pressure uniformity ($b_{P_{S,unif}}$).

The uncertainty flow chart is shown in Figure A.1. Uncertainty results are presented as percent contributions as bar charts in Figure A.2 and tabular form in Tables A.1 - A.6 for all configurations. The static pressure calibration uncertainty is driven by the uncertainty due to the regression.

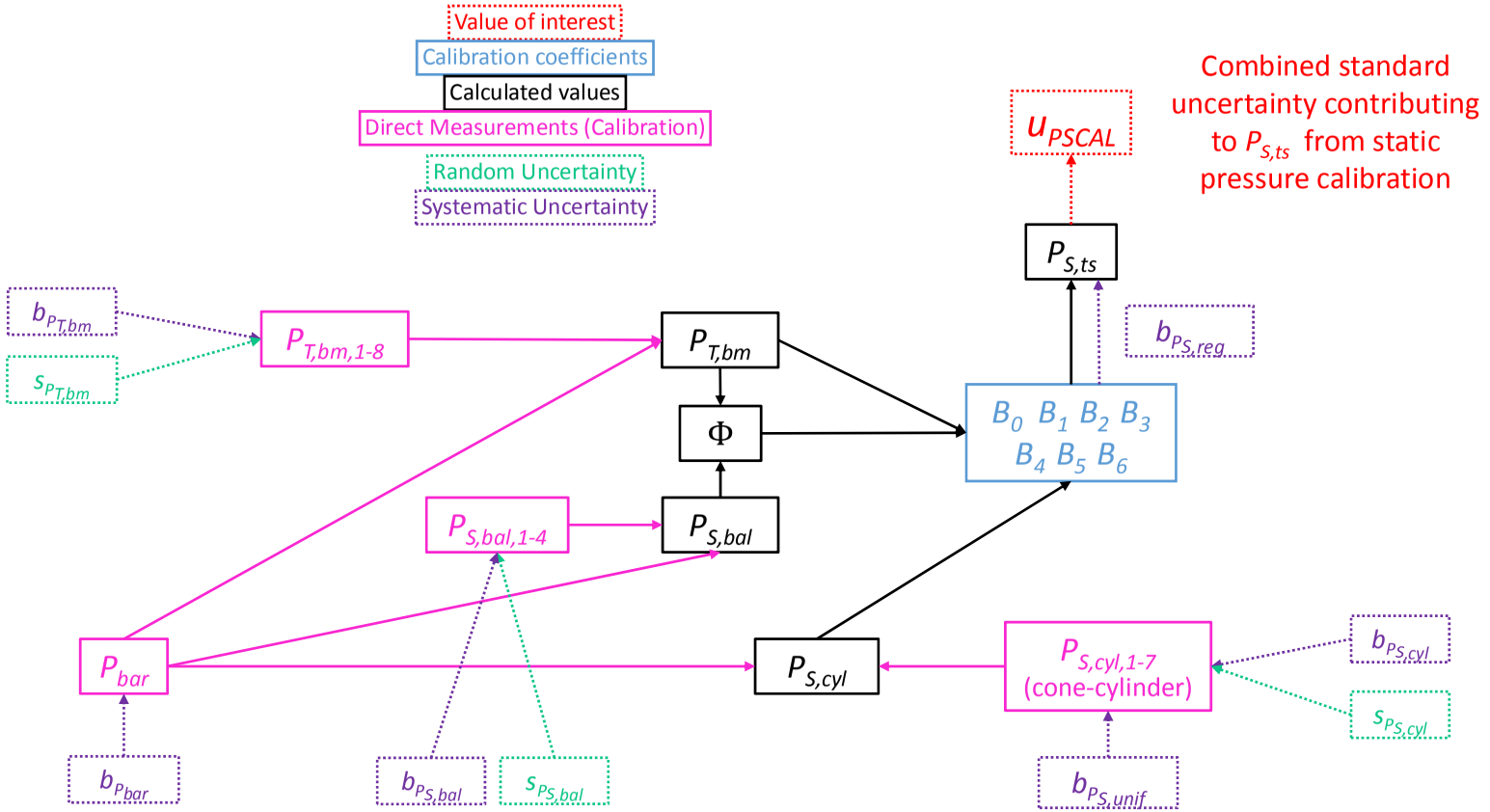

Figure A.1: Flow chart depicting the flow of uncertainty for static pressure calibration

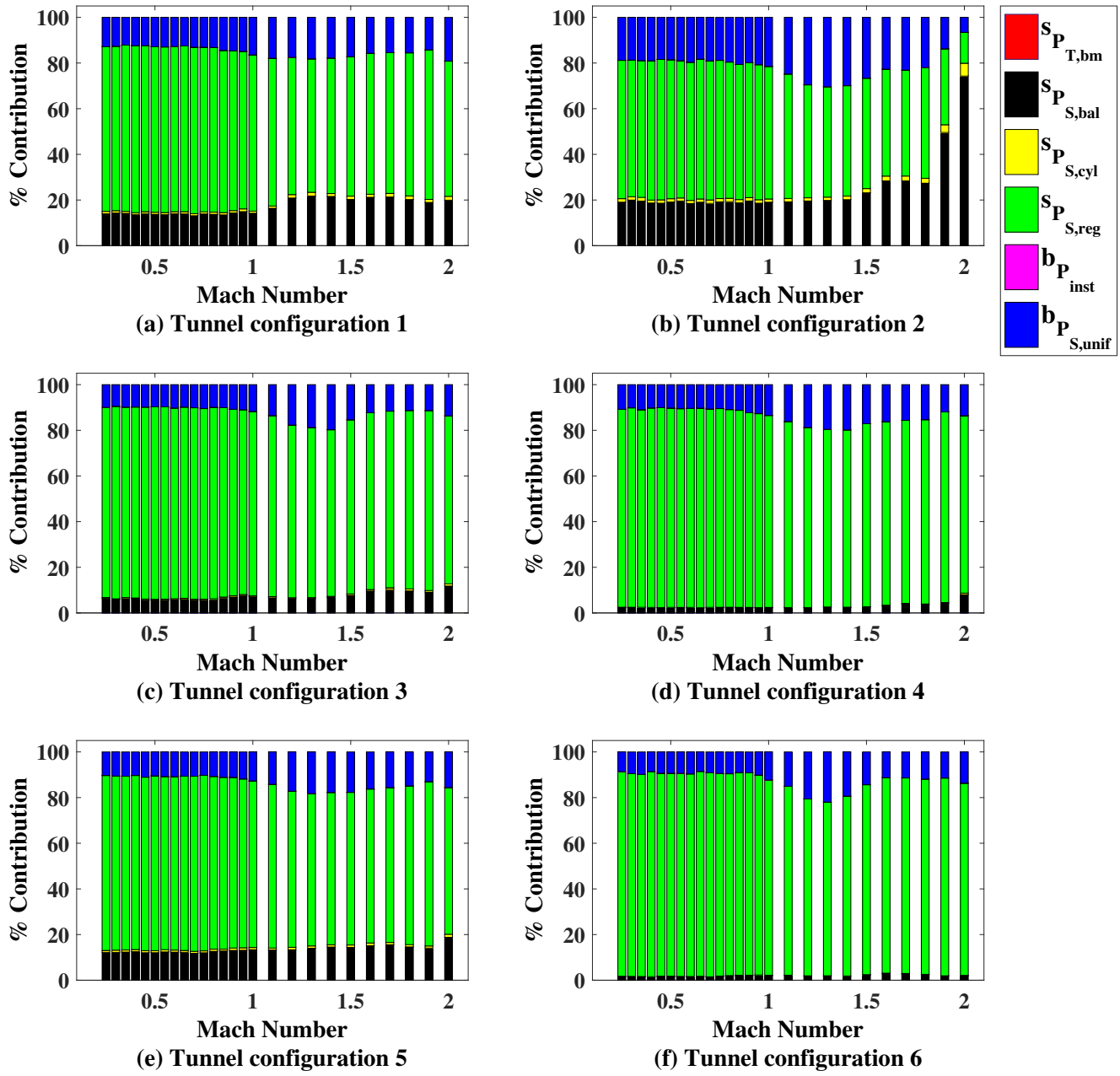

Figure A.2: Percent contributions from all elemental uncertainty sources to the fossilized uncertainty from static pressure calibration u_{PSCAL} as a function of nominal Mach number

Nominal Mach	**Typical $P_{S,cal}$, psia**	$u_{P_{S,cal}}$ **psia k = 2**	$u_{P_{S,cal}}$ **UPC due to** $s_{P_{T,bm}}$	$u_{P_{S,cal}}$ **UPC due to** $s_{P_{S,bal}}$	$u_{P_{S,cal}}$ **UPC due to** $s_{P_{S,cyl}}$	$u_{P_{S,cal}}$ **UPC due to** $b_{P_{S_{reg}}}$	$u_{P_{S,cal}}$ **UPC due to** $b_{P_{inst}}$	$u_{P_{S,cal}}$ **UPC due to** $b_{P_{Sunif}}$
0.25	14.85	0.02	0.00	14.03	1.00	72.12	0.00	12.84
0.40	13.86	0.02	0.00	13.66	0.78	73.14	0.00	12.41
0.60	13.86	0.02	0.00	13.99	0.88	72.38	0.00	12.75
0.80	11.29	0.02	0.00	13.72	0.96	72.11	0.00	13.20
1.00	9.05	0.02	0.00	14.23	0.89	68.41	0.04	16.43
1.20	7.34	0.03	0.00	20.87	1.49	60.12	0.00	17.52
1.40	6.18	0.03	0.00	21.55	1.26	59.37	0.00	17.81
1.60	5.16	0.03	0.00	21.19	1.34	61.73	0.01	15.74
1.80	4.24	0.04	0.01	20.19	1.59	62.69	0.00	15.52
2.00	3.25	0.04	0.01	19.93	1.67	59.20	0.06	19.13

Table A.1: Summary of calculated Static Pressure Calibration percent uncertainty for configuration 1.

Nominal Mach	**Typical $P_{S,cal}$, psia**	$u_{P_{S,cal}}$ **psia k = 2**	$u_{P_{S,cal}}$ **UPC due to** $s_{P_{T,bm}}$	$u_{P_{S,cal}}$ **UPC due to** $s_{P_{S,bal}}$	$u_{P_{S,cal}}$ **UPC due to** $s_{P_{S,cyl}}$	$u_{P_{S,cal}}$ **UPC due to** $b_{P_{S_{reg}}}$	$u_{P_{S,cal}}$ **UPC due to** $b_{P_{inst}}$	$u_{P_{S,cal}}$ **UPC due to** $b_{P_{Sunif}}$
0.25	14.57	0.02	0.00	19.06	1.51	60.60	0.00	18.82
0.40	13.58	0.02	0.00	18.71	1.26	61.01	0.00	19.02
0.60	13.44	0.03	0.00	18.48	1.34	60.54	0.00	19.64
0.80	10.99	0.03	0.01	19.27	1.49	59.66	0.01	19.56
1.00	8.83	0.03	0.00	19.05	1.39	58.06	0.01	21.48
1.20	7.08	0.03	0.00	19.58	1.38	49.49	0.02	29.53
1.40	6.08	0.03	0.00	20.15	1.58	48.36	0.01	29.90
1.60	5.11	0.03	0.01	28.37	2.11	46.82	0.01	22.69
1.80	4.33	0.04	0.00	27.37	2.15	48.52	0.00	21.96
2.00	3.35	0.08	0.01	74.28	5.61	13.55	0.00	6.54

Table A.2: Summary of calculated Static Pressure Calibration percent uncertainty for configuration 2.

Nominal Mach	**Typical $P_{S,cal}$, psia**	$u_{P_{S,cal}}$ **psia k = 2**	$u_{P_{S,cal}}$ **UPC due to** $s_{P_{T,bm}}$	$u_{P_{S,cal}}$ **UPC due to** $s_{P_{S,bal}}$	$u_{P_{S,cal}}$ **UPC due to** $s_{P_{S,cyl}}$	$u_{P_{S,cal}}$ **UPC due to** $b_{P_{S_{reg}}}$	$u_{P_{S,cal}}$ **UPC due to** $b_{P_{inst}}$	$u_{P_{S,cal}}$ **UPC due to** $b_{P_{Sunif}}$
0.25	14.94	0.03	0.00	6.36	0.41	83.27	0.00	9.96
0.40	14.03	0.03	0.00	6.22	0.33	83.66	0.00	9.79
0.60	14.03	0.03	0.00	5.70	0.53	83.53	0.00	10.24
0.80	11.53	0.03	0.00	5.76	0.47	83.86	0.01	9.91
1.00	9.30	0.03	0.00	7.09	0.48	80.68	0.01	11.74
1.20	7.29	0.03	0.00	6.25	0.43	75.59	0.01	17.71
1.40	6.30	0.04	0.00	6.80	0.46	72.99	0.00	19.74
1.60	5.26	0.04	0.00	9.60	0.64	77.49	0.00	12.26
1.80	4.39	0.05	0.00	9.66	0.83	78.16	0.00	11.33
2.00	3.31	0.05	0.00	11.80	0.95	73.59	0.01	13.66

Table A.3: Summary of calculated Static Pressure Calibration percent uncertainty for configuration 3.

Nominal Mach	**Typical $P_{S,cal}$, psia**	$u_{P_{S,cal}}$ **psia k = 2**	$u_{P_{S,cal}}$ **UPC due to** $s_{P_{T,bm}}$	$u_{P_{S,cal}}$ **UPC due to** $s_{P_{S,bal}}$	$u_{P_{S,cal}}$ **UPC due to** $s_{P_{S,cyl}}$	$u_{P_{S,cal}}$ **UPC due to** $b_{P_{S_{reg}}}$	$u_{P_{S,cal}}$ **UPC due to** $b_{P_{inst}}$	$u_{P_{S,cal}}$ **UPC due to** $b_{P_{Sunif}}$
0.25	14.90	0.03	0.00	2.32	0.19	86.72	0.00	10.78
0.40	14.04	0.03	0.00	2.28	0.15	87.37	0.00	10.21
0.60	13.99	0.03	0.00	2.28	0.15	87.19	0.00	10.38
0.80	11.49	0.03	0.00	2.34	0.15	86.61	0.00	10.90
1.00	9.16	0.03	0.00	2.27	0.16	84.08	0.00	13.49
1.20	7.36	0.03	0.00	2.24	0.15	78.85	0.01	18.75
1.40	6.26	0.03	0.00	2.38	0.14	77.66	0.00	19.82
1.60	5.23	0.04	0.00	3.17	0.22	80.40	0.00	16.21
1.80	4.33	0.04	0.00	3.66	0.26	80.73	0.00	15.34
2.00	3.25	0.04	0.00	8.00	0.68	77.68	0.06	13.58

Table A.4: Summary of calculated Static Pressure Calibration percent uncertainty for configuration 4.

Nominal Mach	**Typical $P_{S,cal}$, psia**	$u_{P_{S,cal}}$ **psia k = 2**	$u_{P_{S,cal}}$ **UPC due to** $s_{P_{T,bm}}$	$u_{P_{S,cal}}$ **UPC due to** $s_{P_{S,bal}}$	$u_{P_{S,cal}}$ **UPC due to** $s_{P_{S,cyl}}$	$u_{P_{S,cal}}$ **UPC due to** $b_{P_{S_{reg}}}$	$u_{P_{S,cal}}$ **UPC due to** $b_{P_{inst}}$	$u_{P_{S,cal}}$ **UPC due to** $b_{P_{Sunif}}$
0.25	14.54	0.02	0.01	12.19	0.83	76.67	0.00	10.31
0.40	13.66	0.02	0.00	12.51	0.89	76.30	0.00	10.30
0.60	13.65	0.03	0.00	12.28	0.91	75.98	0.00	10.83
0.80	11.21	0.03	0.00	12.65	0.96	75.66	0.00	10.72
1.00	8.98	0.03	0.00	13.35	0.97	72.98	0.00	12.70
1.20	7.18	0.03	0.00	13.35	1.07	68.37	0.01	17.21
1.40	6.11	0.03	0.00	14.54	0.93	66.78	0.00	17.74
1.60	5.14	0.03	0.00	15.13	1.18	67.44	0.01	16.23
1.80	4.31	0.04	0.00	14.60	0.97	69.54	0.00	14.88
2.00	3.27	0.04	0.00	18.81	1.32	64.24	0.02	15.61

Table A.5: Summary of calculated Static Pressure Calibration percent uncertainty for configuration 5.

Nominal Mach	**Typical $P_{S,cal}$, psia**	$u_{P_{S,cal}}$ **psia k = 2**	$u_{P_{S,cal}}$ **UPC due to** $s_{P_{T,bm}}$	$u_{P_{S,cal}}$ **UPC due to** $s_{P_{S,bal}}$	$u_{P_{S,cal}}$ **UPC due to** $s_{P_{S,cyl}}$	$u_{P_{S,cal}}$ **UPC due to** $b_{P_{S_{reg}}}$	$u_{P_{S,cal}}$ **UPC due to** $b_{P_{inst}}$	$u_{P_{S,cal}}$ **UPC due to** $b_{P_{Sunif}}$
0.25	14.88	0.03	0.00	1.66	0.08	89.63	0.00	8.63
0.40	13.97	0.03	0.00	1.43	0.11	89.84	0.00	8.61
0.60	14.00	0.04	0.00	1.56	0.06	88.77	0.00	9.61
0.80	11.32	0.04	0.00	1.89	0.15	88.40	0.00	9.55
1.00	8.97	0.04	0.00	2.06	0.12	85.50	0.00	12.33
1.20	7.37	0.04	0.00	1.77	0.16	77.50	0.00	20.57
1.40	6.22	0.04	0.00	1.77	0.13	78.73	0.00	19.37
1.60	5.20	0.05	0.00	2.83	0.27	85.61	0.00	11.29
1.80	4.28	0.05	0.00	2.34	0.24	85.53	0.01	11.87
2.00	3.29	0.06	0.00	1.89	0.25	84.13	0.06	13.67

Table A.6: Summary of calculated Static Pressure Calibration percent uncertainty for configuration 6.

A.2 Total Pressure Calibration

Uncertainties that contributed during total pressure calibration include the random uncertainties of the total pressure in the bellmouth, static pressure in the balance chamber and total pressure on the array ($s_{P_{T,bm}}$, $s_{P_{S,bal}}$, and $s_{P_{T,arr}}$), random uncertainty in the total pressure calibration regression ($s_{P_{T,reg}}$), systematic uncertainty in pressure measurement instrumentation (combined as $b_{P_{inst}}$), and systematic uncertainty due to total pressure uniformity ($b_{P_{T,unif}}$).

The uncertainty flow chart for total pressure for subsonic and supersonic ranges are shown in Figures A.3 and A.4. Uncertainty results are presented as percent contributions as bar charts in Figure A.5 and in tabular form in Tables A.7 - A.12 for all configurations. Note that in the supersonic range, the total pressure downstream of a normal shock is measured by the array ($P_{T,2,arr}$). For simplicity, throughout this section $P_{T,2,arr}$ will be referred to as $P_{T,arr}$ and $P_{T,2,ts}$ will be referred to as $P_{T,ts}$, and results are shown on a single chart. Total pressure uniformity drives the total pressure calibration uncertainty, although the regression uncertainty has greater impact in the supersonic regime.

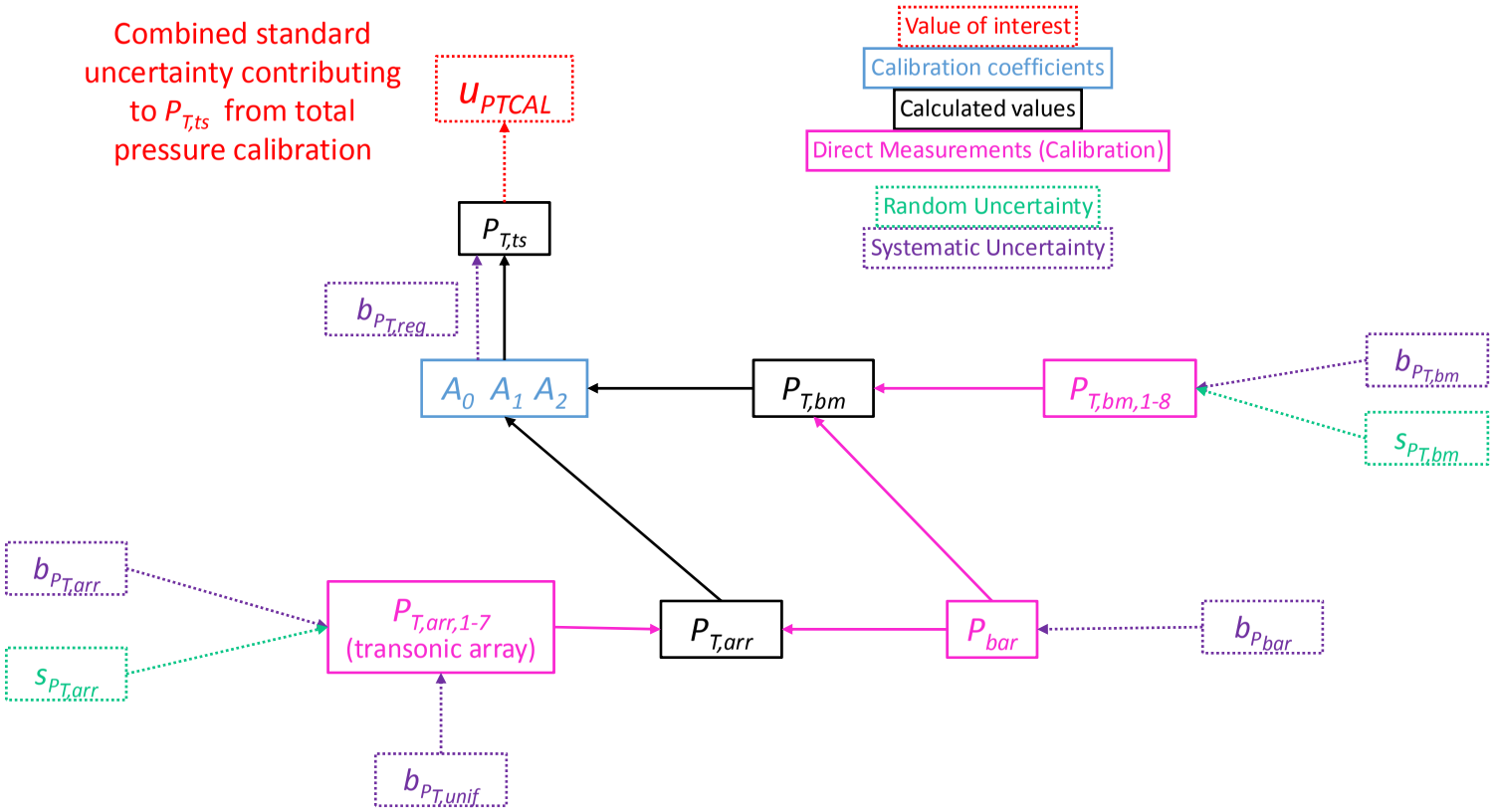

Figure A.3: Flow chart depicting the flow of uncertainty for total pressure calibration: subsonic flow range

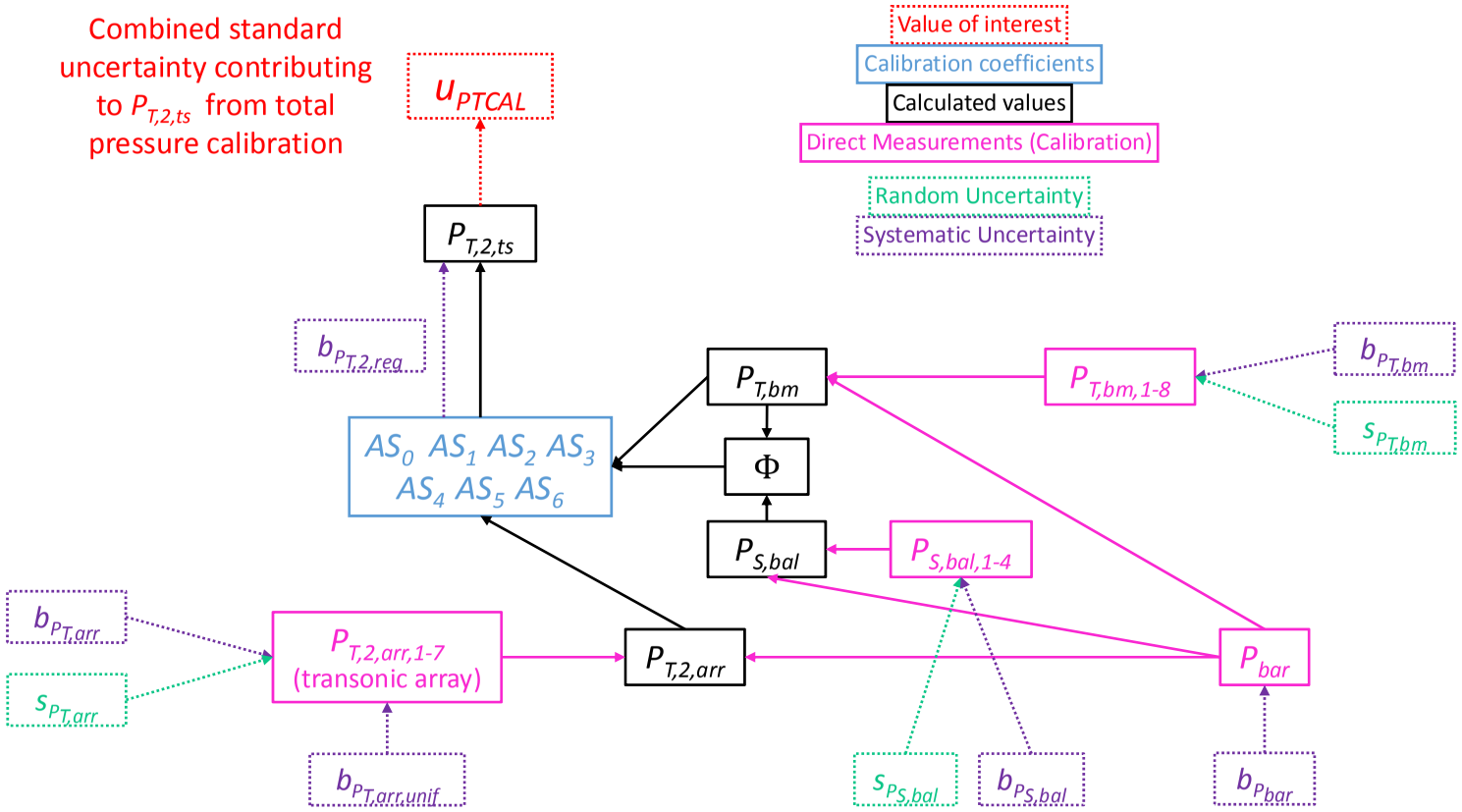

Figure A.4: Flow chart depicting the flow of uncertainty for total pressure calibration: supersonic flow range

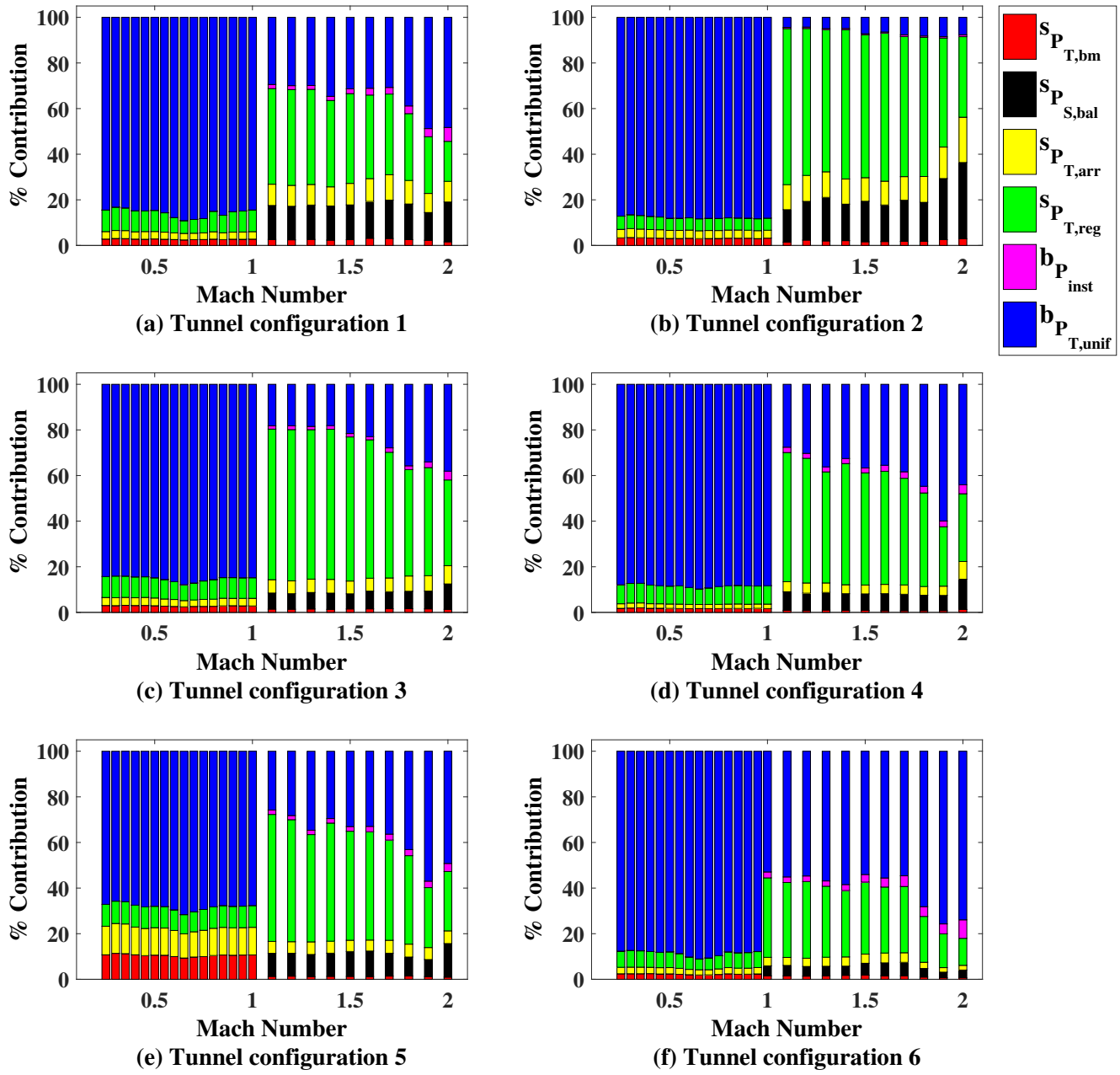

Figure A.5: Percent contributions from all elemental uncertainty sources to the combined uncertainty of the total pressure calibration, as a function of nominal Mach number

Nominal Mach	**Typical $P_{T,cal}$, psia**	$u_{P_{T,cal}}$ **psia k = 2**	$u_{P_{T,cal}}$ **UPC due to** $s_{P_{T,bm}}$	$u_{P_{T,cal}}$ **UPC due to** $s_{P_{S,bal}}$	$u_{P_{T,cal}}$ **UPC due to** $s_{P_{T,arr}}$	$u_{P_{T,cal}}$ **UPC due to** $b_{P_{T_{reg}}}$	$u_{P_{T,cal}}$ **UPC due to** $b_{P_{inst}}$	$u_{P_{T,cal}}$ **UPC due to** $b_{P_{Tunif}}$
0.25	15.51	0.00	2.80	0.00	3.27	9.44	0.00	84.48
0.40	15.54	0.00	2.79	0.00	3.19	9.23	0.00	84.79
0.60	17.74	0.00	2.59	0.00	2.90	6.73	0.01	87.77
0.80	17.31	0.00	2.76	0.00	3.22	9.01	0.00	85.00
1.00	17.15	0.00	2.77	0.00	3.27	9.49	0.01	84.46
1.20	17.32	0.04	2.47	14.70	9.17	41.99	1.73	29.94
1.40	17.86	0.05	2.34	14.97	8.40	37.85	1.82	34.62
1.60	18.72	0.05	3.13	16.17	10.00	36.64	2.96	31.09
1.80	19.45	0.07	2.55	15.62	10.31	29.30	3.37	38.84
2.00	18.14	0.09	1.58	17.48	9.05	17.53	6.09	48.27

Table A.7: Summary of calculated Total Pressure Calibration percent uncertainty for configuration 1.

Nominal Mach	**Typical $P_{T,cal}$, psia**	$u_{P_{T,cal}}$ **psia k = 2**	$u_{P_{T,cal}}$ **UPC due to** $s_{P_{T,bm}}$	$u_{P_{T,cal}}$ **UPC due to** $s_{P_{S,bal}}$	$u_{P_{T,cal}}$ **UPC due to** $s_{P_{T,arr}}$	$u_{P_{T,cal}}$ **UPC due to** $b_{P_{T_{reg}}}$	$u_{P_{T,cal}}$ **UPC due to** $b_{P_{inst}}$	$u_{P_{T,cal}}$ **UPC due to** $b_{P_{Tunif}}$
0.25	15.21	0.00	3.34	0.00	3.71	5.81	0.00	87.14
0.40	15.24	0.00	3.26	0.00	3.71	5.79	0.00	87.24
0.60	17.28	0.00	3.15	0.00	3.58	5.39	0.00	87.88
0.80	16.99	0.00	3.19	0.00	3.54	5.38	0.00	87.89
1.00	16.77	0.00	3.21	0.00	3.46	5.29	0.00	88.04
1.20	16.94	0.11	2.36	16.96	11.38	64.41	0.62	4.27
1.40	17.52	0.12	2.11	15.99	11.03	65.46	0.56	4.84
1.60	18.44	0.13	1.72	16.03	10.42	64.95	0.46	6.42
1.80	19.28	0.15	1.85	17.05	11.33	61.04	0.59	8.14
2.00	18.19	0.21	2.93	33.43	19.85	35.31	0.81	7.67

Table A.8: Summary of calculated Total Pressure Calibration percent uncertainty for configuration 2.

Nominal Mach	**Typical $P_{T,cal}$, psia**	$u_{P_{T,cal}}$ **psia k = 2**	$u_{P_{T,cal}}$ **UPC due to** $s_{P_{T,bm}}$	$u_{P_{T,cal}}$ **UPC due to** $s_{P_{S,bal}}$	$u_{P_{T,cal}}$ **UPC due to** $s_{P_{T,arr}}$	$u_{P_{T,cal}}$ **UPC due to** $b_{P_{T_{reg}}}$	$u_{P_{T,cal}}$ **UPC due to** $b_{P_{inst}}$	$u_{P_{T,cal}}$ **UPC due to** $b_{P_{Tunif}}$
0.25	15.58	0.00	3.03	0.00	3.50	9.19	0.00	84.28
0.40	15.74	0.00	3.02	0.00	3.39	9.16	0.00	84.43
0.60	17.98	0.00	2.61	0.00	3.05	7.84	0.00	86.50
0.80	17.66	0.00	2.67	0.00	3.11	8.59	0.00	85.62
1.00	17.39	0.00	2.82	0.00	3.34	9.04	0.00	84.80
1.20	17.58	0.06	1.38	6.82	5.61	66.32	1.68	18.20
1.40	18.19	0.06	1.31	7.14	6.01	65.82	1.61	18.11
1.60	19.13	0.08	1.55	7.78	5.66	60.66	1.40	22.95
1.80	19.91	0.10	1.62	7.63	6.70	46.64	1.66	35.74
2.00	18.16	0.11	1.36	11.12	7.98	37.61	3.86	38.08

Table A.9: Summary of calculated Total Pressure Calibration percent uncertainty for configuration 3.

Nominal Mach	**Typical $P_{T,cal}$, psia**	$u_{P_{T,cal}}$ **psia k = 2**	$u_{P_{T,cal}}$ **UPC due to** $s_{P_{T,bm}}$	$u_{P_{T,cal}}$ **UPC due to** $s_{P_{S,bal}}$	$u_{P_{T,cal}}$ **UPC due to** $s_{P_{T,arr}}$	$u_{P_{T,cal}}$ **UPC due to** $b_{P_{T_{reg}}}$	$u_{P_{T,cal}}$ **UPC due to** $b_{P_{inst}}$	$u_{P_{T,cal}}$ **UPC due to** $b_{P_{Tunif}}$
0.25	15.56	0.00	1.77	0.00	2.01	8.32	0.00	87.90
0.40	15.74	0.00	1.78	0.00	2.01	8.19	0.00	88.02
0.60	17.94	0.00	1.62	0.00	1.88	7.43	0.01	89.06
0.80	17.64	0.00	1.69	0.00	1.93	8.05	0.00	88.32
1.00	17.35	0.00	1.66	0.00	1.96	8.09	0.00	88.29
1.20	17.52	0.05	0.81	7.60	4.48	54.67	2.15	30.29
1.40	18.08	0.06	0.87	7.33	3.91	53.13	2.21	32.55
1.60	19.07	0.07	0.75	7.46	4.07	49.58	2.64	35.50
1.80	19.82	0.08	0.77	6.74	3.82	41.02	2.92	44.72
2.00	18.23	0.10	1.27	13.26	7.79	29.68	3.96	44.04

Table A.10: Summary of calculated Total Pressure Calibration percent uncertainty for configuration 4.

Nominal Mach	**Typical $P_{T,cal}$, psia**	$u_{P_{T,cal}}$ **psia k = 2**	$u_{P_{T,cal}}$ **UPC due to** $s_{P_{T,bm}}$	$u_{P_{T,cal}}$ **UPC due to** $s_{P_{S,bal}}$	$u_{P_{T,cal}}$ **UPC due to** $s_{P_{T,arr}}$	$u_{P_{T,cal}}$ **UPC due to** $b_{P_{T_{reg}}}$	$u_{P_{T,cal}}$ **UPC due to** $b_{P_{inst}}$	$u_{P_{T,cal}}$ **UPC due to** $b_{P_{Tunif}}$
0.25	15.16	0.00	10.74	0.00	12.53	9.61	0.00	67.12
0.40	15.28	0.00	10.75	0.00	12.16	9.62	0.00	67.47
0.60	17.46	0.00	9.97	0.00	11.44	9.06	0.00	69.52
0.80	17.14	0.00	10.44	0.00	11.93	9.41	0.00	68.23
1.00	16.92	0.00	10.68	0.00	12.11	9.53	0.00	67.68
1.20	17.10	0.05	1.38	10.06	5.06	53.48	1.82	28.21
1.40	17.64	0.06	1.28	10.18	5.25	51.78	1.99	29.51
1.60	18.61	0.07	1.20	11.20	4.81	47.49	2.34	32.96
1.80	19.44	0.08	1.43	8.33	5.66	38.80	2.68	43.11
2.00	18.07	0.11	0.95	14.73	5.56	26.01	3.54	49.21

Table A.11: Summary of calculated Total Pressure Calibration percent uncertainty for configuration 5.

Nominal Mach	**Typical $P_{T,cal}$, psia**	$u_{P_{T,cal}}$ **psia k = 2**	$u_{P_{T,cal}}$ **UPC due to** $s_{P_{T,bm}}$	$u_{P_{T,cal}}$ **UPC due to** $s_{P_{S,bal}}$	$u_{P_{T,cal}}$ **UPC due to** $s_{P_{T,arr}}$	$u_{P_{T,cal}}$ **UPC due to** $b_{P_{T_{reg}}}$	$u_{P_{T,cal}}$ **UPC due to** $b_{P_{inst}}$	$u_{P_{T,cal}}$ **UPC due to** $b_{P_{Tunif}}$
0.25	15.54	0.00	2.43	0.00	2.83	7.10	0.00	87.64
0.40	15.66	0.00	2.50	0.00	2.76	6.93	0.00	87.81
0.60	17.92	0.00	2.03	0.00	2.32	5.43	0.01	90.21
0.80	17.32	0.00	2.41	0.00	2.72	6.91	0.01	87.96
1.00	17.33	0.03	1.53	4.39	3.71	34.85	2.59	52.93
1.20	17.58	0.03	1.38	4.24	3.62	33.62	2.45	54.68
1.40	18.13	0.04	1.74	4.03	4.05	29.10	2.63	58.46
1.60	19.03	0.04	1.59	5.62	4.31	28.93	3.97	55.58
1.80	19.71	0.06	0.98	3.78	2.71	20.11	4.27	68.15
2.00	18.16	0.08	0.65	3.43	2.05	11.83	8.12	73.92

Table A.12: Summary of calculated Total Pressure Calibration percent uncertainty for configuration 6.

A.3 Total Temperature Calibration

Uncertainties that contributed during total temperature calibration include the random uncertainty of the total temperature in the bellmouth ($s_{T_{T,bm}}$), the random uncertainty of the total temperature on the array ($s_{T_{T,arr}}$), random uncertainty in the total temperature calibration regression ($s_{T_{reg}}$), systematic uncertainty due to instrumentation ($b_{T_{inst}}$), and systematic uncertainty due to total temperature uniformity ($b_{T_{T,unif}}$). During the temperature calibration, the thermocouple measurements include individual instrumentation errors as well as correlated errors due to their common reference.

The uncertainty flow chart is shown in Figure A.6. Uncertainty results are presented as percent contributions as bar charts in Figure A.7 and in tabular form in Tables A.13 - A.18 for all configurations. The uncertainty of the total temperature calibration is dominated by the instrumentation uncertainty.

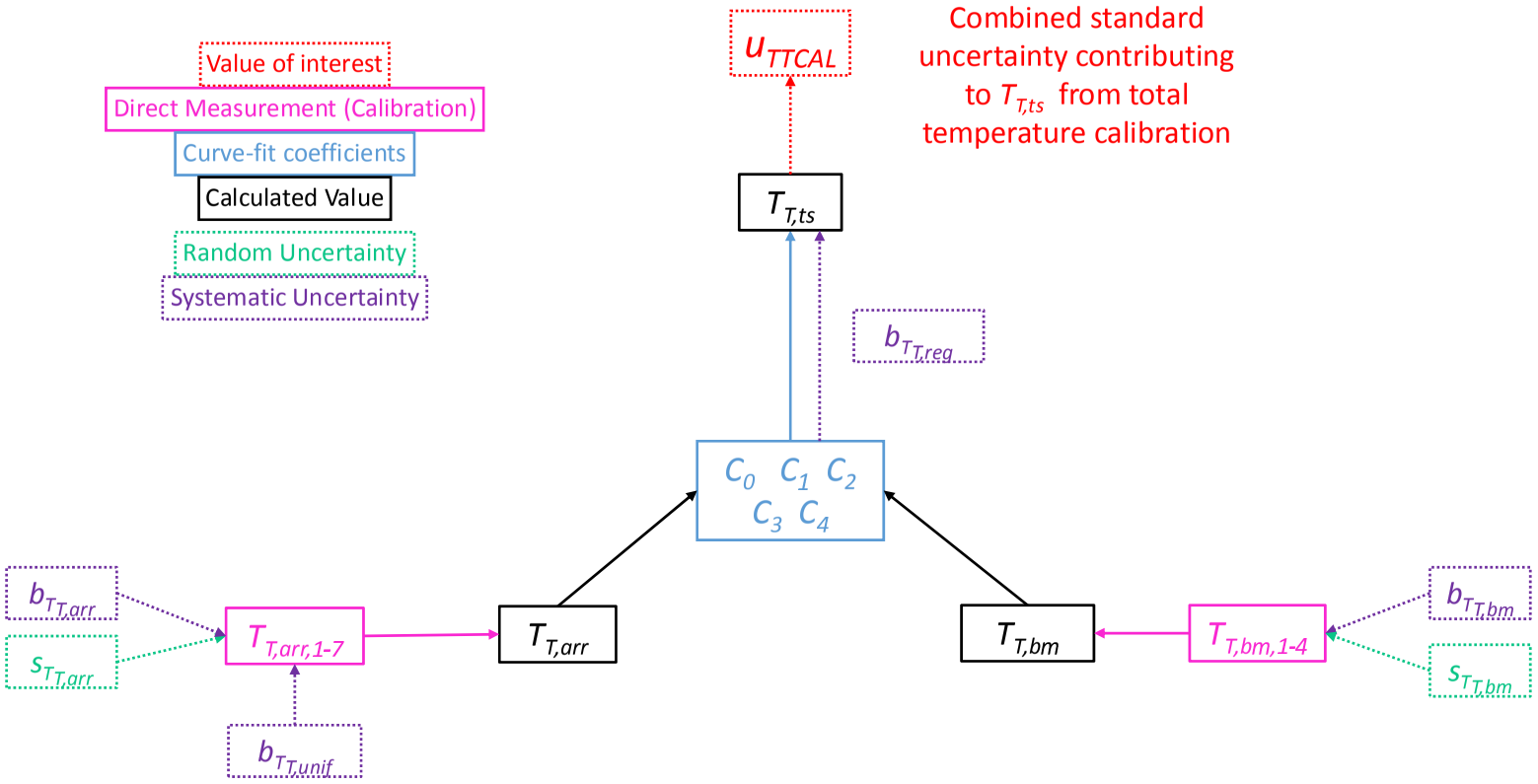

Figure A.6: Flow chart depicting the propagation of uncertainties for total temperature calibration.

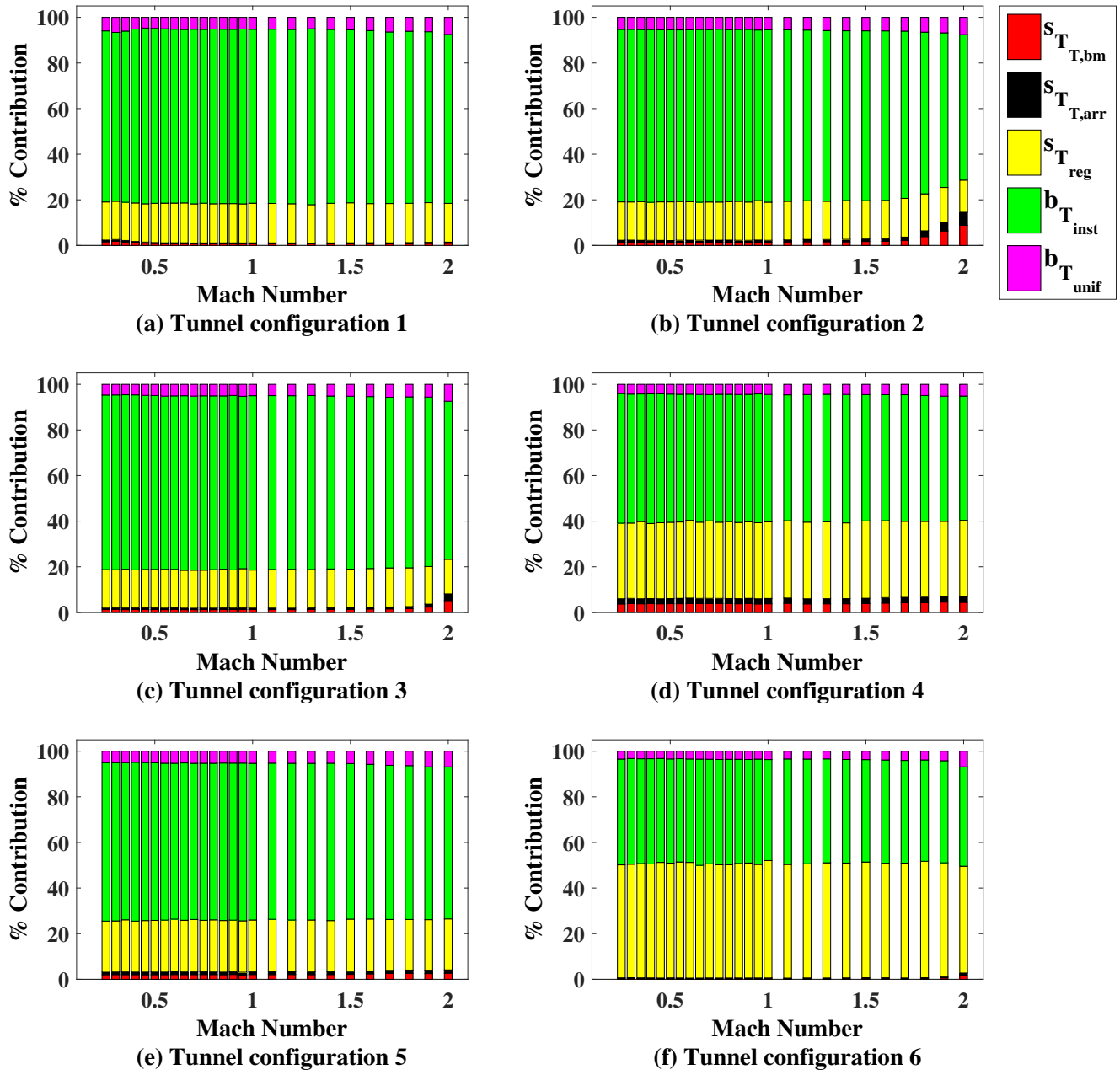

Figure A.7: Percent contributions from all elemental uncertainty sources to the combined uncertainty of the total temperature calibration, as a function of nominal Mach number

Nominal Mach	**Typical $T_{T,cal}$, °R**	$u_{T_{T,cal}}$ **°R k = 2**	$u_{T_{T,cal}}$ **UPC due to** $s_{T_{T,bm}}$	$u_{T_{T,cal}}$ **UPC due to** $s_{T_{T,arr}}$	$u_{T_{T,cal}}$ **UPC due to** $b_{T_{reg}}$	$u_{T_{T,cal}}$ **UPC due to** $b_{T_{inst}}$	$u_{T_{T,cal}}$ **UPC due to** $b_{T_{unif}}$
0.25	519.61	2.77	1.60	0.77	16.71	74.99	5.93
0.40	525.30	2.75	1.21	0.53	16.90	76.23	5.14
0.60	556.67	2.74	0.76	0.41	17.40	76.24	5.19
0.80	565.39	2.73	0.74	0.37	17.15	76.59	5.14
1.00	559.47	2.72	0.75	0.38	17.38	76.26	5.22
1.20	576.39	2.74	0.74	0.36	17.18	76.43	5.29
1.40	585.22	2.71	0.74	0.36	17.36	76.26	5.28
1.60	604.06	2.72	0.78	0.40	17.17	75.83	5.82
1.80	629.67	2.75	0.84	0.41	17.23	75.42	6.11
2.00	648.53	2.74	0.95	0.51	16.98	74.04	7.51

Table A.13: Summary of calculated Total Temperature Calibration percent uncertainty for configuration 1.

Nominal Mach	**Typical $T_{T,cal}$, °R**	$u_{T_{T,cal}}$ **°R k = 2**	$u_{T_{T,cal}}$ **UPC due to** $s_{T_{T,bm}}$	$u_{T_{T,cal}}$ **UPC due to** $s_{T_{T,arr}}$	$u_{T_{T,cal}}$ **UPC due to** $b_{T_{reg}}$	$u_{T_{T,cal}}$ **UPC due to** $b_{T_{inst}}$	$u_{T_{T,cal}}$ **UPC due to** $b_{T_{unif}}$
0.25	532.53	2.78	1.39	0.90	16.82	75.62	5.28
0.40	538.07	2.75	1.41	0.81	16.68	75.76	5.33
0.60	565.80	2.73	1.42	0.87	16.97	75.28	5.46
0.80	567.77	2.74	1.44	0.90	16.92	75.35	5.39
1.00	567.88	2.75	1.45	0.81	16.72	75.62	5.41
1.20	581.81	2.74	1.61	1.02	16.98	74.81	5.58
1.40	589.68	2.74	1.60	1.08	17.01	74.42	5.89
1.60	605.22	2.74	1.80	1.06	16.89	74.31	5.94
1.80	626.79	2.83	3.86	2.56	16.20	70.88	6.49
2.00	639.01	2.99	8.84	5.71	14.08	63.78	7.59

Table A.14: Summary of calculated Total Temperature Calibration percent uncertainty for configuration 2.

Nominal Mach	**Typical $T_{T,cal}$, °R**	$u_{T_{T,cal}}$ **°R k = 2**	$u_{T_{T,cal}}$ **UPC due to** $s_{T_{T,bm}}$	$u_{T_{T,cal}}$ **UPC due to** $s_{T_{T,arr}}$	$u_{T_{T,cal}}$ **UPC due to** $b_{T_{reg}}$	$u_{T_{T,cal}}$ **UPC due to** $b_{T_{inst}}$	$u_{T_{T,cal}}$ **UPC due to** $b_{T_{unif}}$
0.25	516.18	2.77	1.24	0.66	16.84	76.55	4.71
0.40	522.30	2.73	1.28	0.66	16.70	76.73	4.63
0.60	551.17	2.72	1.29	0.68	16.90	76.07	5.06
0.80	553.52	2.74	1.20	0.68	16.86	76.19	5.06
1.00	553.62	2.74	1.23	0.66	16.67	76.45	4.98
1.20	566.43	2.74	1.22	0.65	17.01	76.13	4.99
1.40	574.75	2.72	1.27	0.69	17.07	75.82	5.14
1.60	590.75	2.73	1.47	0.85	16.91	75.41	5.36
1.80	614.36	2.74	1.65	0.90	16.99	74.96	5.50
2.00	640.12	2.86	5.19	2.93	15.17	69.28	7.43

Table A.15: Summary of calculated Total Temperature Calibration percent uncertainty for configuration 3.

Nominal Mach	**Typical $T_{T,cal}$, °R**	$u_{T_{T,cal}}$ **°R k = 2**	$u_{T_{T,cal}}$ **UPC due to** $s_{T_{T,bm}}$	$u_{T_{T,cal}}$ **UPC due to** $s_{T_{T,arr}}$	$u_{T_{T,cal}}$ **UPC due to** $b_{T_{reg}}$	$u_{T_{T,cal}}$ **UPC due to** $b_{T_{inst}}$	$u_{T_{T,cal}}$ **UPC due to** $b_{T_{unif}}$
0.25	511.58	3.20	3.68	2.29	33.13	56.88	4.02
0.40	517.71	3.20	3.83	2.21	32.93	56.84	4.20
0.60	547.83	3.18	3.90	2.36	34.08	55.34	4.32
0.80	550.36	3.20	3.84	2.23	33.70	55.84	4.39
1.00	550.74	3.20	3.78	2.31	33.56	55.88	4.46
1.20	563.77	3.18	3.72	2.24	33.59	55.95	4.49
1.40	571.57	3.19	3.77	2.25	33.21	56.31	4.46
1.60	587.92	3.18	4.06	2.41	33.72	55.25	4.55
1.80	608.76	3.19	4.27	2.62	33.01	55.20	4.91
2.00	622.76	3.19	4.39	2.62	33.33	54.51	5.15

Table A.16: Summary of calculated Total Temperature Calibration percent uncertainty for configuration 4.

Nominal Mach	**Typical $T_{T,cal}$, °R**	$u_{T_{T,cal}}$ **°R k = 2**	$u_{T_{T,cal}}$ **UPC due to** $s_{T_{T,bm}}$	$u_{T_{T,cal}}$ **UPC due to** $s_{T_{T,arr}}$	$u_{T_{T,cal}}$ **UPC due to** $b_{T_{reg}}$	$u_{T_{T,cal}}$ **UPC due to** $b_{T_{inst}}$	$u_{T_{T,cal}}$ **UPC due to** $b_{T_{unif}}$
0.25	529.35	2.89	2.03	1.09	22.40	69.51	4.98
0.40	535.08	2.88	2.04	1.14	22.34	69.63	4.86
0.60	558.96	2.86	2.09	1.20	23.09	68.34	5.29
0.80	561.26	2.88	2.07	1.15	22.86	68.63	5.29
1.00	560.11	2.88	2.08	1.17	22.76	68.67	5.33
1.20	574.94	2.86	2.08	1.20	22.70	68.72	5.30
1.40	582.37	2.87	2.07	1.19	22.48	68.98	5.27
1.60	599.35	2.87	2.38	1.30	22.74	67.80	5.77
1.80	623.10	2.88	2.63	1.42	22.18	67.45	6.32
2.00	636.39	2.89	2.66	1.46	22.36	66.66	6.86

Table A.17: Summary of calculated Total Temperature Calibration percent uncertainty for configuration 5.

Nominal Mach	**Typical $T_{T,cal}$, °R**	$u_{T_{T,cal}}$ **°R k = 2**	$u_{T_{T,cal}}$ **UPC due to** $s_{T_{T,bm}}$	$u_{T_{T,cal}}$ **UPC due to** $s_{T_{T,arr}}$	$u_{T_{T,cal}}$ **UPC due to** $b_{T_{reg}}$	$u_{T_{T,cal}}$ **UPC due to** $b_{T_{inst}}$	$u_{T_{T,cal}}$ **UPC due to** $b_{T_{unif}}$
0.25	513.96	3.59	0.38	0.26	49.54	46.38	3.44
0.40	519.35	3.52	0.38	0.25	49.98	46.12	3.29
0.60	548.49	3.50	0.36	0.17	50.74	45.34	3.40
0.80	565.73	3.52	0.34	0.23	49.67	46.23	3.54
1.00	551.37	3.51	0.38	0.21	51.46	44.30	3.65
1.20	563.95	3.56	0.36	0.24	50.05	45.89	3.45
1.40	572.61	3.51	0.40	0.24	50.33	45.41	3.62
1.60	591.39	3.53	0.42	0.26	50.21	45.27	3.84
1.80	618.21	3.52	0.40	0.30	51.06	44.42	3.82
2.00	641.06	3.66	1.51	1.24	46.83	43.55	6.86

Table A.18: Summary of calculated Total Temperature Calibration percent uncertainty for configuration 6.

Appendix B: Mach Number Uncertainty

Recall from Section 4.2 that the uncertainty in test section Mach number propagates as shown in Figures B.1 and B.2. Results for uncertainty in Mach number for configuration 1 were presented in Section 5. Results for configurations 2-6 are presented in this Appendix. Bar charts depicting the percent contributions are shown, followed by tabulated results detailing dimensional and percent contributions for random, systematic, and total uncertainty.

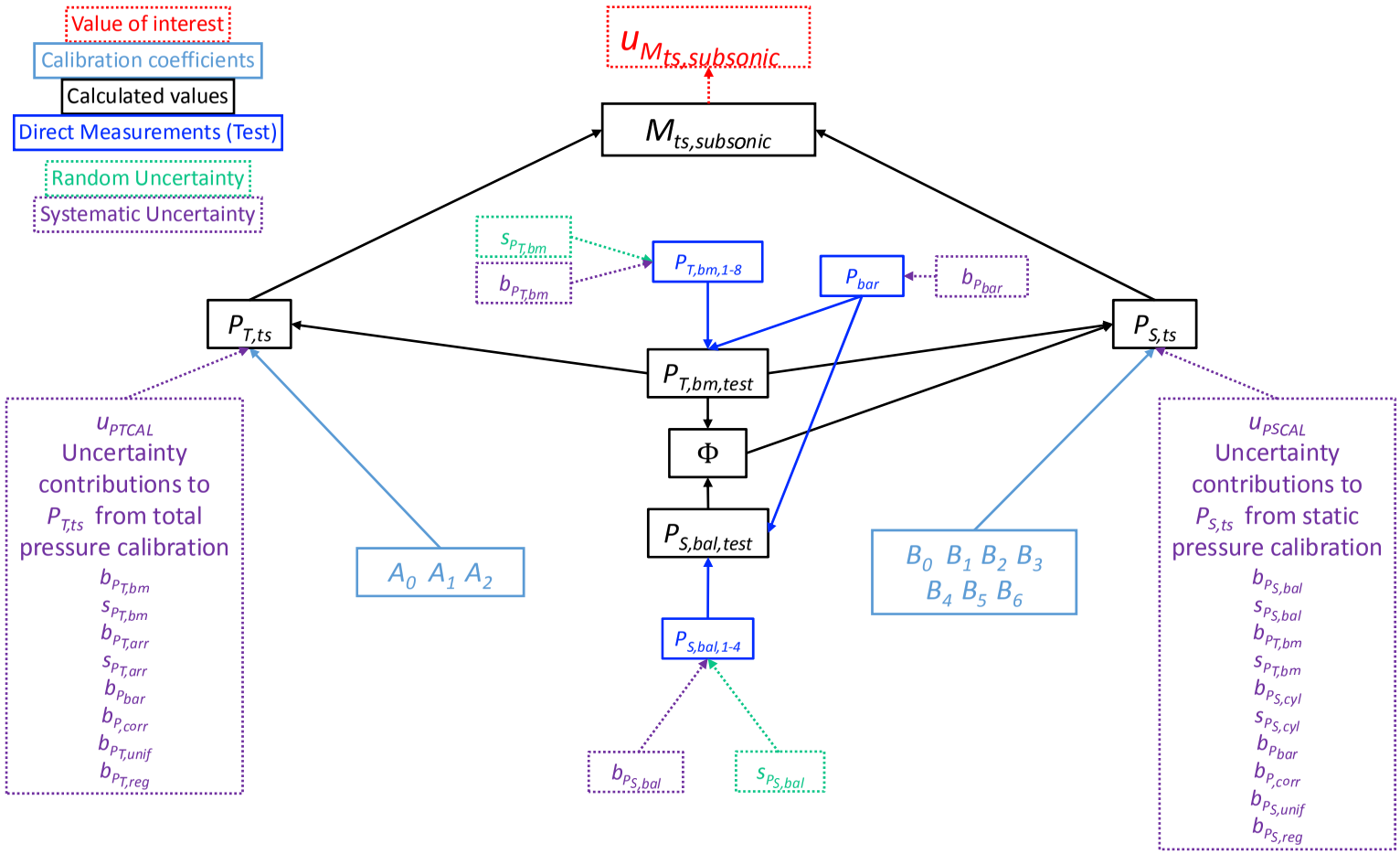

Figure B.1: Flow chart depicting the propagation of uncertainties in Mach number calculation: subsonic flow range

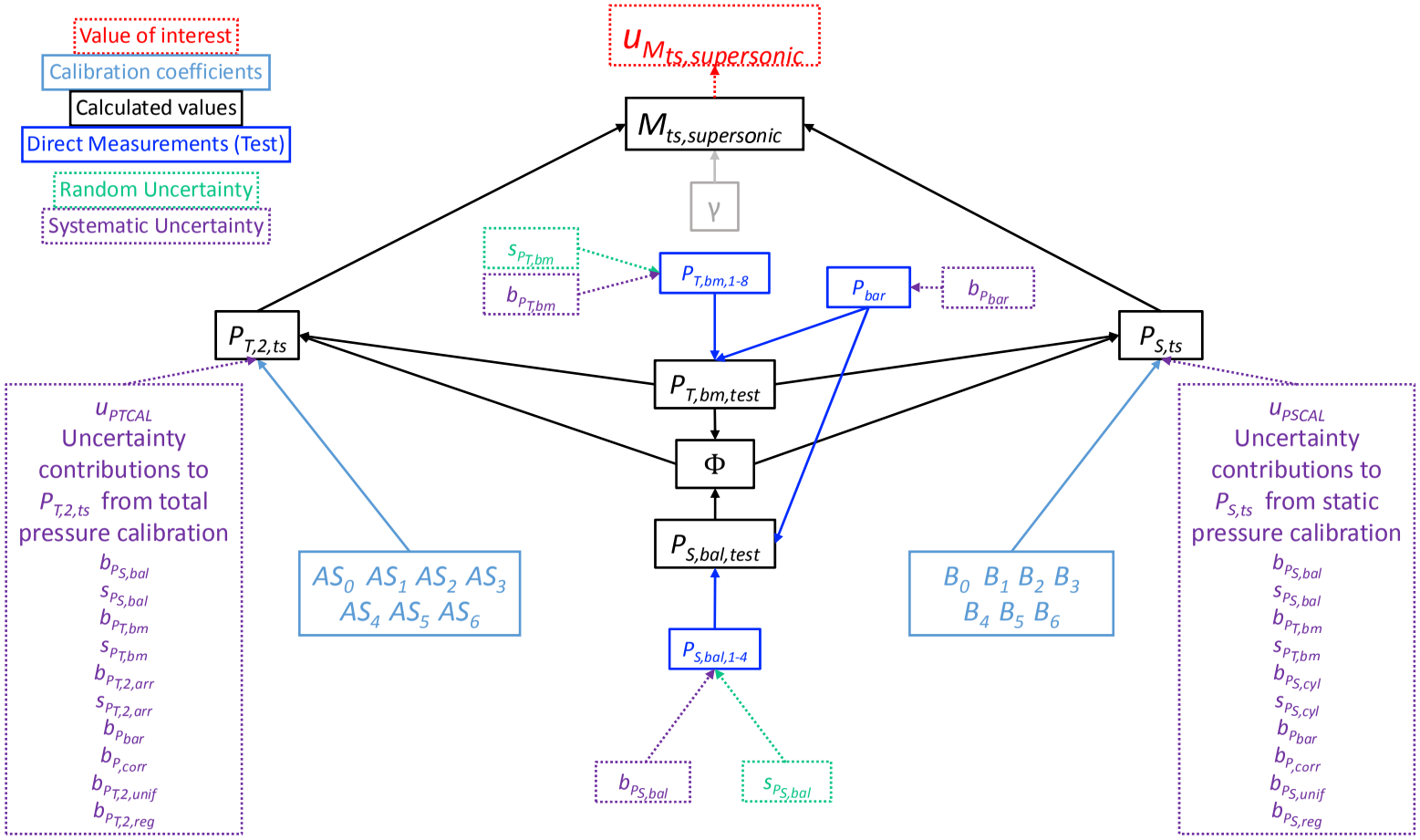

Figure B.2: Flow chart depicting the propagation of uncertainties in Mach number calculation: supersonic flow range

B.1 Random Uncertainty Results for Configurations 2-6

The random uncertainty in Mach number for every configuration is shown in Figure B.3. In the subsonic range, the uncertainty is less than 0.0005 for all configurations. Supersonically there is a bit more spread, but all configurations follow a similar trend. The random uncertainty in Mach number is below 0.005 for all configurations except for configuration 2 at the highest Mach settings.

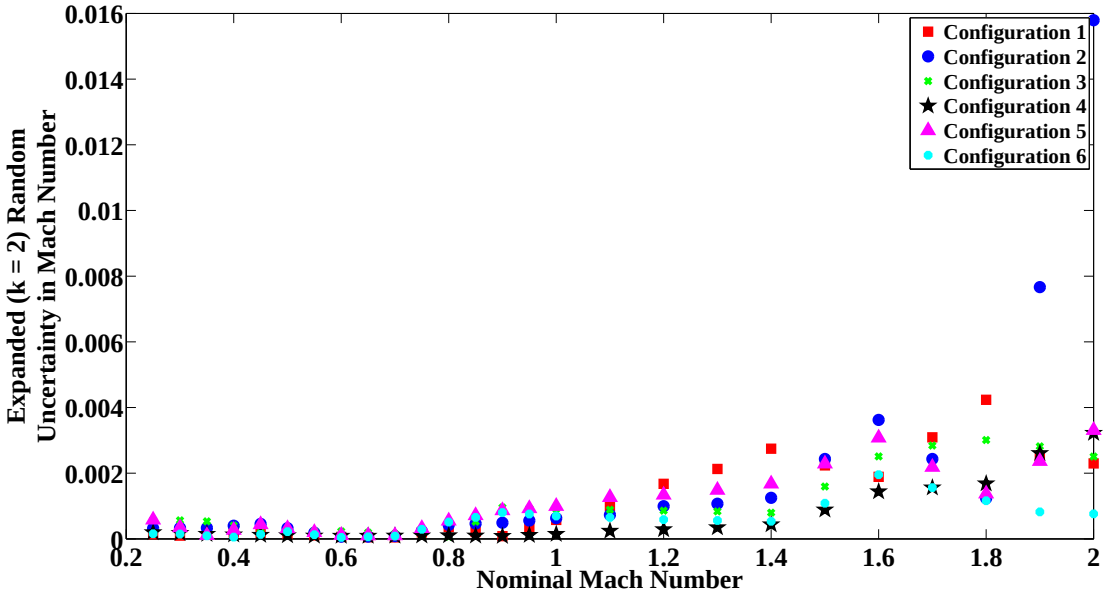

Figure B.3: Expanded random uncertainty of M_{ts} as a function of nominal Mach number for all configurations. The red squares are configuration 1, blue circles are configuration 2, green x's are configuration 3, black stars are configuration 4, purple triangles are configuration 5, and cyan dots are configuration 6.

The elemental random uncertainties contributing to random uncertainty in Mach number are from measurements $P_{T,bm}$ and $P_{S,bal}$. The percent contribution of each of these elemental uncertainties to the total random uncertainty in M_{ts} are shown in Figure B.4. Random variation of the static pressure in the balance chamber drives the random uncertainty in M_{ts}. The tabulated results are shown in Tables B.1 - B.5.

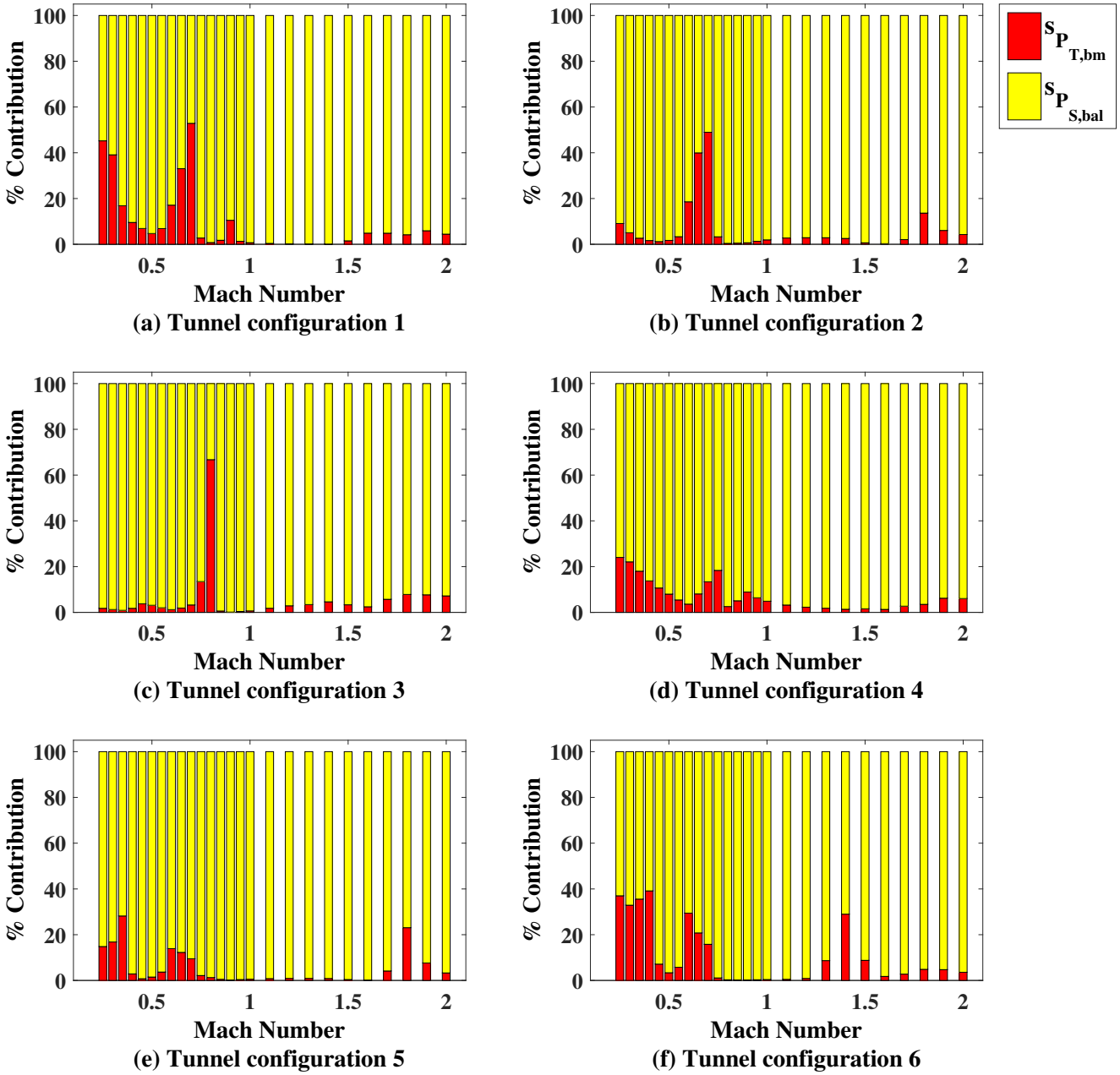

Figure B.4: Random UPC of M_{ts} as a function of nominal Mach number for all configurations. Red is the random uncertainty of the total pressure in the bellmouth, yellow is the random uncertainty of the static pressure in the balance chamber.

Nominal Mach	**Typical** M_{ts}	$s_{M_{ts}}$ **k = 2**	$s_{M_{ts}}$ **due to** $s_{P_{T,bm}}$ **k = 2**	$s_{M_{ts}}$ **due to** $s_{P_{S,bal}}$ **k = 2**	$s_{M_{ts}}$ **UPC due to** $s_{P_{T,bm}}$	$s_{M_{ts}}$ **UPC due to** $s_{P_{S,bal}}$
0.25	0.25	0.0003	0.0001	0.0003	9.1	90.9
0.40	0.41	0.0004	0.0001	0.0004	1.6	98.4
0.60	0.61	0.0001	0.0000	0.0001	18.6	81.4
0.80	0.81	0.0004	0.0000	0.0004	0.4	99.6
1.00	1.00	0.0006	0.0001	0.0006	1.9	98.1
1.20	1.20	0.0010	0.0002	0.0010	2.9	97.1
1.40	1.35	0.0013	0.0002	0.0012	2.6	97.4
1.60	1.55	0.0036	0.0002	0.0036	0.3	99.7
1.80	1.75	0.0012	0.0005	0.0012	13.6	86.4
2.00	1.96	0.0158	0.0033	0.0155	4.3	95.7

Table B.1: Summary of calculated Mach Number random uncertainty with 95% level of confidence for configuration 2.

Nominal Mach	**Typical** M_{ts}	$s_{M_{ts}}$ **k = 2**	$s_{M_{ts}}$ **due to** $s_{P_{T,bm}}$ **k = 2**	$s_{M_{ts}}$ **due to** $s_{P_{S,bal}}$ **k = 2**	$s_{M_{ts}}$ **UPC due to** $s_{P_{T,bm}}$	$s_{M_{ts}}$ **UPC due to** $s_{P_{S,bal}}$
0.25	0.25	0.0006	0.0001	0.0006	1.8	98.2
0.40	0.41	0.0004	0.0001	0.0004	1.8	98.2
0.60	0.61	0.0002	0.0000	0.0002	1.2	98.8
0.80	0.80	0.0001	0.0001	0.0000	66.7	33.3
1.00	0.99	0.0009	0.0001	0.0009	0.6	99.4
1.20	1.20	0.0009	0.0001	0.0008	2.9	97.1
1.40	1.35	0.0008	0.0002	0.0008	4.6	95.4
1.60	1.56	0.0025	0.0004	0.0025	2.5	97.5
1.80	1.77	0.0030	0.0008	0.0029	7.8	92.2
2.00	1.97	0.0025	0.0007	0.0024	7.2	92.8

Table B.2: Summary of calculated Mach Number random uncertainty with 95% level of confidence for configuration 3.

Nominal Mach	**Typical** M_{ts}	$s_{M_{ts}}$ **k = 2**	$s_{M_{ts}}$ **due to** $s_{P_{T,bm}}$ **k = 2**	$s_{M_{ts}}$ **due to** $s_{P_{S,bal}}$ **k = 2**	$s_{M_{ts}}$ **UPC due to** $s_{P_{T,bm}}$	$s_{M_{ts}}$ **UPC due to** $s_{P_{S,bal}}$
0.25	0.25	0.0002	0.0001	0.0002	24.0	76.0
0.40	0.41	0.0001	0.0000	0.0001	13.8	86.2
0.60	0.61	0.0001	0.0000	0.0001	3.6	96.4
0.80	0.81	0.0001	0.0000	0.0001	2.6	97.4
1.00	1.00	0.0001	0.0000	0.0001	4.9	95.1
1.20	1.19	0.0003	0.0000	0.0003	2.3	97.7
1.40	1.35	0.0004	0.0001	0.0004	1.4	98.6
1.60	1.56	0.0014	0.0002	0.0014	1.3	98.7
1.80	1.78	0.0017	0.0003	0.0017	3.5	96.5
2.00	1.99	0.0032	0.0008	0.0031	6.0	94.0

Table B.3: Summary of calculated Mach Number random uncertainty with 95% level of confidence for configuration 4.

Nominal Mach	**Typical** M_{ts}	$s_{M_{ts}}$ **k = 2**	$s_{M_{ts}}$ **due to** $s_{P_{T,bm}}$ **k = 2**	$s_{M_{ts}}$ **due to** $s_{P_{S,bal}}$ **k = 2**	$s_{M_{ts}}$ **UPC due to** $s_{P_{T,bm}}$	$s_{M_{ts}}$ **UPC due to** $s_{P_{S,bal}}$
0.25	0.25	0.0006	0.0002	0.0005	14.8	85.2
0.40	0.40	0.0003	0.0000	0.0003	2.9	97.1
0.60	0.60	0.0001	0.0000	0.0001	13.9	86.1
0.80	0.80	0.0006	0.0001	0.0005	1.3	98.7
1.00	1.00	0.0010	0.0001	0.0010	0.6	99.4
1.20	1.19	0.0013	0.0001	0.0013	0.9	99.1
1.40	1.35	0.0017	0.0002	0.0017	0.9	99.1
1.60	1.55	0.0031	0.0001	0.0031	0.2	99.8
1.80	1.77	0.0014	0.0007	0.0012	23.1	76.9
2.00	1.98	0.0033	0.0006	0.0033	3.3	96.7

Table B.4: Summary of calculated Mach Number random uncertainty with 95% level of confidence for configuration 5.

Nominal Mach	**Typical** M_{ts}	$s_{M_{ts}}$ **k = 2**	$s_{M_{ts}}$ **due to** $s_{P_{T,bm}}$ **k = 2**	$s_{M_{ts}}$ **due to** $s_{P_{S,bal}}$ **k = 2**	$s_{M_{ts}}$ **UPC due to** $s_{P_{T,bm}}$	$s_{M_{ts}}$ **UPC due to** $s_{P_{S,bal}}$
0.25	0.25	0.0002	0.0001	0.0001	37.0	63.0
0.40	0.41	0.0001	0.0000	0.0000	39.1	60.9
0.60	0.60	0.0000	0.0000	0.0000	29.4	70.6
0.80	0.80	0.0005	0.0000	0.0005	0.3	99.7
1.00	1.02	0.0007	0.0000	0.0007	0.4	99.6
1.20	1.19	0.0006	0.0001	0.0006	0.9	99.1
1.40	1.36	0.0005	0.0003	0.0005	29.0	71.0
1.60	1.56	0.0020	0.0003	0.0019	1.8	98.2
1.80	1.79	0.0012	0.0003	0.0011	4.9	95.1
2.00	1.98	0.0008	0.0001	0.0007	3.6	96.4

Table B.5: Summary of calculated Mach Number random uncertainty with 95% level of confidence for configuration 6.

B.2 Systematic Uncertainty Results for Configurations 2-6

The systematic uncertainty in the test section Mach number is shown for all configurations in Figure B.5. All configurations follow a similar trend, remaining below 0.006 subsonically, then increasing supersonically up to 0.02 (0.027 for configuration 2).

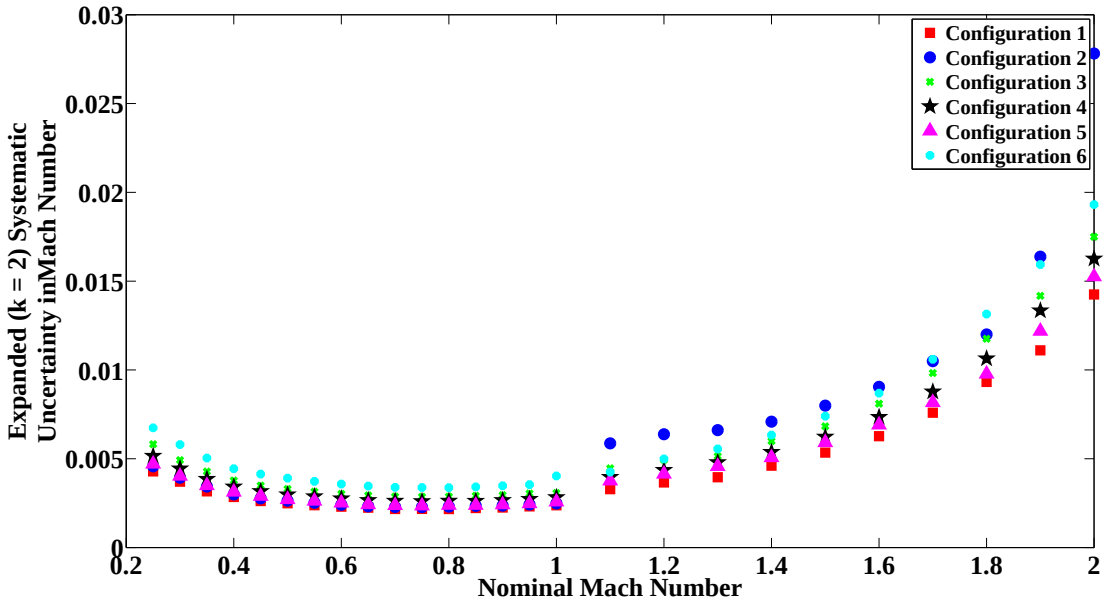

Figure B.5: Systematic uncertainty of M_{ts} as a function of nominal Mach number for all configurations. The red squares are configuration 1, blue circles are configuration 2, green x's are configuration 3, black stars are configuration 4, purple triangles are configuration 5, and cyan dots are configuration 6.

The systematic uncertainty in M_{ts} is due to systematic contributions from total and static pressure calibrations (b_{PTCAL} and b_{PSCAL}), as well as instrumentation uncertainties in test-time bellmouth total pressure, balance chamber static pressure, and barometric pressure (combined as $b_{P_{inst}}$). The percent contributions of each of these uncertainties to the combined systematic uncertainty in M_{ts} are shown in Figure B.6. The tabulated details are shown in Tables B.6 - B.10.

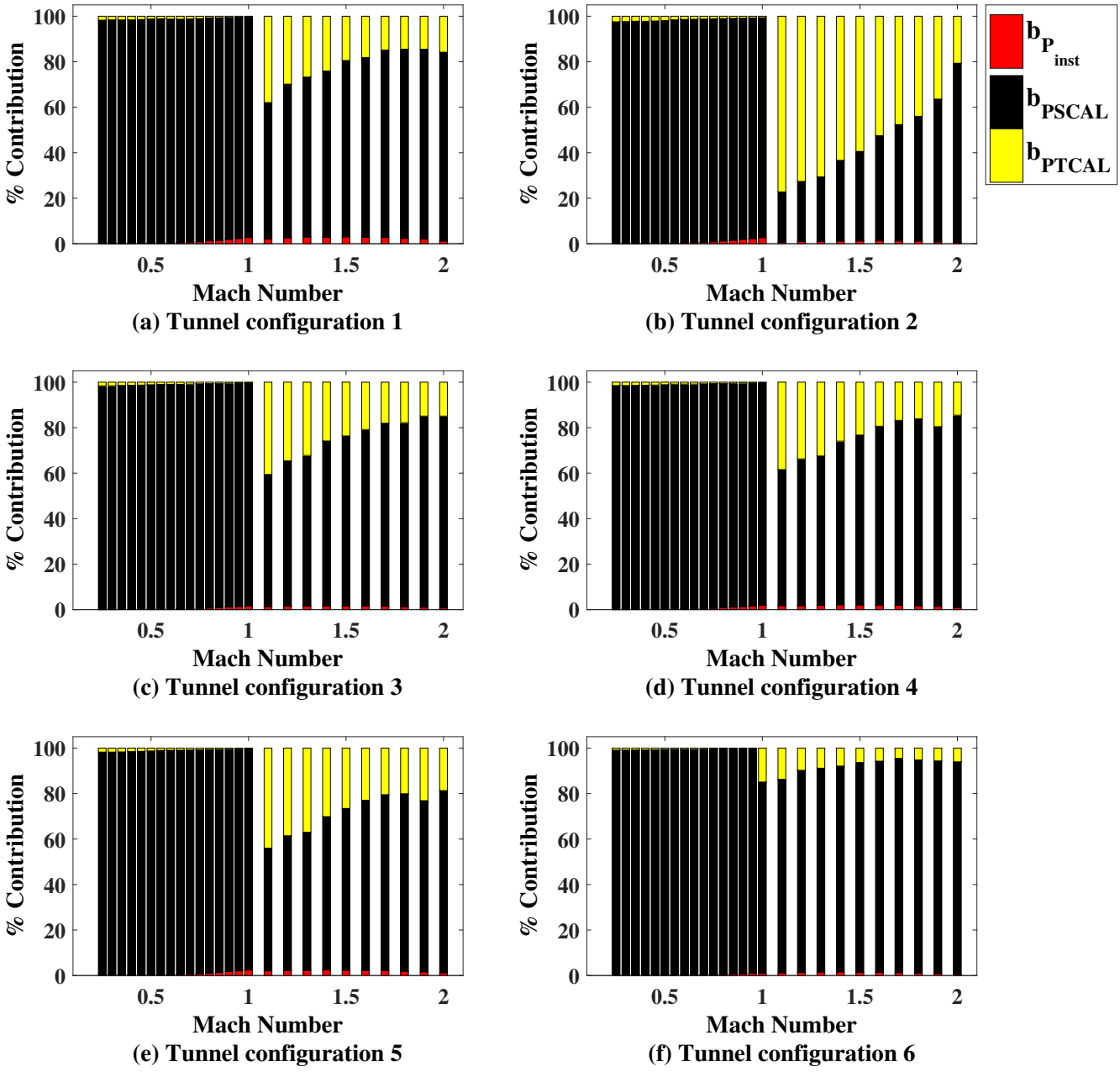

Figure B.6: Systematic UPC of M_{ts} as a function of nominal Mach number for all configurations. Red is the systematic uncertainty due to pressure instrumentation, yellow is the systematic uncertainty due to total pressure calibration, and black is the systematic uncertainty due to static pressure calibration.

Nominal Mach	**Typical** M_{ts}	$b_{M_{ts}}$ **k = 2**	$b_{M_{ts}}$ **due to** $b_{P_{Inst}}$ **k = 2**	$b_{M_{ts}}$ b_{PSCAL} **k = 2**	$b_{M_{ts}}$ b_{PTCAL} **k = 2**	$b_{M_{ts}}$ **UPC due to** $b_{P_{Inst}}$	$b_{M_{ts}}$ **UPC due to** b_{PSCAL}	$b_{M_{ts}}$ **UPC due to** b_{PTCAL}
0.25	0.25	0.0046	0.0001	0.0045	0.0007	0.0	97.5	2.5
0.40	0.41	0.0030	0.0001	0.0030	0.0004	0.1	97.6	2.2
0.60	0.61	0.0024	0.0001	0.0024	0.0003	0.4	98.2	1.4
0.80	0.81	0.0023	0.0003	0.0023	0.0002	1.2	97.8	1.0
1.00	1.00	0.0025	0.0004	0.0024	0.0002	2.7	96.7	0.6
1.20	1.20	0.0064	0.0006	0.0033	0.0054	0.9	26.4	72.6
1.40	1.35	0.0071	0.0008	0.0042	0.0056	1.2	35.5	63.4
1.60	1.55	0.0090	0.0010	0.0061	0.0066	1.3	46.2	52.5
1.80	1.75	0.0120	0.0013	0.0089	0.0080	1.2	54.8	44.0
2.00	1.96	0.0278	0.0018	0.0247	0.0126	0.4	78.9	20.6

Table B.6: Summary of calculated Mach Number systematic uncertainty with 95% level of confidence for configuration 2.

Nominal Mach	**Typical** M_{ts}	$b_{M_{ts}}$ **k = 2**	$b_{M_{ts}}$ **due to** $b_{P_{Inst}}$ **k = 2**	$b_{M_{ts}}$ b_{PSCAL} **k = 2**	$b_{M_{ts}}$ b_{PTCAL} **k = 2**	$b_{M_{ts}}$ **UPC due to** $b_{P_{Inst}}$	$b_{M_{ts}}$ **UPC due to** b_{PSCAL}	$b_{M_{ts}}$ **UPC due to** b_{PTCAL}
0.25	0.25	0.0058	0.0001	0.0058	0.0007	0.0	98.4	1.6
0.40	0.41	0.0038	0.0001	0.0037	0.0004	0.1	98.5	1.4
0.60	0.61	0.0030	0.0001	0.0030	0.0003	0.2	98.9	0.9
0.80	0.80	0.0029	0.0002	0.0028	0.0002	0.7	98.7	0.6
1.00	0.99	0.0031	0.0004	0.0030	0.0002	1.6	98.0	0.4
1.20	1.20	0.0049	0.0006	0.0039	0.0029	1.5	63.9	34.6
1.40	1.35	0.0060	0.0008	0.0051	0.0030	1.6	72.6	25.9
1.60	1.56	0.0081	0.0010	0.0071	0.0037	1.6	77.6	20.8
1.80	1.77	0.0118	0.0013	0.0106	0.0050	1.3	80.9	17.8
2.00	1.97	0.0175	0.0015	0.0161	0.0068	0.7	84.4	14.9

Table B.7: Summary of calculated Mach Number systematic uncertainty with 95% level of confidence for configuration 3.

Nominal Mach	**Typical** M_{ts}	$b_{M_{ts}}$ **k = 2**	$b_{M_{ts}}$ **due to** $b_{P_{Inst}}$ **k = 2**	$b_{M_{ts}}$ b_{PSCAL} **k = 2**	$b_{M_{ts}}$ b_{PTCAL} **k = 2**	$b_{M_{ts}}$ **UPC due to** $b_{P_{Inst}}$	$b_{M_{ts}}$ **UPC due to** b_{PSCAL}	$b_{M_{ts}}$ **UPC due to** b_{PTCAL}
0.25	0.25	0.0052	0.0001	0.0051	0.0006	0.0	98.5	1.5
0.40	0.41	0.0034	0.0001	0.0034	0.0004	0.1	98.6	1.3
0.60	0.61	0.0028	0.0001	0.0027	0.0003	0.2	98.9	0.8
0.80	0.81	0.0026	0.0002	0.0026	0.0002	0.8	98.7	0.5
1.00	1.00	0.0028	0.0004	0.0028	0.0002	1.8	97.8	0.4
1.20	1.19	0.0044	0.0006	0.0035	0.0025	1.7	64.5	33.7
1.40	1.35	0.0054	0.0008	0.0046	0.0027	2.1	72.0	25.9
1.60	1.56	0.0073	0.0010	0.0065	0.0032	2.0	78.6	19.4
1.80	1.78	0.0106	0.0014	0.0096	0.0043	1.7	82.2	16.1
2.00	1.99	0.0163	0.0016	0.0149	0.0062	1.0	84.5	14.5

Table B.8: Summary of calculated Mach Number systematic uncertainty with 95% level of confidence for configuration 4.

Nominal Mach	**Typical** M_{ts}	$b_{M_{ts}}$ **k = 2**	$b_{M_{ts}}$ **due to** $b_{P_{Inst}}$ **k = 2**	$b_{M_{ts}}$ b_{PSCAL} **k = 2**	$b_{M_{ts}}$ b_{PTCAL} **k = 2**	$b_{M_{ts}}$ **UPC due to** $b_{P_{Inst}}$	$b_{M_{ts}}$ **UPC due to** b_{PSCAL}	$b_{M_{ts}}$ **UPC due to** b_{PTCAL}
0.25	0.25	0.0047	0.0001	0.0047	0.0006	0.0	98.2	1.8
0.40	0.40	0.0031	0.0001	0.0031	0.0004	0.1	98.3	1.5
0.60	0.60	0.0025	0.0001	0.0025	0.0002	0.3	98.8	0.9
0.80	0.80	0.0024	0.0002	0.0024	0.0002	1.0	98.3	0.6
1.00	1.00	0.0026	0.0004	0.0025	0.0002	2.4	97.2	0.4
1.20	1.19	0.0041	0.0006	0.0032	0.0026	2.1	59.4	38.5
1.40	1.35	0.0051	0.0008	0.0042	0.0028	2.4	67.4	30.2
1.60	1.55	0.0069	0.0010	0.0060	0.0033	2.2	74.9	22.9
1.80	1.77	0.0098	0.0013	0.0086	0.0044	1.9	78.0	20.1
2.00	1.98	0.0153	0.0017	0.0137	0.0066	1.2	80.1	18.7

Table B.9: Summary of calculated Mach Number systematic uncertainty with 95% level of confidence for configuration 5.

Nominal Mach	**Typical** M_{ts}	$b_{M_{ts}}$ **k = 2**	$b_{M_{ts}}$ **due to** $b_{P_{Inst}}$ **k = 2**	$b_{M_{ts}}$ b_{PSCAL} **k = 2**	$b_{M_{ts}}$ b_{PTCAL} **k = 2**	$b_{M_{ts}}$ **UPC due to** $b_{P_{Inst}}$	$b_{M_{ts}}$ **UPC due to** b_{PSCAL}	$b_{M_{ts}}$ **UPC due to** b_{PTCAL}
0.25	0.25	0.0067	0.0001	0.0067	0.0006	0.0	99.1	0.9
0.40	0.41	0.0044	0.0001	0.0044	0.0004	0.1	99.1	0.8
0.60	0.60	0.0036	0.0001	0.0036	0.0003	0.1	99.3	0.6
0.80	0.80	0.0034	0.0002	0.0034	0.0002	0.5	99.1	0.3
1.00	1.02	0.0040	0.0004	0.0037	0.0016	1.0	84.1	14.9
1.20	1.19	0.0050	0.0006	0.0047	0.0016	1.4	88.8	9.8
1.40	1.36	0.0063	0.0008	0.0060	0.0018	1.5	90.5	7.9
1.60	1.56	0.0087	0.0010	0.0084	0.0021	1.4	92.8	5.8
1.80	1.79	0.0131	0.0013	0.0127	0.0030	1.0	93.8	5.2
2.00	1.98	0.0193	0.0014	0.0187	0.0047	0.5	93.4	6.0

Table B.10: Summary of calculated Mach Number systematic uncertainty with 95% level of confidence for configuration 6.

B.3 Total Uncertainty Results for Configurations 2-6

The total uncertainty in M_{ts} for each of the six configurations is shown in Figure B.7. Each configuration follows a very similar trend, although values for configuration 2 are slightly higher than the other configurations. The combined uncertainty in M_{ts} is tabulated for configurations 2-6 in Tables B.11 - B.15.

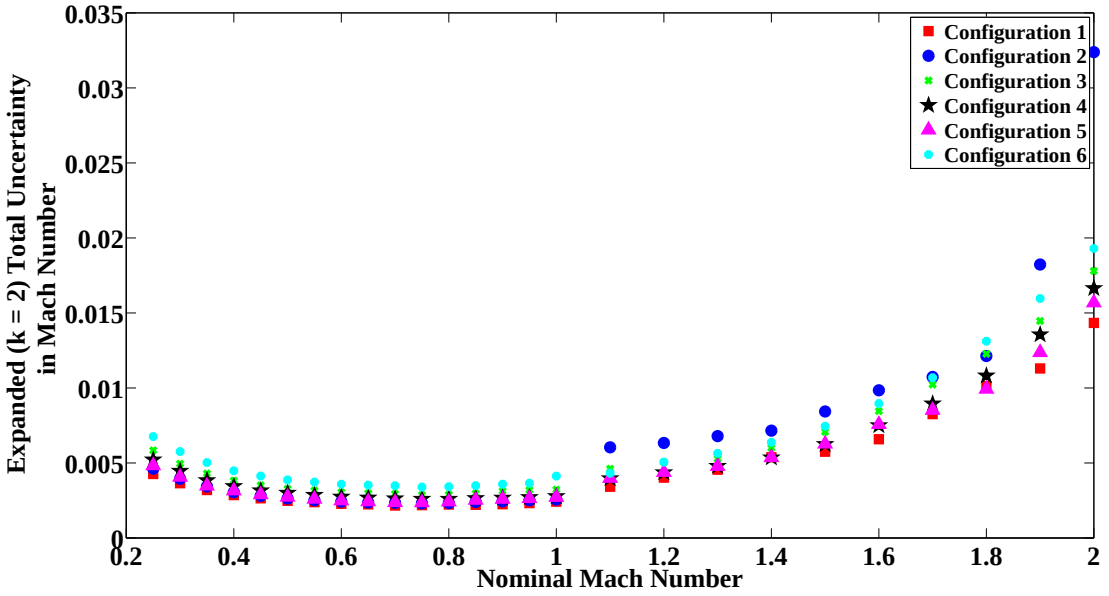

Figure B.7: Total uncertainty of M_{ts} as a function of nominal Mach number for all configurations.

Nominal Mach	**Typical** M_{ts}	$s_{M_{ts}}$ **k = 2**	$b_{M_{ts}}$ **k = 2**	$u_{M_{ts}}$ **k = 2**	$s_{M_{ts}}$ **UPC**	$b_{M_{ts}}$ **UPC**
0.25	0.25	0.0003	0.0046	0.0046	0.5	99.5
0.40	0.41	0.0004	0.0030	0.0031	1.8	98.2
0.60	0.61	0.0001	0.0024	0.0024	0.1	99.9
0.80	0.81	0.0004	0.0023	0.0023	3.3	96.7
1.00	1.00	0.0006	0.0025	0.0026	6.1	93.9
1.20	1.20	0.0010	0.0064	0.0063	2.4	97.6
1.40	1.35	0.0013	0.0071	0.0072	3.0	97.0
1.60	1.55	0.0036	0.0090	0.0098	13.8	86.2
1.80	1.75	0.0012	0.0120	0.0121	1.1	98.9
2.00	1.96	0.0158	0.0278	0.0324	24.4	75.6

Table B.11: Summary of calculated Mach Number uncertainty with 95% level of confidence for configuration 2.

Nominal Mach	**Typical** M_{ts}	$s_{M_{ts}}$ **k = 2**	$b_{M_{ts}}$ **k = 2**	$u_{M_{ts}}$ **k = 2**	$s_{M_{ts}}$ **UPC**	$b_{M_{ts}}$ **UPC**
0.25	0.25	0.0006	0.0058	0.0058	1.0	99.0
0.40	0.41	0.0004	0.0038	0.0038	1.1	98.9
0.60	0.61	0.0002	0.0030	0.0030	0.6	99.4
0.80	0.80	0.0001	0.0029	0.0029	0.0	100.0
1.00	0.99	0.0009	0.0031	0.0032	8.1	91.9
1.20	1.20	0.0009	0.0049	0.0050	2.9	97.1
1.40	1.35	0.0008	0.0060	0.0060	1.7	98.3
1.60	1.56	0.0025	0.0081	0.0085	8.8	91.2
1.80	1.77	0.0030	0.0118	0.0123	6.2	93.8
2.00	1.97	0.0025	0.0175	0.0178	2.0	98.0

Table B.12: Summary of calculated Mach Number uncertainty with 95% level of confidence for configuration 3.

Nominal Mach	**Typical** M_{ts}	$s_{M_{ts}}$ **k = 2**	$b_{M_{ts}}$ **k = 2**	$u_{M_{ts}}$ **k = 2**	$s_{M_{ts}}$ **UPC**	$b_{M_{ts}}$ **UPC**
0.25	0.25	0.0002	0.0052	0.0052	0.1	99.9
0.40	0.41	0.0001	0.0034	0.0034	0.1	99.9
0.60	0.61	0.0001	0.0028	0.0027	0.1	99.9
0.80	0.81	0.0001	0.0026	0.0026	0.2	99.8
1.00	1.00	0.0001	0.0028	0.0028	0.3	99.7
1.20	1.19	0.0003	0.0044	0.0044	0.4	99.6
1.40	1.35	0.0004	0.0054	0.0054	0.7	99.3
1.60	1.56	0.0014	0.0073	0.0075	3.7	96.3
1.80	1.78	0.0017	0.0106	0.0108	2.4	97.6
2.00	1.99	0.0032	0.0163	0.0166	3.8	96.2

Table B.13: Summary of calculated Mach Number uncertainty with 95% level of confidence for configuration 4.

Nominal Mach	**Typical** M_{ts}	$s_{M_{ts}}$ **k = 2**	$b_{M_{ts}}$ **k = 2**	$u_{M_{ts}}$ **k = 2**	$s_{M_{ts}}$ **UPC**	$b_{M_{ts}}$ **UPC**
0.25	0.25	0.0006	0.0047	0.0048	1.5	98.5
0.40	0.40	0.0003	0.0031	0.0031	0.7	99.3
0.60	0.60	0.0001	0.0025	0.0025	0.2	99.8
0.80	0.80	0.0006	0.0024	0.0024	5.0	95.0
1.00	1.00	0.0010	0.0026	0.0027	13.0	87.0
1.20	1.19	0.0013	0.0041	0.0044	9.5	90.5
1.40	1.35	0.0017	0.0051	0.0054	9.9	90.1
1.60	1.55	0.0031	0.0069	0.0076	16.5	83.5
1.80	1.77	0.0014	0.0098	0.0099	1.9	98.1
2.00	1.98	0.0033	0.0153	0.0157	4.5	95.5

Table B.14: Summary of calculated Mach Number uncertainty with 95% level of confidence for configuration 5.

Nominal Mach	**Typical** M_{ts}	$s_{M_{ts}}$ **k = 2**	$b_{M_{ts}}$ **k = 2**	$u_{M_{ts}}$ **k = 2**	$s_{M_{ts}}$ **UPC**	$b_{M_{ts}}$ **UPC**
0.25	0.25	0.0002	0.0067	0.0068	0.1	99.9
0.40	0.41	0.0001	0.0044	0.0045	0.0	100.0
0.60	0.60	0.0000	0.0036	0.0036	0.0	100.0
0.80	0.80	0.0005	0.0034	0.0034	2.3	97.7
1.00	1.02	0.0007	0.0040	0.0041	2.9	97.1
1.20	1.19	0.0006	0.0050	0.0051	1.4	98.6
1.40	1.36	0.0005	0.0063	0.0064	0.7	99.3
1.60	1.56	0.0020	0.0087	0.0090	4.8	95.2
1.80	1.79	0.0012	0.0131	0.0131	0.8	99.2
2.00	1.98	0.0008	0.0193	0.0193	0.2	99.8

Table B.15: Summary of calculated Mach Number uncertainty with 95% level of confidence for configuration 6.

Appendix C: Static Pressure Uncertainty

The uncertainty from measured values to test section static pressure propagates as shown in Figure C.1. Results for uncertainty in test section static pressure for configuration 1 were presented in Section 5. Results for configurations 2-6 are presented in this Appendix. Bar charts depicting the percent contributions are shown, followed by tabulated results detailing dimensional and percent contributions for random, systematic, and total uncertainty.

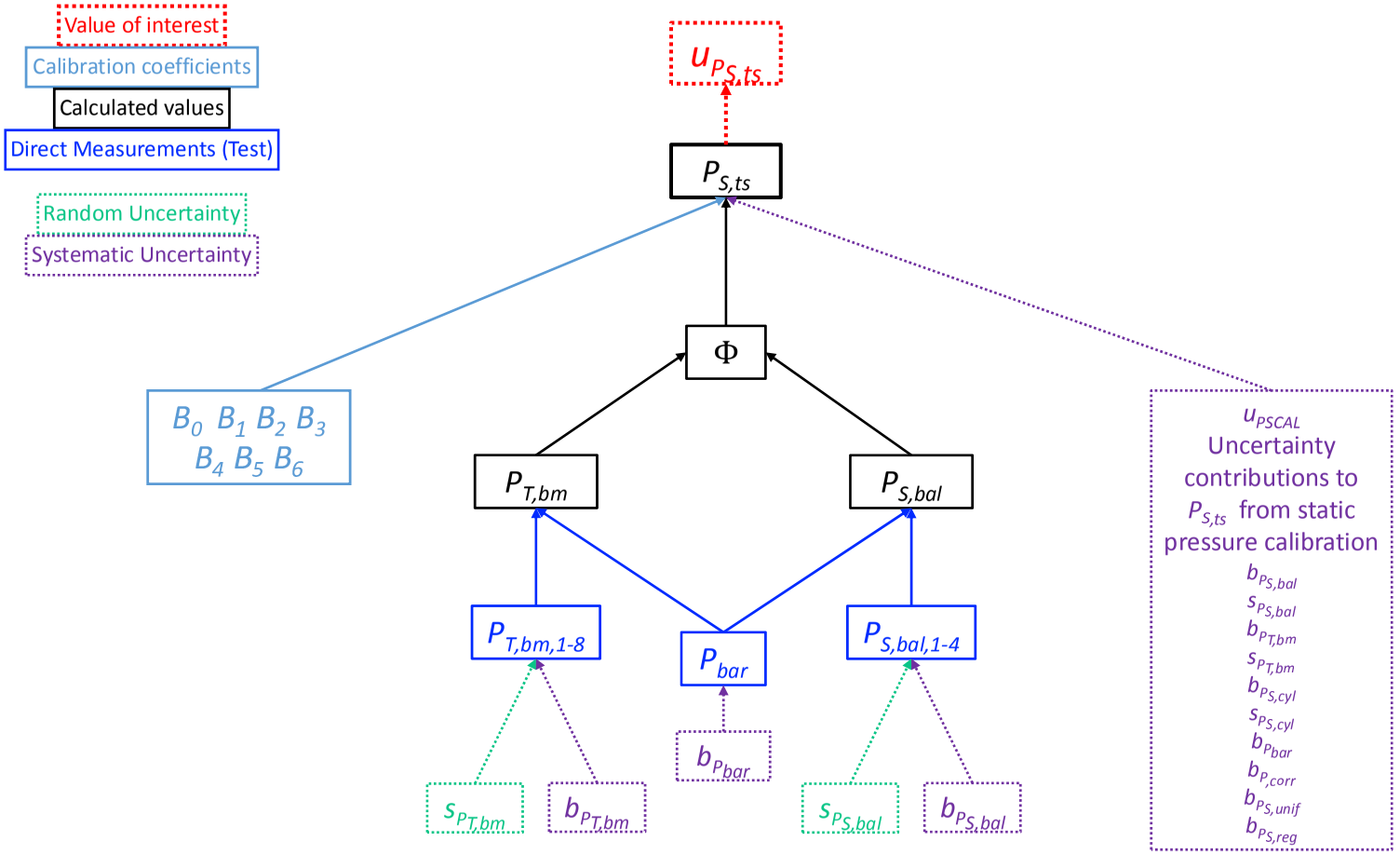

Figure C.1: Uncertainty flow from measured values to calculated static pressure in the test section.

C.1 Random Uncertainty Results for Configurations 2-6

The random uncertainty in the static pressure is shown for all configurations in Figure C.2. All configurations follow a similar trend, remaining below 0.005 psia subsonically then increasing supersonically. Configuration 2 shows a sharp increase at the highest Mach numbers, not seen in the other configurations, which remain below 0.03 psia.

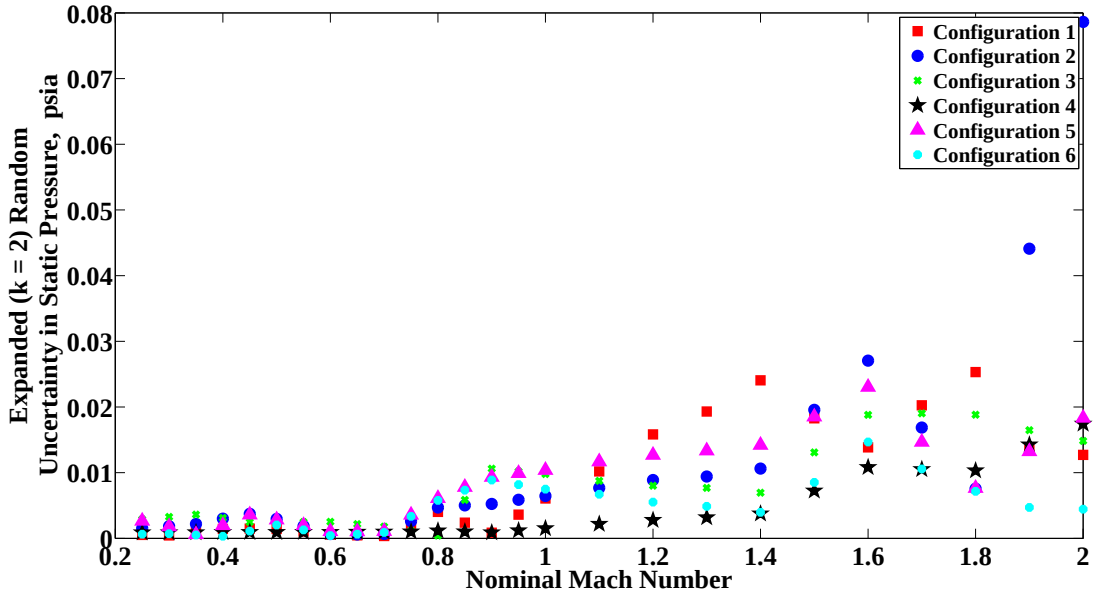

Figure C.2: Random uncertainty of $P_{S,ts}$ as a function of nominal Mach number for all configurations. The red squares are configuration 1, blue circles are configuration 2, green x's are configuration 3, black stars are configuration 4, purple triangles are configuration 5, and cyan dots are configuration 6.

The elemental random uncertainties contributing to random uncertainty in test section static pressure are from measurements $P_{T,bm}$ and $P_{S,bal}$. The percent contribution of each of these elemental uncertainties to the total random uncertainty in $P_{S,ts}$ are shown in Figure C.3. The tabulated details are shown in Tables C.1 - C.5.

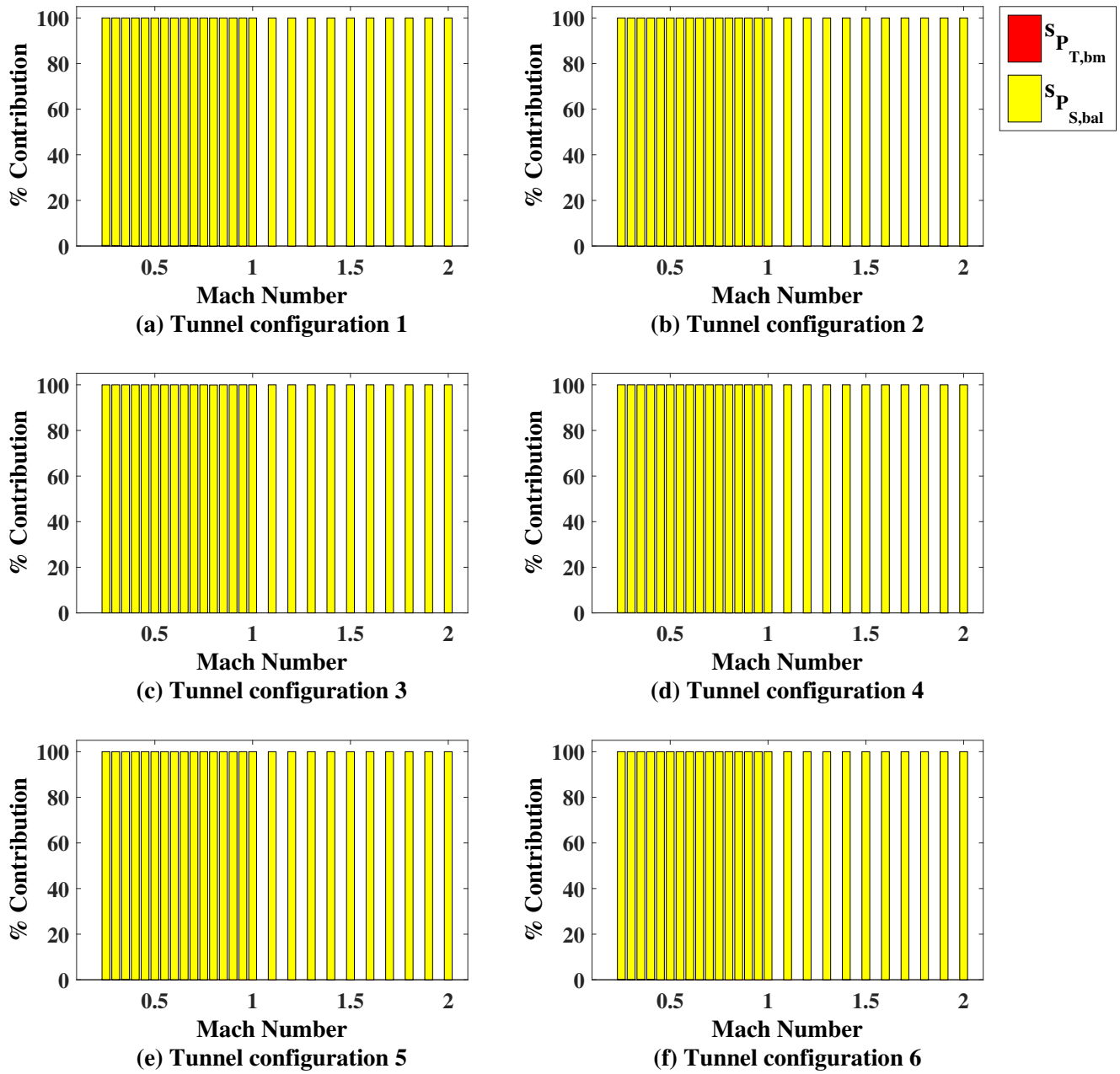

Figure C.3: Random UPC of $P_{S,ts}$ as a function of nominal Mach number for all configurations. Red is the random uncertainty of the total pressure in the bellmouth, yellow is the random uncertainty of the static pressure in the balance chamber.

Nominal Mach	**Typical** $P_{S,ts}$ **psia**	$s_{P_{S,ts}}$ **psia k = 2**	$s_{P_{S,ts}}$ **due to** $s_{P_{T,bm}}$ **psia k = 2**	$s_{P_{S,ts}}$ **due to** $s_{P_{S,bal}}$ **psia k = 2**	$s_{P_{S,ts}}$ **UPC due to** $s_{P_{T,bm}}$	$s_{P_{S,ts}}$ **UPC due to** $s_{P_{S,bal}}$
0.25	14.57	0.0015	0.0000	0.0015	0.0	100.0
0.40	13.58	0.0030	0.0000	0.0030	0.0	100.0
0.60	13.44	0.0007	0.0000	0.0007	0.1	99.9
0.80	10.99	0.0047	0.0000	0.0047	0.0	100.0
1.00	8.83	0.0065	0.0000	0.0065	0.0	100.0
1.20	7.08	0.0089	0.0000	0.0089	0.0	100.0
1.40	6.08	0.0106	0.0000	0.0106	0.0	100.0
1.60	5.11	0.0271	0.0000	0.0271	0.0	100.0
1.80	4.33	0.0076	0.0001	0.0076	0.0	100.0
2.00	3.35	0.0786	0.0008	0.0786	0.0	100.0

Table C.1: Summary of calculated Static Pressure random uncertainty with 95% level of confidence for configuration 2.

Nominal Mach	**Typical** $P_{S,ts}$ **psia**	$s_{P_{S,ts}}$ **psia k = 2**	$s_{P_{S,ts}}$ **due to** $s_{P_{T,bm}}$ **psia k = 2**	$s_{P_{S,ts}}$ **due to** $s_{P_{S,bal}}$ **psia k = 2**	$s_{P_{S,ts}}$ **UPC due to** $s_{P_{T,bm}}$	$s_{P_{S,ts}}$ **UPC due to** $s_{P_{S,bal}}$
0.25	14.94	0.0029	0.0000	0.0029	0.0	100.0
0.40	14.03	0.0031	0.0000	0.0031	0.0	100.0
0.60	14.03	0.0025	0.0000	0.0025	0.0	100.0
0.80	11.53	0.0004	0.0000	0.0004	0.1	99.9
1.00	9.30	0.0098	0.0000	0.0098	0.0	100.0
1.20	7.29	0.0080	0.0000	0.0080	0.0	100.0
1.40	6.30	0.0070	0.0000	0.0070	0.0	100.0
1.60	5.26	0.0188	0.0001	0.0188	0.0	100.0
1.80	4.39	0.0188	0.0002	0.0188	0.0	100.0
2.00	3.31	0.0148	0.0001	0.0148	0.0	100.0

Table C.2: Summary of calculated Static Pressure random uncertainty with 95% level of confidence for configuration 3.

Nominal Mach	**Typical** $P_{S,ts}$ **psia**	$s_{P_{S,ts}}$ **psia** **k = 2**	$s_{P_{S,ts}}$ **due to** $s_{P_{T,bm}}$ **psia** **k = 2**	$s_{P_{S,ts}}$ **due to** $s_{P_{S,bal}}$ **psia** **k = 2**	$s_{P_{S,ts}}$ **UPC due to** $s_{P_{T,bm}}$	$s_{P_{S,ts}}$ **UPC due to** $s_{P_{S,bal}}$
0.25	14.90	0.0009	0.0000	0.0009	0.1	99.9
0.40	14.04	0.0009	0.0000	0.0009	0.1	99.9
0.60	13.99	0.0009	0.0000	0.0009	0.0	100.0
0.80	11.49	0.0012	0.0000	0.0012	0.0	100.0
1.00	9.16	0.0015	0.0000	0.0015	0.0	100.0
1.20	7.36	0.0028	0.0000	0.0028	0.0	100.0
1.40	6.26	0.0038	0.0000	0.0038	0.0	100.0
1.60	5.23	0.0108	0.0001	0.0108	0.0	100.0
1.80	4.33	0.0103	0.0001	0.0103	0.0	100.0
2.00	3.25	0.0174	0.0001	0.0174	0.0	100.0

Table C.3: Summary of calculated Static Pressure random uncertainty with 95% level of confidence for configuration 4.

Nominal Mach	**Typical** $P_{S,ts}$ **psia**	$s_{P_{S,ts}}$ **psia** **k = 2**	$s_{P_{S,ts}}$ **due to** $s_{P_{T,bm}}$ **psia** **k = 2**	$s_{P_{S,ts}}$ **due to** $s_{P_{S,bal}}$ **psia** **k = 2**	$s_{P_{S,ts}}$ **UPC due to** $s_{P_{T,bm}}$	$s_{P_{S,ts}}$ **UPC due to** $s_{P_{S,bal}}$
0.25	14.54	0.0026	0.0001	0.0026	0.1	99.9
0.40	13.66	0.0020	0.0000	0.0020	0.0	100.0
0.60	13.65	0.0011	0.0000	0.0011	0.0	100.0
0.80	11.21	0.0061	0.0000	0.0061	0.0	100.0
1.00	8.98	0.0104	0.0000	0.0104	0.0	100.0
1.20	7.18	0.0127	0.0000	0.0127	0.0	100.0
1.40	6.11	0.0142	0.0000	0.0142	0.0	100.0
1.60	5.14	0.0230	0.0000	0.0230	0.0	100.0
1.80	4.31	0.0076	0.0002	0.0076	0.0	100.0
2.00	3.27	0.0183	0.0002	0.0183	0.0	100.0

Table C.4: Summary of calculated Static Pressure random uncertainty with 95% level of confidence for configuration 5.

Nominal Mach	**Typical** $P_{S,ts}$ **psia**	$s_{P_{S,ts}}$ **psia k = 2**	$s_{P_{S,ts}}$ **due to** $s_{P_{T,bm}}$ **psia k = 2**	$s_{P_{S,ts}}$ **due to** $s_{P_{S,bal}}$ **psia k = 2**	$s_{P_{S,ts}}$ **UPC due to** $s_{P_{T,bm}}$	$s_{P_{S,ts}}$ **UPC due to** $s_{P_{S,bal}}$
0.25	14.88	0.0006	0.0000	0.0006	0.2	99.8
0.40	13.97	0.0003	0.0000	0.0003	0.2	99.8
0.60	14.00	0.0004	0.0000	0.0004	0.1	99.9
0.80	11.32	0.0058	0.0000	0.0058	0.0	100.0
1.00	8.97	0.0075	0.0000	0.0075	0.0	100.0
1.20	7.37	0.0055	0.0000	0.0055	0.0	100.0
1.40	6.22	0.0040	0.0001	0.0040	0.1	99.9
1.60	5.20	0.0147	0.0001	0.0147	0.0	100.0
1.80	4.28	0.0072	0.0001	0.0072	0.0	100.0
2.00	3.29	0.0044	0.0000	0.0044	0.0	100.0

Table C.5: Summary of calculated Static Pressure random uncertainty with 95% level of confidence for configuration 6.

C.2 Systematic Uncertainty Results for Configurations 2-6

The systematic uncertainty in the test section static pressure is shown for all configurations in Figure C.4. All configurations follow a similar trend, although configuration 6 is notably higher at all Mach numbers.

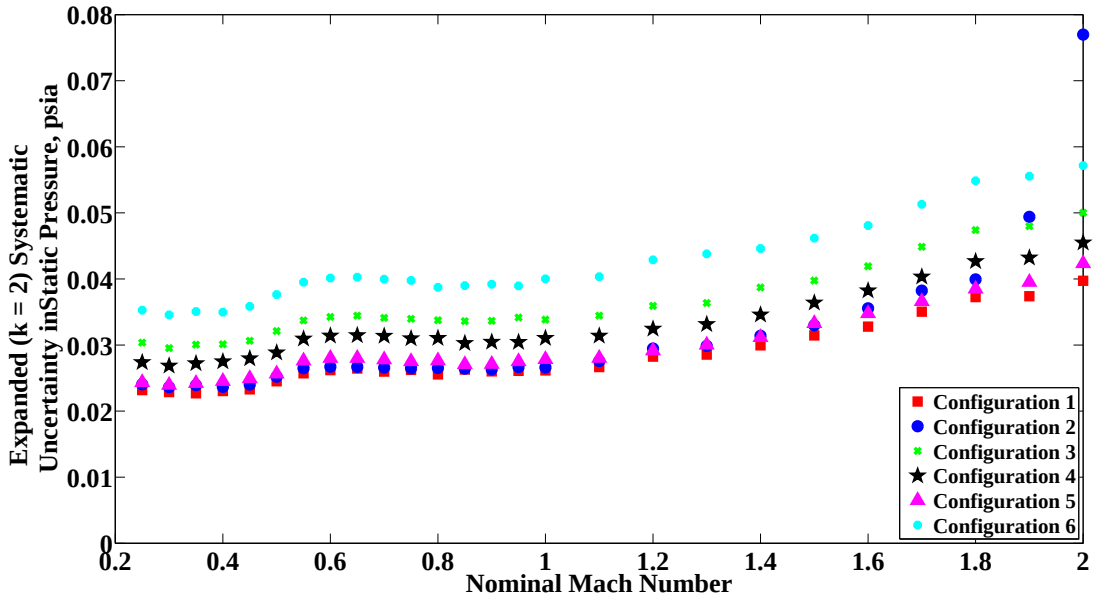

Figure C.4: Systematic uncertainty of $P_{S,ts}$ as a function of nominal Mach number for all configurations. The red squares are configuration 1, blue circles are configuration 2, green x's are configuration 3, black stars are configuration 4, purple triangles are configuration 5, and cyan dots are configuration 6.

The systematic uncertainty in $P_{S,ts}$ is due to systematic contributions from static pressure calibration (b_{PSCAL}) and instrumentation uncertainties in test-time bellmouth total pressure, balance chamber static pressure, and barometric pressure (combined as $b_{P_{inst}}$). The percent contributions of each of these uncertainties to the combined systematic uncertainty in $P_{S,ts}$ are shown in Figure C.5. The tabulated details are shown in Tables C.6 - C.10.

C.3 Total Uncertainty Results for Configurations 2-6

The overall uncertainty in $P_{S,ts}$ for all configurations is shown in Figure C.6. The plots follow a general trend, especially subsonically, although there is a noticeable difference in magnitude particularly for configuration 6. The overall uncertainty in $P_{S,ts}$ is presented for configurations 2-6 in Tables C.11 - C.15.

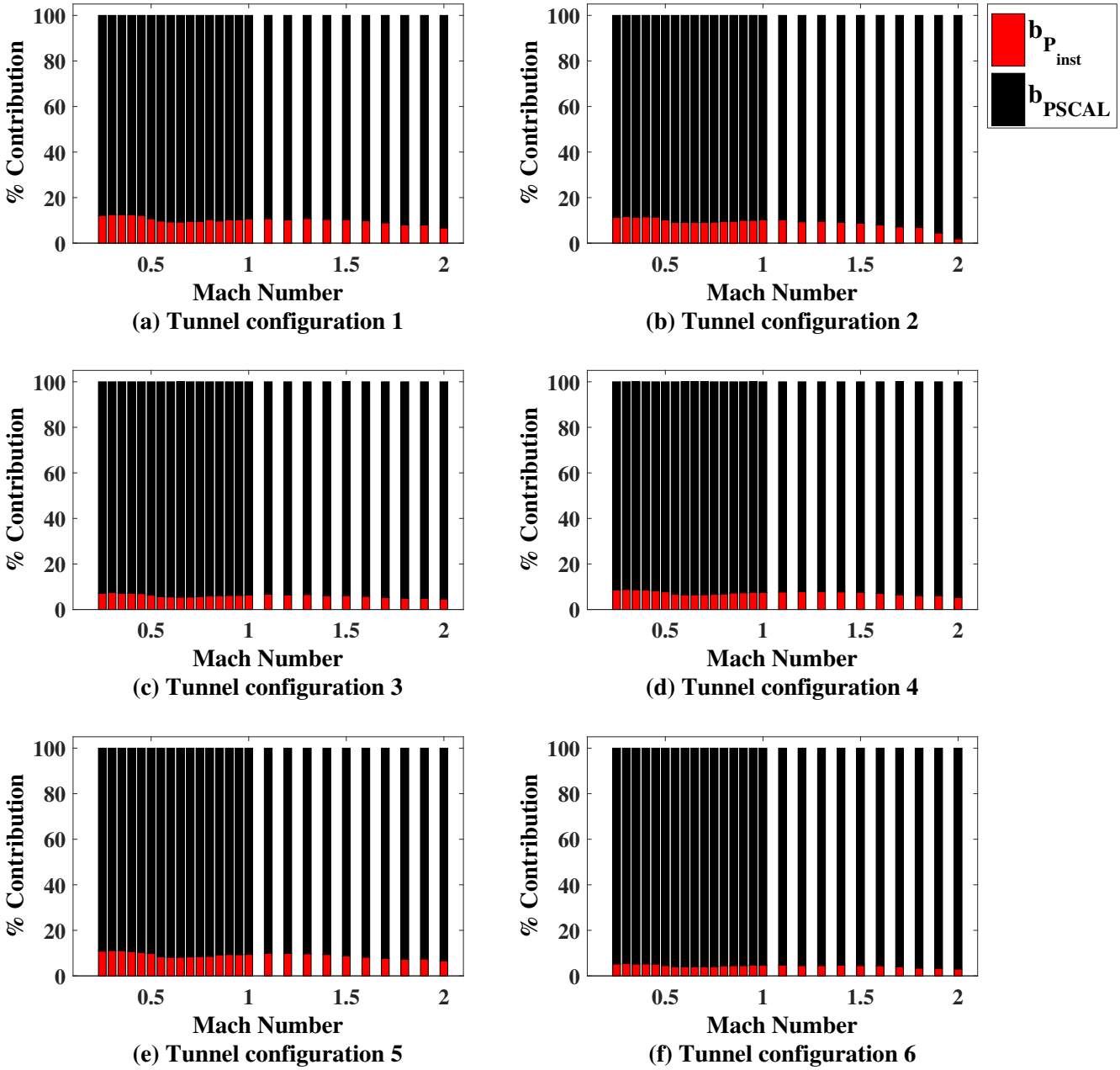

Figure C.5: Systematic UPC of $P_{S,ts}$ as a function of nominal Mach number for all configurations. Red is the systematic uncertainty due to pressure instrumentation and black is the systematic uncertainty due to static pressure calibration.

Nominal Mach	**Typical** $P_{S,ts}$ **psia**	$b_{P_{S,ts}}$ **psia k = 2**	$b_{P_{S,ts}}$ **due to** $b_{P_{Inst}}$ **psia k = 2**	$b_{P_{S,ts}}$ **due to** b_{PSCAL} **psia k = 2**	$b_{P_{S,ts}}$ **UPC due to** $b_{P_{Inst}}$	$b_{P_{S,ts}}$ **UPC due to** b_{PSCAL}
0.25	14.57	0.0240	0.0081	0.0227	11.3	88.7
0.40	13.58	0.0237	0.0081	0.0223	11.6	88.4
0.60	13.44	0.0267	0.0081	0.0255	9.1	90.9
0.80	10.99	0.0265	0.0082	0.0252	9.6	90.4
1.00	8.83	0.0266	0.0085	0.0252	10.3	89.7
1.20	7.08	0.0295	0.0090	0.0280	9.4	90.6
1.40	6.08	0.0314	0.0095	0.0299	9.1	90.9
1.60	5.11	0.0356	0.0100	0.0341	8.0	92.0
1.80	4.33	0.0399	0.0104	0.0385	6.8	93.2
2.00	3.35	0.0770	0.0106	0.0763	1.9	98.1

Table C.6: Summary of calculated Static Pressure systematic uncertainty with 95% level of confidence for configuration 2.

Nominal Mach	**Typical** $P_{S,ts}$ **psia**	$b_{P_{S,ts}}$ **psia k = 2**	$b_{P_{S,ts}}$ **due to** $b_{P_{Inst}}$ **psia k = 2**	$b_{P_{S,ts}}$ **due to** b_{PSCAL} **psia k = 2**	$b_{P_{S,ts}}$ **UPC due to** $b_{P_{Inst}}$	$b_{P_{S,ts}}$ **UPC due to** b_{PSCAL}
0.25	14.94	0.0304	0.0081	0.0293	7.1	92.9
0.40	14.03	0.0301	0.0081	0.0290	7.2	92.8
0.60	14.03	0.0343	0.0081	0.0333	5.5	94.5
0.80	11.53	0.0338	0.0082	0.0328	5.9	94.1
1.00	9.30	0.0338	0.0086	0.0327	6.4	93.6
1.20	7.29	0.0359	0.0091	0.0348	6.4	93.6
1.40	6.30	0.0387	0.0095	0.0375	6.1	93.9
1.60	5.26	0.0419	0.0101	0.0407	5.8	94.2
1.80	4.39	0.0474	0.0105	0.0462	4.9	95.1
2.00	3.31	0.0500	0.0107	0.0489	4.6	95.4

Table C.7: Summary of calculated Static Pressure systematic uncertainty with 95% level of confidence for configuration 3.

Nominal Mach	**Typical $P_{S,ts}$ psia**	**$b_{P_{S,ts}}$ psia k = 2**	**$b_{P_{S,ts}}$ due to $b_{P_{Inst}}$ psia k = 2**	**$b_{P_{S,ts}}$ due to b_{PSCAL} psia k = 2**	**$b_{P_{S,ts}}$ UPC due to $b_{P_{Inst}}$**	**$b_{P_{S,ts}}$ UPC due to b_{PSCAL}**
0.25	14.90	0.0274	0.0080	0.0262	8.6	91.4
0.40	14.04	0.0275	0.0080	0.0263	8.6	91.4
0.60	13.99	0.0314	0.0080	0.0304	6.5	93.5
0.80	11.49	0.0310	0.0081	0.0300	6.8	93.2
1.00	9.16	0.0310	0.0085	0.0299	7.4	92.6
1.20	7.36	0.0324	0.0091	0.0312	7.8	92.2
1.40	6.26	0.0346	0.0096	0.0332	7.7	92.3
1.60	5.23	0.0382	0.0101	0.0369	7.0	93.0
1.80	4.33	0.0427	0.0105	0.0414	6.0	94.0
2.00	3.25	0.0455	0.0105	0.0443	5.3	94.7

Table C.8: Summary of calculated Static Pressure systematic uncertainty with 95% level of confidence for configuration 4.

Nominal Mach	**Typical $P_{S,ts}$ psia**	**$b_{P_{S,ts}}$ psia k = 2**	**$b_{P_{S,ts}}$ due to $b_{P_{Inst}}$ psia k = 2**	**$b_{P_{S,ts}}$ due to b_{PSCAL} psia k = 2**	**$b_{P_{S,ts}}$ UPC due to $b_{P_{Inst}}$**	**$b_{P_{S,ts}}$ UPC due to b_{PSCAL}**
0.25	14.54	0.0243	0.0080	0.0230	10.9	89.1
0.40	13.66	0.0245	0.0080	0.0232	10.8	89.2
0.60	13.65	0.0280	0.0080	0.0268	8.2	91.8
0.80	11.21	0.0276	0.0081	0.0264	8.6	91.4
1.00	8.98	0.0278	0.0086	0.0265	9.4	90.6
1.20	7.18	0.0291	0.0091	0.0277	9.8	90.2
1.40	6.11	0.0312	0.0096	0.0297	9.4	90.6
1.60	5.14	0.0348	0.0100	0.0333	8.2	91.8
1.80	4.31	0.0385	0.0104	0.0371	7.3	92.7
2.00	3.27	0.0423	0.0109	0.0409	6.6	93.4

Table C.9: Summary of calculated Static Pressure systematic uncertainty with 95% level of confidence for configuration 5.

Nominal Mach	**Typical $P_{S,ts}$ psia**	**$b_{P_{S,ts}}$ psia k = 2**	**$b_{P_{S,ts}}$ due to $b_{P_{Inst}}$ psia k = 2**	**$b_{P_{S,ts}}$ due to b_{PSCAL} psia k = 2**	**$b_{P_{S,ts}}$ UPC due to $b_{P_{Inst}}$**	**$b_{P_{S,ts}}$ UPC due to b_{PSCAL}**
0.25	14.88	0.0353	0.0081	0.0343	5.2	94.8
0.40	13.97	0.0350	0.0080	0.0340	5.3	94.7
0.60	14.00	0.0401	0.0081	0.0393	4.0	96.0
0.80	11.32	0.0387	0.0081	0.0379	4.4	95.6
1.00	8.97	0.0400	0.0086	0.0391	4.6	95.4
1.20	7.37	0.0429	0.0091	0.0419	4.6	95.4
1.40	6.22	0.0446	0.0097	0.0435	4.8	95.2
1.60	5.20	0.0481	0.0101	0.0470	4.4	95.6
1.80	4.28	0.0549	0.0102	0.0539	3.5	96.5
2.00	3.29	0.0572	0.0099	0.0563	3.0	97.0

Table C.10: Summary of calculated Static Pressure systematic uncertainty with 95% level of confidence for configuration 6.

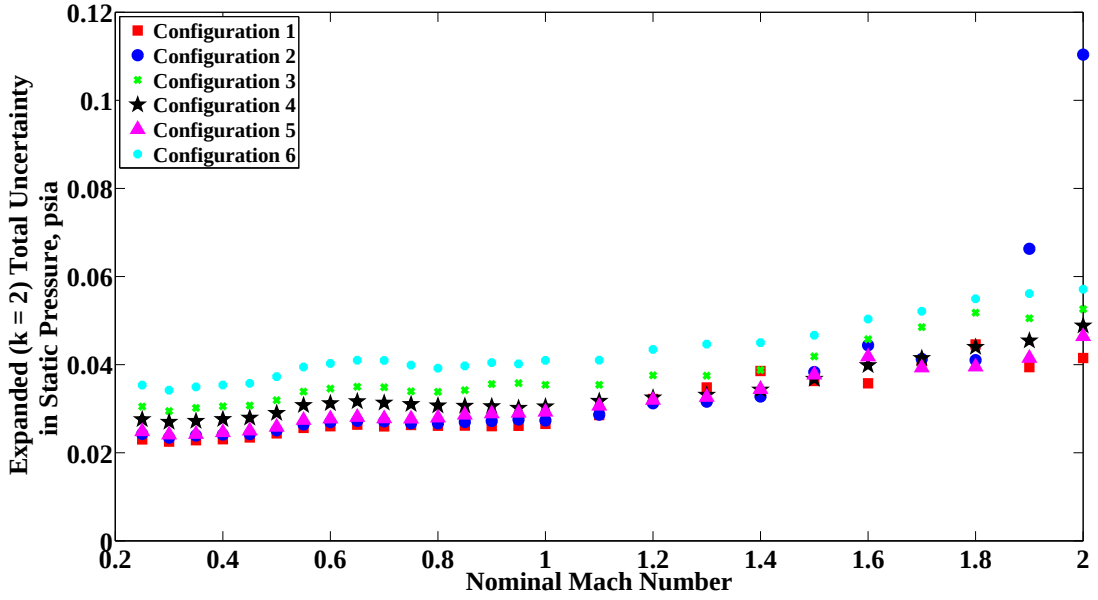

Figure C.6: Total uncertainty of $P_{S,ts}$ as a function of nominal Mach number for all configurations.

Nominal Mach	**Typical $P_{S,ts}$, psia**	$s_{P_{S,ts}}$ **psia k = 2**	$b_{P_{S,ts}}$ **psia k = 2**	$u_{P_{S,ts}}$ **psia k = 2**	$s_{P_{S,ts}}$ **UPC**	$b_{P_{S,ts}}$ **UPC**
0.25	14.57	0.0015	0.0240	0.0243	0.4	99.6
0.40	13.58	0.0030	0.0237	0.0241	1.6	98.4
0.60	13.44	0.0007	0.0267	0.0270	0.1	99.9
0.80	10.99	0.0047	0.0265	0.0267	3.0	97.0
1.00	8.83	0.0065	0.0266	0.0273	5.6	94.4
1.20	7.08	0.0089	0.0295	0.0312	8.3	91.7
1.40	6.08	0.0106	0.0314	0.0328	10.3	89.7
1.60	5.11	0.0271	0.0356	0.0444	36.7	63.3
1.80	4.33	0.0076	0.0399	0.0410	3.5	96.5
2.00	3.35	0.0786	0.0770	0.1104	51.1	48.9

Table C.11: Summary of calculated Static Pressure uncertainty with 95% level of confidence for configuration 2.

Nominal Mach	**Typical $P_{S,ts}$, psia**	$s_{P_{S,ts}}$ **psia k = 2**	$b_{P_{S,ts}}$ **psia k = 2**	$u_{P_{S,ts}}$ **psia k = 2**	$s_{P_{S,ts}}$ **UPC**	$b_{P_{S,ts}}$ **UPC**
0.25	14.94	0.0029	0.0304	0.0305	0.9	99.1
0.40	14.03	0.0031	0.0301	0.0305	1.1	98.9
0.60	14.03	0.0025	0.0343	0.0345	0.5	99.5
0.80	11.53	0.0004	0.0338	0.0338	0.0	100.0
1.00	9.30	0.0098	0.0338	0.0354	7.7	92.3
1.20	7.29	0.0080	0.0359	0.0376	4.7	95.3
1.40	6.30	0.0070	0.0387	0.0388	3.1	96.9
1.60	5.26	0.0188	0.0419	0.0458	16.8	83.2
1.80	4.39	0.0188	0.0474	0.0518	13.6	86.4
2.00	3.31	0.0148	0.0500	0.0526	8.1	91.9

Table C.12: Summary of calculated Static Pressure uncertainty with 95% level of confidence for configuration 3.

Nominal Mach	**Typical $P_{S,ts}$, psia**	$s_{P_{S,ts}}$ **psia k = 2**	$b_{P_{S,ts}}$ **psia k = 2**	$u_{P_{S,ts}}$ **psia k = 2**	$s_{P_{S,ts}}$ **UPC**	$b_{P_{S,ts}}$ **UPC**
0.25	14.90	0.0009	0.0274	0.0276	0.1	99.9
0.40	14.04	0.0009	0.0275	0.0276	0.1	99.9
0.60	13.99	0.0009	0.0314	0.0312	0.1	99.9
0.80	11.49	0.0012	0.0310	0.0307	0.1	99.9
1.00	9.16	0.0015	0.0310	0.0305	0.2	99.8
1.20	7.36	0.0028	0.0324	0.0325	0.7	99.3
1.40	6.26	0.0038	0.0346	0.0343	1.2	98.8
1.60	5.23	0.0108	0.0382	0.0399	7.4	92.6
1.80	4.33	0.0103	0.0427	0.0440	5.5	94.5
2.00	3.25	0.0174	0.0455	0.0488	12.8	87.2

Table C.13: Summary of calculated Static Pressure uncertainty with 95% level of confidence for configuration 4.

Nominal Mach	**Typical $P_{S,ts}$, psia**	$s_{P_{S,ts}}$ **psia k = 2**	$b_{P_{S,ts}}$ **psia k = 2**	$u_{P_{S,ts}}$ **psia k = 2**	$s_{P_{S,ts}}$ **UPC**	$b_{P_{S,ts}}$ **UPC**
0.25	14.54	0.0026	0.0243	0.0248	1.2	98.8
0.40	13.66	0.0020	0.0245	0.0246	0.6	99.4
0.60	13.65	0.0011	0.0280	0.0277	0.1	99.9
0.80	11.21	0.0061	0.0276	0.0279	4.7	95.3
1.00	8.98	0.0104	0.0278	0.0293	12.2	87.8
1.20	7.18	0.0127	0.0291	0.0319	15.9	84.1
1.40	6.11	0.0142	0.0312	0.0344	17.2	82.8
1.60	5.14	0.0230	0.0348	0.0418	30.5	69.5
1.80	4.31	0.0076	0.0385	0.0395	3.8	96.2
2.00	3.27	0.0183	0.0423	0.0464	15.8	84.2

Table C.14: Summary of calculated Static Pressure uncertainty with 95% level of confidence for configuration 5.

Nominal Mach	**Typical** $P_{S,ts}$**, psia**	$s_{P_{S,ts}}$ **psia** **k = 2**	$b_{P_{S,ts}}$ **psia** **k = 2**	$u_{P_{S,ts}}$ **psia** **k = 2**	$s_{P_{S,ts}}$ **UPC**	$b_{P_{S,ts}}$ **UPC**
0.25	14.88	0.0006	0.0353	0.0354	0.0	100.0
0.40	13.97	0.0003	0.0350	0.0354	0.0	100.0
0.60	14.00	0.0004	0.0401	0.0403	0.0	100.0
0.80	11.32	0.0058	0.0387	0.0392	2.2	97.8
1.00	8.97	0.0075	0.0400	0.0410	3.4	96.6
1.20	7.37	0.0055	0.0429	0.0435	1.6	98.4
1.40	6.22	0.0040	0.0446	0.0450	0.8	99.2
1.60	5.20	0.0147	0.0481	0.0504	8.5	91.5
1.80	4.28	0.0072	0.0549	0.0550	1.7	98.3
2.00	3.29	0.0044	0.0572	0.0571	0.6	99.4

Table C.15: Summary of calculated Static Pressure uncertainty with 95% level of confidence for configuration 6.

Appendix D: Total Pressure Uncertainty

The uncertainty from measured values to test section total pressure propagates as shown in Figure D.1. Results for uncertainty in test section total pressure for configuration 1 were presented in Section 5. Results for configurations 2-6 are presented in this Appendix. Bar charts depicting the percent contributions are shown, followed by tabulated results detailing dimensional and percent contributions for random, systematic, and total uncertainty.

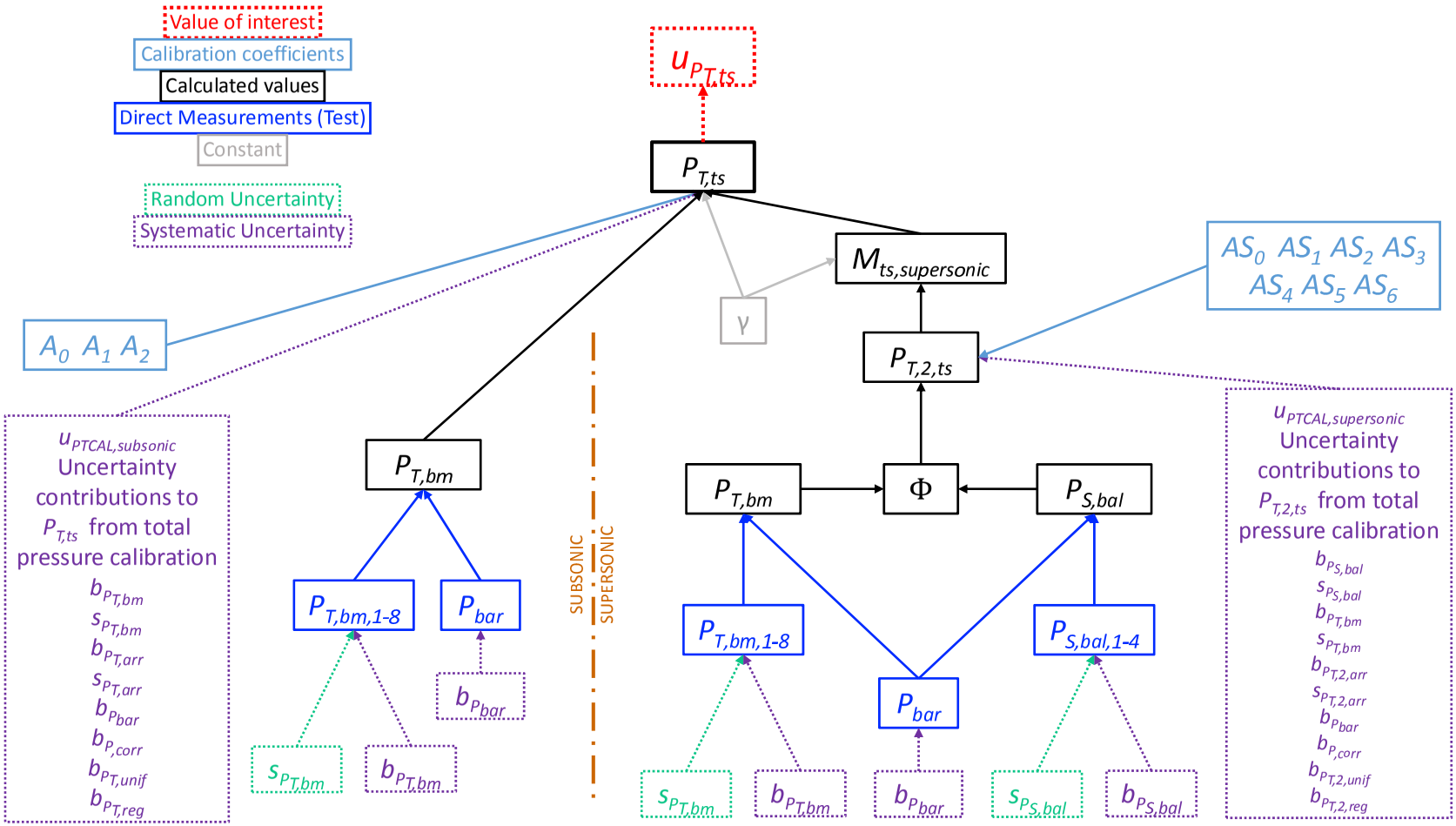

Figure D.1: Uncertainty flow from measured values to calculated total pressure in the test section.

D.1 Random Uncertainty Results for Configurations 2-6

The random uncertainty in the total pressure is shown for all configurations in Figure D.2. All configurations follow a similar trend, remaining below 0.0005 psia subsonically then increasing supersonically to between 0.02 and 0.04 psia, with two exceptions. Configuration 2 shows a sharp increase at the highest Mach numbers, not seen in the other configurations, up to 0.12 psia. Configuration 6 never sees an uncertainty above 0.01 psia.

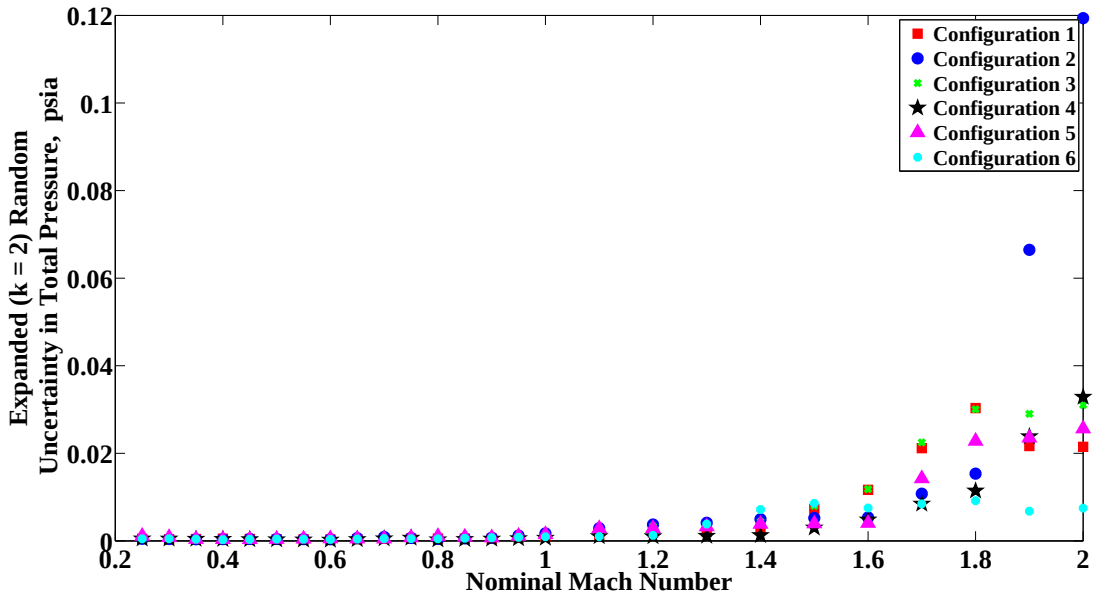

Figure D.2: Random uncertainty of $P_{T,ts}$ as a function of nominal Mach number for all configurations. The red squares are configuration 1, blue circles are configuration 2, green x's are configuration 3, black stars are configuration 4, purple triangles are configuration 5, and cyan dots are configuration 6.

Contributors to random uncertainty in test section total pressure are the random uncertainties in $P_{T,bm}$ and $P_{S,bal}$. The percent contribution of each of these elemental uncertainties to the total random uncertainty in $P_{T,ts}$ are shown in Figure D.3. The tabulated details are shown in Tables D.1 - D.5.

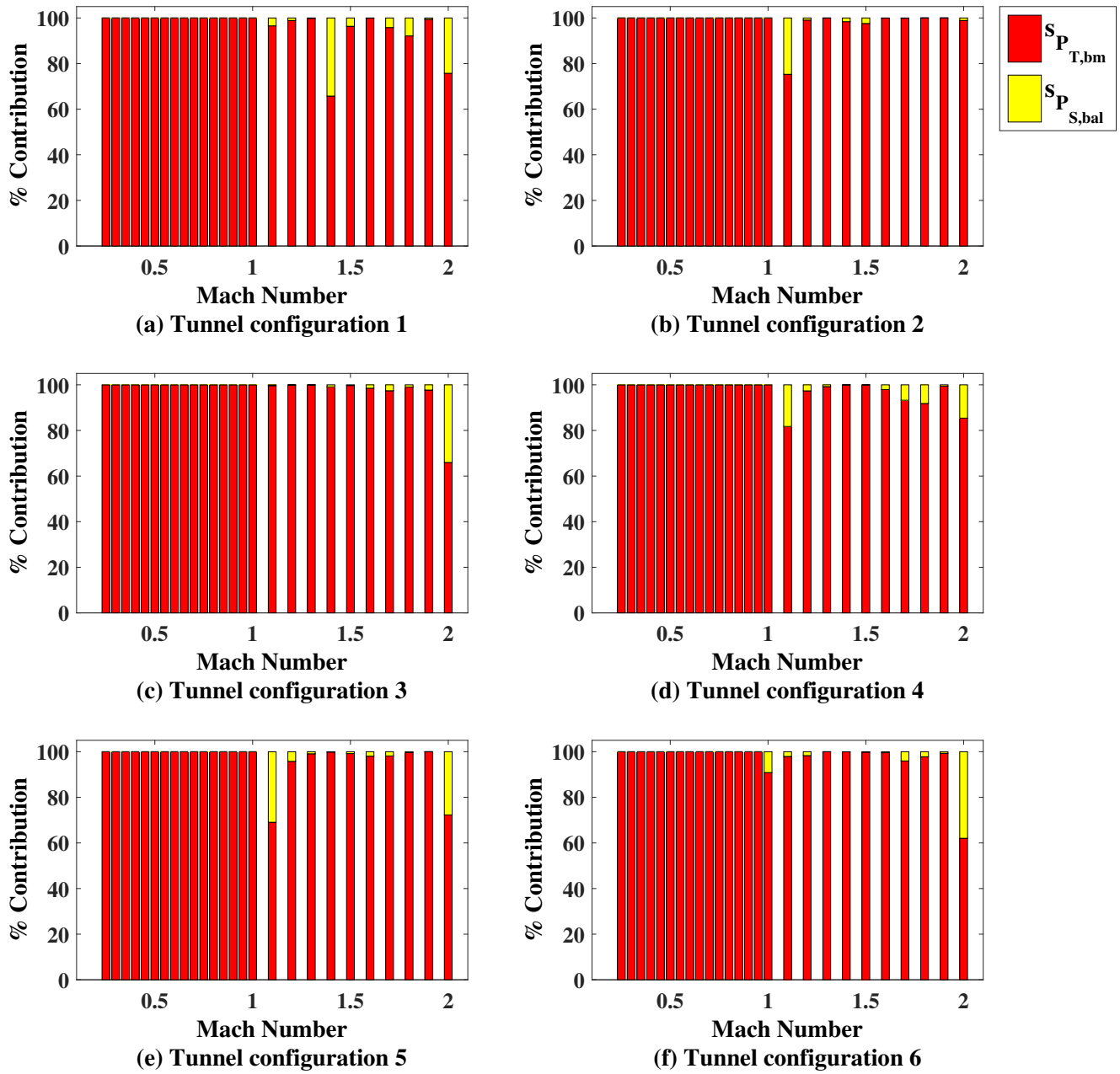

Figure D.3: Random UPC of $P_{T,ts}$ as a function of nominal Mach number for all configurations. Red is the random uncertainty of the total pressure in the bellmouth, yellow is the random uncertainty of the static pressure in the balance chamber.

Nominal Mach	**Typical** $P_{T,ts}$ **psia**	$s_{P_{T,ts}}$ **psia k = 2**	$s_{P_{T,ts}}$ **due to** $s_{P_{T,bm}}$ **psia k = 2**	$s_{P_{T,ts}}$ **due to** $s_{P_{S,bal}}$ **psia k = 2**	$s_{P_{T,ts}}$ **UPC due to** $s_{P_{T,bm}}$	$s_{P_{T,ts}}$ **UPC due to** $s_{P_{S,bal}}$
0.25	15.21	0.0005	0.0005	0.0000	100.0	0.0
0.40	15.24	0.0004	0.0004	0.0000	100.0	0.0
0.60	17.28	0.0004	0.0004	0.0000	100.0	0.0
0.80	16.99	0.0005	0.0005	0.0000	100.0	0.0
1.00	16.77	0.0017	0.0017	0.0000	100.0	0.0
1.20	17.06	0.0037	0.0037	0.0004	99.1	0.9
1.40	18.06	0.0050	0.0049	0.0006	98.4	1.6
1.60	20.20	0.0054	0.0054	0.0002	99.9	0.1
1.80	23.13	0.0153	0.0153	0.0000	100.0	0.0
2.00	24.58	0.1194	0.1187	0.0125	98.9	1.1

Table D.1: Summary of calculated Total Pressure random uncertainty with 95% level of confidence for configuration 2.

Nominal Mach	**Typical** $P_{T,ts}$ **psia**	$s_{P_{T,ts}}$ **psia k = 2**	$s_{P_{T,ts}}$ **due to** $s_{P_{T,bm}}$ **psia k = 2**	$s_{P_{T,ts}}$ **due to** $s_{P_{S,bal}}$ **psia k = 2**	$s_{P_{T,ts}}$ **UPC due to** $s_{P_{T,bm}}$	$s_{P_{T,ts}}$ **UPC due to** $s_{P_{S,bal}}$
0.25	15.58	0.0004	0.0004	0.0000	100.0	0.0
0.40	15.74	0.0004	0.0004	0.0000	100.0	0.0
0.60	17.98	0.0003	0.0003	0.0000	100.0	0.0
0.80	17.66	0.0009	0.0009	0.0000	100.0	0.0
1.00	17.39	0.0015	0.0015	0.0000	100.0	0.0
1.20	17.72	0.0033	0.0033	0.0001	99.9	0.1
1.40	18.77	0.0044	0.0044	0.0004	99.1	0.9
1.60	21.00	0.0118	0.0117	0.0014	98.5	1.5
1.80	24.11	0.0301	0.0299	0.0029	99.1	0.9
2.00	24.71	0.0310	0.0252	0.0181	65.9	34.1

Table D.2: Summary of calculated Total Pressure random uncertainty with 95% level of confidence for configuration 3.

Nominal Mach	**Typical** $P_{T,ts}$ **psia**	$s_{P_{T,ts}}$ **psia k = 2**	$s_{P_{T,ts}}$ **due to** $s_{P_{T,bm}}$ **psia k = 2**	$s_{P_{T,ts}}$ **due to** $s_{P_{S,bal}}$ **psia k = 2**	$s_{P_{T,ts}}$ **UPC due to** $s_{P_{T,bm}}$	$s_{P_{T,ts}}$ **UPC due to** $s_{P_{S,bal}}$
0.25	15.56	0.0005	0.0005	0.0000	100.0	0.0
0.40	15.74	0.0004	0.0004	0.0000	100.0	0.0
0.60	17.94	0.0002	0.0002	0.0000	100.0	0.0
0.80	17.64	0.0003	0.0003	0.0000	100.0	0.0
1.00	17.35	0.0007	0.0007	0.0000	100.0	0.0
1.20	17.64	0.0010	0.0010	0.0002	97.3	2.7
1.40	18.65	0.0013	0.0013	0.0000	100.0	0.0
1.60	20.96	0.0048	0.0048	0.0007	97.9	2.1
1.80	24.13	0.0114	0.0110	0.0033	91.8	8.2
2.00	25.17	0.0329	0.0304	0.0126	85.4	14.6

Table D.3: Summary of calculated Total Pressure random uncertainty with 95% level of confidence for configuration 4.

Nominal Mach	**Typical** $P_{T,ts}$ **psia**	$s_{P_{T,ts}}$ **psia k = 2**	$s_{P_{T,ts}}$ **due to** $s_{P_{T,bm}}$ **psia k = 2**	$s_{P_{T,ts}}$ **due to** $s_{P_{S,bal}}$ **psia k = 2**	$s_{P_{T,ts}}$ **UPC due to** $s_{P_{T,bm}}$	$s_{P_{T,ts}}$ **UPC due to** $s_{P_{S,bal}}$
0.25	15.16	0.0011	0.0011	0.0000	100.0	0.0
0.40	15.28	0.0004	0.0004	0.0000	100.0	0.0
0.60	17.46	0.0005	0.0005	0.0000	100.0	0.0
0.80	17.14	0.0010	0.0010	0.0000	100.0	0.0
1.00	16.92	0.0015	0.0015	0.0000	100.0	0.0
1.20	17.21	0.0029	0.0028	0.0006	95.8	4.2
1.40	18.20	0.0038	0.0038	0.0001	99.8	0.2
1.60	20.41	0.0040	0.0040	0.0006	98.0	2.0
1.80	23.48	0.0228	0.0227	0.0015	99.6	0.4
2.00	24.68	0.0256	0.0218	0.0135	72.3	27.7

Table D.4: Summary of calculated Total Pressure random uncertainty with 95% level of confidence for configuration 5.

Nominal Mach	**Typical** $P_{T,ts}$ **psia**	$s_{P_{T,ts}}$ **psia k = 2**	$s_{P_{T,ts}}$ **due to** $s_{P_{T,bm}}$ **psia k = 2**	$s_{P_{T,ts}}$ **due to** $s_{P_{S,bal}}$ **psia k = 2**	$s_{P_{T,ts}}$ **UPC due to** $s_{P_{T,bm}}$	$s_{P_{T,ts}}$ **UPC due to** $s_{P_{S,bal}}$
0.25	15.54	0.0005	0.0005	0.0000	100.0	0.0
0.40	15.66	0.0003	0.0003	0.0000	100.0	0.0
0.60	17.92	0.0003	0.0003	0.0000	100.0	0.0
0.80	17.32	0.0005	0.0005	0.0000	100.0	0.0
1.00	17.33	0.0009	0.0009	0.0003	90.8	9.2
1.20	17.69	0.0013	0.0012	0.0002	98.3	1.7
1.40	18.74	0.0072	0.0072	0.0002	99.9	0.1
1.60	20.96	0.0075	0.0075	0.0005	99.6	0.4
1.80	24.06	0.0092	0.0091	0.0014	97.8	2.2
2.00	24.81	0.0075	0.0059	0.0046	62.0	38.0

Table D.5: Summary of calculated Total Pressure random uncertainty with 95% level of confidence for configuration 6.

D.2 Systematic Uncertainty Results for Configurations 2-6

The systematic uncertainty in the test section total pressure is shown for all configurations in Figure D.4. All configurations follow a similar trend, remaining around 0.01 psia subsonically, and increasing supersonically up to 0.4 psia, with the exception of configuration 2, which is higher supersonically.

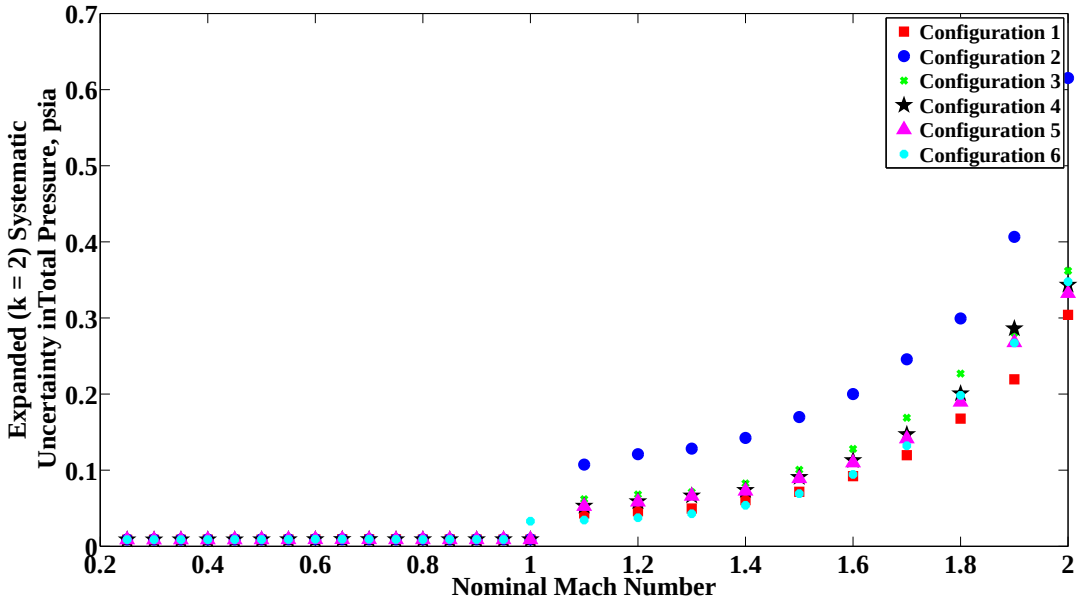

Figure D.4: Systematic uncertainty of $P_{T,ts}$ as a function of nominal Mach number for all configurations. The red squares are configuration 1, blue circles are configuration 2, green x's are configuration 3, black stars are configuration 4, purple triangles are configuration 5, and cyan dots are configuration 6.

The systematic uncertainty in $P_{T,ts}$ is due to systematic contributions from total and static pressure calibrations (b_{PTCAL} and b_{PSCAL}), as well as instrumentation uncertainties in test-time bellmouth total pressure, balance chamber static pressure, and barometric pressure (combined as $b_{P_{inst}}$). The percent contributions of each of these uncertainties to the combined systematic uncertainty in $P_{T,ts}$ are shown in Figure D.5. The tabulated details are shown in Tables D.6 - D.10.

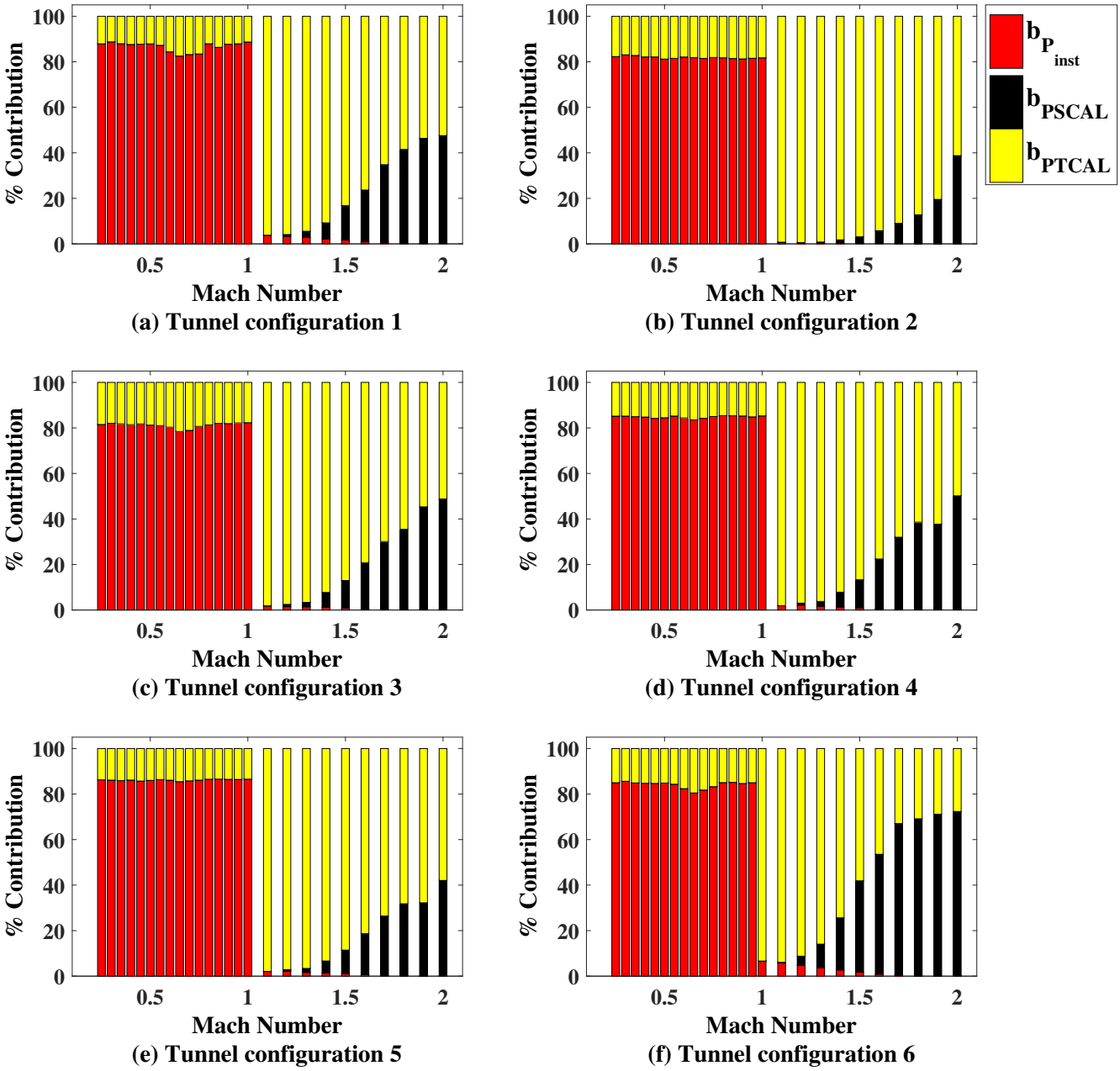

Figure D.5: Systematic UPC of $P_{T,ts}$ as a function of nominal Mach number for all configurations. Red is the systematic uncertainty due to pressure instrumentation, yellow is the systematic uncertainty due to total pressure calibration, and black is the systematic uncertainty due to static pressure calibration.

Nominal Mach	**Typical** $P_{T,ts}$ **psia**	$b_{P_{T,ts}}$, **psia k = 2**	$b_{P_{T,ts}}$ **due to** $b_{P_{Inst}}$, **psia k = 2**	$b_{P_{T,ts}}$ b_{PSCAL}, **psia k = 2**	$b_{P_{T,ts}}$ b_{PTCAL}, **psia k = 2**	$b_{P_{T,ts}}$ **UPC due to** $b_{P_{Inst}}$	$b_{P_{T,ts}}$ **UPC due to** b_{PSCAL}	$b_{P_{T,ts}}$ **UPC due to** b_{PTCAL}
0.25	15.21	0.0089	0.0081	0.0000	0.0038	82.3	0.0	17.7
0.40	15.24	0.0089	0.0081	0.0000	0.0038	82.2	0.0	17.8
0.60	17.28	0.0092	0.0084	0.0000	0.0039	82.1	0.0	17.9
0.80	16.99	0.0092	0.0083	0.0000	0.0039	81.8	0.0	18.2
1.00	16.77	0.0091	0.0082	0.0000	0.0039	81.8	0.0	18.2
1.20	17.06	0.1210	0.0080	0.0052	0.1206	0.4	0.2	99.4
1.40	18.06	0.1424	0.0088	0.0167	0.1411	0.4	1.4	98.2
1.60	20.20	0.2000	0.0089	0.0471	0.1942	0.2	5.6	94.2
1.80	23.13	0.2994	0.0101	0.1064	0.2796	0.1	12.6	87.2
2.00	24.58	0.6153	0.0091	0.3829	0.4815	0.0	38.7	61.2

Table D.6: Summary of calculated Total Pressure systematic uncertainty with 95% level of confidence for configuration 2.

Nominal Mach	**Typical** $P_{T,ts}$ **psia**	$b_{P_{T,ts}}$, **psia k = 2**	$b_{P_{T,ts}}$ **due to** $b_{P_{Inst}}$, **psia k = 2**	$b_{P_{T,ts}}$ b_{PSCAL}, **psia k = 2**	$b_{P_{T,ts}}$ b_{PTCAL}, **psia k = 2**	$b_{P_{T,ts}}$ **UPC due to** $b_{P_{Inst}}$	$b_{P_{T,ts}}$ **UPC due to** b_{PSCAL}	$b_{P_{T,ts}}$ **UPC due to** b_{PTCAL}
0.25	15.58	0.0090	0.0081	0.0000	0.0039	81.5	0.0	18.5
0.40	15.74	0.0090	0.0081	0.0000	0.0039	81.4	0.0	18.6
0.60	17.98	0.0094	0.0084	0.0000	0.0042	80.3	0.0	19.7
0.80	17.66	0.0093	0.0084	0.0000	0.0040	81.3	0.0	18.7
1.00	17.39	0.0091	0.0083	0.0000	0.0038	82.3	0.0	17.7
1.20	17.72	0.0681	0.0082	0.0068	0.0672	1.5	1.0	97.5
1.40	18.77	0.0826	0.0089	0.0212	0.0793	1.2	6.6	92.3
1.60	21.00	0.1280	0.0086	0.0576	0.1139	0.4	20.3	79.3
1.80	24.11	0.2268	0.0091	0.1348	0.1822	0.2	35.3	64.5
2.00	24.71	0.3620	0.0218	0.2519	0.2590	0.4	48.4	51.2

Table D.7: Summary of calculated Total Pressure systematic uncertainty with 95% level of confidence for configuration 3.

Nominal Mach	**Typical** $P_{T,ts}$ **psia**	$b_{P_{T,ts}}$, **psia k = 2**	$b_{P_{T,ts}}$ **due to** $b_{P_{Inst}}$, **psia k = 2**	$b_{P_{T,ts}}$ b_{PSCAL}, **psia k = 2**	$b_{P_{T,ts}}$ b_{PTCAL}, **psia k = 2**	$b_{P_{T,ts}}$ **UPC due to** $b_{P_{Inst}}$	$b_{P_{T,ts}}$ **UPC due to** b_{PSCAL}	$b_{P_{T,ts}}$ **UPC due to** b_{PTCAL}
0.25	15.56	0.0087	0.0081	0.0000	0.0034	85.2	0.0	14.8
0.40	15.74	0.0088	0.0081	0.0000	0.0034	84.8	0.0	15.2
0.60	17.94	0.0091	0.0084	0.0000	0.0036	84.4	0.0	15.6
0.80	17.64	0.0090	0.0083	0.0000	0.0034	85.4	0.0	14.6
1.00	17.35	0.0090	0.0083	0.0000	0.0034	85.3	0.0	14.7
1.20	17.64	0.0589	0.0086	0.0056	0.0580	2.2	0.9	97.0
1.40	18.65	0.0737	0.0085	0.0188	0.0708	1.3	6.5	92.1
1.60	20.96	0.1130	0.0086	0.0528	0.0995	0.6	21.8	77.6
1.80	24.13	0.2007	0.0077	0.1245	0.1572	0.1	38.5	61.4
2.00	25.17	0.3434	0.0174	0.2426	0.2424	0.3	49.9	49.8

Table D.8: Summary of calculated Total Pressure systematic uncertainty with 95% level of confidence for configuration 4.

Nominal Mach	**Typical** $P_{T,ts}$ **psia**	$b_{P_{T,ts}}$, **psia k = 2**	$b_{P_{T,ts}}$ **due to** $b_{P_{Inst}}$, **psia k = 2**	$b_{P_{T,ts}}$ b_{PSCAL}, **psia k = 2**	$b_{P_{T,ts}}$ b_{PTCAL}, **psia k = 2**	$b_{P_{T,ts}}$ **UPC due to** $b_{P_{Inst}}$	$b_{P_{T,ts}}$ **UPC due to** b_{PSCAL}	$b_{P_{T,ts}}$ **UPC due to** b_{PTCAL}
0.25	15.16	0.0087	0.0081	0.0000	0.0032	86.3	0.0	13.7
0.40	15.28	0.0087	0.0081	0.0000	0.0032	86.1	0.0	13.9
0.60	17.46	0.0090	0.0083	0.0000	0.0033	86.1	0.0	13.9
0.80	17.14	0.0089	0.0083	0.0000	0.0033	86.5	0.0	13.5
1.00	16.92	0.0089	0.0082	0.0000	0.0033	86.6	0.0	13.4
1.20	17.21	0.0583	0.0085	0.0049	0.0575	2.1	0.7	97.1
1.40	18.20	0.0727	0.0085	0.0167	0.0703	1.4	5.3	93.3
1.60	20.41	0.1098	0.0088	0.0466	0.0990	0.6	18.0	81.3
1.80	23.48	0.1896	0.0086	0.1066	0.1566	0.2	31.6	68.2
2.00	24.68	0.3324	0.0177	0.2148	0.2530	0.3	41.8	57.9

Table D.9: Summary of calculated Total Pressure systematic uncertainty with 95% level of confidence for configuration 5.

Nominal Mach	**Typical** $P_{T,ts}$ **psia**	$b_{P_{T,ts}}$, **psia k = 2**	$b_{P_{T,ts}}$ **due to** $b_{P_{Inst}}$, **psia k = 2**	$b_{P_{T,ts}}$ b_{PSCAL}, **psia k = 2**	$b_{P_{T,ts}}$ b_{PTCAL}, **psia k = 2**	$b_{P_{T,ts}}$ **UPC due to** $b_{P_{Inst}}$	$b_{P_{T,ts}}$ **UPC due to** b_{PSCAL}	$b_{P_{T,ts}}$ **UPC due to** b_{PTCAL}
0.25	15.54	0.0088	0.0081	0.0000	0.0034	85.0	0.0	15.0
0.40	15.66	0.0088	0.0081	0.0000	0.0034	84.8	0.0	15.2
0.60	17.92	0.0093	0.0084	0.0000	0.0039	82.4	0.0	17.6
0.80	17.32	0.0089	0.0082	0.0000	0.0034	85.0	0.0	15.0
1.00	17.33	0.0330	0.0085	0.0001	0.0318	6.6	0.0	93.4
1.20	17.69	0.0376	0.0082	0.0075	0.0359	4.7	4.0	91.2
1.40	18.74	0.0539	0.0089	0.0258	0.0464	2.7	22.9	74.4
1.60	20.96	0.0944	0.0088	0.0685	0.0643	0.9	52.7	46.4
1.80	24.06	0.1983	0.0088	0.1647	0.1102	0.2	68.9	30.9
2.00	24.81	0.3477	0.0194	0.2951	0.1829	0.3	72.0	27.7

Table D.10: Summary of calculated Total Pressure systematic uncertainty with 95% level of confidence for configuration 6.

D.3 Total Uncertainty Results for Configurations 2-6

Total uncertainty in $P_{T,ts}$ for all six configurations are shown in Figure D.6. Each configuration follows the same trend, although supersonically configuration 2 is noticeably higher. The combined uncertainty in $P_{T,ts}$ is presented for configurations 2-6 in Tables D.11 - D.15.

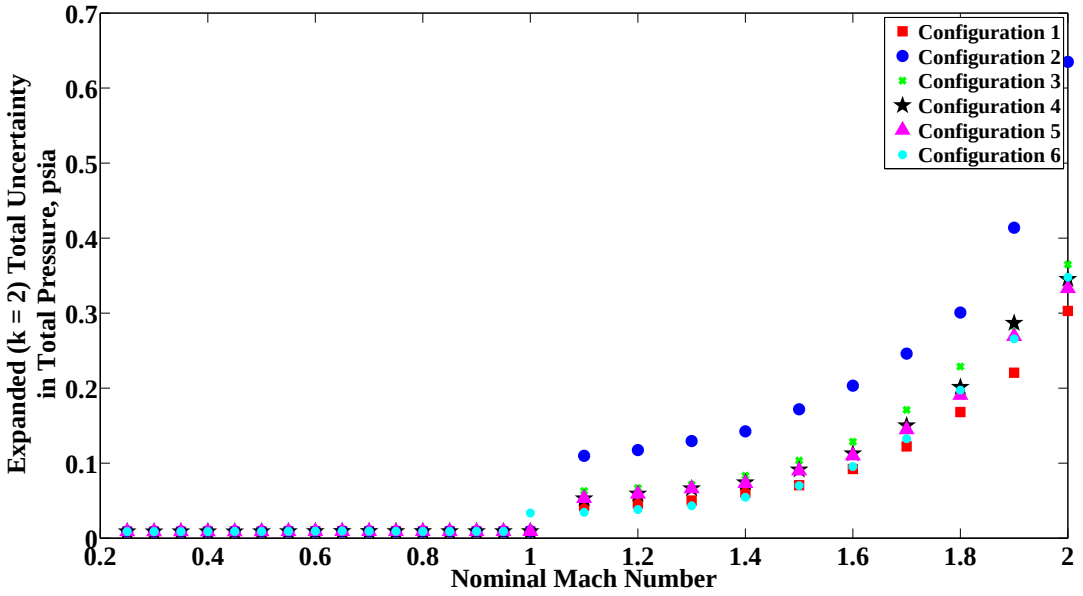

Figure D.6: Total uncertainty of $P_{T,ts}$ as a function of nominal Mach number for all configurations.

Nominal Mach	**Typical $P_{T,ts}$, psia**	$s_{P_{T,ts}}$ **psia k = 2**	$b_{P_{T,ts}}$ **psia k = 2**	$u_{P_{T,ts}}$ **psia k = 2**	$s_{P_{T,ts}}$ **UPC**	$b_{P_{T,ts}}$ **UPC**
0.25	15.21	0.0005	0.0089	0.0090	0.3	99.7
0.40	15.24	0.0004	0.0089	0.0090	0.2	99.8
0.60	17.28	0.0004	0.0092	0.0092	0.2	99.8
0.80	16.99	0.0005	0.0092	0.0092	0.2	99.8
1.00	16.77	0.0017	0.0091	0.0093	3.4	96.6
1.20	17.06	0.0037	0.1210	0.1174	0.1	99.9
1.40	18.06	0.0050	0.1424	0.1424	0.1	99.9
1.60	20.20	0.0054	0.2000	0.2032	0.1	99.9
1.80	23.13	0.0153	0.2994	0.3008	0.3	99.7
2.00	24.58	0.1194	0.6153	0.6350	3.6	96.4

Table D.11: Summary of calculated Total Pressure uncertainty with 95% level of confidence for configuration 2.

Nominal Mach	**Typical $P_{T,ts}$, psia**	$s_{P_{T,ts}}$ **psia k = 2**	$b_{P_{T,ts}}$ **psia k = 2**	$u_{P_{T,ts}}$ **psia k = 2**	$s_{P_{T,ts}}$ **UPC**	$b_{P_{T,ts}}$ **UPC**
0.25	15.58	0.0004	0.0090	0.0090	0.2	99.8
0.40	15.74	0.0004	0.0090	0.0091	0.2	99.8
0.60	17.98	0.0003	0.0094	0.0094	0.1	99.9
0.80	17.66	0.0009	0.0093	0.0093	0.9	99.1
1.00	17.39	0.0015	0.0091	0.0093	2.5	97.5
1.20	17.72	0.0033	0.0681	0.0668	0.2	99.8
1.40	18.77	0.0044	0.0826	0.0833	0.3	99.7
1.60	21.00	0.0118	0.1280	0.1286	0.8	99.2
1.80	24.11	0.0301	0.2268	0.2287	1.7	98.3
2.00	24.71	0.0310	0.3620	0.3648	0.7	99.3

Table D.12: Summary of calculated Total Pressure uncertainty with 95% level of confidence for configuration 3.

Nominal Mach	**Typical $P_{T,ts}$, psia**	$s_{P_{T,ts}}$ **psia k = 2**	$b_{P_{T,ts}}$ **psia k = 2**	$u_{P_{T,ts}}$ **psia k = 2**	$s_{P_{T,ts}}$ **UPC**	$b_{P_{T,ts}}$ **UPC**
0.25	15.56	0.0005	0.0087	0.0088	0.3	99.7
0.40	15.74	0.0004	0.0088	0.0088	0.2	99.8
0.60	17.94	0.0002	0.0091	0.0091	0.1	99.9
0.80	17.64	0.0003	0.0090	0.0090	0.1	99.9
1.00	17.35	0.0007	0.0090	0.0090	0.5	99.5
1.20	17.64	0.0010	0.0589	0.0590	0.0	100.0
1.40	18.65	0.0013	0.0737	0.0741	0.0	100.0
1.60	20.96	0.0048	0.1130	0.1128	0.2	99.8
1.80	24.13	0.0114	0.2007	0.2014	0.3	99.7
2.00	25.17	0.0329	0.3434	0.3453	0.9	99.1

Table D.13: Summary of calculated Total Pressure uncertainty with 95% level of confidence for configuration 4.

Nominal Mach	**Typical $P_{T,ts}$, psia**	$s_{P_{T,ts}}$ **psia k = 2**	$b_{P_{T,ts}}$ **psia k = 2**	$u_{P_{T,ts}}$ **psia k = 2**	$s_{P_{T,ts}}$ **UPC**	$b_{P_{T,ts}}$ **UPC**
0.25	15.16	0.0011	0.0087	0.0088	1.5	98.5
0.40	15.28	0.0004	0.0087	0.0087	0.2	99.8
0.60	17.46	0.0005	0.0090	0.0090	0.3	99.7
0.80	17.14	0.0010	0.0089	0.0090	1.4	98.6
1.00	16.92	0.0015	0.0089	0.0090	2.7	97.3
1.20	17.21	0.0029	0.0583	0.0588	0.2	99.8
1.40	18.20	0.0038	0.0727	0.0730	0.3	99.7
1.60	20.41	0.0040	0.1098	0.1100	0.1	99.9
1.80	23.48	0.0228	0.1896	0.1906	1.4	98.6
2.00	24.68	0.0256	0.3324	0.3329	0.6	99.4

Table D.14: Summary of calculated Total Pressure uncertainty with 95% level of confidence for configuration 5.

Nominal Mach	**Typical $P_{T,ts}$, psia**	$s_{P_{T,ts}}$ **psia** **k = 2**	$b_{P_{T,ts}}$ **psia** **k = 2**	$u_{P_{T,ts}}$ **psia** **k = 2**	$s_{P_{T,ts}}$ **UPC**	$b_{P_{T,ts}}$ **UPC**
0.25	15.54	0.0005	0.0088	0.0088	0.3	99.7
0.40	15.66	0.0003	0.0088	0.0088	0.1	99.9
0.60	17.92	0.0003	0.0093	0.0093	0.1	99.9
0.80	17.32	0.0005	0.0089	0.0088	0.3	99.7
1.00	17.33	0.0009	0.0330	0.0336	0.1	99.9
1.20	17.69	0.0013	0.0376	0.0382	0.1	99.9
1.40	18.74	0.0072	0.0539	0.0545	1.7	98.3
1.60	20.96	0.0075	0.0944	0.0954	0.6	99.4
1.80	24.06	0.0092	0.1983	0.1974	0.2	99.8
2.00	24.81	0.0075	0.3477	0.3478	0.0	100.0

Table D.15: Summary of calculated Total Pressure uncertainty with 95% level of confidence for configuration 6.

Appendix E: Dynamic Pressure Uncertainty

Dynamic pressure is a function of Mach number and total pressure, as shown in Figure E.1. Refer to Appendices B and D respectively to see uncertainty flow to those variables, which are propagated through the data reduction equations shown in Section 3.2.2 to attain uncertainty in dynamic pressure. Results for uncertainty in dynamic pressure for configuration 1 were presented in Section 5. Results for configurations 2-6 are presented in this Appendix. Bar charts depicting the percent contributions are shown, followed by tabulated results detailing dimensional and percent contributions for random, systematic, and total uncertainty.

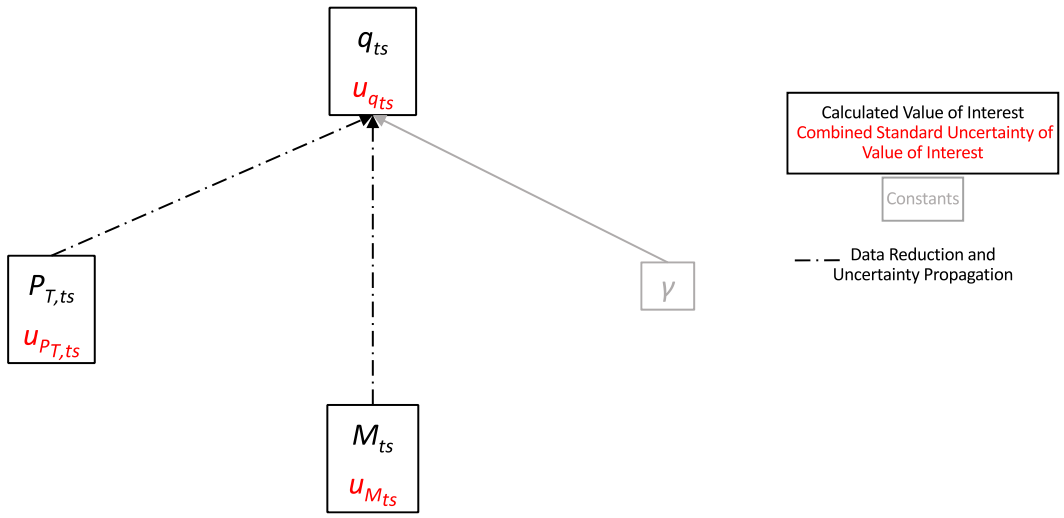

Figure E.1: Uncertainty flow from measured value to calculated dynamic pressure in the test section.

E.1 Random Uncertainty Results for Configurations 2-6

The random uncertainty in the dynamic pressure is shown for all configurations in Figure E.2. All configurations follow a similar trend, remaining below 0.005 psia subsonically then increasing supersonically. Configuration 2 shows a sharp increase at the highest Mach numbers, not seen in the other configurations, which remain below 0.02 psia.

The elemental random uncertainties contributing to random uncertainty in test section dynamic pressure are the random uncertainty in $P_{T,bm}$ and $P_{S,bal}$. The percent contributions of each of these parameters to the total random uncertainty in q_{ts} are shown in Figure E.3. The tabulated details are shown in Tables E.1 - E.5.

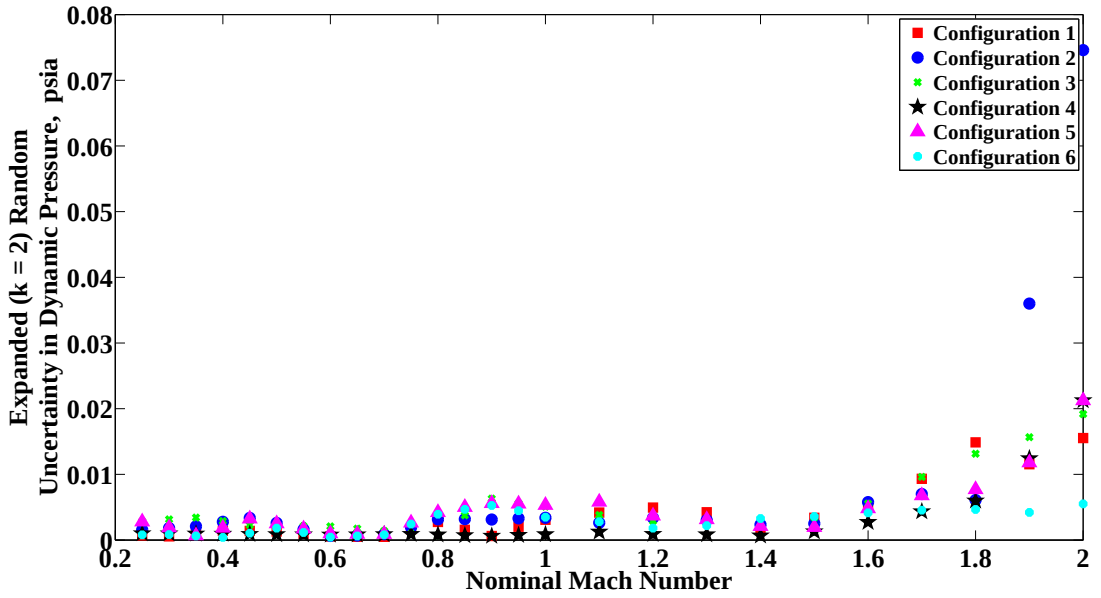

Figure E.2: Random uncertainty of q_{ts} as a function of nominal Mach number for all configurations. The red squares are configuration 1, blue circles are configuration 2, green x's are configuration 3, black stars are configuration 4, purple triangles are configuration 5, and cyan dots are configuration 6.

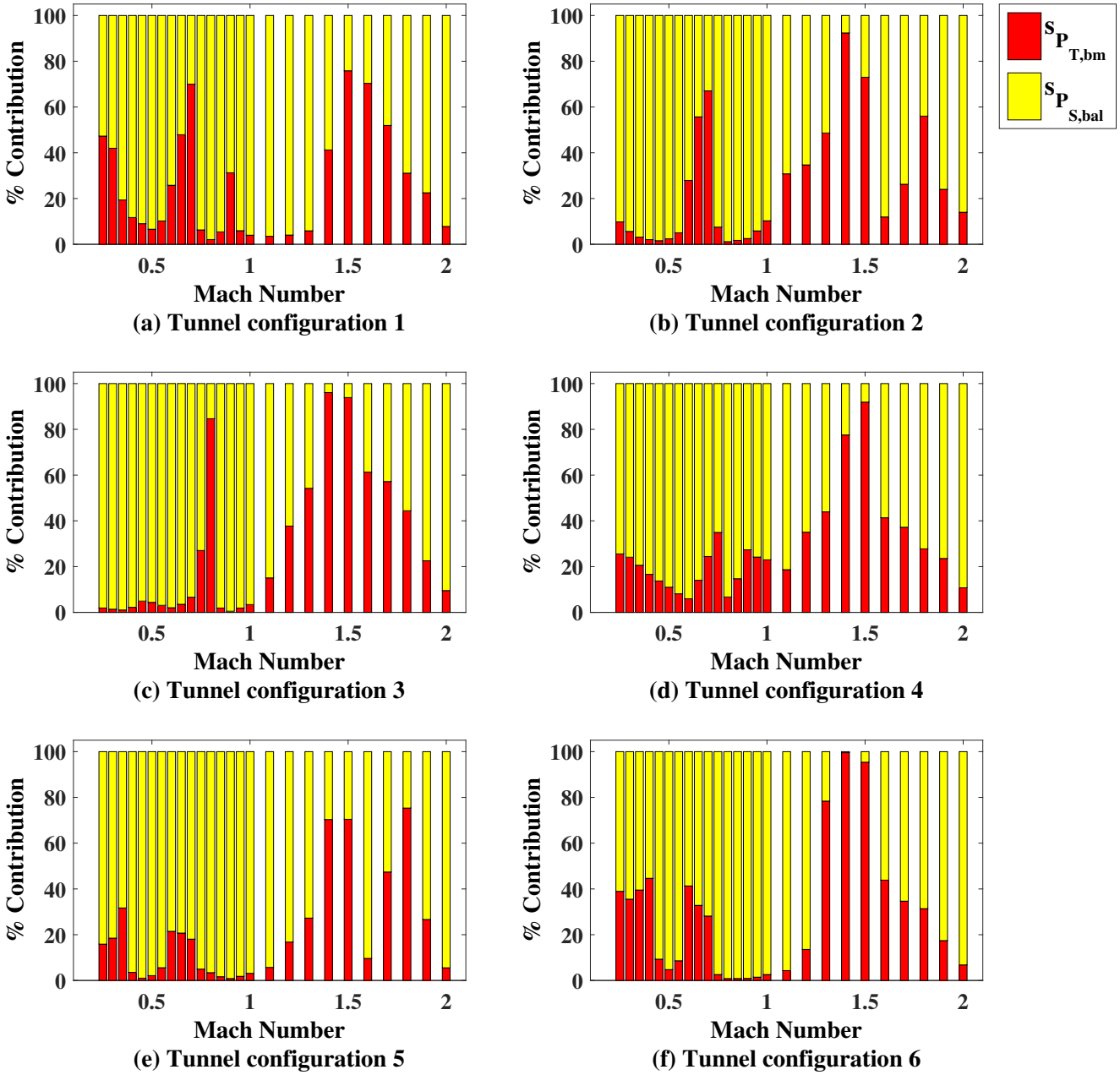

Figure E.3: Random UPC of q_{ts} as a function of nominal Mach number for all configurations. Red is the random uncertainty of the total pressure in the bellmouth, yellow is the random uncertainty of the static pressure in the balance chamber.

Nominal Mach	**Typical** q_{ts} **psia**	$s_{q_{ts}}$ **psia** **k = 2**	$s_{q_{ts}}$ **due to** $s_{P_{T,bm}}$ **psia** **k = 2**	$s_{q_{ts}}$ **due to** $s_{P_{S,bal}}$ **psia** **k = 2**	$s_{q_{ts}}$ **UPC due to** $s_{P_{T,bm}}$	$s_{q_{ts}}$ **UPC due to** $s_{P_{S,bal}}$
0.25	0.63	0.002	0.000	0.001	9.8	90.2
0.40	1.59	0.003	0.000	0.003	2.0	98.0
0.60	3.50	0.001	0.000	0.001	27.9	72.1
0.80	5.10	0.003	0.000	0.003	1.1	98.9
1.00	6.22	0.003	0.001	0.003	10.3	89.7
1.20	7.08	0.003	0.002	0.003	34.7	65.3
1.40	7.77	0.002	0.002	0.001	92.4	7.6
1.60	8.60	0.006	0.002	0.005	11.9	88.1
1.80	9.31	0.006	0.005	0.004	56.0	44.0
2.00	8.99	0.075	0.028	0.069	14.0	86.0

Table E.1: Summary of calculated Dynamic Pressure random uncertainty with 95% level of confidence for configuration 2.

Nominal Mach	**Typical** q_{ts} **psia**	$s_{q_{ts}}$ **psia** **k = 2**	$s_{q_{ts}}$ **due to** $s_{P_{T,bm}}$ **psia** **k = 2**	$s_{q_{ts}}$ **due to** $s_{P_{S,bal}}$ **psia** **k = 2**	$s_{q_{ts}}$ **UPC due to** $s_{P_{T,bm}}$	$s_{q_{ts}}$ **UPC due to** $s_{P_{S,bal}}$
0.25	0.63	0.003	0.000	0.003	1.9	98.1
0.40	1.63	0.003	0.000	0.003	2.2	97.8
0.60	3.60	0.002	0.000	0.002	2.0	98.0
0.80	5.22	0.001	0.001	0.000	84.6	15.4
1.00	6.37	0.005	0.001	0.005	3.4	96.6
1.20	7.37	0.003	0.002	0.002	37.7	62.3
1.40	8.07	0.002	0.002	0.000	96.1	3.9
1.60	8.93	0.006	0.004	0.003	61.3	38.7
1.80	9.63	0.013	0.009	0.010	44.4	55.6
2.00	8.99	0.019	0.006	0.018	9.5	90.5

Table E.2: Summary of calculated Dynamic Pressure random uncertainty with 95% level of confidence for configuration 3.

Nominal Mach	**Typical** q_{ts} **psia**	$s_{q_{ts}}$ **psia** **k = 2**	$s_{q_{ts}}$ **due to** $s_{P_{T,bm}}$ **psia** **k = 2**	$s_{q_{ts}}$ **due to** $s_{P_{S,bal}}$ **psia** **k = 2**	$s_{q_{ts}}$ **UPC due to** $s_{P_{T,bm}}$	$s_{q_{ts}}$ **UPC due to** $s_{P_{S,bal}}$
0.25	0.64	0.001	0.001	0.001	25.6	74.4
0.40	1.63	0.001	0.000	0.001	16.6	83.4
0.60	3.61	0.001	0.000	0.001	5.9	94.1
0.80	5.24	0.001	0.000	0.001	6.7	93.3
1.00	6.42	0.001	0.000	0.001	23.0	77.0
1.20	7.31	0.001	0.001	0.001	35.1	64.9
1.40	8.02	0.001	0.001	0.000	77.5	22.5
1.60	8.91	0.003	0.002	0.002	41.4	58.6
1.80	9.60	0.006	0.003	0.005	27.8	72.2
2.00	9.04	0.021	0.007	0.020	10.7	89.3

Table E.3: Summary of calculated Dynamic Pressure random uncertainty with 95% level of confidence for configuration 4.

Nominal Mach	**Typical** q_{ts} **psia**	$s_{q_{ts}}$ **psia** **k = 2**	$s_{q_{ts}}$ **due to** $s_{P_{T,bm}}$ **psia** **k = 2**	$s_{q_{ts}}$ **due to** $s_{P_{S,bal}}$ **psia** **k = 2**	$s_{q_{ts}}$ **UPC due to** $s_{P_{T,bm}}$	$s_{q_{ts}}$ **UPC due to** $s_{P_{S,bal}}$
0.25	0.61	0.003	0.001	0.003	15.9	84.1
0.40	1.56	0.002	0.000	0.002	3.5	96.5
0.60	3.48	0.001	0.000	0.001	21.5	78.5
0.80	5.06	0.004	0.001	0.004	3.4	96.6
1.00	6.24	0.005	0.001	0.005	3.1	96.9
1.20	7.13	0.004	0.002	0.003	16.8	83.2
1.40	7.83	0.002	0.002	0.001	70.3	29.7
1.60	8.69	0.005	0.001	0.005	9.6	90.4
1.80	9.40	0.008	0.007	0.004	75.3	24.7
2.00	8.95	0.021	0.005	0.021	5.5	94.5

Table E.4: Summary of calculated Dynamic Pressure random uncertainty with 95% level of confidence for configuration 5.

Nominal Mach	**Typical** q_{ts} **psia**	$s_{q_{ts}}$ **psia** **k = 2**	$s_{q_{ts}}$ **due to** $s_{P_{T,bm}}$ **psia** **k = 2**	$s_{q_{ts}}$ **due to** $s_{P_{S,bal}}$ **psia** **k = 2**	$s_{q_{ts}}$ **UPC due to** $s_{P_{T,bm}}$	$s_{q_{ts}}$ **UPC due to** $s_{P_{S,bal}}$
0.25	0.64	0.001	0.000	0.001	39.0	61.0
0.40	1.62	0.000	0.000	0.000	44.6	55.4
0.60	3.58	0.000	0.000	0.000	41.3	58.7
0.80	5.12	0.004	0.000	0.004	0.8	99.2
1.00	6.50	0.003	0.001	0.003	2.6	97.4
1.20	7.33	0.002	0.001	0.002	13.6	86.4
1.40	8.06	0.003	0.003	0.000	99.6	0.4
1.60	8.90	0.004	0.003	0.003	43.8	56.2
1.80	9.55	0.005	0.003	0.004	31.4	68.6
2.00	9.00	0.006	0.001	0.005	6.8	93.2

Table E.5: Summary of calculated Dynamic Pressure random uncertainty with 95% level of confidence for configuration 6.

E.2 Systematic Uncertainty Results for Configurations 2-6

The systematic uncertainty in the test section dynamic pressure is shown for all configurations in Figure E.4. All configurations follow a similar trend, although there is variation in magnitude dependent on configuration, especially supersonically.

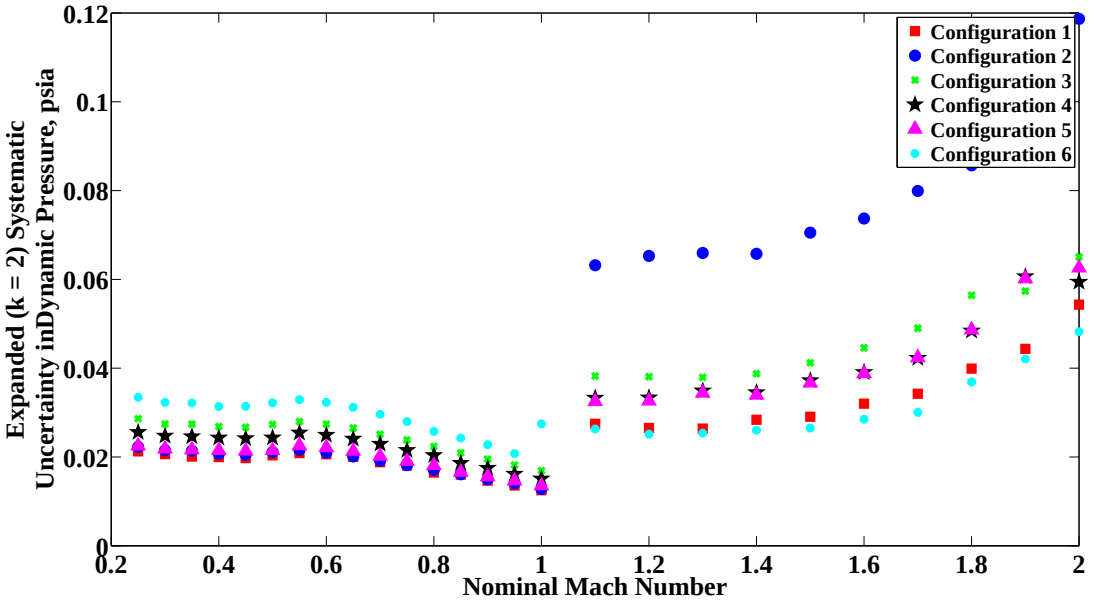

Figure E.4: Systematic uncertainty of q_{ts} as a function of nominal Mach number for all configurations. The red squares are configuration 1, blue circles are configuration 2, green x's are configuration 3, black stars are configuration 4, purple triangles are configuration 5, and cyan dots are configuration 6.

The systematic uncertainty in q_{ts} is due to systematic contributions from total and static pressure calibrations (b_{PTCAL} and b_{PSCAL}), as well as instrumentation uncertainties in test-time bellmouth total pressure, balance chamber static pressure, and barometric pressure (combined as $b_{P_{inst}}$). The percent contributions of each of these uncertainties to the combined systematic uncertainty in q_{ts} are shown in Figure E.5. The tabulated details are shown in Tables E.6 - E.10.

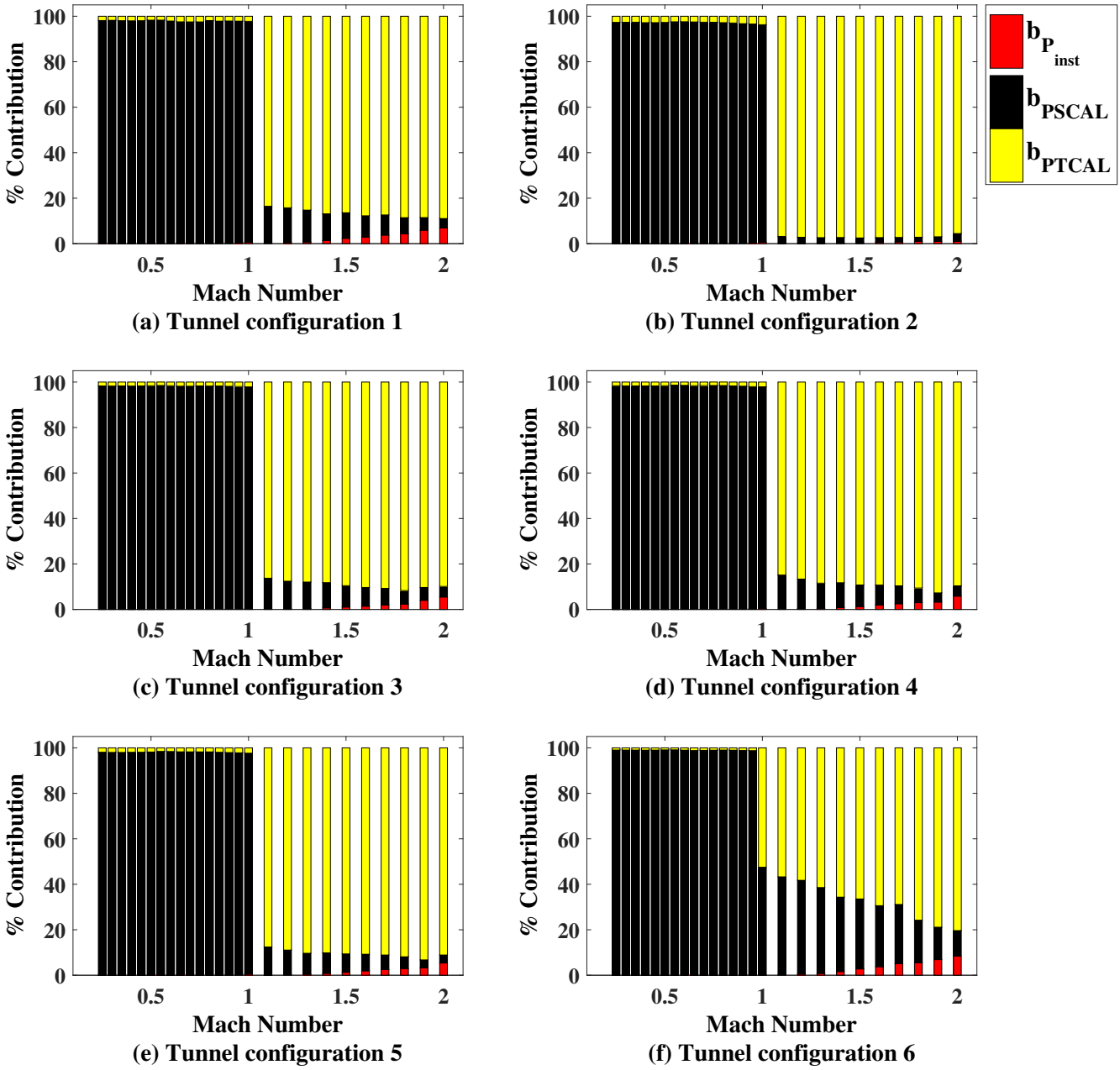

Figure E.5: Systematic UPC of q_{ts} as a function of nominal Mach number for all configurations. Red is the systematic uncertainty due to pressure instrumentation, yellow is the systematic uncertainty due to total pressure calibration, and black is the systematic uncertainty due to static pressure calibration.

Nominal Mach	**Typical** q_{ts} **psia**	$b_{q_{ts}}$ **psia** **k = 2**	$b_{q_{ts}}$ **due to** $b_{P_{Inst}}$ **psia** **k = 2**	$b_{q_{ts}}$ **due to** b_{PSCAL} **psia** **k = 2**	$b_{q_{ts}}$ **due to** b_{PTCAL} **psia** **k = 2**	$b_{q_{ts}}$ **UPC due to** $b_{P_{Inst}}$	$b_{q_{ts}}$ **UPC due to** b_{PSCAL}	$b_{q_{ts}}$ **UPC due to** b_{PTCAL}
0.25	0.63	0.022	0.000	0.022	0.004	0.0	97.3	2.7
0.40	1.59	0.021	0.000	0.020	0.003	0.0	97.2	2.8
0.60	3.50	0.021	0.000	0.021	0.003	0.0	97.5	2.4
0.80	5.10	0.017	0.001	0.017	0.003	0.1	97.1	2.8
1.00	6.22	0.013	0.001	0.013	0.002	0.6	95.7	3.7
1.20	7.08	0.065	0.002	0.011	0.064	0.1	2.7	97.2
1.40	7.77	0.066	0.003	0.010	0.065	0.2	2.5	97.3
1.60	8.60	0.074	0.005	0.011	0.073	0.5	2.1	97.3
1.80	9.31	0.086	0.009	0.012	0.084	1.0	1.8	97.2
2.00	8.99	0.119	0.012	0.022	0.116	1.0	3.4	95.6

Table E.6: Summary of calculated Dynamic Pressure systematic uncertainty with 95% level of confidence for configuration 2.

Nominal Mach	**Typical** q_{ts} **psia**	$b_{q_{ts}}$ **psia** **k = 2**	$b_{q_{ts}}$ **due to** $b_{P_{Inst}}$ **psia** **k = 2**	$b_{q_{ts}}$ **due to** b_{PSCAL} **psia** **k = 2**	$b_{q_{ts}}$ **due to** b_{PTCAL} **psia** **k = 2**	$b_{q_{ts}}$ **UPC due to** $b_{P_{Inst}}$	$b_{q_{ts}}$ **UPC due to** b_{PSCAL}	$b_{q_{ts}}$ **UPC due to** b_{PTCAL}
0.25	0.63	0.029	0.000	0.028	0.004	0.0	98.3	1.7
0.40	1.63	0.027	0.000	0.027	0.004	0.0	98.2	1.8
0.60	3.60	0.027	0.001	0.027	0.003	0.0	98.3	1.6
0.80	5.22	0.022	0.001	0.022	0.003	0.1	98.2	1.8
1.00	6.37	0.017	0.001	0.017	0.002	0.3	97.6	2.1
1.20	7.37	0.038	0.002	0.013	0.036	0.2	12.2	87.6
1.40	8.07	0.039	0.003	0.013	0.036	0.7	11.1	88.2
1.60	8.93	0.045	0.005	0.013	0.042	1.4	8.2	90.3
1.80	9.63	0.056	0.009	0.014	0.054	2.4	5.9	91.7
2.00	8.99	0.065	0.015	0.014	0.062	5.5	4.6	89.9

Table E.7: Summary of calculated Dynamic Pressure systematic uncertainty with 95% level of confidence for configuration 3.

Nominal Mach	**Typical** q_{ts} **psia**	$b_{q_{ts}}$ **psia** **k = 2**	$b_{q_{ts}}$ **due to** $b_{P_{Inst}}$ **psia** **k = 2**	$b_{q_{ts}}$ **due to** b_{PSCAL} **psia** **k = 2**	$b_{q_{ts}}$ **due to** b_{PTCAL} **psia** **k = 2**	$b_{q_{ts}}$ **UPC due to** $b_{P_{Inst}}$	$b_{q_{ts}}$ **UPC due to** b_{PSCAL}	$b_{q_{ts}}$ **UPC due to** b_{PTCAL}
0.25	0.64	0.026	0.000	0.025	0.003	0.0	98.4	1.6
0.40	1.63	0.024	0.000	0.024	0.003	0.0	98.3	1.7
0.60	3.61	0.025	0.000	0.025	0.003	0.0	98.5	1.5
0.80	5.24	0.020	0.001	0.020	0.003	0.1	98.4	1.5
1.00	6.42	0.015	0.001	0.015	0.002	0.5	97.5	2.1
1.20	7.31	0.033	0.002	0.012	0.031	0.4	13.0	86.7
1.40	8.02	0.035	0.003	0.011	0.032	0.8	10.9	88.3
1.60	8.91	0.039	0.005	0.012	0.037	1.9	8.8	89.3
1.80	9.60	0.048	0.008	0.012	0.046	3.0	6.4	90.6
2.00	9.04	0.059	0.014	0.013	0.056	5.9	4.5	89.6

Table E.8: Summary of calculated Dynamic Pressure systematic uncertainty with 95% level of confidence for configuration 4.

Nominal Mach	**Typical** q_{ts} **psia**	$b_{q_{ts}}$ **psia** **k = 2**	$b_{q_{ts}}$ **due to** $b_{P_{Inst}}$ **psia** **k = 2**	$b_{q_{ts}}$ **due to** b_{PSCAL} **psia** **k = 2**	$b_{q_{ts}}$ **due to** b_{PTCAL} **psia** **k = 2**	$b_{q_{ts}}$ **UPC due to** $b_{P_{Inst}}$	$b_{q_{ts}}$ **UPC due to** b_{PSCAL}	$b_{q_{ts}}$ **UPC due to** b_{PTCAL}
0.25	0.61	0.023	0.000	0.022	0.003	0.0	98.1	1.9
0.40	1.56	0.021	0.000	0.021	0.003	0.0	98.1	1.9
0.60	3.48	0.022	0.000	0.022	0.003	0.0	98.3	1.6
0.80	5.06	0.018	0.001	0.018	0.002	0.1	98.1	1.8
1.00	6.24	0.014	0.001	0.013	0.002	0.5	97.2	2.3
1.20	7.13	0.033	0.002	0.011	0.031	0.4	10.7	88.9
1.40	7.83	0.034	0.003	0.010	0.032	0.8	9.0	90.1
1.60	8.69	0.039	0.005	0.011	0.037	1.9	7.3	90.8
1.80	9.40	0.049	0.008	0.011	0.047	3.0	5.2	91.9
2.00	8.95	0.063	0.015	0.012	0.060	5.4	3.5	91.1

Table E.9: Summary of calculated Dynamic Pressure systematic uncertainty with 95% level of confidence for configuration 5.

Nominal Mach	**Typical** q_{ts} **psia**	$b_{q_{ts}}$ **psia** **k = 2**	$b_{q_{ts}}$ **due to** $b_{P_{Inst}}$ **psia** **k = 2**	$b_{q_{ts}}$ **due to** b_{PSCAL} **psia** **k = 2**	$b_{q_{ts}}$ **due to** b_{PTCAL} **psia** **k = 2**	$b_{q_{ts}}$ **UPC due to** $b_{P_{Inst}}$	$b_{q_{ts}}$ **UPC due to** b_{PSCAL}	$b_{q_{ts}}$ **UPC due to** b_{PTCAL}
0.25	0.64	0.033	0.000	0.033	0.003	0.0	99.0	1.0
0.40	1.62	0.031	0.000	0.031	0.003	0.0	99.0	1.0
0.60	3.58	0.032	0.000	0.032	0.003	0.0	99.0	1.0
0.80	5.12	0.026	0.001	0.026	0.003	0.1	99.0	1.0
1.00	6.50	0.027	0.001	0.019	0.020	0.2	47.3	52.5
1.20	7.33	0.025	0.002	0.016	0.019	0.5	41.3	58.3
1.40	8.06	0.026	0.003	0.015	0.021	1.6	32.7	65.7
1.60	8.90	0.029	0.006	0.015	0.024	3.7	26.8	69.4
1.80	9.55	0.037	0.009	0.016	0.032	5.4	18.8	75.8
2.00	9.00	0.048	0.014	0.016	0.043	8.4	11.2	80.4

Table E.10: Summary of calculated Dynamic Pressure systematic uncertainty with 95% level of confidence for configuration 6.

E.3 Total Uncertainty Results for Configurations 2-6

The total uncertainty in q_{ts} for all configurations is shown in Figure E.6. The trends are the same for every configuration, although the magnitudes vary, especially configuration 2 which is above 0.06 psia for all supersonic Mach numbers. The combined uncertainty in q_{ts} is presented for configurations 2-6 in Tables E.11 - E.15.

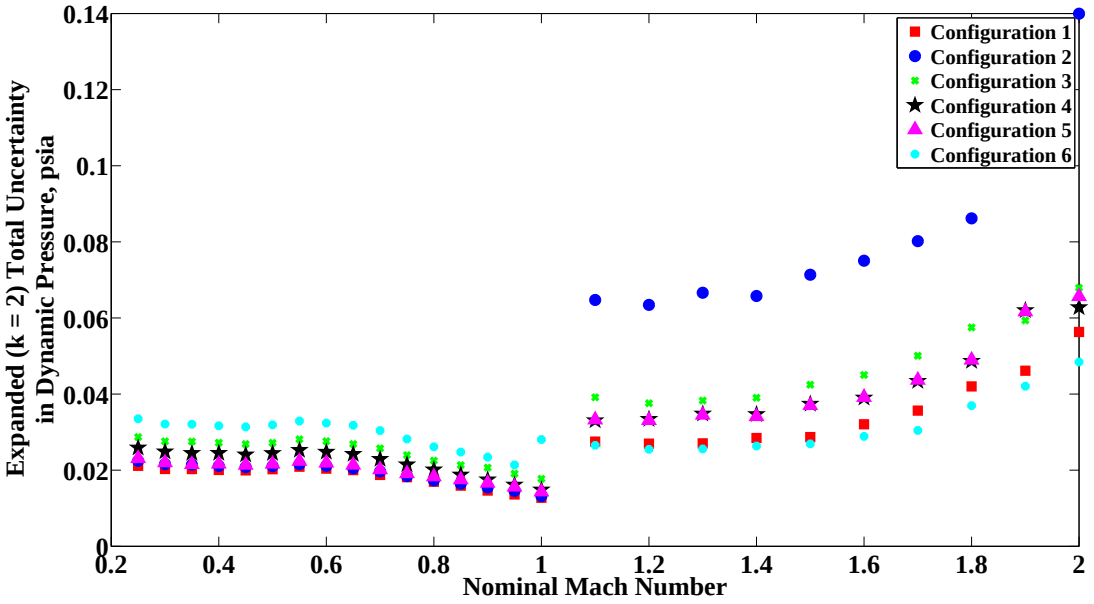

Figure E.6: Total uncertainty in q_{ts} as a function of nominal Mach number for all configurations.

Nominal Mach	**Typical q_{ts}, psia**	$s_{q_{ts}}$ **psia k = 2**	$b_{q_{ts}}$ **psia k = 2**	$u_{q_{ts}}$ **psia k = 2**	$s_{q_{ts}}$ **UPC**	$b_{q_{ts}}$ **UPC**
0.25	0.63	0.002	0.022	0.022	0.5	99.5
0.40	1.59	0.003	0.021	0.021	1.8	98.2
0.60	3.50	0.001	0.021	0.021	0.1	99.9
0.80	5.10	0.003	0.017	0.017	3.3	96.7
1.00	6.22	0.003	0.013	0.013	6.5	93.5
1.20	7.08	0.003	0.065	0.063	0.3	99.7
1.40	7.77	0.002	0.066	0.066	0.1	99.9
1.60	8.60	0.006	0.074	0.075	0.6	99.4
1.80	9.31	0.006	0.086	0.086	0.5	99.5
2.00	8.99	0.075	0.119	0.140	28.3	71.7

Table E.11: Summary of calculated Dynamic Pressure uncertainty with 95% level of confidence for configuration 2.

Nominal Mach	**Typical q_{ts}, psia**	$s_{q_{ts}}$ **psia k = 2**	$b_{q_{ts}}$ **psia k = 2**	$u_{q_{ts}}$ **psia k = 2**	$s_{q_{ts}}$ **UPC**	$b_{q_{ts}}$ **UPC**
0.25	0.63	0.003	0.029	0.029	1.0	99.0
0.40	1.63	0.003	0.027	0.027	1.1	98.9
0.60	3.60	0.002	0.027	0.028	0.6	99.4
0.80	5.22	0.001	0.022	0.023	0.1	99.9
1.00	6.37	0.005	0.017	0.018	8.3	91.7
1.20	7.37	0.003	0.038	0.038	0.6	99.4
1.40	8.07	0.002	0.039	0.039	0.3	99.7
1.60	8.93	0.006	0.045	0.045	1.5	98.5
1.80	9.63	0.013	0.056	0.058	5.2	94.8
2.00	8.99	0.019	0.065	0.068	8.0	92.0

Table E.12: Summary of calculated Dynamic Pressure uncertainty with 95% level of confidence for configuration 3.

Nominal Mach	**Typical q_{ts}, psia**	$s_{q_{ts}}$ **psia k = 2**	$b_{q_{ts}}$ **psia k = 2**	$u_{q_{ts}}$ **psia k = 2**	$s_{q_{ts}}$ **UPC**	$b_{q_{ts}}$ **UPC**
0.25	0.64	0.001	0.026	0.026	0.1	99.9
0.40	1.63	0.001	0.024	0.024	0.1	99.9
0.60	3.61	0.001	0.025	0.025	0.1	99.9
0.80	5.24	0.001	0.020	0.020	0.2	99.8
1.00	6.42	0.001	0.015	0.015	0.3	99.7
1.20	7.31	0.001	0.033	0.033	0.1	99.9
1.40	8.02	0.001	0.035	0.035	0.0	100.0
1.60	8.91	0.003	0.039	0.039	0.5	99.5
1.80	9.60	0.006	0.048	0.049	1.5	98.5
2.00	9.04	0.021	0.059	0.063	11.3	88.7

Table E.13: Summary of calculated Dynamic Pressure uncertainty with 95% level of confidence for configuration 4.

Nominal Mach	**Typical q_{ts}, psia**	$s_{q_{ts}}$ **psia k = 2**	$b_{q_{ts}}$ **psia k = 2**	$u_{q_{ts}}$ **psia k = 2**	$s_{q_{ts}}$ **UPC**	$b_{q_{ts}}$ **UPC**
0.25	0.61	0.003	0.023	0.023	1.5	98.5
0.40	1.56	0.002	0.021	0.022	0.7	99.3
0.60	3.48	0.001	0.022	0.022	0.2	99.8
0.80	5.06	0.004	0.018	0.018	5.1	94.9
1.00	6.24	0.005	0.014	0.014	13.3	86.7
1.20	7.13	0.004	0.033	0.033	1.3	98.7
1.40	7.83	0.002	0.034	0.034	0.4	99.6
1.60	8.69	0.005	0.039	0.039	1.5	98.5
1.80	9.40	0.008	0.049	0.049	2.4	97.6
2.00	8.95	0.021	0.063	0.066	10.3	89.7

Table E.14: Summary of calculated Dynamic Pressure uncertainty with 95% level of confidence for configuration 5.

Nominal Mach	**Typical q_{ts}, psia**	$s_{q_{ts}}$ **psia** **k = 2**	$b_{q_{ts}}$ **psia** **k = 2**	$u_{q_{ts}}$ **psia** **k = 2**	$s_{q_{ts}}$ **UPC**	$b_{q_{ts}}$ **UPC**
0.25	0.64	0.001	0.033	0.034	0.1	99.9
0.40	1.62	0.000	0.031	0.032	0.0	100.0
0.60	3.58	0.000	0.032	0.032	0.0	100.0
0.80	5.12	0.004	0.026	0.026	2.3	97.7
1.00	6.50	0.003	0.027	0.028	1.6	98.4
1.20	7.33	0.002	0.025	0.025	0.5	99.5
1.40	8.06	0.003	0.026	0.026	1.6	98.4
1.60	8.90	0.004	0.029	0.029	2.1	97.9
1.80	9.55	0.005	0.037	0.037	1.6	98.4
2.00	9.00	0.006	0.048	0.048	1.3	98.7

Table E.15: Summary of calculated Dynamic Pressure uncertainty with 95% level of confidence for configuration 6.

Appendix F: Total Temperature Uncertainty

The uncertainty from measured values to test section total temperature propagates as shown in Figure F.1. Results for uncertainty in test section total temperature for configuration 1 were presented in Section 5. Results for configurations 2-6 are presented in this Appendix. Bar charts depicting the percent contributions are shown, followed by tabulated results detailing dimensional and percent contributions for random, systematic, and total uncertainty.

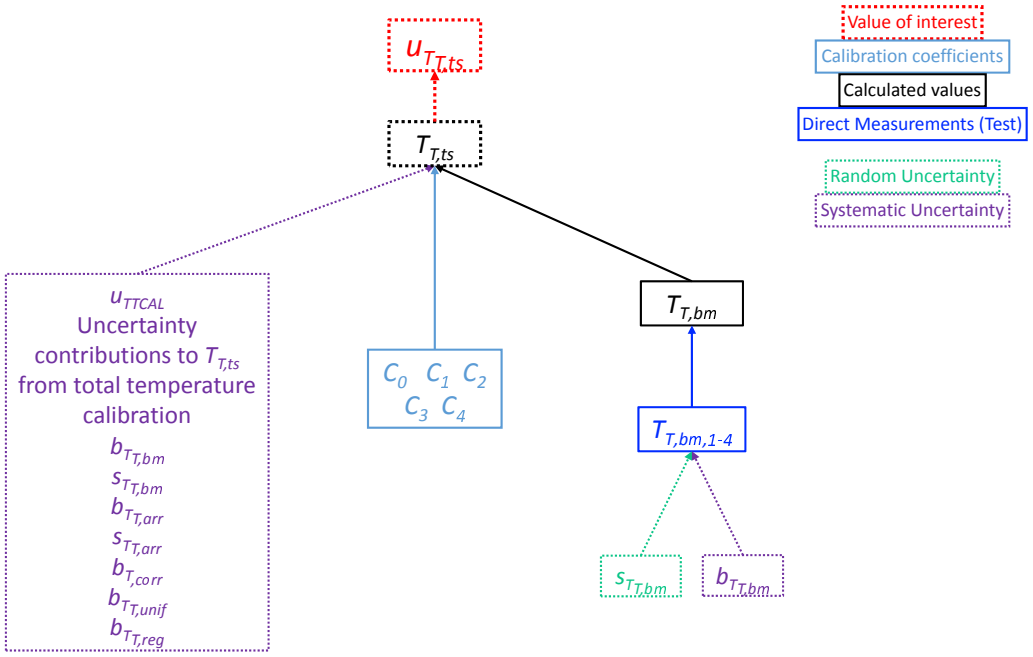

Figure F.1: Uncertainty flow from measured value to calculated total temperature in the test section.

F.1 Random Uncertainty Results for Configurations 2-6

The random uncertainty in the test section total temperature is shown for all configurations in Figure F.2. All configurations follow a similar trend transonically, remaining below 0.5 °R. There is more scatter at the low and high end of the Mach range.

The only elemental random uncertainty contributing to random uncertainty in test section static pressure is that of measurement $T_{T,bm}$.

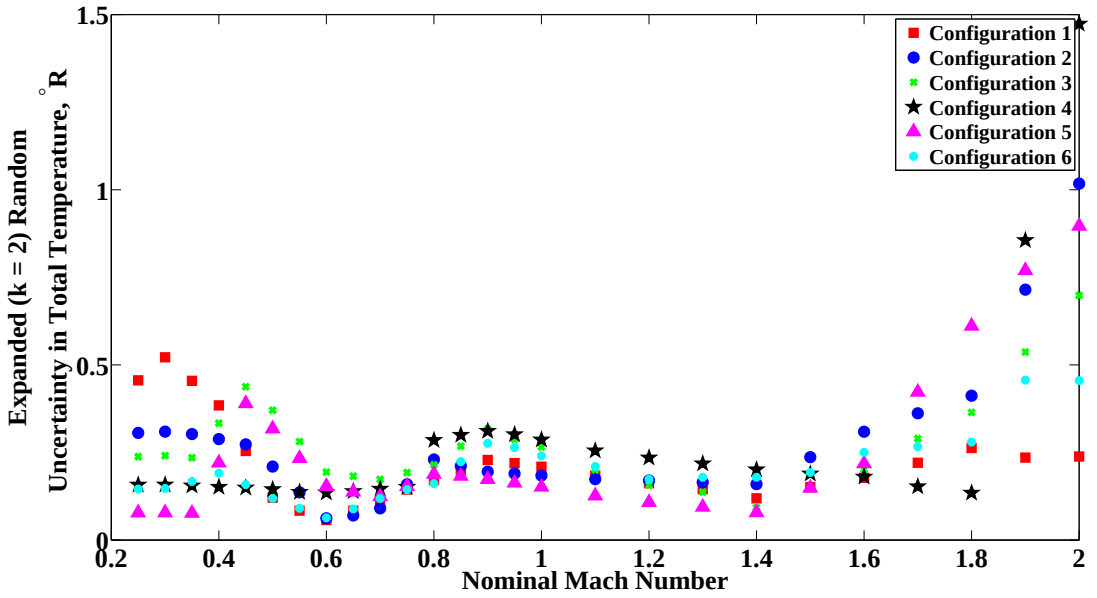

Figure F.2: Random uncertainty of $T_{T,ts}$ as a function of nominal Mach number for all configurations. The red squares are configuration 1, blue circles are configuration 2, green x's are configuration 3, black stars are configuration 4, purple triangles are configuration 5, and cyan dots are configuration 6.

Nominal Mach	**Typical** $T_{T,ts}$ **°R**	$s_{T_{T,ts}}$ **°R k = 2**	$s_{T_{T,ts}}$ **due to** $s_{T_{T,bm}}$ **°R k = 2**	$s_{T_{T,ts}}$ **UPC due to** $s_{T_{T,bm}}$
0.25	533	0.31	0.31	100.0
0.40	538	0.29	0.29	100.0
0.60	566	0.06	0.06	100.0
0.80	568	0.23	0.23	100.0
1.00	568	0.18	0.18	100.0
1.20	582	0.17	0.17	100.0
1.40	590	0.16	0.16	100.0
1.60	605	0.31	0.31	100.0
1.80	627	0.41	0.41	100.0
2.00	639	1.02	1.02	100.0

Table F.1: Summary of calculated Total Temperature random uncertainty with 95% level of confidence for configuration 2.

Nominal Mach	**Typical** $T_{T,ts}$ **°R**	$s_{T_{T,ts}}$ **°R k = 2**	$s_{T_{T,ts}}$ **due to** $s_{T_{T,bm}}$ **°R k = 2**	$s_{T_{T,ts}}$ **UPC due to** $s_{T_{T,bm}}$
0.25	516	0.24	0.24	100.0
0.40	522	0.33	0.33	100.0
0.60	551	0.19	0.19	100.0
0.80	554	0.21	0.21	100.0
1.00	554	0.27	0.27	100.0
1.20	566	0.16	0.16	100.0
1.40	575	0.09	0.09	100.0
1.60	591	0.20	0.20	100.0
1.80	614	0.36	0.36	100.0
2.00	640	0.70	0.70	100.0

Table F.2: Summary of calculated Total Temperature random uncertainty with 95% level of confidence for configuration 3.

Nominal Mach	**Typical** $T_{T,ts}$ **°R**	$s_{T_{T,ts}}$ **°R k = 2**	$s_{T_{T,ts}}$ **due to** $s_{T_{T,bm}}$ **°R k = 2**	$s_{T_{T,ts}}$ **UPC due to** $s_{T_{T,bm}}$
0.25	512	0.16	0.16	100.0
0.40	518	0.15	0.15	100.0
0.60	548	0.14	0.14	100.0
0.80	550	0.29	0.29	100.0
1.00	551	0.29	0.29	100.0
1.20	564	0.24	0.24	100.0
1.40	572	0.20	0.20	100.0
1.60	588	0.18	0.18	100.0
1.80	609	0.13	0.13	100.0
2.00	623	1.47	1.47	100.0

Table F.3: Summary of calculated Total Temperature random uncertainty with 95% level of confidence for configuration 4.

Nominal Mach	**Typical** $T_{T,ts}$ **°R**	$s_{T_{T,ts}}$ **°R k = 2**	$s_{T_{T,ts}}$ **due to** $s_{T_{T,bm}}$ **°R k = 2**	$s_{T_{T,ts}}$ **UPC due to** $s_{T_{T,bm}}$
0.25	529	0.08	0.08	100.0
0.40	535	0.22	0.22	100.0
0.60	559	0.15	0.15	100.0
0.80	561	0.19	0.19	100.0
1.00	560	0.15	0.15	100.0
1.20	575	0.11	0.11	100.0
1.40	582	0.08	0.08	100.0
1.60	599	0.22	0.22	100.0
1.80	623	0.61	0.61	100.0
2.00	636	0.90	0.90	100.0

Table F.4: Summary of calculated Total Temperature random uncertainty with 95% level of confidence for configuration 5.

Nominal Mach	**Typical** $T_{T,ts}$ **°R**	$s_{T_{T,ts}}$ **°R k = 2**	$s_{T_{T,ts}}$ **due to** $s_{T_{T,bm}}$ **°R k = 2**	$s_{T_{T,ts}}$ **UPC due to** $s_{T_{T,bm}}$
0.25	514	0.15	0.15	100.0
0.40	519	0.19	0.19	100.0
0.60	548	0.06	0.06	100.0
0.80	566	0.16	0.16	100.0
1.00	551	0.24	0.24	100.0
1.20	564	0.17	0.17	100.0
1.40	573	0.18	0.18	100.0
1.60	591	0.25	0.25	100.0
1.80	618	0.28	0.28	100.0
2.00	641	0.46	0.46	100.0

Table F.5: Summary of calculated Total Temperature random uncertainty with 95% level of confidence for configuration 6.

F.2 Systematic Uncertainty Results for Configurations 2-6

The systematic uncertainty in the test section total temperature is shown for all configurations in Figure F.3. All configurations show relatively steady values, although there is some variation in the magnitude (between 2.75 and 3.6 °R).

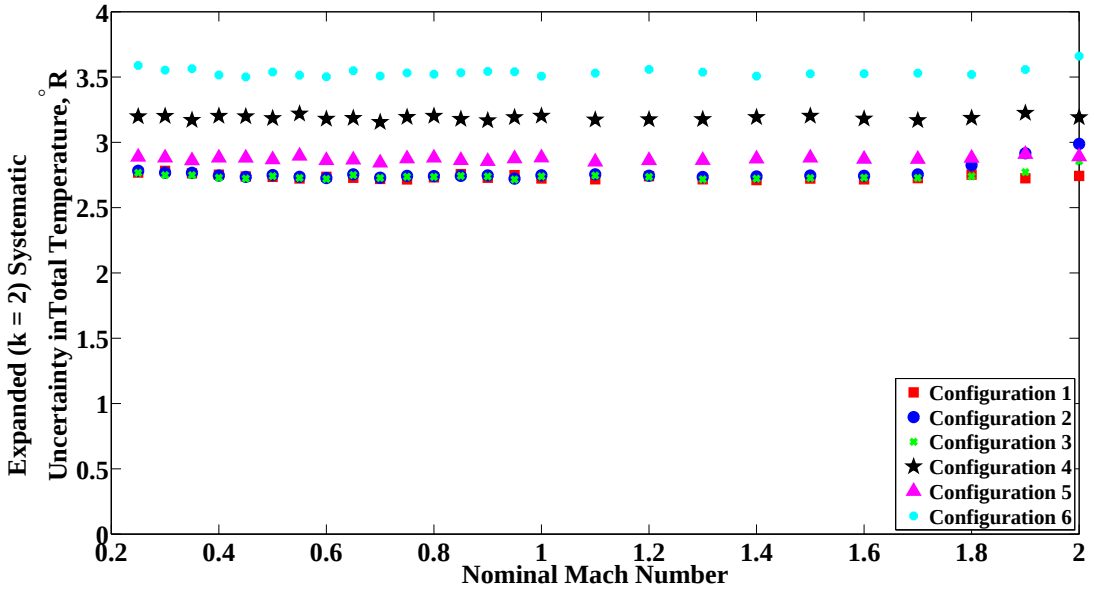

Figure F.3: Systematic UPC of $T_{T,ts}$ as a function of nominal Mach number for all configurations. The red squares are configuration 1, blue circles are configuration 2, green x's are configuration 3, black stars are configuration 4, purple triangles are configuration 5, and cyan dots are configuration 6.

The systematic uncertainty in $T_{T,ts}$ is due to systematic contributions from total temperature calibration (b_{TTCAL}). The systematic uncertainty due to test time bellmouth total temperature measurement is fully correlated with the calibration, so the calibration uncertainty is the only contributor. The tabulated details of these uncertainties are shown in Tables F.6 - F.10.

Nominal Mach	**Typical** $T_{T,ts}$ **°R**	$b_{T_{T,ts}}$ **°R k = 2**	$b_{T_{T,ts}}$ **due to** b_{TTCAL} **°R k = 2**	$b_{T_{T,ts}}$ **UPC due to** b_{TTCAL}
0.25	533	2.78	2.78	100.0
0.40	538	2.75	2.75	100.0
0.60	566	2.73	2.73	100.0
0.80	568	2.74	2.74	100.0
1.00	568	2.75	2.75	100.0
1.20	582	2.74	2.74	100.0
1.40	590	2.74	2.74	100.0
1.60	605	2.74	2.74	100.0
1.80	627	2.83	2.83	100.0
2.00	639	2.99	2.99	100.0

Table F.6: Summary of calculated Total Temperature systematic uncertainty with 95% level of confidence for configuration 2.

Nominal Mach	**Typical** $T_{T,ts}$ **°R**	$b_{T_{T,ts}}$ **°R k = 2**	$b_{T_{T,ts}}$ **due to** b_{TTCAL} **°R k = 2**	$b_{T_{T,ts}}$ **UPC due to** b_{TTCAL}
0.25	516	2.77	2.77	100.0
0.40	522	2.73	2.73	100.0
0.60	551	2.72	2.72	100.0
0.80	554	2.74	2.74	100.0
1.00	554	2.74	2.74	100.0
1.20	566	2.74	2.74	100.0
1.40	575	2.72	2.72	100.0
1.60	591	2.73	2.73	100.0
1.80	614	2.74	2.74	100.0
2.00	640	2.86	2.86	100.0

Table F.7: Summary of calculated Total Temperature systematic uncertainty with 95% level of confidence for configuration 3.

Nominal Mach	**Typical** $T_{T,ts}$ **°R**	$b_{T_{T,ts}}$ **°R k = 2**	$b_{T_{T,ts}}$ **due to** b_{TTCAL} **°R k = 2**	$b_{T_{T,ts}}$ **UPC due to** b_{TTCAL}
0.25	512	3.20	3.20	100.0
0.40	518	3.20	3.20	100.0
0.60	548	3.18	3.18	100.0
0.80	550	3.20	3.20	100.0
1.00	551	3.20	3.20	100.0
1.20	564	3.18	3.18	100.0
1.40	572	3.19	3.19	100.0
1.60	588	3.18	3.18	100.0
1.80	609	3.19	3.19	100.0
2.00	623	3.19	3.19	100.0

Table F.8: Summary of calculated Total Temperature systematic uncertainty with 95% level of confidence for configuration 4.

Nominal Mach	**Typical** $T_{T,ts}$ **°R**	$b_{T_{T,ts}}$ **°R k = 2**	$b_{T_{T,ts}}$ **due to** b_{TTCAL} **°R k = 2**	$b_{T_{T,ts}}$ **UPC due to** b_{TTCAL}
0.25	529	2.89	2.89	100.0
0.40	535	2.88	2.88	100.0
0.60	559	2.86	2.86	100.0
0.80	561	2.88	2.88	100.0
1.00	560	2.88	2.88	100.0
1.20	575	2.86	2.86	100.0
1.40	582	2.87	2.87	100.0
1.60	599	2.87	2.87	100.0
1.80	623	2.88	2.88	100.0
2.00	636	2.89	2.89	100.0

Table F.9: Summary of calculated Total Temperature systematic uncertainty with 95% level of confidence for configuration 5.

Nominal Mach	**Typical** $T_{T,ts}$ **°R**	$b_{T_{T,ts}}$ **°R k = 2**	$b_{T_{T,ts}}$ **due to** b_{TTCAL} **°R k = 2**	$b_{T_{T,ts}}$ **UPC due to** b_{TTCAL}
0.25	514	3.59	3.59	100.0
0.40	519	3.52	3.52	100.0
0.60	548	3.50	3.50	100.0
0.80	566	3.52	3.52	100.0
1.00	551	3.51	3.51	100.0
1.20	564	3.56	3.56	100.0
1.40	573	3.51	3.51	100.0
1.60	591	3.53	3.53	100.0
1.80	618	3.52	3.52	100.0
2.00	641	3.66	3.66	100.0

Table F.10: Summary of calculated Total Temperature systematic uncertainty with 95% level of confidence for configuration 6.

F.3 Total Uncertainty Results for Configurations 2-6

The total uncertainty in $T_{T,ts}$ for all configurations is shown in Figure F.4. The trend is the same for every configuration, although the magnitudes vary. The combined uncertainty in $T_{T,ts}$ is presented for configurations 2-6 in Tables F.11 - F.15.

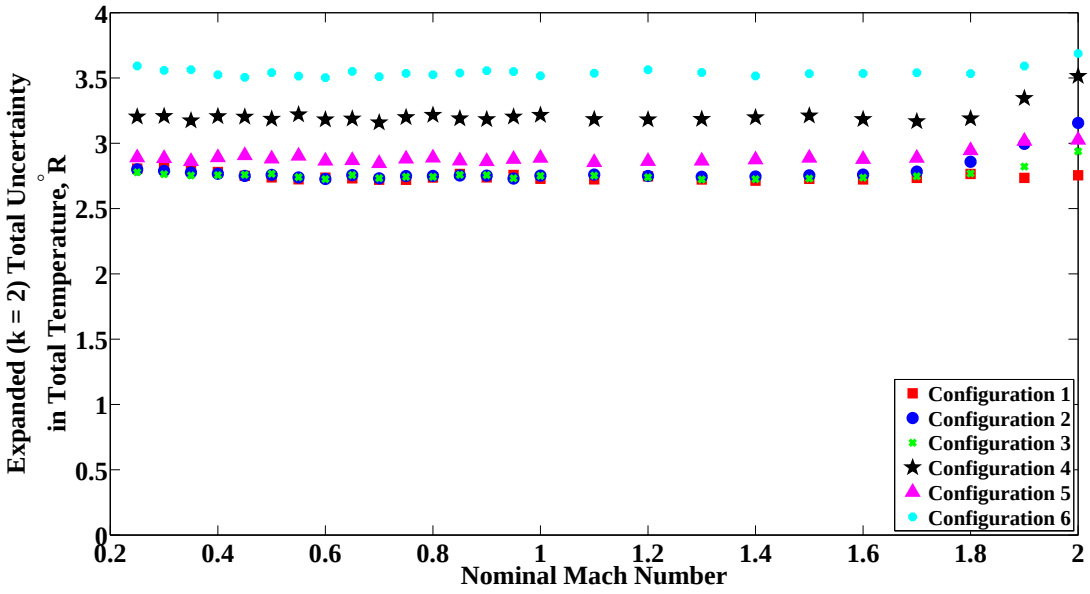

Figure F.4: Total uncertainty of $T_{T,ts}$ as a function of nominal Mach number for all configurations.

Nominal Mach	**Typical $T_{T,ts}$, °R**	$s_{T_{T,ts}}$ **°R k = 2**	$b_{T_{T,ts}}$ **°R k = 2**	$u_{T_{T,ts}}$ **°R k = 2**	$s_{T_{T,ts}}$ **UPC**	$b_{T_{T,ts}}$ **UPC**
0.25	533	0.31	2.78	2.80	1.2	98.8
0.40	538	0.29	2.75	2.77	1.1	98.9
0.60	566	0.06	2.73	2.73	0.1	99.9
0.80	568	0.23	2.74	2.75	0.7	99.3
1.00	568	0.18	2.75	2.75	0.4	99.6
1.20	582	0.17	2.74	2.75	0.4	99.6
1.40	590	0.16	2.74	2.75	0.3	99.7
1.60	605	0.31	2.74	2.76	1.3	98.7
1.80	627	0.41	2.83	2.86	2.1	97.9
2.00	639	1.02	2.99	3.16	10.4	89.6

Table F.11: Summary of calculated Total Temperature uncertainty with 95% level of confidence for configuration 2.

Nominal Mach	**Typical $T_{T,ts}$, °R**	$s_{T_{T,ts}}$ **°R k = 2**	$b_{T_{T,ts}}$ **°R k = 2**	$u_{T_{T,ts}}$ **°R k = 2**	$s_{T_{T,ts}}$ **UPC**	$b_{T_{T,ts}}$ **UPC**
0.25	516	0.24	2.77	2.78	0.7	99.3
0.40	522	0.33	2.73	2.76	1.5	98.5
0.60	551	0.19	2.72	2.73	0.5	99.5
0.80	554	0.21	2.74	2.74	0.6	99.4
1.00	554	0.27	2.74	2.75	0.9	99.1
1.20	566	0.16	2.74	2.74	0.3	99.7
1.40	575	0.09	2.72	2.73	0.1	99.9
1.60	591	0.20	2.73	2.74	0.5	99.5
1.80	614	0.36	2.74	2.77	1.7	98.3
2.00	640	0.70	2.86	2.94	5.6	94.4

Table F.12: Summary of calculated Total Temperature uncertainty with 95% level of confidence for configuration 3.

Nominal Mach	**Typical $T_{T,ts}$, °R**	$s_{T_{T,ts}}$ **°R k = 2**	$b_{T_{T,ts}}$ **°R k = 2**	$u_{T_{T,ts}}$ **°R k = 2**	$s_{T_{T,ts}}$ **UPC**	$b_{T_{T,ts}}$ **UPC**
0.25	512	0.16	3.20	3.20	0.2	99.8
0.40	518	0.15	3.20	3.21	0.2	99.8
0.60	548	0.14	3.18	3.18	0.2	99.8
0.80	550	0.29	3.20	3.22	0.8	99.2
1.00	551	0.29	3.20	3.22	0.8	99.2
1.20	564	0.24	3.18	3.18	0.5	99.5
1.40	572	0.20	3.19	3.20	0.4	99.6
1.60	588	0.18	3.18	3.18	0.3	99.7
1.80	609	0.13	3.19	3.19	0.2	99.8
2.00	623	1.47	3.19	3.51	17.6	82.4

Table F.13: Summary of calculated Total Temperature uncertainty with 95% level of confidence for configuration 4.

Nominal Mach	**Typical $T_{T,ts}$, °R**	$s_{T_{T,ts}}$ **°R k = 2**	$b_{T_{T,ts}}$ **°R k = 2**	$u_{T_{T,ts}}$ **°R k = 2**	$s_{T_{T,ts}}$ **UPC**	$b_{T_{T,ts}}$ **UPC**
0.25	529	0.08	2.89	2.89	0.1	99.9
0.40	535	0.22	2.88	2.89	0.6	99.4
0.60	559	0.15	2.86	2.87	0.3	99.7
0.80	561	0.19	2.88	2.89	0.4	99.6
1.00	560	0.15	2.88	2.89	0.3	99.7
1.20	575	0.11	2.86	2.86	0.1	99.9
1.40	582	0.08	2.87	2.87	0.1	99.9
1.60	599	0.22	2.87	2.88	0.6	99.4
1.80	623	0.61	2.88	2.95	4.3	95.7
2.00	636	0.90	2.89	3.03	8.8	91.2

Table F.14: Summary of calculated Total Temperature uncertainty with 95% level of confidence for configuration 5.

Nominal Mach	**Typical $T_{T,ts}$, °R**	$s_{T_{T,ts}}$ **°R k = 2**	$b_{T_{T,ts}}$ **°R k = 2**	$u_{T_{T,ts}}$ **°R k = 2**	$s_{T_{T,ts}}$ **UPC**	$b_{T_{T,ts}}$ **UPC**
0.25	514	0.15	3.59	3.59	0.2	99.8
0.40	519	0.19	3.52	3.52	0.3	99.7
0.60	548	0.06	3.50	3.50	0.0	100.0
0.80	566	0.16	3.52	3.53	0.2	99.8
1.00	551	0.24	3.51	3.52	0.5	99.5
1.20	564	0.17	3.56	3.56	0.2	99.8
1.40	573	0.18	3.51	3.52	0.3	99.7
1.60	591	0.25	3.53	3.53	0.5	99.5
1.80	618	0.28	3.52	3.53	0.6	99.4
2.00	641	0.46	3.66	3.69	1.5	98.5

Table F.15: Summary of calculated Total Temperature uncertainty with 95% level of confidence for configuration 6.

Appendix G: Static Temperature Uncertainty

Static temperature is a function of Mach number and total temperature, as shown in Figure G.1. Refer to Appendices B and F respectively to see uncertainty flow to those variables, which are propagated through the data reduction equations shown in Section 3.2.2 to attain uncertainty in static temperature. Results for uncertainty in static temperature for configuration 1 were presented in Section 5. Results for configurations 2-6 are presented in this Appendix. Bar charts depicting the percent contributions are shown, followed by tabulated results detailing dimensional and percent contributions for random, systematic, and total uncertainty.

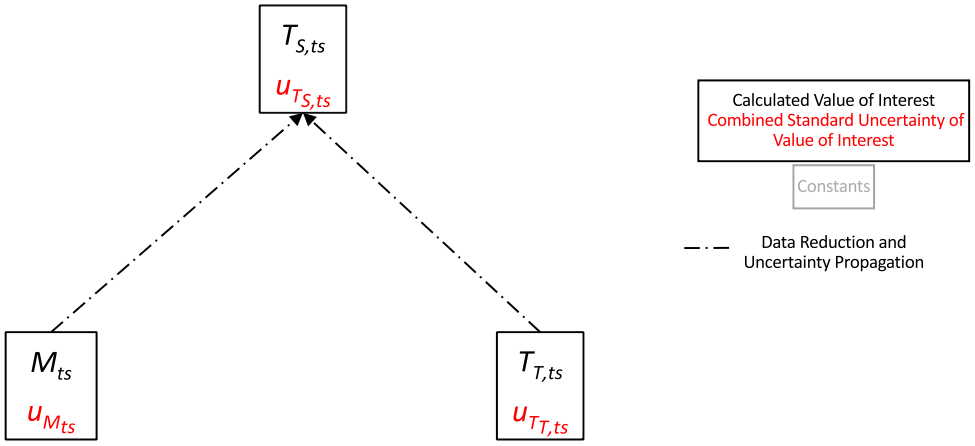

Figure G.1: Uncertainty flow from measured value to calculated static temperature in the test section.

G.1 Random Uncertainty Results for Configurations 2-6

The random uncertainty in the test section static temperature is shown for all configurations in Figure G.2. All configurations follow a similar trend, remaining below 0.5 °R subsonically then increasing supersonically. Configuration 2 shows a sharp increase at the highest Mach numbers, not seen in the other configurations, which remain below 1 °R, while configuration 2 peaks at almost 3 °R.

The elemental random uncertainties contributing to random uncertainty in test section static temperature are the random uncertainties in $P_{T,bm}$, $P_{S,bal}$, and $T_{T,bm}$. The percent contributions of each of these elemental uncertainties to the total random uncertainty in $T_{S,ts}$ are shown in Figure G.3. The tabulated details are shown in Tables G.1 - G.5.

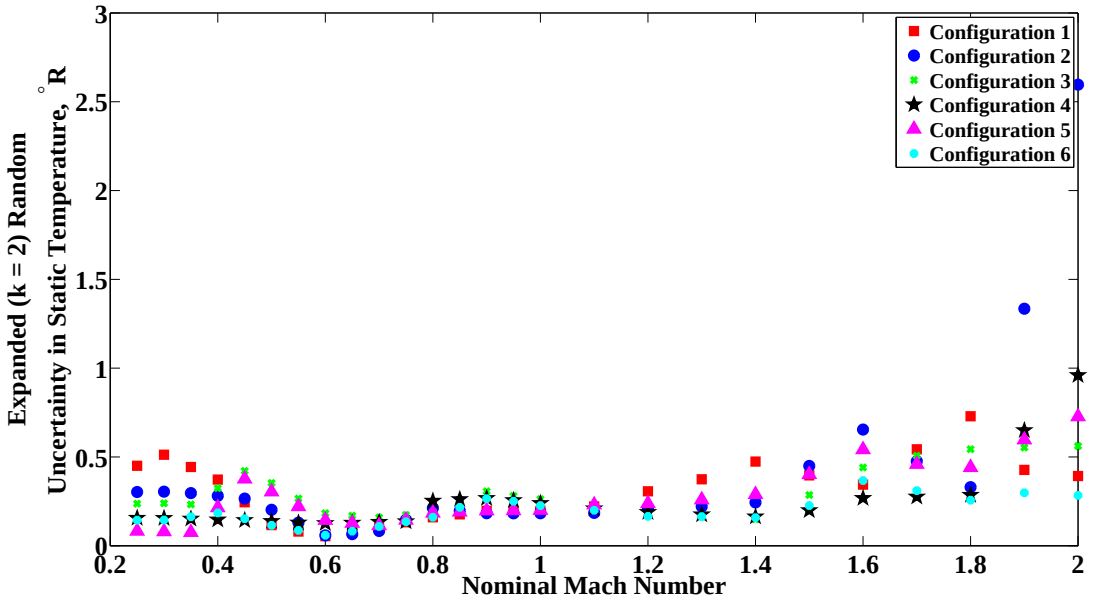

Figure G.2: Random uncertainty of $T_{S,ts}$ as a function of nominal Mach number for all configurations. The red squares are configuration 1, blue circles are configuration 2, green x's are configuration 3, black stars are configuration 4, purple triangles are configuration 5, and cyan dots are configuration 6.

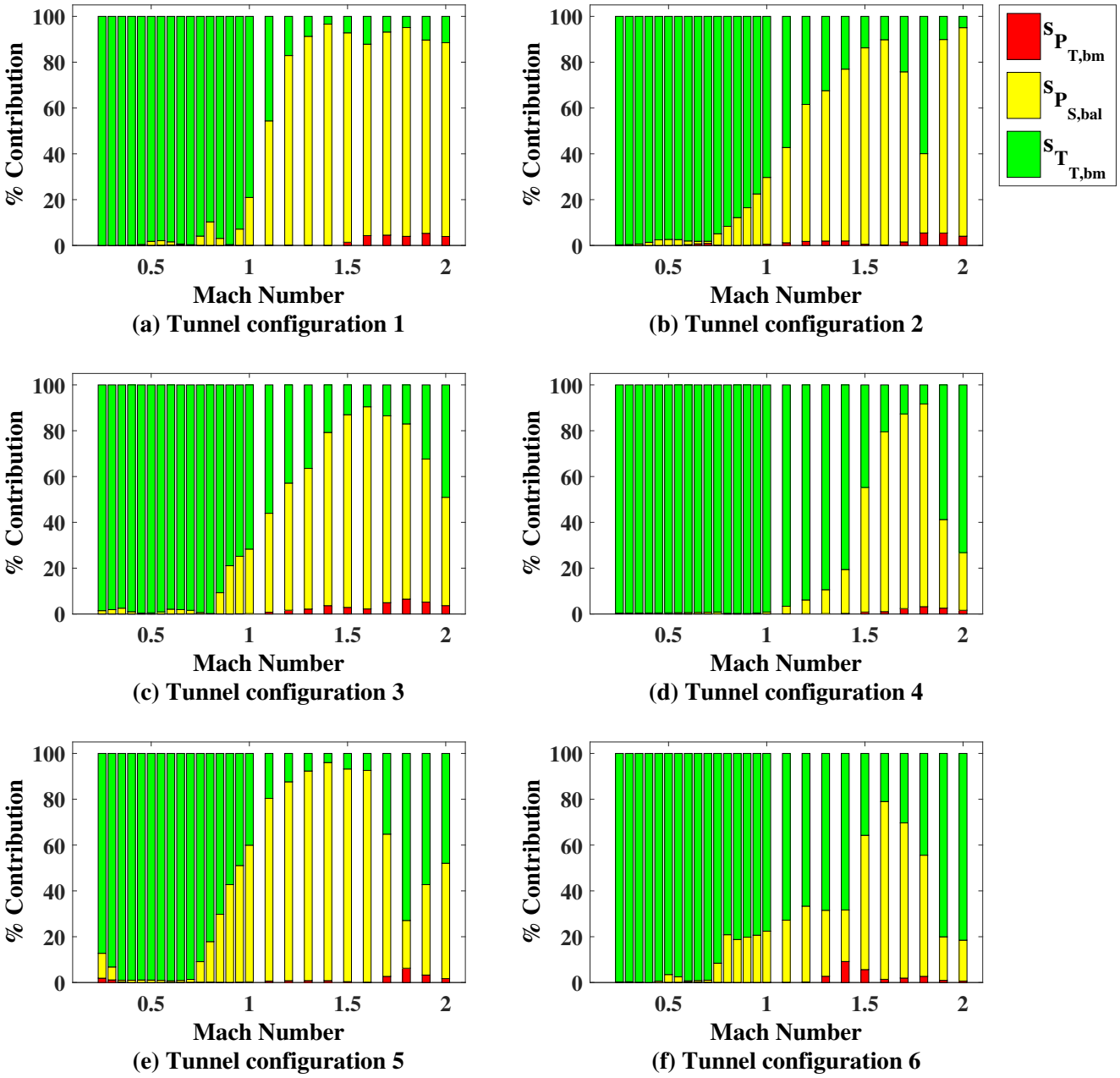

Figure G.3: Random UPC of $T_{S,ts}$ as a function of nominal Mach number for all configurations. Red is the random uncertainty of the total pressure in the bellmouth, yellow is the random uncertainty of the static pressure in the balance chamber, and green is the random uncertainty of the total temperature in the bellmouth.

Nominal Mach	**Typical** $T_{S,ts}$ **°R**	$s_{T_{S,ts}}$ **°R k = 2**	$s_{T_{S,ts}}$ **due to** $s_{P_{T,bm}}$ **°R k = 2**	$s_{T_{S,ts}}$ **due to** $s_{P_{S,bal}}$ **°R k = 2**	$s_{T_{S,ts}}$ **due to** $s_{T_{T,bm}}$ **°R k = 2**	$s_{T_{S,ts}}$ **UPC due to** $s_{P_{T,bm}}$	$s_{T_{S,ts}}$ **UPC due to** $s_{P_{S,bal}}$	$s_{T_{S,ts}}$ **UPC due to** $s_{T_{T,bm}}$
0.25	526	0.30	0.00	0.02	0.30	0.0	0.3	99.7
0.40	521	0.28	0.00	0.03	0.28	0.0	1.4	98.6
0.60	527	0.06	0.00	0.01	0.06	0.4	1.6	98.0
0.80	501	0.21	0.00	0.06	0.20	0.0	8.3	91.6
1.00	473	0.18	0.01	0.10	0.15	0.6	29.1	70.3
1.20	453	0.21	0.03	0.16	0.13	1.8	59.8	38.4
1.40	432	0.24	0.03	0.21	0.12	2.0	75.0	23.0
1.60	409	0.65	0.03	0.62	0.21	0.2	89.6	10.2
1.80	388	0.33	0.08	0.19	0.26	5.5	34.6	59.9
2.00	362	2.60	0.52	2.48	0.58	4.0	91.0	4.9

Table G.1: Summary of calculated Static Temperature random uncertainty with 95% level of confidence for configuration 2.

Nominal Mach	**Typical** $T_{S,ts}$ **°R**	$s_{T_{S,ts}}$ **°R k = 2**	$s_{T_{S,ts}}$ **due to** $s_{P_{T,bm}}$ **°R k = 2**	$s_{T_{S,ts}}$ **due to** $s_{P_{S,bal}}$ **°R k = 2**	$s_{T_{S,ts}}$ **due to** $s_{T_{T,bm}}$ **°R k = 2**	$s_{T_{S,ts}}$ **UPC due to** $s_{P_{T,bm}}$	$s_{T_{S,ts}}$ **UPC due to** $s_{P_{S,bal}}$	$s_{T_{S,ts}}$ **UPC due to** $s_{T_{T,bm}}$
0.25	510	0.24	0.00	0.03	0.24	0.0	1.4	98.5
0.40	505	0.32	0.00	0.03	0.32	0.0	1.0	99.0
0.60	514	0.18	0.00	0.03	0.18	0.0	2.1	97.9
0.80	490	0.19	0.01	0.01	0.19	0.1	0.1	99.8
1.00	463	0.26	0.01	0.14	0.22	0.2	28.2	71.7
1.20	440	0.19	0.02	0.14	0.12	1.6	55.5	42.9
1.40	421	0.15	0.03	0.13	0.07	3.6	75.6	20.7
1.60	398	0.44	0.07	0.41	0.14	2.2	88.2	9.5
1.80	378	0.54	0.14	0.48	0.22	6.5	76.5	17.0
2.00	360	0.56	0.11	0.39	0.39	3.7	47.3	49.1

Table G.2: Summary of calculated Static Temperature random uncertainty with 95% level of confidence for configuration 3.

Nominal Mach	**Typical** $T_{S,ts}$ **°R**	$s_{T_{S,ts}}$ **°R k = 2**	$s_{T_{S,ts}}$ **due to** $s_{P_{T,bm}}$ **°R k = 2**	$s_{T_{S,ts}}$ **due to** $s_{P_{S,bal}}$ **°R k = 2**	$s_{T_{S,ts}}$ **due to** $s_{T_{T,bm}}$ **°R k = 2**	$s_{T_{S,ts}}$ **UPC due to** $s_{P_{T,bm}}$	$s_{T_{S,ts}}$ **UPC due to** $s_{P_{S,bal}}$	$s_{T_{S,ts}}$ **UPC due to** $s_{T_{T,bm}}$
0.25	505	0.16	0.00	0.01	0.16	0.1	0.3	99.6
0.40	501	0.15	0.00	0.01	0.15	0.1	0.4	99.5
0.60	510	0.13	0.00	0.01	0.13	0.0	0.6	99.4
0.80	487	0.25	0.00	0.01	0.25	0.0	0.3	99.7
1.00	459	0.24	0.00	0.02	0.24	0.0	0.8	99.1
1.20	439	0.19	0.01	0.05	0.18	0.1	6.0	93.9
1.40	418	0.16	0.01	0.07	0.15	0.3	19.2	80.6
1.60	395	0.27	0.03	0.24	0.12	1.0	78.5	20.5
1.80	373	0.29	0.05	0.27	0.08	3.2	88.5	8.3
2.00	347	0.96	0.12	0.48	0.82	1.6	25.2	73.2

Table G.3: Summary of calculated Static Temperature random uncertainty with 95% level of confidence for configuration 4.

Nominal Mach	**Typical** $T_{S,ts}$ **°R**	$s_{T_{S,ts}}$ **°R k = 2**	$s_{T_{S,ts}}$ **due to** $s_{P_{T,bm}}$ **°R k = 2**	$s_{T_{S,ts}}$ **due to** $s_{P_{S,bal}}$ **°R k = 2**	$s_{T_{S,ts}}$ **due to** $s_{T_{T,bm}}$ **°R k = 2**	$s_{T_{S,ts}}$ **UPC due to** $s_{P_{T,bm}}$	$s_{T_{S,ts}}$ **UPC due to** $s_{P_{S,bal}}$	$s_{T_{S,ts}}$ **UPC due to** $s_{T_{T,bm}}$
0.25	523	0.08	0.01	0.03	0.08	1.9	10.9	87.2
0.40	518	0.21	0.00	0.02	0.21	0.0	1.0	99.0
0.60	521	0.14	0.00	0.01	0.14	0.1	0.7	99.2
0.80	497	0.18	0.01	0.08	0.17	0.2	17.6	82.1
1.00	467	0.20	0.01	0.15	0.13	0.3	59.6	40.0
1.20	448	0.24	0.02	0.22	0.08	0.8	86.8	12.4
1.40	426	0.29	0.03	0.28	0.06	0.8	95.2	4.0
1.60	404	0.54	0.02	0.52	0.15	0.2	92.4	7.4
1.80	384	0.44	0.11	0.20	0.38	6.3	20.8	72.9
2.00	357	0.73	0.10	0.52	0.50	1.7	50.4	47.9

Table G.4: Summary of calculated Static Temperature random uncertainty with 95% level of confidence for configuration 5.

Nominal Mach	**Typical** $T_{S,ts}$ **°R**	$s_{T_{S,ts}}$ **°R k = 2**	$s_{T_{S,ts}}$ **due to** $s_{P_{T,bm}}$ **°R k = 2**	$s_{T_{S,ts}}$ **due to** $s_{P_{S,bal}}$ **°R k = 2**	$s_{T_{S,ts}}$ **due to** $s_{T_{T,bm}}$ **°R k = 2**	$s_{T_{S,ts}}$ **UPC due to** $s_{P_{T,bm}}$	$s_{T_{S,ts}}$ **UPC due to** $s_{P_{S,bal}}$	$s_{T_{S,ts}}$ **UPC due to** $s_{T_{T,bm}}$
0.25	508	0.14	0.00	0.01	0.14	0.1	0.2	99.7
0.40	503	0.18	0.00	0.00	0.18	0.0	0.0	99.9
0.60	511	0.06	0.00	0.00	0.06	0.2	0.5	99.3
0.80	501	0.16	0.00	0.07	0.14	0.1	20.8	79.1
1.00	457	0.23	0.01	0.11	0.20	0.1	22.3	77.6
1.20	439	0.17	0.01	0.10	0.14	0.3	33.0	66.7
1.40	418	0.16	0.05	0.08	0.13	9.2	22.5	68.3
1.60	397	0.37	0.04	0.32	0.17	1.4	77.6	21.0
1.80	378	0.26	0.04	0.19	0.17	2.7	52.9	44.4
2.00	360	0.28	0.02	0.12	0.26	0.7	17.8	81.5

Table G.5: Summary of calculated Static Temperature random uncertainty with 95% level of confidence for configuration 6.

G.2 Systematic Uncertainty Results for Configurations 2-6

The systematic uncertainty in the test section static temperature is shown for all configurations in Figure G.4. All configurations follow a similar trend, again with different magnitudes for different configurations.

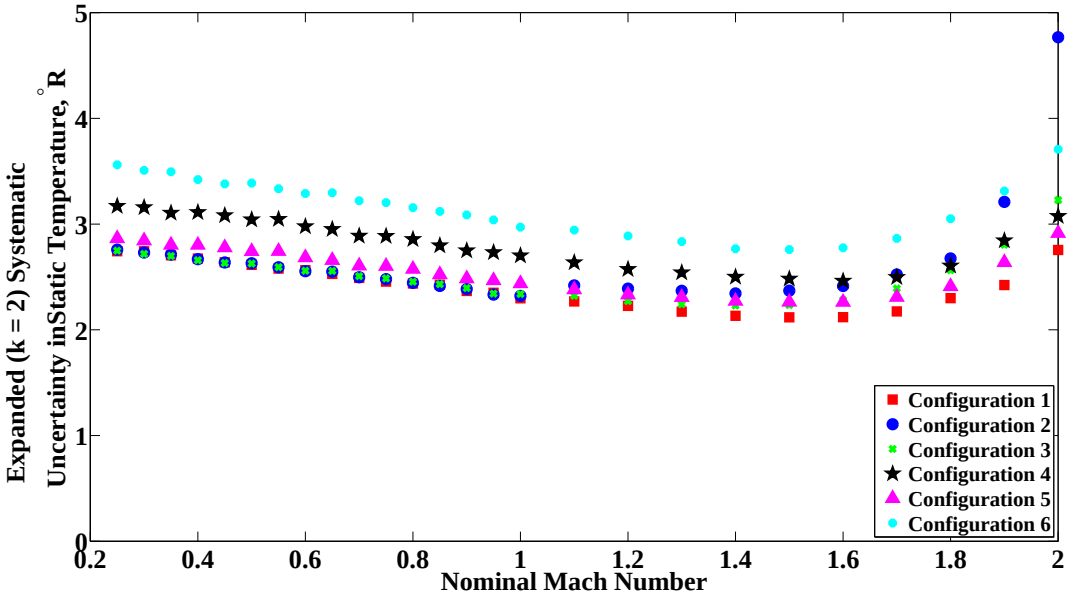

Figure G.4: Systematic uncertainty of $T_{S,ts}$ as a function of nominal Mach number for all configurations. The red squares are configuration 1, blue circles are configuration 2, green x's are configuration 3, black stars are configuration 4, purple triangles are configuration 5, and cyan dots are configuration 6.

The systematic uncertainty in $T_{S,ts}$ is due to systematic contributions from all tunnel calibrations (b_{PSCAL}, b_{PTCAL}, and b_{TTCAL}), and instrumentation uncertainties in test-time bellmouth total pressure, balance chamber static pressure, and barometric pressure (combined as $b_{P_{inst}}$). Instrumentation uncertainty in bellmouth total temperature is fully correlated to the uncertainty due to the Total Temperature calibration and is therefore inherantly included in that value. The percent contributions of each of these uncertainties to the combined systematic uncertainty in $T_{S,ts}$ are shown in Figure G.5. The tabulated details are shown in Tables G.6 - G.10.

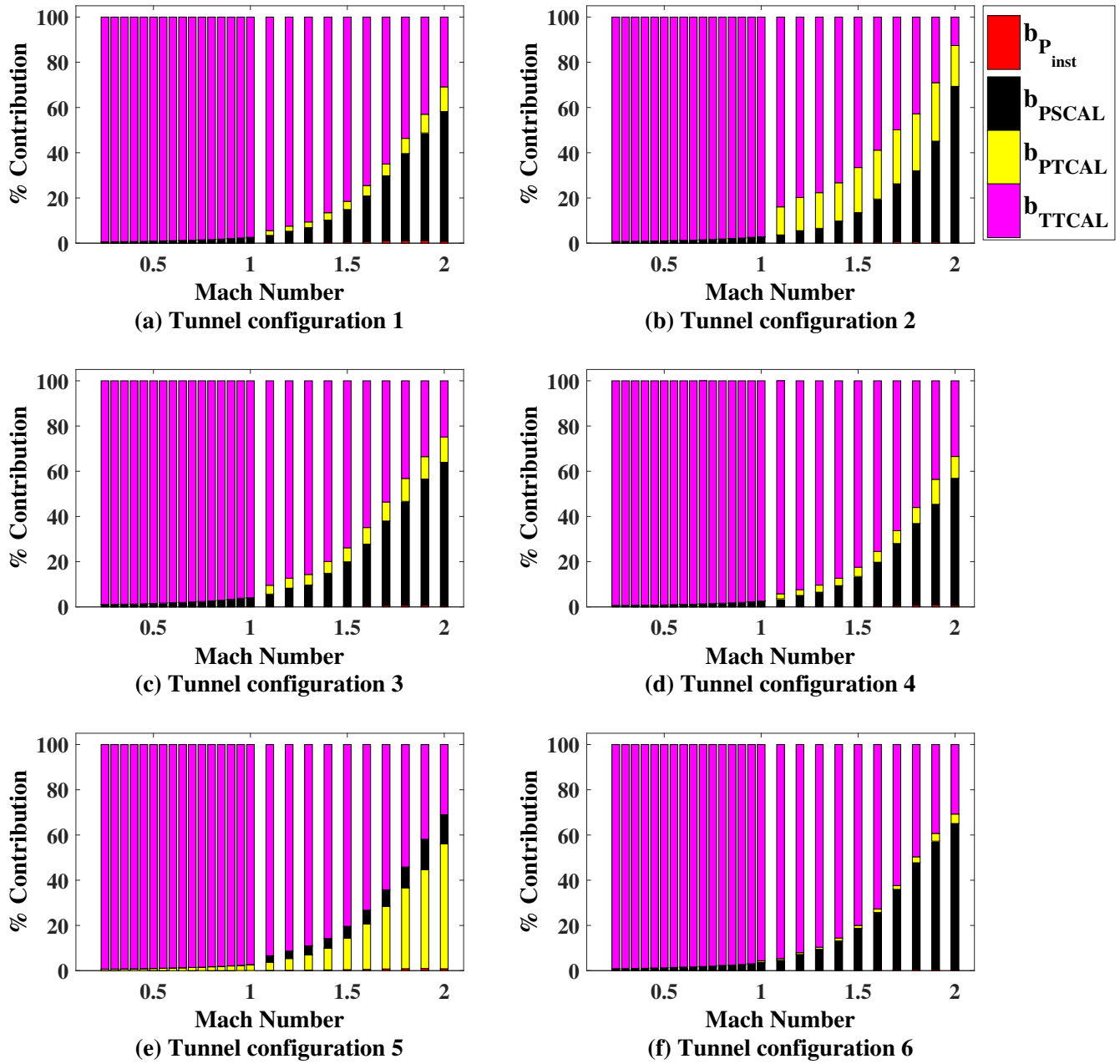

Figure G.5: Systematic UPC of $T_{S,ts}$ as a function of nominal Mach number for all configurations. Red is the systematic uncertainty due to pressure instrumentation, yellow is the systematic uncertainty due to total pressure calibration, black is the systematic uncertainty due to static pressure calibration, green is the systematic uncertainty due to temperature instrumentation, and purple is the systematic uncertainty due to total temperature calibration.

Nominal Mach	**Typical** $T_{S,ts}$ **°R**	$b_{T_{S,ts}}$ **°R k = 2**	$b_{T_{S,ts}}$ **due to** $b_{P_{Inst}}$ **°R k = 2**	$b_{T_{S,ts}}$ **due to** b_{PSCAL} **°R k = 2**	$b_{T_{S,ts}}$ **due to** b_{PTCAL} **°R k = 2**	$b_{T_{S,ts}}$ **due to** b_{TTCAL} **°R k = 2**	$b_{T_{S,ts}}$ **UPC due to** $b_{P_{Inst}}$	$b_{T_{S,ts}}$ **UPC due to** b_{PSCAL}	$b_{T_{S,ts}}$ **UPC due to** b_{PTCAL}	$b_{T_{S,ts}}$ **UPC due to** b_{TTCAL}
0.25	526	2.76	0.00	0.23	0.04	2.75	0.0	0.7	0.0	99.3
0.40	521	2.67	0.01	0.24	0.04	2.66	0.0	0.8	0.0	99.1
0.60	527	2.55	0.02	0.29	0.03	2.54	0.0	1.2	0.0	98.7
0.80	501	2.44	0.04	0.33	0.03	2.42	0.0	1.8	0.0	98.2
1.00	473	2.32	0.06	0.39	0.03	2.29	0.1	2.8	0.0	97.1
1.20	453	2.39	0.10	0.55	0.91	2.13	0.2	5.3	14.7	79.8
1.40	432	2.34	0.13	0.72	0.96	2.01	0.3	9.5	16.9	73.3
1.60	409	2.41	0.18	1.05	1.12	1.85	0.5	19.0	21.6	58.9
1.80	388	2.67	0.22	1.50	1.34	1.75	0.7	31.4	25.2	42.8
2.00	362	4.77	0.29	3.96	2.03	1.69	0.4	69.0	18.1	12.6

Table G.6: Summary of calculated Static Temperature systematic uncertainty with 95% level of confidence for configuration 2.

Nominal Mach	**Typical** $T_{S,ts}$ **°R**	$b_{T_{S,ts}}$ **°R k = 2**	$b_{T_{S,ts}}$ **due to** $b_{P_{Inst}}$ **°R k = 2**	$b_{T_{S,ts}}$ **due to** b_{PSCAL} **°R k = 2**	$b_{T_{S,ts}}$ **due to** b_{PTCAL} **°R k = 2**	$b_{T_{S,ts}}$ **due to** b_{TTCAL} **°R k = 2**	$b_{T_{S,ts}}$ **UPC due to** $b_{P_{Inst}}$	$b_{T_{S,ts}}$ **UPC due to** b_{PSCAL}	$b_{T_{S,ts}}$ **UPC due to** b_{PTCAL}	$b_{T_{S,ts}}$ **UPC due to** b_{TTCAL}
0.25	510	2.75	0.00	0.29	0.04	2.73	0.0	1.1	0.0	98.9
0.40	505	2.66	0.01	0.30	0.04	2.64	0.0	1.3	0.0	98.7
0.60	514	2.56	0.02	0.35	0.03	2.53	0.0	1.9	0.0	98.1
0.80	490	2.46	0.03	0.40	0.03	2.42	0.0	2.6	0.0	97.3
1.00	463	2.34	0.06	0.47	0.03	2.29	0.1	4.0	0.0	96.0
1.20	440	2.27	0.10	0.65	0.48	2.12	0.2	8.1	4.4	87.3
1.40	421	2.23	0.13	0.85	0.51	1.99	0.3	14.6	5.2	79.9
1.60	398	2.28	0.17	1.19	0.62	1.84	0.6	27.2	7.3	64.9
1.80	378	2.56	0.22	1.74	0.82	1.68	0.7	46.0	10.1	43.2
2.00	360	3.23	0.24	2.57	1.08	1.61	0.6	63.4	11.2	24.8

Table G.7: Summary of calculated Static Temperature systematic uncertainty with 95% level of confidence for configuration 3.

Nominal Mach	**Typical** $T_{S,ts}$ **°R**	$b_{T_{S,ts}}$ **°R k = 2**	$b_{T_{S,ts}}$ **due to** $b_{P_{Inst}}$ **°R k = 2**	$b_{T_{S,ts}}$ **due to** b_{PSCAL} **°R k = 2**	$b_{T_{S,ts}}$ **due to** b_{PTCAL} **°R k = 2**	$b_{T_{S,ts}}$ **due to** b_{TTCAL} **°R k = 2**	$b_{T_{S,ts}}$ **UPC due to** $b_{P_{Inst}}$	$b_{T_{S,ts}}$ **UPC due to** b_{PSCAL}	$b_{T_{S,ts}}$ **UPC due to** b_{PTCAL}	$b_{T_{S,ts}}$ **UPC due to** b_{TTCAL}
0.25	505	3.17	0.00	0.25	0.03	3.16	0.0	0.6	0.0	99.4
0.40	501	3.11	0.01	0.27	0.03	3.10	0.0	0.7	0.0	99.2
0.60	510	2.98	0.02	0.32	0.03	2.96	0.0	1.1	0.0	98.9
0.80	487	2.86	0.03	0.36	0.03	2.83	0.0	1.6	0.0	98.4
1.00	459	2.70	0.06	0.43	0.03	2.67	0.0	2.5	0.0	97.4
1.20	439	2.57	0.09	0.57	0.41	2.47	0.1	4.9	2.6	92.4
1.40	418	2.50	0.13	0.76	0.45	2.34	0.3	9.1	3.3	87.3
1.60	395	2.46	0.17	1.08	0.54	2.14	0.5	19.3	4.7	75.5
1.80	373	2.61	0.22	1.57	0.69	1.95	0.7	36.2	7.1	56.0
2.00	347	3.07	0.25	2.31	0.96	1.78	0.7	56.2	9.7	33.5

Table G.8: Summary of calculated Static Temperature systematic uncertainty with 95% level of confidence for configuration 4.

Nominal Mach	**Typical** $T_{S,ts}$ **°R**	$b_{T_{S,ts}}$ **°R k = 2**	$b_{T_{S,ts}}$ **due to** $b_{P_{Inst}}$ **°R k = 2**	$b_{T_{S,ts}}$ **due to** b_{PSCAL} **°R k = 2**	$b_{T_{S,ts}}$ **due to** b_{PTCAL} **°R k = 2**	$b_{T_{S,ts}}$ **due to** b_{TTCAL} **°R k = 2**	$b_{T_{S,ts}}$ **UPC due to** $b_{P_{Inst}}$	$b_{T_{S,ts}}$ **UPC due to** b_{PSCAL}	$b_{T_{S,ts}}$ **UPC due to** b_{PTCAL}	$b_{T_{S,ts}}$ **UPC due to** b_{TTCAL}
0.25	523	2.86	0.00	0.24	0.03	2.85	0.0	0.7	0.0	99.3
0.40	518	2.80	0.01	0.25	0.03	2.79	0.0	0.8	0.0	99.2
0.60	521	2.68	0.02	0.29	0.03	2.67	0.0	1.2	0.0	98.8
0.80	497	2.57	0.03	0.33	0.03	2.55	0.0	1.7	0.0	98.3
1.00	467	2.44	0.06	0.39	0.03	2.40	0.1	2.6	0.0	97.3
1.20	448	2.33	0.10	0.53	0.43	2.23	0.2	5.2	3.4	91.3
1.40	426	2.27	0.13	0.70	0.47	2.10	0.3	9.6	4.3	85.8
1.60	404	2.26	0.17	1.01	0.56	1.94	0.6	20.0	6.1	73.2
1.80	384	2.41	0.22	1.44	0.73	1.77	0.9	35.8	9.2	54.2
2.00	357	2.91	0.27	2.17	1.05	1.62	0.8	55.2	12.9	31.0

Table G.9: Summary of calculated Static Temperature systematic uncertainty with 95% level of confidence for configuration 5.

Nominal Mach	**Typical** $T_{S,ts}$ **°R**	$b_{T_{S,ts}}$ **°R k = 2**	$b_{T_{S,ts}}$ **due to** $b_{P_{Inst}}$ **°R k = 2**	$b_{T_{S,ts}}$ **due to** b_{PSCAL} **°R k = 2**	$b_{T_{S,ts}}$ **due to** b_{PTCAL} **°R k = 2**	$b_{T_{S,ts}}$ **due to** b_{TTCAL} **°R k = 2**	$b_{T_{S,ts}}$ **UPC due to** $b_{P_{Inst}}$	$b_{T_{S,ts}}$ **UPC due to** b_{PSCAL}	$b_{T_{S,ts}}$ **UPC due to** b_{PTCAL}	$b_{T_{S,ts}}$ **UPC due to** b_{TTCAL}
0.25	508	3.56	0.00	0.33	0.03	3.54	0.0	0.9	0.0	99.1
0.40	503	3.42	0.01	0.35	0.03	3.40	0.0	1.0	0.0	98.9
0.60	511	3.29	0.02	0.41	0.03	3.26	0.0	1.6	0.0	98.4
0.80	501	3.16	0.03	0.48	0.03	3.12	0.0	2.3	0.0	97.7
1.00	457	2.97	0.06	0.57	0.24	2.91	0.0	3.7	0.7	95.6
1.20	439	2.89	0.10	0.77	0.25	2.77	0.1	7.0	0.8	92.1
1.40	418	2.77	0.13	1.00	0.30	2.56	0.2	13.1	1.1	85.6
1.60	397	2.78	0.17	1.40	0.35	2.37	0.4	25.3	1.6	72.7
1.80	378	3.05	0.22	2.10	0.49	2.15	0.5	47.2	2.6	49.7
2.00	360	3.71	0.23	2.98	0.76	2.06	0.4	64.7	4.2	30.7

Table G.10: Summary of calculated Static Temperature systematic uncertainty with 95% level of confidence for configuration 6.

G.3 Total Uncertainty Results for Configurations 2-6

The total uncertainty in $T_{S,ts}$ for all configurations is shown in Figure G.6. Each configuration follows the same trend as configuration 1, although the magnitudes vary significantly. The combined uncertainty in $T_{S,ts}$ is presented for configurations 2-6 in Tables G.11 - G.15.

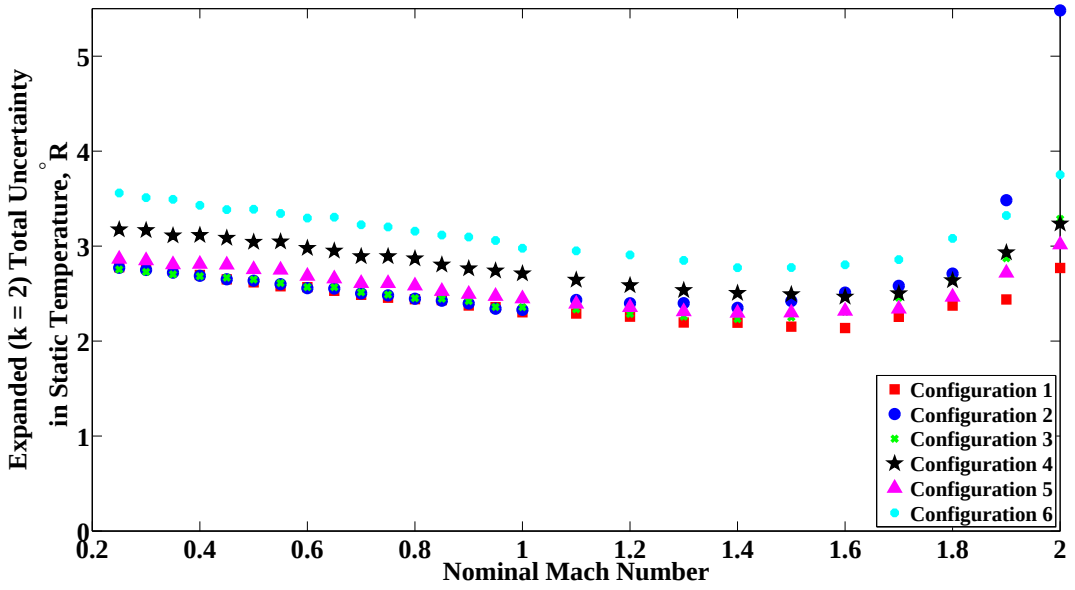

Figure G.6: Total uncertainty of $T_{S,ts}$ as a function of nominal Mach number for all configurations.

Nominal Mach	**Typical $T_{S,ts}$, °R**	$s_{T_{S,ts}}$ **°R k = 2**	$b_{T_{S,ts}}$ **°R k = 2**	$u_{T_{S,ts}}$ **°R k = 2**	$s_{T_{S,ts}}$ **UPC**	$b_{T_{S,ts}}$ **UPC**
0.25	526	0.30	2.76	2.77	1.2	98.8
0.40	521	0.28	2.67	2.69	1.1	98.9
0.60	527	0.06	2.55	2.56	0.1	99.9
0.80	501	0.21	2.44	2.45	0.7	99.3
1.00	473	0.18	2.32	2.33	0.6	99.4
1.20	453	0.21	2.39	2.40	0.8	99.2
1.40	432	0.24	2.34	2.35	1.1	98.9
1.60	409	0.65	2.41	2.51	6.8	93.2
1.80	388	0.33	2.67	2.71	1.5	98.5
2.00	362	2.60	4.77	5.48	22.9	77.1

Table G.11: Summary of calculated Static Temperature uncertainty with 95% level of confidence for configuration 2.

Nominal Mach	**Typical $T_{S,ts}$, °R**	$s_{T_{S,ts}}$ **°R k = 2**	$b_{T_{S,ts}}$ **°R k = 2**	$u_{T_{S,ts}}$ **°R k = 2**	$s_{T_{S,ts}}$ **UPC**	$b_{T_{S,ts}}$ **UPC**
0.25	510	0.24	2.75	2.75	0.7	99.3
0.40	505	0.32	2.66	2.68	1.5	98.5
0.60	514	0.18	2.56	2.57	0.5	99.5
0.80	490	0.19	2.46	2.45	0.6	99.4
1.00	463	0.26	2.34	2.36	1.2	98.8
1.20	440	0.19	2.27	2.29	0.7	99.3
1.40	421	0.15	2.23	2.23	0.4	99.6
1.60	398	0.44	2.28	2.31	3.6	96.4
1.80	378	0.54	2.56	2.64	4.3	95.7
2.00	360	0.56	3.23	3.29	2.9	97.1

Table G.12: Summary of calculated Static Temperature uncertainty with 95% level of confidence for configuration 3.

Nominal Mach	**Typical $T_{S,ts}$, °R**	$s_{T_{S,ts}}$ **°R k = 2**	$b_{T_{S,ts}}$ **°R k = 2**	$u_{T_{S,ts}}$ **°R k = 2**	$s_{T_{S,ts}}$ **UPC**	$b_{T_{S,ts}}$ **UPC**
0.25	505	0.16	3.17	3.17	0.2	99.8
0.40	501	0.15	3.11	3.11	0.2	99.8
0.60	510	0.13	2.98	2.98	0.2	99.8
0.80	487	0.25	2.86	2.87	0.8	99.2
1.00	459	0.24	2.70	2.71	0.8	99.2
1.20	439	0.19	2.57	2.59	0.5	99.5
1.40	418	0.16	2.50	2.50	0.4	99.6
1.60	395	0.27	2.46	2.47	1.2	98.8
1.80	373	0.29	2.61	2.64	1.2	98.8
2.00	347	0.96	3.07	3.24	8.9	91.1

Table G.13: Summary of calculated Static Temperature uncertainty with 95% level of confidence for configuration 4.

Nominal Mach	**Typical $T_{S,ts}$, °R**	$s_{T_{S,ts}}$ **°R k = 2**	$b_{T_{S,ts}}$ **°R k = 2**	$u_{T_{S,ts}}$ **°R k = 2**	$s_{T_{S,ts}}$ **UPC**	$b_{T_{S,ts}}$ **UPC**
0.25	523	0.08	2.86	2.86	0.1	99.9
0.40	518	0.21	2.80	2.81	0.6	99.4
0.60	521	0.14	2.68	2.69	0.3	99.7
0.80	497	0.18	2.57	2.58	0.5	99.5
1.00	467	0.20	2.44	2.45	0.7	99.3
1.20	448	0.24	2.33	2.36	1.0	99.0
1.40	426	0.29	2.27	2.30	1.6	98.4
1.60	404	0.54	2.26	2.32	5.4	94.6
1.80	384	0.44	2.41	2.46	3.2	96.8
2.00	357	0.73	2.91	3.02	5.9	94.1

Table G.14: Summary of calculated Static Temperature uncertainty with 95% level of confidence for configuration 5.

Nominal Mach	**Typical $T_{S,ts}$, °R**	$s_{T_{S,ts}}$ **°R k = 2**	$b_{T_{S,ts}}$ **°R k = 2**	$u_{T_{S,ts}}$ **°R k = 2**	$s_{T_{S,ts}}$ **UPC**	$b_{T_{S,ts}}$ **UPC**
0.25	508	0.14	3.56	3.56	0.2	99.8
0.40	503	0.18	3.42	3.43	0.3	99.7
0.60	511	0.06	3.29	3.30	0.0	100.0
0.80	501	0.16	3.16	3.16	0.3	99.7
1.00	457	0.23	2.97	2.98	0.6	99.4
1.20	439	0.17	2.89	2.91	0.3	99.7
1.40	418	0.16	2.77	2.77	0.3	99.7
1.60	397	0.37	2.78	2.80	1.7	98.3
1.80	378	0.26	3.05	3.08	0.7	99.3
2.00	360	0.28	3.71	3.75	0.6	99.4

Table G.15: Summary of calculated Static Temperature uncertainty with 95% level of confidence for configuration 6.

Appendix H: Reynolds Number Uncertainty

Reynolds number is a function of Mach number, static pressure, and total temperature as shown in Figure H.1. Refer to Appendices B, C and F respectively to see uncertainty flow from measured values to those variables, which are propagated through the data reduction equations shown in Section 3.2.2 to attain uncertainty in Reynolds number. Results for uncertainty in Reynolds number for configuration 1 were presented in Section 5. Results for configurations 2-6 are presented in this Appendix. Bar charts depicting the percent contributions are shown, followed by tabulated results detailing dimensional and percent contributions for random, systematic, and total uncertainty.

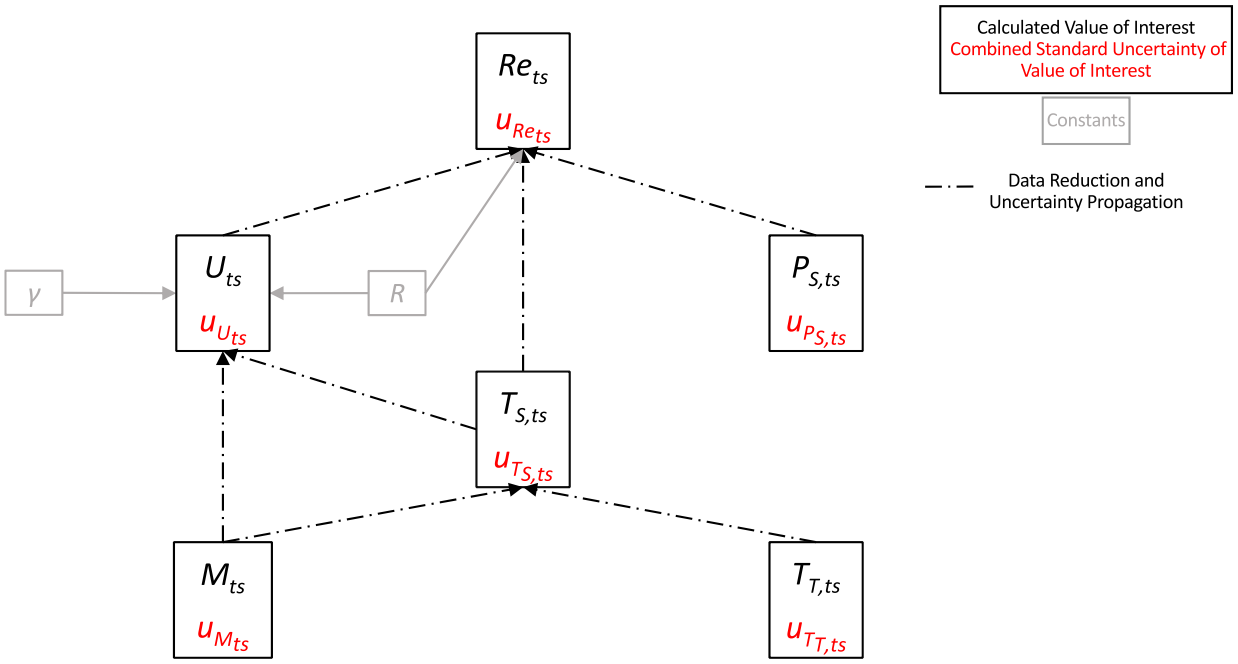

Figure H.1: Uncertainty flow from measured value to calculated Reynolds number in the test section.

H.1 Random Uncertainty Results for Configurations 2-6

The random uncertainty in the Reynolds number is shown for all configurations in Figure H.2. All configurations follow a similar trend, remaining below 0.005 x 10^6 ft^{-1} subsonically then increasing supersonically. Configuration 2 shows a sharp increase at the highest Mach numbers, not seen in the other configurations, which remain below 0.02 x 10^6 ft^{-1}.

The elemental random uncertainties contributing to random uncertainty in test section Reynolds number are the random uncertainty in $P_{T,bm}$ and $P_{S,bal}$. The percent contribution of each of these elemental uncertainties to the total random uncertainty in Re_{ts} are shown in Figure H.3. The tabulated details are shown in Tables H.1 - H.5.

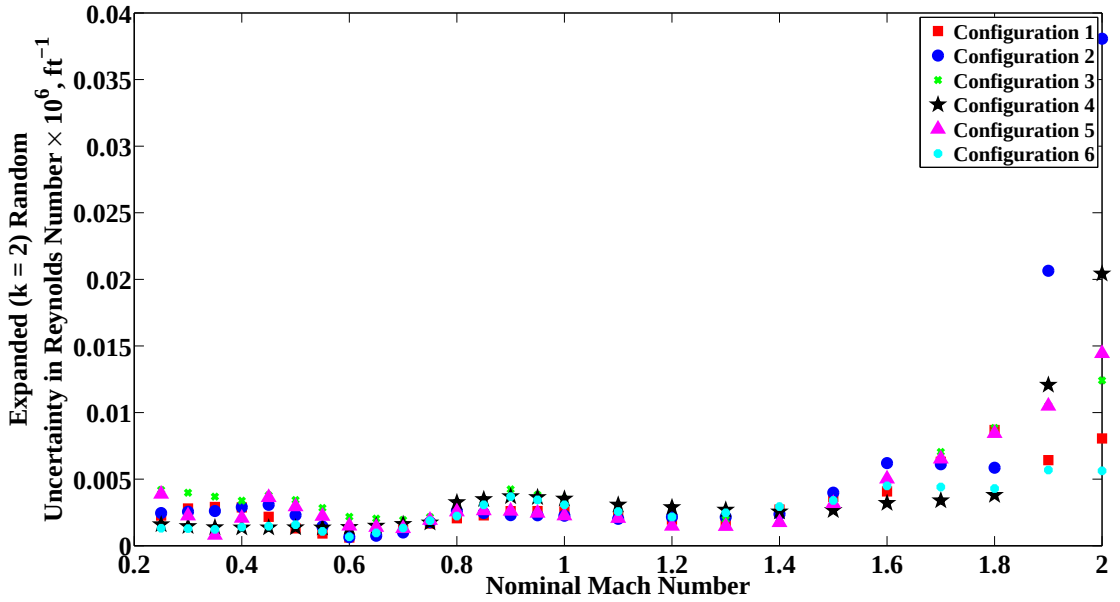

Figure H.2: Random uncertainty of R_{ts} as a function of nominal Mach number for all configurations. The red squares are configuration 1, blue circles are configuration 2, green x's are configuration 3, black stars are configuration 4, purple triangles are configuration 5, and cyan dots are configuration 6.

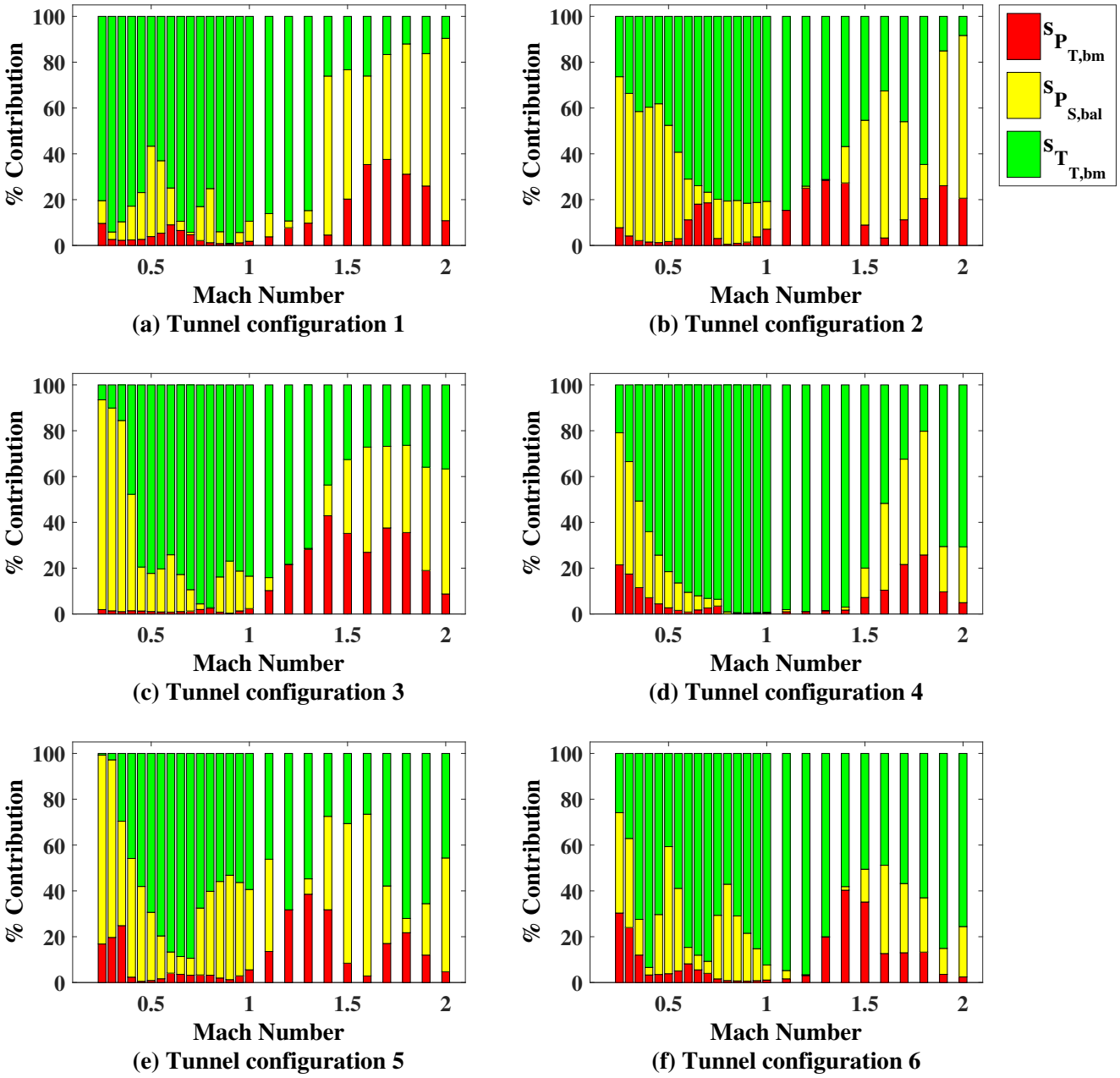

Figure H.3: Random UPC of Re_{ts} as a function of nominal Mach number for all configurations. Red is the random uncertainty of the total pressure in the bellmouth, yellow is the random uncertainty of the static pressure in the balance chamber, and green is the random uncertainty of the total temperature in the bellmouth.

Nominal Mach	**Typical** Re_{ts} $\times 10^6$ **ft^{-1}**	$s_{Re_{ts}}$, $\times 10^6$, **ft^{-1}** **k = 2**	$s_{Re_{ts}}$, **due to** $s_{P_{T,bm}}$, $\times 10^6$ **ft^{-1}** **k = 2**	$s_{Re_{ts}}$ **due to** $s_{P_{S,bal}}$, $\times 10^6$ **ft^{-1}** **k = 2**	$s_{Re_{ts}}$ **due to** $s_{T_{T,bm}}$, $\times 10^6$ **ft^{-1}** **k = 2**	$s_{Re_{ts}}$ **UPC due to** $s_{P_{T,bm}}$	$s_{Re_{ts}}$ **UPC due to** $s_{P_{S,bal}}$	$s_{Re_{ts}}$ **UPC due to** $s_{T_{T,bm}}$
0.25	1.72	0.0025	0.0007	0.0020	0.0013	7.8	65.9	26.3
0.40	2.67	0.0029	0.0004	0.0022	0.0018	1.5	58.8	39.6
0.60	3.88	0.0006	0.0002	0.0003	0.0005	11.2	17.8	71.0
0.80	4.51	0.0026	0.0002	0.0011	0.0023	0.5	18.8	80.6
1.00	4.82	0.0023	0.0006	0.0008	0.0020	7.1	12.2	80.7
1.20	4.87	0.0022	0.0011	0.0002	0.0019	25.0	0.9	74.1
1.40	5.03	0.0024	0.0012	0.0009	0.0018	27.3	15.9	56.8
1.60	5.22	0.0062	0.0011	0.0050	0.0035	3.3	64.2	32.6
1.80	5.35	0.0059	0.0026	0.0023	0.0047	20.5	14.9	64.6
2.00	5.09	0.0381	0.0173	0.0321	0.0110	20.6	71.1	8.3

Table H.1: Summary of calculated Reynolds Number random uncertainty with 95% level of confidence for configuration 2.

Nominal Mach	**Typical** Re_{ts} $\times 10^6$ **ft^{-1}**	$s_{Re_{ts}}$, $\times 10^6$, **ft^{-1}** **k = 2**	$s_{Re_{ts}}$, **due to** $s_{P_{T,bm}}$, $\times 10^6$ **ft^{-1}** **k = 2**	$s_{Re_{ts}}$ **due to** $s_{P_{S,bal}}$, $\times 10^6$ **ft^{-1}** **k = 2**	$s_{Re_{ts}}$ **due to** $s_{T_{T,bm}}$, $\times 10^6$ **ft^{-1}** **k = 2**	$s_{Re_{ts}}$ **UPC due to** $s_{P_{T,bm}}$	$s_{Re_{ts}}$ **UPC due to** $s_{P_{S,bal}}$	$s_{Re_{ts}}$ **UPC due to** $s_{T_{T,bm}}$
0.25	1.81	0.0042	0.0006	0.0040	0.0011	1.9	91.6	6.5
0.40	2.86	0.0034	0.0004	0.0024	0.0023	1.4	50.8	47.8
0.60	4.16	0.0022	0.0002	0.0011	0.0019	0.8	25.0	74.2
0.80	4.82	0.0024	0.0004	0.0001	0.0024	2.6	0.2	97.3
1.00	5.14	0.0035	0.0005	0.0013	0.0032	2.4	14.2	83.5
1.20	5.24	0.0022	0.0010	0.0001	0.0019	21.5	0.2	78.3
1.40	5.40	0.0017	0.0011	0.0006	0.0012	42.9	13.4	43.7
1.60	5.60	0.0049	0.0025	0.0033	0.0026	26.9	45.9	27.1
1.80	5.69	0.0088	0.0053	0.0055	0.0045	35.6	38.1	26.4
2.00	5.08	0.0124	0.0037	0.0092	0.0075	8.7	54.6	36.7

Table H.2: Summary of calculated Reynolds Number random uncertainty with 95% level of confidence for configuration 3.

Nominal Mach	**Typical** Re_{ts} $\times 10^6$ **ft^{-1}**	$s_{Re_{ts}}$, $\times 10^6$, **ft^{-1} k = 2**	$s_{Re_{ts}}$, **due to** $s_{P_{T,bm}}$, $\times 10^6$ **ft^{-1} k = 2**	$s_{Re_{ts}}$ **due to** $s_{P_{S,bal}}$, $\times 10^6$ **ft^{-1} k = 2**	$s_{Re_{ts}}$ **due to** $s_{T_{T,bm}}$, $\times 10^6$ **ft^{-1} k = 2**	$s_{Re_{ts}}$ **UPC due to** $s_{P_{T,bm}}$	$s_{Re_{ts}}$ **UPC due to** $s_{P_{S,bal}}$	$s_{Re_{ts}}$ **UPC due to** $s_{T_{T,bm}}$
0.25	1.85	0.0016	0.0007	0.0012	0.0007	21.5	57.6	20.9
0.40	2.88	0.0014	0.0004	0.0007	0.0011	7.1	28.8	64.0
0.60	4.19	0.0014	0.0001	0.0004	0.0013	0.9	8.6	90.5
0.80	4.86	0.0033	0.0001	0.0003	0.0032	0.2	0.8	99.0
1.00	5.19	0.0035	0.0002	0.0002	0.0035	0.5	0.3	99.2
1.20	5.25	0.0029	0.0003	0.0000	0.0029	1.1	0.0	98.9
1.40	5.41	0.0026	0.0003	0.0003	0.0025	1.7	1.3	97.0
1.60	5.62	0.0032	0.0010	0.0020	0.0023	10.4	37.9	51.7
1.80	5.74	0.0038	0.0019	0.0028	0.0017	25.8	54.0	20.2
2.00	5.33	0.0204	0.0045	0.0101	0.0172	4.9	24.4	70.7

Table H.3: Summary of calculated Reynolds Number random uncertainty with 95% level of confidence for configuration 4.

Nominal Mach	**Typical** Re_{ts} $\times 10^6$ **ft^{-1}**	$s_{Re_{ts}}$, $\times 10^6$, **ft^{-1} k = 2**	$s_{Re_{ts}}$, **due to** $s_{P_{T,bm}}$, $\times 10^6$ **ft^{-1} k = 2**	$s_{Re_{ts}}$ **due to** $s_{P_{S,bal}}$, $\times 10^6$ **ft^{-1} k = 2**	$s_{Re_{ts}}$ **due to** $s_{T_{T,bm}}$, $\times 10^6$ **ft^{-1} k = 2**	$s_{Re_{ts}}$ **UPC due to** $s_{P_{T,bm}}$	$s_{Re_{ts}}$ **UPC due to** $s_{P_{S,bal}}$	$s_{Re_{ts}}$ **UPC due to** $s_{T_{T,bm}}$
0.25	1.70	0.0039	0.0016	0.0035	0.0003	16.8	82.5	0.7
0.40	2.67	0.0021	0.0003	0.0015	0.0014	2.4	51.8	45.8
0.60	3.96	0.0015	0.0003	0.0005	0.0014	4.1	9.2	86.7
0.80	4.59	0.0026	0.0005	0.0015	0.0020	3.2	36.6	60.2
1.00	4.94	0.0023	0.0005	0.0013	0.0017	5.6	35.1	59.4
1.20	4.99	0.0015	0.0008	0.0000	0.0012	31.8	0.0	68.2
1.40	5.15	0.0017	0.0010	0.0011	0.0009	31.8	40.8	27.5
1.60	5.34	0.0050	0.0009	0.0042	0.0026	2.9	70.6	26.5
1.80	5.45	0.0084	0.0039	0.0021	0.0072	21.8	6.2	72.0
2.00	5.11	0.0144	0.0031	0.0102	0.0098	4.7	49.6	45.6

Table H.4: Summary of calculated Reynolds Number random uncertainty with 95% level of confidence for configuration 5.

Nominal Mach	**Typical** Re_{ts} $\times 10^6$ **ft^{-1}**	$s_{Re_{ts}}$, $\times 10^6$, **ft^{-1} k = 2**	$s_{Re_{ts}}$, **due to** $s_{P_{T,bm}}$, $\times 10^6$ **ft^{-1} k = 2**	$s_{Re_{ts}}$ **due to** $s_{P_{S,bal}}$, $\times 10^6$ **ft^{-1} k = 2**	$s_{Re_{ts}}$ **due to** $s_{T_{T,bm}}$, $\times 10^6$ **ft^{-1} k = 2**	$s_{Re_{ts}}$ **UPC due to** $s_{P_{T,bm}}$	$s_{Re_{ts}}$ **UPC due to** $s_{P_{S,bal}}$	$s_{Re_{ts}}$ **UPC due to** $s_{T_{T,bm}}$
0.25	1.84	0.0013	0.0007	0.0009	0.0007	30.3	43.8	25.8
0.40	2.86	0.0014	0.0003	0.0003	0.0013	3.3	3.3	93.4
0.60	4.17	0.0007	0.0002	0.0002	0.0006	8.2	7.2	84.7
0.80	4.60	0.0022	0.0002	0.0014	0.0017	0.9	42.0	57.1
1.00	5.19	0.0031	0.0003	0.0008	0.0030	1.1	6.6	92.3
1.20	5.26	0.0022	0.0004	0.0001	0.0021	3.0	0.4	96.6
1.40	5.41	0.0029	0.0019	0.0004	0.0022	40.3	1.6	58.1
1.60	5.56	0.0045	0.0016	0.0028	0.0031	12.7	38.5	48.8
1.80	5.60	0.0043	0.0016	0.0021	0.0034	13.3	23.7	63.0
2.00	5.08	0.0056	0.0009	0.0026	0.0049	2.4	22.0	75.6

Table H.5: Summary of calculated Reynolds Number random uncertainty with 95% level of confidence for configuration 6.

H.2 Systematic Uncertainty Results for Configurations 2-6

The systematic uncertainty in the test section Reynolds number is shown for all configurations in Figure H.4. All configurations follow a similar trend with varying magnitudes.

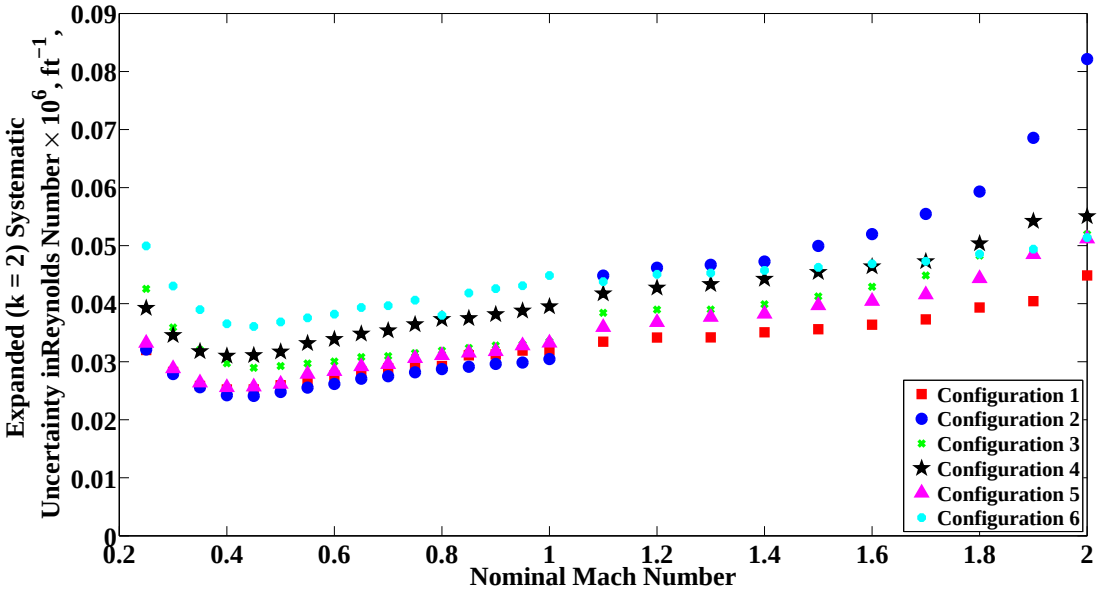

Figure H.4: Systematic uncertainty of Re_{ts} as a function of nominal Mach number for all configurations. The red squares are configuration 1, blue circles are configuration 2, green x's are configuration 3, black stars are configuration 4, purple triangles are configuration 5, and cyan dots are configuration 6.

The systematic uncertainty in Re_{ts} is due to systematic contributions from all tunnel calibrations (b_{PSCAL}, b_{PTCAL}, and b_{TTCAL}), instrumentation uncertainties in test-time bellmouth total pressure, balance chamber static pressure, and barometric pressure (combined as $b_{P_{inst}}$). The percent contributions of each of these uncertainties to the combined systematic uncertainty in Re_{ts} are shown in Figure H.5. The tabulated details are shown in Tables H.6 - H.10.

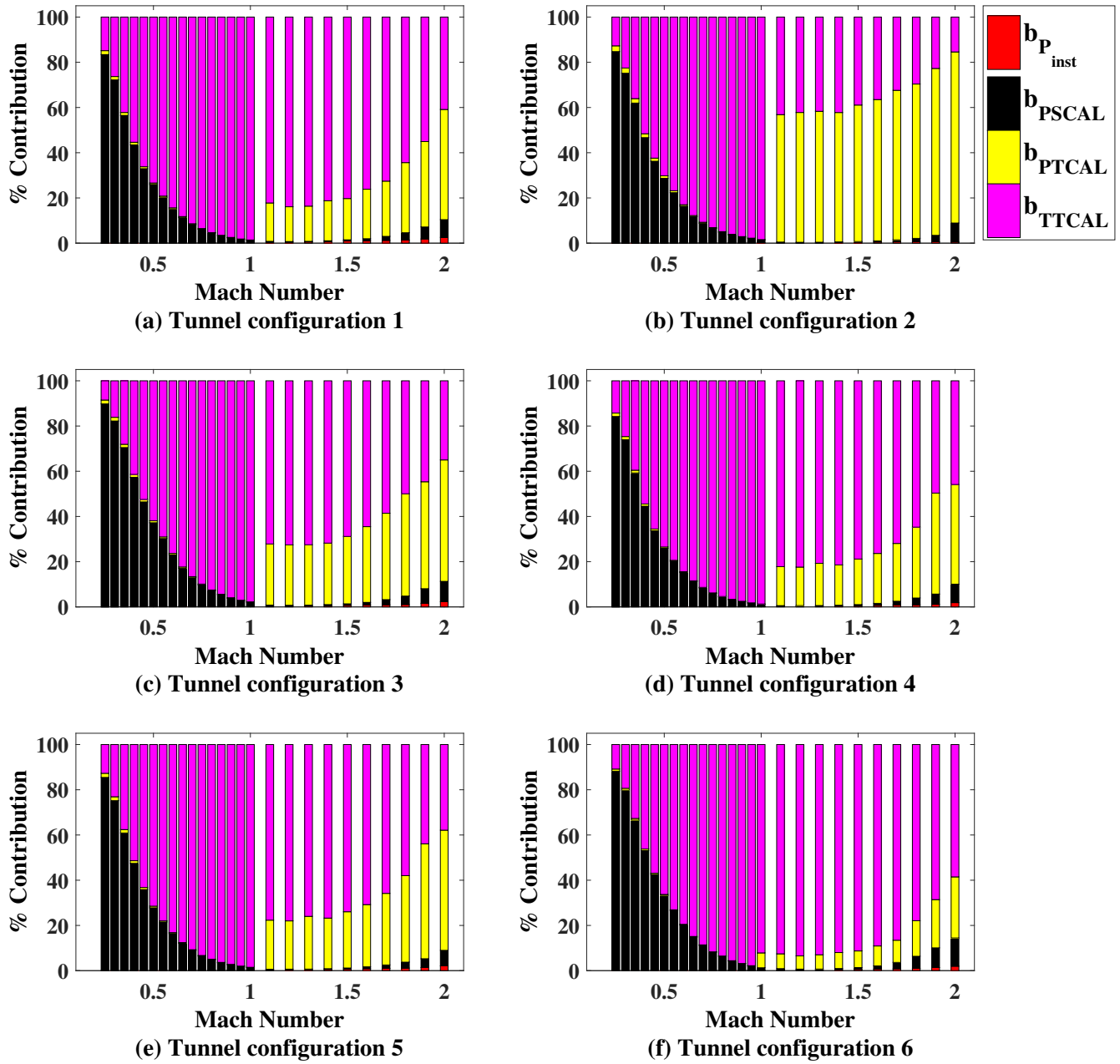

Figure H.5: Systematic UPC of Re_{ts} as a function of nominal Mach number for all configurations. Red is the systematic uncertainty due to pressure instrumentation, yellow is the systematic uncertainty due to total pressure calibration, black is the systematic uncertainty due to static pressure calibration, and purple is the systematic uncertainty due to total temperature calibration.

Nominal Mach	**Typical** Re_{ts} $\times 10^6$ **ft^{-1}**	$b_{Re_{ts}}$ $\times 10^6$ **ft^{-1} k = 2**	$b_{Re_{ts}}$ **due to** $b_{P_{Inst}}$ $\times 10^6$ **ft^{-1} k = 2**	$b_{Re_{ts}}$ **due to** b_{PSCAL}, $\times 10^6$ **ft^{-1} k = 2**	$b_{Re_{ts}}$ **due to** b_{PTCAL}, $\times 10^6$ **ft^{-1} k = 2**	$b_{Re_{ts}}$ **due to** b_{TTCAL}, $\times 10^6$ **ft^{-1} k = 2**	$b_{Re_{ts}}$ **UPC due to** $b_{P_{Inst}}$	$b_{Re_{ts}}$ **UPC due to** b_{PSCAL}	$b_{Re_{ts}}$ **UPC due to** b_{PTCAL}	$b_{Re_{ts}}$ **UPC due to** b_{TTCAL}
0.25	1.72	0.0321	0.0005	0.0295	0.0051	0.0114	0.0	84.7	2.5	12.7
0.40	2.67	0.0242	0.0008	0.0165	0.0032	0.0174	0.1	46.6	1.7	51.6
0.60	3.88	0.0262	0.0012	0.0105	0.0021	0.0238	0.2	16.1	0.7	83.0
0.80	4.51	0.0287	0.0015	0.0061	0.0017	0.0280	0.3	4.5	0.3	94.9
1.00	4.82	0.0305	0.0019	0.0031	0.0014	0.0302	0.4	1.0	0.2	98.4
1.20	4.87	0.0462	0.0022	0.0018	0.0350	0.0300	0.2	0.2	57.4	42.2
1.40	5.03	0.0473	0.0029	0.0020	0.0358	0.0307	0.4	0.2	57.2	42.2
1.60	5.22	0.0520	0.0037	0.0037	0.0411	0.0314	0.5	0.5	62.5	36.5
1.80	5.35	0.0593	0.0049	0.0071	0.0490	0.0323	0.7	1.4	68.3	29.6
2.00	5.09	0.0821	0.0059	0.0238	0.0715	0.0323	0.5	8.4	75.7	15.4

Table H.6: Summary of calculated Reynolds Number systematic uncertainty with 95% level of confidence for configuration 2.

Nominal Mach	**Typical** Re_{ts} $\times 10^6$ **ft^{-1}**	$b_{Re_{ts}}$ $\times 10^6$ **ft^{-1} k = 2**	$b_{Re_{ts}}$ **due to** $b_{P_{Inst}}$ $\times 10^6$ **ft^{-1} k = 2**	$b_{Re_{ts}}$ **due to** b_{PSCAL}, $\times 10^6$ **ft^{-1} k = 2**	$b_{Re_{ts}}$ **due to** b_{PTCAL}, $\times 10^6$ **ft^{-1} k = 2**	$b_{Re_{ts}}$ **due to** b_{TTCAL}, $\times 10^6$ **ft^{-1} k = 2**	$b_{Re_{ts}}$ **UPC due to** $b_{P_{Inst}}$	$b_{Re_{ts}}$ **UPC due to** b_{PSCAL}	$b_{Re_{ts}}$ **UPC due to** b_{PTCAL}	$b_{Re_{ts}}$ **UPC due to** b_{TTCAL}
0.25	1.81	0.0426	0.0005	0.0403	0.0055	0.0124	0.0	89.8	1.7	8.5
0.40	2.86	0.0297	0.0008	0.0225	0.0034	0.0191	0.1	57.2	1.3	41.4
0.60	4.16	0.0300	0.0013	0.0144	0.0024	0.0262	0.2	22.9	0.6	76.3
0.80	4.82	0.0319	0.0016	0.0084	0.0018	0.0307	0.2	7.0	0.3	92.5
1.00	5.14	0.0335	0.0019	0.0044	0.0014	0.0331	0.3	1.7	0.2	97.8
1.20	5.24	0.0390	0.0024	0.0024	0.0201	0.0332	0.4	0.4	26.7	72.6
1.40	5.40	0.0399	0.0031	0.0027	0.0208	0.0338	0.6	0.4	27.2	71.8
1.60	5.60	0.0429	0.0038	0.0047	0.0248	0.0345	0.8	1.2	33.5	64.5
1.80	5.69	0.0483	0.0050	0.0093	0.0325	0.0341	1.1	3.7	45.2	50.0
2.00	5.08	0.0519	0.0079	0.0156	0.0381	0.0307	2.3	9.0	53.7	35.0

Table H.7: Summary of calculated Reynolds Number systematic uncertainty with 95% level of confidence for configuration 3.

Nominal Mach	**Typical** Re_{ts} $\times 10^6$ **ft^{-1}**	$b_{Re_{ts}}$ $\times 10^6$ **ft^{-1} k = 2**	$b_{Re_{ts}}$ **due to** $b_{P_{Inst}}$ $\times 10^6$ **ft^{-1} k = 2**	$b_{Re_{ts}}$ **due to** b_{PSCAL}, $\times 10^6$ **ft^{-1} k = 2**	$b_{Re_{ts}}$ **due to** b_{PTCAL}, $\times 10^6$ **ft^{-1} k = 2**	$b_{Re_{ts}}$ **due to** b_{TTCAL}, $\times 10^6$ **ft^{-1} k = 2**	$b_{Re_{ts}}$ **UPC due to** $b_{P_{Inst}}$	$b_{Re_{ts}}$ **UPC due to** b_{PSCAL}	$b_{Re_{ts}}$ **UPC due to** b_{PTCAL}	$b_{Re_{ts}}$ **UPC due to** b_{TTCAL}
0.25	1.85	0.0392	0.0005	0.0360	0.0048	0.0148	0.0	84.2	1.5	14.3
0.40	2.88	0.0310	0.0008	0.0207	0.0030	0.0229	0.1	44.5	1.0	54.5
0.60	4.19	0.0339	0.0013	0.0131	0.0021	0.0311	0.1	15.1	0.4	84.4
0.80	4.86	0.0373	0.0016	0.0077	0.0015	0.0364	0.2	4.3	0.2	95.4
1.00	5.19	0.0395	0.0019	0.0039	0.0013	0.0392	0.2	1.0	0.1	98.7
1.20	5.25	0.0427	0.0025	0.0022	0.0176	0.0388	0.3	0.3	17.0	82.4
1.40	5.41	0.0442	0.0030	0.0024	0.0187	0.0399	0.5	0.3	17.8	81.4
1.60	5.62	0.0464	0.0039	0.0043	0.0218	0.0405	0.7	0.9	22.1	76.3
1.80	5.74	0.0504	0.0048	0.0088	0.0282	0.0405	0.9	3.0	31.3	64.7
2.00	5.33	0.0550	0.0076	0.0157	0.0365	0.0373	1.9	8.2	44.1	45.9

Table H.8: Summary of calculated Reynolds Number systematic uncertainty with 95% level of confidence for configuration 4.

Nominal Mach	**Typical** Re_{ts} $\times 10^6$ **ft^{-1}**	$b_{Re_{ts}}$ $\times 10^6$ **ft^{-1} k = 2**	$b_{Re_{ts}}$ **due to** $b_{P_{Inst}}$ $\times 10^6$ **ft^{-1} k = 2**	$b_{Re_{ts}}$ **due to** b_{PSCAL}, $\times 10^6$ **ft^{-1} k = 2**	$b_{Re_{ts}}$ **due to** b_{PTCAL}, $\times 10^6$ **ft^{-1} k = 2**	$b_{Re_{ts}}$ **due to** b_{TTCAL}, $\times 10^6$ **ft^{-1} k = 2**	$b_{Re_{ts}}$ **UPC due to** $b_{P_{Inst}}$	$b_{Re_{ts}}$ **UPC due to** b_{PSCAL}	$b_{Re_{ts}}$ **UPC due to** b_{PTCAL}	$b_{Re_{ts}}$ **UPC due to** b_{TTCAL}
0.25	1.70	0.0332	0.0005	0.0307	0.0045	0.0118	0.0	85.4	1.8	12.7
0.40	2.67	0.0256	0.0008	0.0176	0.0028	0.0183	0.1	47.4	1.2	51.4
0.60	3.96	0.0284	0.0013	0.0114	0.0019	0.0259	0.2	16.2	0.4	83.2
0.80	4.59	0.0311	0.0015	0.0067	0.0014	0.0303	0.2	4.6	0.2	94.9
1.00	4.94	0.0333	0.0019	0.0034	0.0012	0.0330	0.3	1.0	0.1	98.5
1.20	4.99	0.0368	0.0024	0.0018	0.0170	0.0325	0.4	0.2	21.3	78.0
1.40	5.15	0.0382	0.0029	0.0021	0.0181	0.0335	0.6	0.3	22.4	76.8
1.60	5.34	0.0404	0.0038	0.0037	0.0212	0.0340	0.9	0.8	27.5	70.8
1.80	5.45	0.0443	0.0047	0.0072	0.0274	0.0338	1.1	2.6	38.3	58.0
2.00	5.11	0.0512	0.0075	0.0134	0.0373	0.0315	2.1	6.9	53.1	37.9

Table H.9: Summary of calculated Reynolds Number systematic uncertainty with 95% level of confidence for configuration 5.

Nominal Mach	**Typical** Re_{ts} $\times 10^6$ **ft^{-1}**	$b_{Re_{ts}}$ $\times 10^6$ **ft^{-1} k = 2**	$b_{Re_{ts}}$ **due to** $b_{P_{Inst}}$ $\times 10^6$ **ft^{-1} k = 2**	$b_{Re_{ts}}$ **due to** b_{PSCAL}, $\times 10^6$ **ft^{-1} k = 2**	$b_{Re_{ts}}$ **due to** b_{PTCAL}, $\times 10^6$ **ft^{-1} k = 2**	$b_{Re_{ts}}$ **due to** b_{TTCAL}, $\times 10^6$ **ft^{-1} k = 2**	$b_{Re_{ts}}$ **UPC due to** $b_{P_{Inst}}$	$b_{Re_{ts}}$ **UPC due to** b_{PSCAL}	$b_{Re_{ts}}$ **UPC due to** b_{PTCAL}	$b_{Re_{ts}}$ **UPC due to** b_{TTCAL}
0.25	1.84	0.0499	0.0005	0.0469	0.0049	0.0164	0.0	88.2	0.9	10.8
0.40	2.86	0.0365	0.0008	0.0266	0.0030	0.0248	0.1	53.1	0.7	46.2
0.60	4.17	0.0382	0.0013	0.0171	0.0022	0.0341	0.1	20.1	0.3	79.5
0.80	4.60	0.0380	0.0015	0.0094	0.0015	0.0367	0.2	6.2	0.2	93.5
1.00	5.19	0.0449	0.0020	0.0047	0.0115	0.0431	0.2	1.1	6.6	92.1
1.20	5.26	0.0451	0.0024	0.0029	0.0109	0.0436	0.3	0.4	5.8	93.5
1.40	5.41	0.0457	0.0031	0.0032	0.0122	0.0439	0.5	0.5	7.1	92.0
1.60	5.56	0.0469	0.0039	0.0056	0.0139	0.0442	0.7	1.4	8.8	89.1
1.80	5.60	0.0486	0.0049	0.0112	0.0193	0.0429	1.0	5.4	15.7	77.9
2.00	5.08	0.0514	0.0072	0.0182	0.0267	0.0393	2.0	12.5	27.0	58.5

Table H.10: Summary of calculated Reynolds Number systematic uncertainty with 95% level of confidence for configuration 6.

H.3 Total Uncertainty Results for Configurations 2-6

The overall uncertainty in Re_{ts} for all configurations is shown in Figure H.6. The trends are similar for all configurations. The combined uncertainty in Re_{ts} is tabulated for configurations 2-6 in Tables H.11 - H.15.

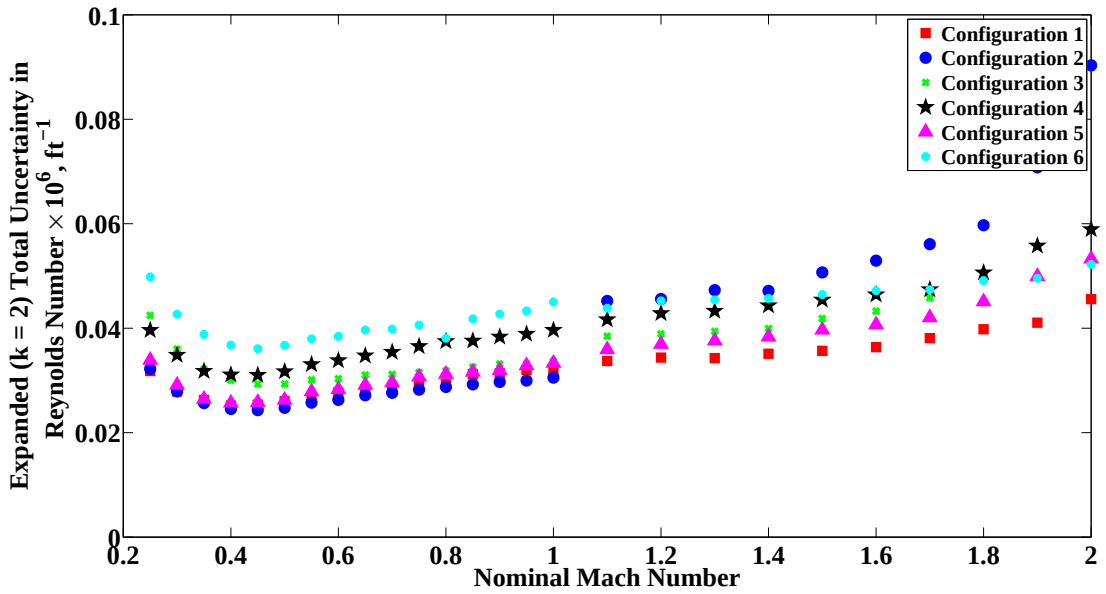

Figure H.6: Total uncertainty of Re_{ts} as a function of nominal Mach number for all configurations.

Nominal Mach	**Typical** Re_{ts} $\times 10^6$ **ft^{-1}**	$s_{Re_{ts}}$ $\times 10^6$ **ft^{-1}** **k = 2**	$b_{Re_{ts}}$ $\times 10^6$ **ft^{-1}** **k = 2**	$u_{Re_{ts}}$ $\times 10^6$ **ft^{-1}** **k = 2**	$s_{Re_{ts}}$ **UPC**	$b_{Re_{ts}}$ **UPC**
0.25	1.72	0.0025	0.0321	0.0322	0.6	99.4
0.40	2.67	0.0029	0.0242	0.0245	1.4	98.6
0.60	3.88	0.0006	0.0262	0.0263	0.1	99.9
0.80	4.51	0.0026	0.0287	0.0288	0.8	99.2
1.00	4.82	0.0023	0.0305	0.0305	0.5	99.5
1.20	4.87	0.0022	0.0462	0.0456	0.2	99.8
1.40	5.03	0.0024	0.0473	0.0471	0.3	99.7
1.60	5.22	0.0062	0.0520	0.0529	1.4	98.6
1.80	5.35	0.0059	0.0593	0.0597	1.0	99.0
2.00	5.09	0.0381	0.0821	0.0903	17.7	82.3

Table H.11: Summary of calculated Reynolds Number uncertainty with 95% level of confidence for configuration 2.

Nominal Mach	**Typical** Re_{ts} $\times 10^6$ **ft^{-1}**	$s_{Re_{ts}}$ $\times 10^6$ **ft^{-1}** **k = 2**	$b_{Re_{ts}}$ $\times 10^6$ **ft^{-1}** **k = 2**	$u_{Re_{ts}}$ $\times 10^6$ **ft^{-1}** **k = 2**	$s_{Re_{ts}}$ **UPC**	$b_{Re_{ts}}$ **UPC**
0.25	1.81	0.0042	0.0426	0.0425	1.0	99.0
0.40	2.86	0.0034	0.0297	0.0300	1.3	98.7
0.60	4.16	0.0022	0.0300	0.0303	0.5	99.5
0.80	4.82	0.0024	0.0319	0.0318	0.6	99.4
1.00	5.14	0.0035	0.0335	0.0337	1.1	98.9
1.20	5.24	0.0022	0.0390	0.0389	0.3	99.7
1.40	5.40	0.0017	0.0399	0.0399	0.2	99.8
1.60	5.60	0.0049	0.0429	0.0433	1.3	98.7
1.80	5.69	0.0088	0.0483	0.0493	3.2	96.8
2.00	5.08	0.0124	0.0519	0.0534	5.4	94.6

Table H.12: Summary of calculated Reynolds Number uncertainty with 95% level of confidence for configuration 3.

Nominal Mach	**Typical** Re_{ts} $\times 10^6$ **ft^{-1}**	$s_{Re_{ts}}$ $\times 10^6$ **ft^{-1}** **k = 2**	$b_{Re_{ts}}$ $\times 10^6$ **ft^{-1}** **k = 2**	$u_{Re_{ts}}$ $\times 10^6$ **ft^{-1}** **k = 2**	$s_{Re_{ts}}$ **UPC**	$b_{Re_{ts}}$ **UPC**
0.25	1.85	0.0016	0.0392	0.0396	0.2	99.8
0.40	2.88	0.0014	0.0310	0.0311	0.2	99.8
0.60	4.19	0.0014	0.0339	0.0338	0.2	99.8
0.80	4.86	0.0033	0.0373	0.0375	0.8	99.2
1.00	5.19	0.0035	0.0395	0.0396	0.8	99.2
1.20	5.25	0.0029	0.0427	0.0428	0.5	99.5
1.40	5.41	0.0026	0.0442	0.0443	0.3	99.7
1.60	5.62	0.0032	0.0464	0.0464	0.5	99.5
1.80	5.74	0.0038	0.0504	0.0506	0.6	99.4
2.00	5.33	0.0204	0.0550	0.0589	12.1	87.9

Table H.13: Summary of calculated Reynolds Number uncertainty with 95% level of confidence for configuration 4.

Nominal Mach	**Typical** Re_{ts} $\times 10^6$ **ft^{-1}**	$s_{Re_{ts}}$ $\times 10^6$ **ft^{-1}** **k = 2**	$b_{Re_{ts}}$ $\times 10^6$ **ft^{-1}** **k = 2**	$u_{Re_{ts}}$ $\times 10^6$ **ft^{-1}** **k = 2**	$s_{Re_{ts}}$ **UPC**	$b_{Re_{ts}}$ **UPC**
0.25	1.70	0.0039	0.0332	0.0339	1.3	98.7
0.40	2.67	0.0021	0.0256	0.0257	0.7	99.3
0.60	3.96	0.0015	0.0284	0.0283	0.3	99.7
0.80	4.59	0.0026	0.0311	0.0312	0.7	99.3
1.00	4.94	0.0023	0.0333	0.0333	0.5	99.5
1.20	4.99	0.0015	0.0368	0.0369	0.2	99.8
1.40	5.15	0.0017	0.0382	0.0383	0.2	99.8
1.60	5.34	0.0050	0.0404	0.0407	1.5	98.5
1.80	5.45	0.0084	0.0443	0.0451	3.5	96.5
2.00	5.11	0.0144	0.0512	0.0533	7.4	92.6

Table H.14: Summary of calculated Reynolds Number uncertainty with 95% level of confidence for configuration 5.

Nominal Mach	**Typical** Re_{ts} $\times 10^6$ **ft^{-1}**	$s_{Re_{ts}}$ $\times 10^6$ **ft^{-1}** **k = 2**	$b_{Re_{ts}}$ $\times 10^6$ **ft^{-1}** **k = 2**	$u_{Re_{ts}}$ $\times 10^6$ **ft^{-1}** **k = 2**	$s_{Re_{ts}}$ **UPC**	$b_{Re_{ts}}$ **UPC**
0.25	1.84	0.0013	0.0499	0.0498	0.1	99.9
0.40	2.86	0.0014	0.0365	0.0368	0.1	99.9
0.60	4.17	0.0007	0.0382	0.0384	0.0	100.0
0.80	4.60	0.0022	0.0380	0.0381	0.3	99.7
1.00	5.19	0.0031	0.0449	0.0450	0.5	99.5
1.20	5.26	0.0022	0.0451	0.0452	0.2	99.8
1.40	5.41	0.0029	0.0457	0.0457	0.4	99.6
1.60	5.56	0.0045	0.0469	0.0472	0.9	99.1
1.80	5.60	0.0043	0.0486	0.0491	0.8	99.2
2.00	5.08	0.0056	0.0514	0.0522	1.2	98.8

Table H.15: Summary of calculated Reynolds Number uncertainty with 95% level of confidence for configuration 6.

Appendix I: Free Stream Air Speed Uncertainty

Free stream air speed is a function of Mach number and total temperature, as shown in Figure I.1. Refer to Appendices B and F respectively to see uncertainty flow from measured values to those variables, which are propagated through the data reduction equations shown in Section 3.2.2 to attain uncertainty in air speed. Results for uncertainty in free stream air speed for configuration 1 were presented in Section 5. Results for configurations 2-6 are presented in this Appendix. Bar charts depicting the percent contributions are shown, followed by tabulated results detailing dimensional and percent contributions for random, systematic, and total uncertainty.

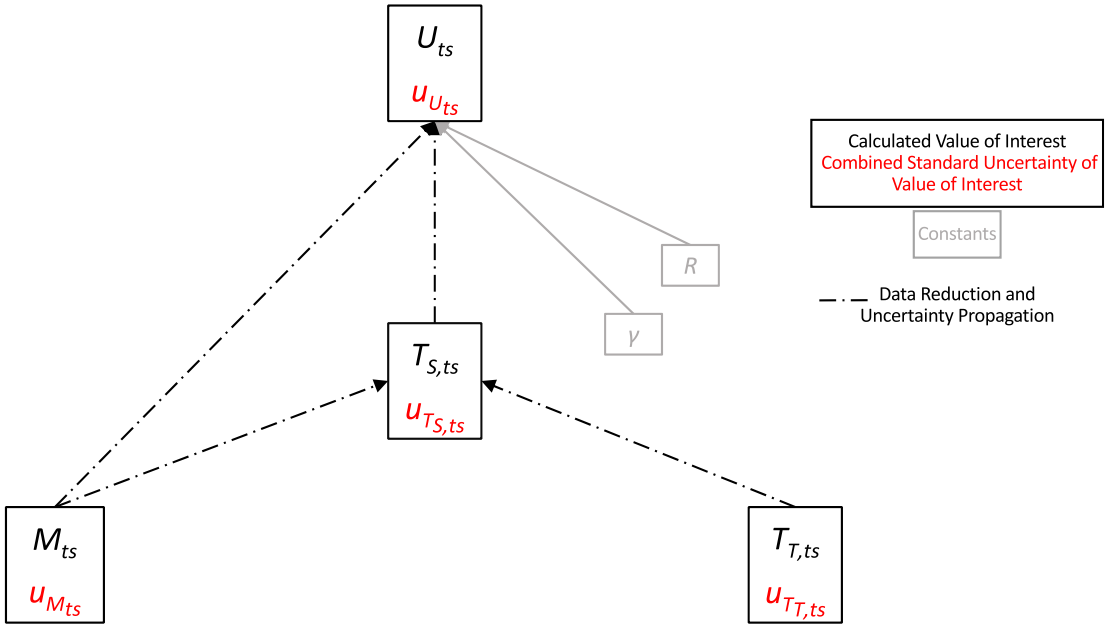

Figure I.1: Uncertainty flow from measured value to calculated free stream air speed in the test section.

I.1 Random Uncertainty Results for Configurations 2-6

The random uncertainty in the free stream air speed is shown for all configurations in Figure I.2. All configurations follow a similar trend, remaining below 1 ft/s subsonically then increasing supersonically. Configuration 2 shows a sharp increase at the highest Mach numbers, not seen in the other configurations, which remain below 3 ft/s.

The elemental random uncertainties contributing to random uncertainty in free stream air speed are the random uncertainties in $P_{T,bm}$, $P_{S,bal}$, and $T_{T,bm}$. The percent contributions of each of these elemental uncertainties to the total random uncertainty in U_{ts} are shown in Figure I.3. The tabulated details are shown in Tables I.1 - I.5.

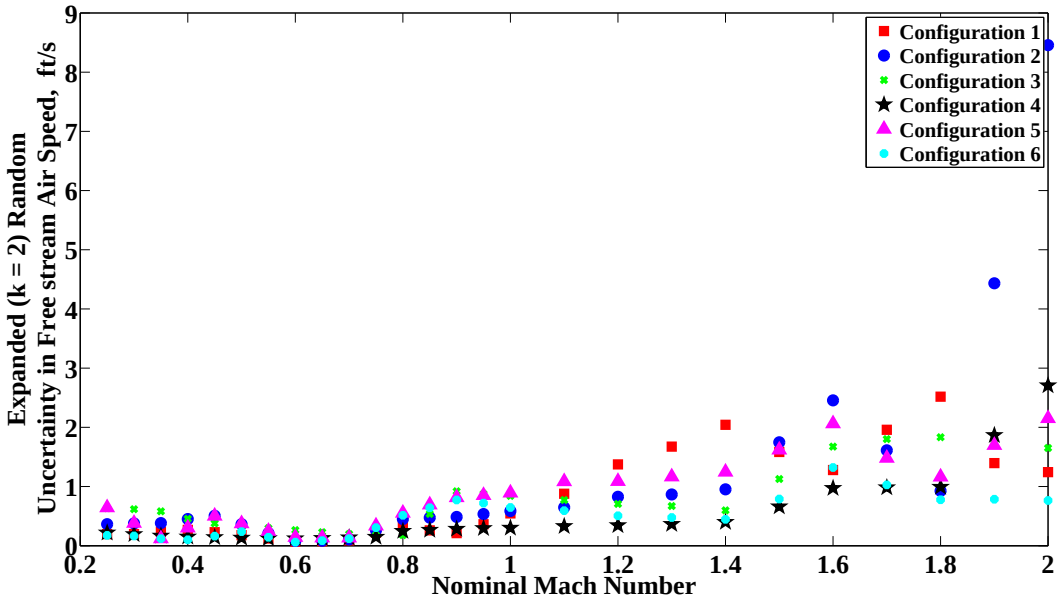

Figure I.2: Random uncertainty of U_{ts} as a function of nominal Mach number for all configurations. The red squares are configuration 1, blue circles are configuration 2, green x's are configuration 3, black stars are configuration 4, purple triangles are configuration 5, and cyan dots are configuration 6.

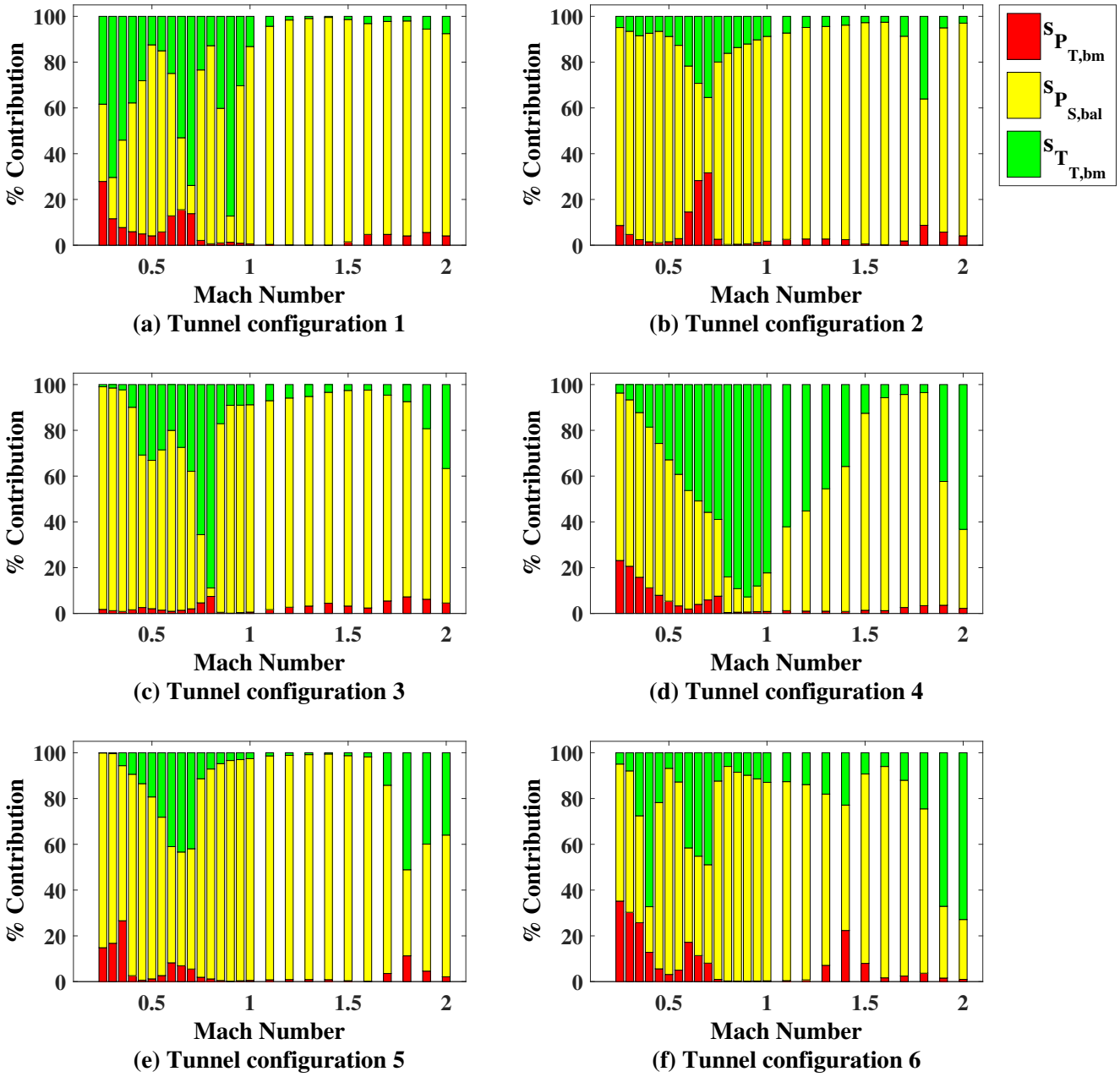

Figure I.3: Random UPC of U_{ts} as a function of nominal Mach number for all configurations. Red is the random uncertainty of the total pressure in the bellmouth, yellow is the random uncertainty of the static pressure in the balance chamber, and green is the random uncertainty of the total temperature in the bellmouth..

Nominal Mach	Typical U_{ts} ft/s	$s_{U_{ts}}$ ft/s k = 2	$s_{U_{ts}}$ due to $s_{P_{T,bm}}$ ft/s k = 2	$s_{U_{ts}}$ due to $s_{P_{S,bal}}$ ft/s k = 2	$s_{U_{ts}}$ due to $s_{T_{T,bm}}$ ft/s k = 2	$s_{U_{ts}}$ UPC due to $s_{P_{T,bm}}$	$s_{U_{ts}}$ UPC due to $s_{P_{S,bal}}$	$s_{U_{ts}}$ UPC due to $s_{T_{T,bm}}$
0.25	280	0.36	0.11	0.34	0.08	8.6	86.5	4.9
0.40	460	0.45	0.06	0.43	0.12	1.5	91.1	7.4
0.60	690	0.08	0.03	0.06	0.04	14.5	63.8	21.7
0.80	890	0.45	0.03	0.41	0.18	0.3	83.5	16.1
1.00	1070	0.59	0.08	0.56	0.17	1.8	89.5	8.7
1.20	1250	0.83	0.14	0.80	0.18	2.7	92.4	4.8
1.40	1380	0.95	0.15	0.92	0.19	2.5	93.7	3.8
1.60	1540	2.46	0.13	2.42	0.39	0.3	97.2	2.6
1.80	1690	0.93	0.27	0.69	0.56	8.7	55.2	36.1
2.00	1830	8.46	1.72	8.15	1.45	4.1	92.9	3.0

Table I.1: Summary of calculated Free stream Air Speed random uncertainty with 95% level of confidence for configuration 2.

Nominal Mach	Typical U_{ts} ft/s	$s_{U_{ts}}$ ft/s k = 2	$s_{U_{ts}}$ due to $s_{P_{T,bm}}$ ft/s k = 2	$s_{U_{ts}}$ due to $s_{P_{S,bal}}$ ft/s k = 2	$s_{U_{ts}}$ due to $s_{T_{T,bm}}$ ft/s k = 2	$s_{U_{ts}}$ UPC due to $s_{P_{T,bm}}$	$s_{U_{ts}}$ UPC due to $s_{P_{S,bal}}$	$s_{U_{ts}}$ UPC due to $s_{T_{T,bm}}$
0.25	270	0.64	0.08	0.63	0.06	1.8	97.3	1.0
0.40	450	0.46	0.06	0.43	0.14	1.6	88.5	9.9
0.60	670	0.26	0.03	0.24	0.12	1.0	79.0	20.0
0.80	870	0.18	0.05	0.03	0.17	7.4	3.7	88.9
1.00	1040	0.84	0.06	0.80	0.25	0.6	90.6	8.8
1.20	1230	0.71	0.12	0.68	0.17	2.7	91.4	5.9
1.40	1360	0.60	0.13	0.57	0.11	4.4	92.2	3.4
1.60	1520	1.67	0.26	1.63	0.26	2.4	95.2	2.4
1.80	1690	1.83	0.49	1.69	0.50	7.2	85.3	7.4
2.00	1830	1.65	0.35	1.27	1.00	4.6	58.8	36.7

Table I.2: Summary of calculated Free stream Air Speed random uncertainty with 95% level of confidence for configuration 3.

Nominal Mach	**Typical** U_{ts} **ft/s**	$s_{U_{ts}}$ **ft/s k = 2**	$s_{U_{ts}}$ **due to** $s_{P_{T,bm}}$ **ft/s k = 2**	$s_{U_{ts}}$ **due to** $s_{P_{S,bal}}$ **ft/s k = 2**	$s_{U_{ts}}$ **due to** $s_{T_{T,bm}}$ **ft/s k = 2**	$s_{U_{ts}}$ **UPC due to** $s_{P_{T,bm}}$	$s_{U_{ts}}$ **UPC due to** $s_{P_{S,bal}}$	$s_{U_{ts}}$ **UPC due to** $s_{T_{T,bm}}$
0.25	270	0.22	0.11	0.19	0.04	23.1	73.2	3.7
0.40	450	0.15	0.05	0.13	0.07	11.2	70.2	18.6
0.60	670	0.12	0.02	0.09	0.08	1.9	51.8	46.3
0.80	870	0.25	0.02	0.10	0.23	0.4	15.5	84.1
1.00	1050	0.30	0.03	0.12	0.27	0.9	16.9	82.3
1.20	1220	0.34	0.03	0.23	0.26	1.0	43.8	55.2
1.40	1360	0.40	0.04	0.32	0.24	0.9	63.4	35.8
1.60	1520	0.97	0.11	0.94	0.23	1.2	93.0	5.7
1.80	1680	0.99	0.18	0.96	0.19	3.4	93.1	3.5
2.00	1820	2.71	0.40	1.59	2.15	2.2	34.5	63.3

Table I.3: Summary of calculated Free stream Air Speed random uncertainty with 95% level of confidence for configuration 4.

Nominal Mach	**Typical** U_{ts} **ft/s**	$s_{U_{ts}}$ **ft/s k = 2**	$s_{U_{ts}}$ **due to** $s_{P_{T,bm}}$ **ft/s k = 2**	$s_{U_{ts}}$ **due to** $s_{P_{S,bal}}$ **ft/s k = 2**	$s_{U_{ts}}$ **due to** $s_{T_{T,bm}}$ **ft/s k = 2**	$s_{U_{ts}}$ **UPC due to** $s_{P_{T,bm}}$	$s_{U_{ts}}$ **UPC due to** $s_{P_{S,bal}}$	$s_{U_{ts}}$ **UPC due to** $s_{T_{T,bm}}$
0.25	270	0.64	0.25	0.59	0.02	14.8	85.1	0.1
0.40	450	0.30	0.05	0.28	0.09	2.6	88.0	9.4
0.60	680	0.14	0.04	0.10	0.09	8.2	50.8	41.0
0.80	880	0.55	0.06	0.53	0.15	1.2	91.7	7.1
1.00	1060	0.89	0.07	0.88	0.14	0.6	96.9	2.6
1.20	1240	1.09	0.10	1.08	0.12	0.9	98.0	1.1
1.40	1370	1.25	0.12	1.24	0.09	0.9	98.6	0.6
1.60	1530	2.06	0.09	2.04	0.28	0.2	98.0	1.8
1.80	1700	1.16	0.39	0.71	0.83	11.3	37.6	51.1
2.00	1830	2.15	0.31	1.69	1.29	2.1	61.9	36.0

Table I.4: Summary of calculated Free stream Air Speed random uncertainty with 95% level of confidence for configuration 5.

Nominal Mach	**Typical** U_{ts} **ft/s**	$s_{U_{ts}}$ **ft/s k = 2**	$s_{U_{ts}}$ **due to** $s_{P_{T,bm}}$ **ft/s k = 2**	$s_{U_{ts}}$ **due to** $s_{P_{S,bal}}$ **ft/s k = 2**	$s_{U_{ts}}$ **due to** $s_{T_{T,bm}}$ **ft/s k = 2**	$s_{U_{ts}}$ **UPC due to** $s_{P_{T,bm}}$	$s_{U_{ts}}$ **UPC due to** $s_{P_{S,bal}}$	$s_{U_{ts}}$ **UPC due to** $s_{T_{T,bm}}$
0.25	270	0.18	0.10	0.14	0.04	35.2	59.9	4.9
0.40	450	0.10	0.04	0.04	0.08	12.8	19.9	67.3
0.60	670	0.06	0.02	0.04	0.04	17.2	41.2	41.6
0.80	880	0.51	0.03	0.50	0.13	0.3	93.7	6.0
1.00	1070	0.65	0.04	0.60	0.23	0.3	86.7	12.9
1.20	1220	0.51	0.04	0.47	0.19	0.8	85.3	13.9
1.40	1360	0.45	0.21	0.33	0.21	22.4	54.8	22.9
1.60	1530	1.32	0.17	1.27	0.32	1.7	92.4	6.0
1.80	1700	0.78	0.15	0.66	0.38	3.7	71.8	24.5
2.00	1840	0.76	0.08	0.39	0.65	1.0	26.2	72.9

Table I.5: Summary of calculated Free stream Air Speed random uncertainty with 95% level of confidence for configuration 6.

I.2 Systematic Uncertainty Results for Configurations 2-6

The systematic uncertainty in the test section free stream air speed is shown for all configurations in Figure I.4. All configurations follow a similar trend.

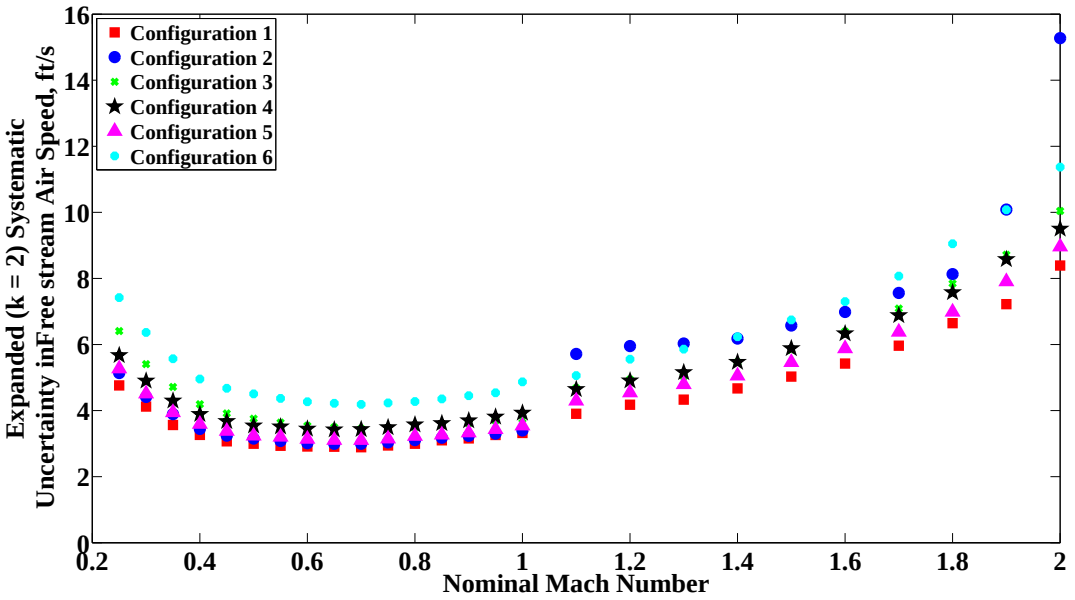

Figure I.4: Systematic uncertainty of U_{ts} as a function of nominal Mach number for all configurations. The red squares are configuration 1, blue circles are configuration 2, green x's are configuration 3, black stars are configuration 4, purple triangles are configuration 5, and cyan dots are configuration 6.

The systematic uncertainty in U_{ts} is due to systematic contributions from all tunnel calibrations (b_{PSCAL}, b_{PTCAL}, and b_{TTCAL}), and instrumentation uncertainties in test-time bellmouth total pressure, balance chamber static pressure, and barometric pressure (combined as $b_{P_{inst}}$). The percent contributions of each of these uncertainties to the combined systematic uncertainty in U_{ts} are shown in Figure I.5. The tabulated details are shown in Tables I.6 - I.10.

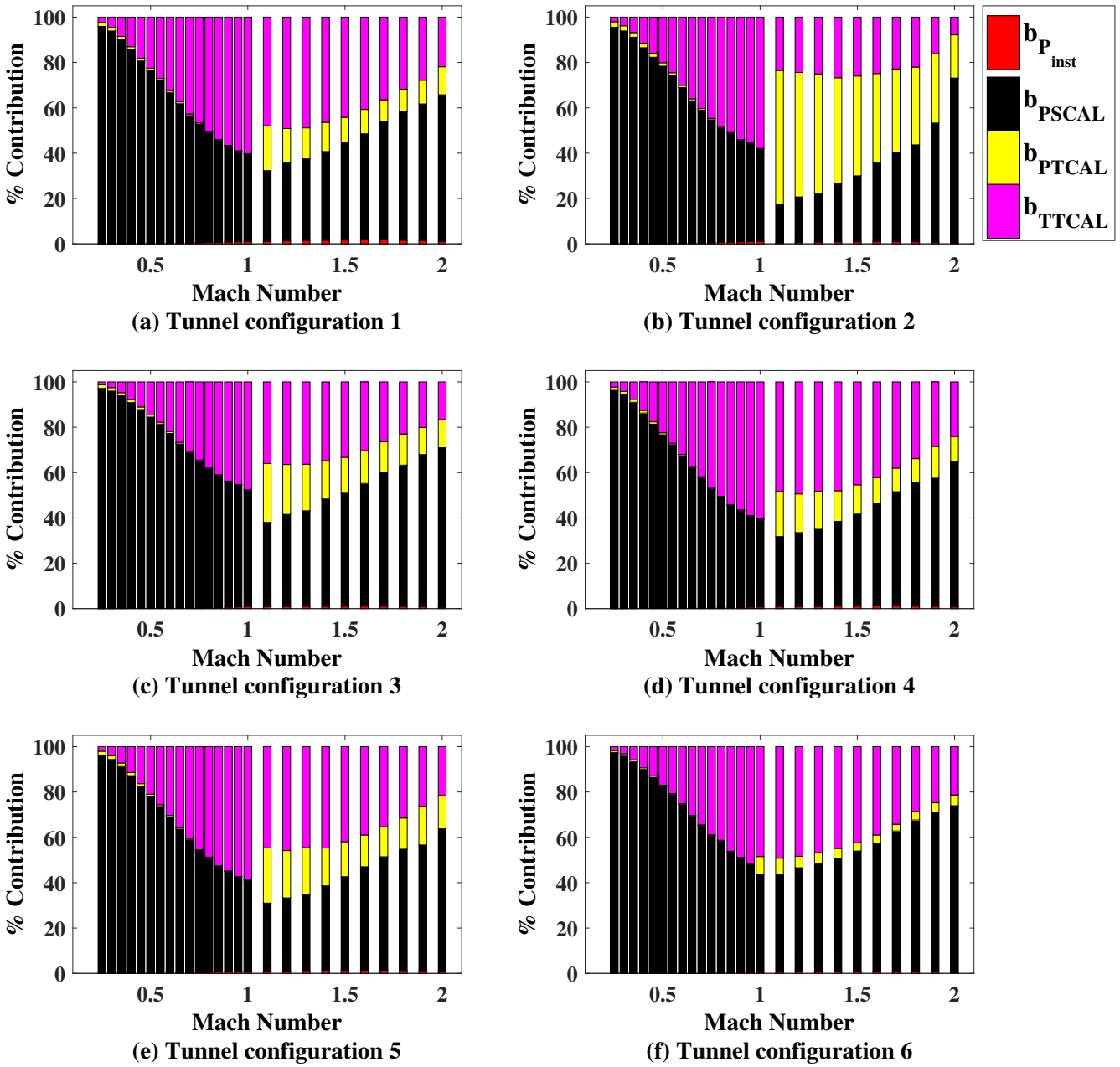

Figure I.5: Systematic UPC of U_{ts} as a function of nominal Mach number for all configurations. Red is the systematic uncertainty due to pressure instrumentation, yellow is the systematic uncertainty due to total pressure calibration, black is the systematic uncertainty due to static pressure calibration, and purple is the systematic uncertainty due to total temperature calibration.

Nominal Mach	**Typical** U_{ts} **ft/s**	$b_{U_{ts}}$ **ft/s k = 2**	$b_{U_{ts}}$ **due to** $b_{P_{Inst}}$ **ft/s k = 2**	$b_{U_{ts}}$ **due to** b_{PSCAL} **ft/s k = 2**	$b_{U_{ts}}$ **due to** b_{PTCAL} **ft/s k = 2**	$b_{U_{ts}}$ **due to** b_{TTCAL} **ft/s k = 2**	$b_{U_{ts}}$ **UPC due to** $b_{P_{Inst}}$	$b_{U_{ts}}$ **UPC due to** b_{PSCAL}	$b_{U_{ts}}$ **UPC due to** b_{PTCAL}	$b_{U_{ts}}$ **UPC due to** b_{TTCAL}
0.25	280	5.14	0.07	5.02	0.80	0.73	0.0	95.5	2.4	2.0
0.40	460	3.44	0.12	3.20	0.48	1.17	0.1	86.4	2.0	11.5
0.60	690	3.01	0.15	2.50	0.30	1.65	0.3	68.7	1.0	30.1
0.80	890	3.11	0.25	2.21	0.22	2.16	0.6	50.6	0.5	48.2
1.00	1070	3.40	0.36	2.17	0.18	2.59	1.1	40.7	0.3	57.9
1.20	1250	5.95	0.50	2.66	4.41	2.94	0.7	20.0	54.9	24.4
1.40	1380	6.18	0.58	3.15	4.21	3.20	0.9	26.0	46.4	26.7
1.60	1540	6.98	0.69	4.11	4.39	3.48	1.0	34.7	39.4	24.9
1.80	1690	8.13	0.78	5.32	4.76	3.82	0.9	42.8	34.3	22.0
2.00	1830	15.27	0.95	13.03	6.67	4.27	0.4	72.7	19.1	7.8

Table I.6: Summary of calculated Free stream Air Speed systematic uncertainty with 95% level of confidence for configuration 2.

Nominal Mach	**Typical** U_{ts} **ft/s**	$b_{U_{ts}}$ **ft/s k = 2**	$b_{U_{ts}}$ **due to** $b_{P_{Inst}}$ **ft/s k = 2**	$b_{U_{ts}}$ **due to** b_{PSCAL} **ft/s k = 2**	$b_{U_{ts}}$ **due to** b_{PTCAL} **ft/s k = 2**	$b_{U_{ts}}$ **due to** b_{TTCAL} **ft/s k = 2**	$b_{U_{ts}}$ **UPC due to** $b_{P_{Inst}}$	$b_{U_{ts}}$ **UPC due to** b_{PSCAL}	$b_{U_{ts}}$ **UPC due to** b_{PTCAL}	$b_{U_{ts}}$ **UPC due to** b_{TTCAL}
0.25	270	6.41	0.07	6.31	0.80	0.73	0.0	97.1	1.6	1.3
0.40	450	4.19	0.11	3.99	0.47	1.17	0.1	90.8	1.3	7.8
0.60	670	3.54	0.14	3.11	0.30	1.66	0.2	77.1	0.7	22.0
0.80	870	3.50	0.23	2.74	0.22	2.16	0.4	61.2	0.4	38.0
1.00	1040	3.74	0.34	2.68	0.17	2.58	0.8	51.4	0.2	47.6
1.20	1230	4.94	0.48	3.15	2.32	2.98	1.0	40.6	22.0	36.4
1.40	1360	5.46	0.55	3.76	2.24	3.22	1.0	47.3	16.9	34.8
1.60	1520	6.39	0.68	4.70	2.43	3.52	1.1	54.1	14.5	30.3
1.80	1690	7.84	0.78	6.19	2.91	3.76	1.0	62.3	13.7	23.0
2.00	1830	10.04	0.79	8.42	3.54	4.09	0.6	70.4	12.4	16.6

Table I.7: Summary of calculated Free stream Air Speed systematic uncertainty with 95% level of confidence for configuration 3.

Nominal Mach	**Typical** U_{ts} **ft/s**	$b_{U_{ts}}$ **ft/s k = 2**	$b_{U_{ts}}$ **due to** $b_{P_{Inst}}$ **ft/s k = 2**	$b_{U_{ts}}$ **due to** b_{PSCAL} **ft/s k = 2**	$b_{U_{ts}}$ **due to** b_{PTCAL} **ft/s k = 2**	$b_{U_{ts}}$ **due to** b_{TTCAL} **ft/s k = 2**	$b_{U_{ts}}$ **UPC due to** $b_{P_{Inst}}$	$b_{U_{ts}}$ **UPC due to** b_{PSCAL}	$b_{U_{ts}}$ **UPC due to** b_{PTCAL}	$b_{U_{ts}}$ **UPC due to** b_{TTCAL}
0.25	270	5.67	0.06	5.57	0.69	0.86	0.0	96.3	1.5	2.3
0.40	450	3.89	0.11	3.61	0.42	1.38	0.1	86.2	1.2	12.6
0.60	670	3.45	0.14	2.83	0.26	1.95	0.2	67.2	0.6	32.0
0.80	870	3.57	0.22	2.50	0.19	2.54	0.4	48.8	0.3	50.5
1.00	1050	3.93	0.34	2.44	0.15	3.06	0.7	38.7	0.1	60.4
1.20	1220	4.90	0.46	2.80	2.03	3.45	0.9	32.7	17.1	49.4
1.40	1360	5.47	0.57	3.34	2.01	3.79	1.1	37.4	13.5	48.0
1.60	1520	6.33	0.68	4.27	2.12	4.11	1.2	45.5	11.2	42.2
1.80	1680	7.58	0.80	5.59	2.47	4.41	1.1	54.4	10.7	33.9
2.00	1820	9.50	0.83	7.61	3.15	4.66	0.8	64.1	11.0	24.1

Table I.8: Summary of calculated Free stream Air Speed systematic uncertainty with 95% level of confidence for configuration 4.

Nominal Mach	**Typical** U_{ts} **ft/s**	$b_{U_{ts}}$ **ft/s k = 2**	$b_{U_{ts}}$ **due to** $b_{P_{Inst}}$ **ft/s k = 2**	$b_{U_{ts}}$ **due to** b_{PSCAL} **ft/s k = 2**	$b_{U_{ts}}$ **due to** b_{PTCAL} **ft/s k = 2**	$b_{U_{ts}}$ **due to** b_{TTCAL} **ft/s k = 2**	$b_{U_{ts}}$ **UPC due to** $b_{P_{Inst}}$	$b_{U_{ts}}$ **UPC due to** b_{PSCAL}	$b_{U_{ts}}$ **UPC due to** b_{PTCAL}	$b_{U_{ts}}$ **UPC due to** b_{TTCAL}
0.25	270	5.27	0.07	5.17	0.69	0.75	0.0	96.2	1.7	2.0
0.40	450	3.59	0.12	3.35	0.42	1.21	0.1	87.1	1.4	11.4
0.60	680	3.14	0.15	2.60	0.25	1.73	0.2	68.8	0.7	30.3
0.80	880	3.23	0.23	2.29	0.19	2.25	0.5	50.4	0.3	48.7
1.00	1060	3.54	0.35	2.24	0.15	2.72	1.0	40.1	0.2	58.8
1.20	1240	4.54	0.48	2.58	2.08	3.08	1.1	32.2	20.9	45.8
1.40	1370	5.05	0.59	3.09	2.06	3.38	1.4	37.3	16.7	44.7
1.60	1530	5.88	0.68	3.97	2.20	3.67	1.4	45.7	14.0	39.0
1.80	1700	6.98	0.80	5.11	2.59	3.92	1.3	53.5	13.8	31.5
2.00	1830	8.96	0.87	7.10	3.43	4.16	0.9	62.8	14.7	21.5

Table I.9: Summary of calculated Free stream Air Speed systematic uncertainty with 95% level of confidence for configuration 5.

Nominal Mach	**Typical** U_{ts} **ft/s**	$b_{U_{ts}}$ **ft/s k = 2**	$b_{U_{ts}}$ **due to** $b_{P_{Inst}}$ **ft/s k = 2**	$b_{U_{ts}}$ **due to** b_{PSCAL} **ft/s k = 2**	$b_{U_{ts}}$ **due to** b_{PTCAL} **ft/s k = 2**	$b_{U_{ts}}$ **due to** b_{TTCAL} **ft/s k = 2**	$b_{U_{ts}}$ **UPC due to** $b_{P_{Inst}}$	$b_{U_{ts}}$ **UPC due to** b_{PSCAL}	$b_{U_{ts}}$ **UPC due to** b_{PTCAL}	$b_{U_{ts}}$ **UPC due to** b_{TTCAL}
0.25	270	7.42	0.07	7.32	0.70	0.96	0.0	97.4	0.9	1.7
0.40	450	4.96	0.11	4.70	0.42	1.51	0.1	89.9	0.7	9.3
0.60	670	4.27	0.14	3.68	0.28	2.14	0.1	74.3	0.4	25.2
0.80	880	4.27	0.24	3.26	0.19	2.75	0.3	58.2	0.2	41.3
1.00	1070	4.87	0.35	3.21	1.35	3.39	0.5	43.3	7.7	48.5
1.20	1220	5.56	0.48	3.76	1.25	3.86	0.7	45.8	5.1	48.4
1.40	1360	6.24	0.58	4.41	1.30	4.18	0.9	49.9	4.4	44.9
1.60	1530	7.30	0.68	5.49	1.37	4.56	0.9	56.7	3.5	39.0
1.80	1700	9.05	0.77	7.41	1.75	4.84	0.7	66.9	3.7	28.6
2.00	1840	11.37	0.75	9.75	2.48	5.25	0.4	73.5	4.8	21.3

Table I.10: Summary of calculated Free stream Air Speed systematic uncertainty with 95% level of confidence for configuration 6.

I.3 Total Uncertainty Results for Configurations 2-6

The total uncertainty in U_{ts} for all configurations is shown in Figure I.6. Every configuration follows the same trend, although they have slightly different magnitudes. The combined uncertainty in U_{ts} is presented for configurations 2-6 in Tables I.11 - I.15.

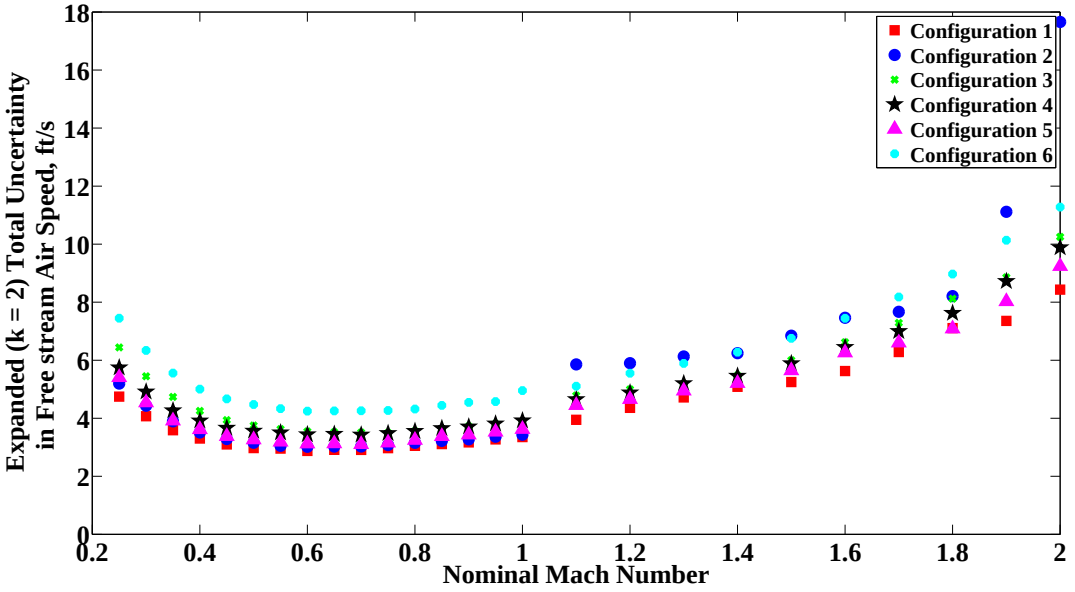

Figure I.6: Total uncertainty in U_{ts} as a function of nominal Mach number for all configurations.

Nominal Mach	**Typical U_{ts}, ft/s**	$s_{U_{ts}}$ **ft/s k = 2**	$b_{U_{ts}}$ **ft/s k = 2**	$u_{U_{ts}}$ **ft/s k = 2**	$s_{U_{ts}}$ **UPC**	$b_{U_{ts}}$ **UPC**
0.25	280	0.36	5.14	5.20	0.5	99.5
0.40	460	0.45	3.44	3.51	1.7	98.3
0.60	690	0.08	3.01	3.02	0.1	99.9
0.80	890	0.45	3.11	3.15	2.1	97.9
1.00	1070	0.59	3.40	3.43	2.9	97.1
1.20	1250	0.83	5.95	5.90	1.9	98.1
1.40	1380	0.95	6.18	6.24	2.3	97.7
1.60	1540	2.46	6.98	7.46	11.0	89.0
1.80	1690	0.93	8.13	8.21	1.3	98.7
2.00	1830	8.46	15.27	17.66	23.5	76.5

Table I.11: Summary of calculated Free stream Air Speed uncertainty with 95% level of confidence for configuration 2.

Nominal Mach	**Typical U_{ts}, ft/s**	$s_{U_{ts}}$ **ft/s k = 2**	$b_{U_{ts}}$ **ft/s k = 2**	$u_{U_{ts}}$ **ft/s k = 2**	$s_{U_{ts}}$ **UPC**	$b_{U_{ts}}$ **UPC**
0.25	270	0.64	6.41	6.44	1.0	99.0
0.40	450	0.46	4.19	4.25	1.2	98.8
0.60	670	0.26	3.54	3.54	0.6	99.4
0.80	870	0.18	3.50	3.55	0.3	99.7
1.00	1040	0.84	3.74	3.82	4.8	95.2
1.20	1230	0.71	4.94	5.00	2.0	98.0
1.40	1360	0.60	5.46	5.47	1.2	98.8
1.60	1520	1.67	6.39	6.62	6.4	93.6
1.80	1690	1.83	7.84	8.12	5.2	94.8
2.00	1830	1.65	10.04	10.25	2.6	97.4

Table I.12: Summary of calculated Free stream Air Speed uncertainty with 95% level of confidence for configuration 3.

Nominal Mach	**Typical U_{ts}, ft/s**	$s_{U_{ts}}$ **ft/s k = 2**	$b_{U_{ts}}$ **ft/s k = 2**	$u_{U_{ts}}$ **ft/s k = 2**	$s_{U_{ts}}$ **UPC**	$b_{U_{ts}}$ **UPC**
0.25	270	0.22	5.67	5.74	0.1	99.9
0.40	450	0.15	3.89	3.91	0.2	99.8
0.60	670	0.12	3.45	3.44	0.1	99.9
0.80	870	0.25	3.57	3.56	0.5	99.5
1.00	1050	0.30	3.93	3.92	0.6	99.4
1.20	1220	0.34	4.90	4.88	0.5	99.5
1.40	1360	0.40	5.47	5.46	0.5	99.5
1.60	1520	0.97	6.33	6.45	2.3	97.7
1.80	1680	0.99	7.58	7.62	1.7	98.3
2.00	1820	2.71	9.50	9.88	7.5	92.5

Table I.13: Summary of calculated Free stream Air Speed uncertainty with 95% level of confidence for configuration 4.

Nominal Mach	**Typical U_{ts}, ft/s**	$s_{U_{ts}}$ **ft/s k = 2**	$b_{U_{ts}}$ **ft/s k = 2**	$u_{U_{ts}}$ **ft/s k = 2**	$s_{U_{ts}}$ **UPC**	$b_{U_{ts}}$ **UPC**
0.25	270	0.64	5.27	5.41	1.5	98.5
0.40	450	0.30	3.59	3.62	0.7	99.3
0.60	680	0.14	3.14	3.12	0.2	99.8
0.80	880	0.55	3.23	3.25	2.9	97.1
1.00	1060	0.89	3.54	3.62	6.0	94.0
1.20	1240	1.09	4.54	4.66	5.4	94.6
1.40	1370	1.25	5.05	5.21	5.7	94.3
1.60	1530	2.06	5.88	6.26	11.0	89.0
1.80	1700	1.16	6.98	7.09	2.7	97.3
2.00	1830	2.15	8.96	9.24	5.4	94.6

Table I.14: Summary of calculated Free stream Air Speed uncertainty with 95% level of confidence for configuration 5.

Nominal Mach	**Typical U_{ts}, ft/s**	$s_{U_{ts}}$ **ft/s k = 2**	$b_{U_{ts}}$ **ft/s k = 2**	$u_{U_{ts}}$ **ft/s k = 2**	$s_{U_{ts}}$ **UPC**	$b_{U_{ts}}$ **UPC**
0.25	270	0.18	7.42	7.45	0.1	99.9
0.40	450	0.10	4.96	5.00	0.0	100.0
0.60	670	0.06	4.27	4.25	0.0	100.0
0.80	880	0.51	4.27	4.32	1.4	98.6
1.00	1070	0.65	4.87	4.95	1.7	98.3
1.20	1220	0.51	5.56	5.55	0.8	99.2
1.40	1360	0.45	6.24	6.28	0.5	99.5
1.60	1530	1.32	7.30	7.45	3.2	96.8
1.80	1700	0.78	9.05	8.97	0.7	99.3
2.00	1840	0.76	11.37	11.28	0.5	99.5

Table I.15: Summary of calculated Free stream Air Speed uncertainty with 95% level of confidence for configuration 6.

Appendix J: Spatial Uniformity Considerations

For the 8- by 6-foot SWT uncertainty study, estimating and applying uncertainty in spatial uniformity of total temperature, total pressure and static pressure was limited to the effect of uniformity on the calibration tests, described in Section 6.1.5. If the uncertainty of a variable of interest as it applies to a randomly selected point on a cross-sectional plane or volume of the test section is desired, spatial uniformity uncertainty would be applied additionally within the test-time analysis.

Section 6.1.5 describes initial spatial uniformity uncertainty estimation attempts. The cone-cylinder was analyzed, but data indicated static pressure variations, suspected to be due to the presence of shock effects. This effect averages out for calibration purposes, but the variation is undesirable as an uncertainty estimate since the shocks are an artifact of the calibration hardware.

Alternatively, static pressure measured by the transonic array is considered. Flow quality data was obtained at a total of five rake heights in the tunnel, providing 35 test-section representative static pressure port locations (data from the outer two probes on each end of the array are omitted to exclude boundary layer effects, leaving the 7 center pressure probes). This cross-sectional data provides a good spatial picture of what is happening with static pressure behavior at the test section entrance.

A standard deviation across those 35 data points measured by the array can provide an estimate of spatial uniformity standard uncertainty using Equation 22 (see the resulting blue line "Raw data" in Figure J.1). When this is done outright on the raw data, however, the estimate appears quite high, and a problem becomes apparent: due to the fact that the tunnel is set to the pressure ratio $P_{S,bal}/P_{T,bm}$, static and total pressure can vary independently for a nominal Mach setting, so long as the ratio does not vary. Therefore, data taken at different rake heights (likely on different test days with different atmospheric conditions, which directly impact this atmospheric tunnel) can have large random variation, as seen and explained in more detail in Section 6.1.3. Techniques must be explored to eliminate unwanted variations while preserving spatial uniformity characteristics.

Two methods were used to visually explore spatial uniformity data in attempts to isolate its uncertainty from other potential contributors (i.e. instrumentation, random). Figure J.2 shows raw differential static pressure data measured by the transonic array at all five rake height settings at two different tunnel set points. The same data is displayed in pressure distribution "blob plots" (top) and line plots (bottom). Both plot types are useful in determining data trends. For example, in the blob plots there is a magnitude trend that is obvious across different rake heights, clearly displaying the variation due to different atmospheric conditions, discussed above. In the line plots, a probe-type bias becomes very apparent, with a clear up-down "W" pattern where probes located at 24", 36" and 48" are 5-hole probes and measure a slightly lower pressure, while probes located at 18", 30", 42" and 54" are Pitot-static probes and measure a slightly higher pressure.

One way to "normalize" the five rake heights (while maintaining dimensionality) to isolate spatial uniformity uncertainty from changing atmospheric conditions is to average pressure readings horizontally across the 7 probes at each rake height, and subtract the average from each individual measurement on the rake at that height. Spatial visualization results

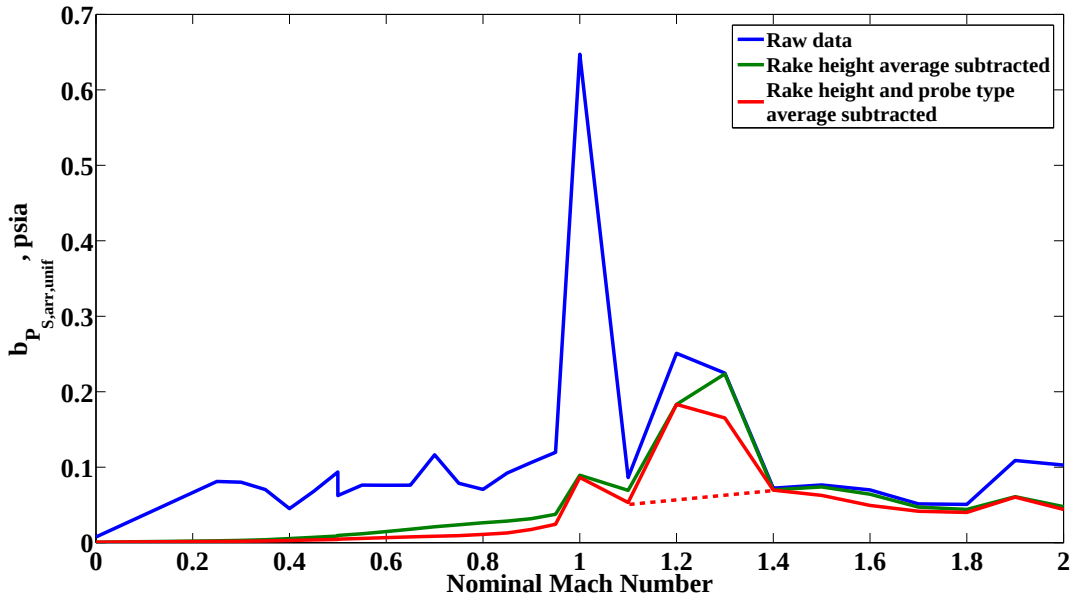

Figure J.1: Systematic Standard Uncertainty due to Static Pressure Uniformity: Techniques to Isolate Uniformity Uncertainty. Note the dotted red line, indicating an interpolation could be done to eliminate suspected shock interactions affecting measurements in the Mach 1.1-1.4 range.

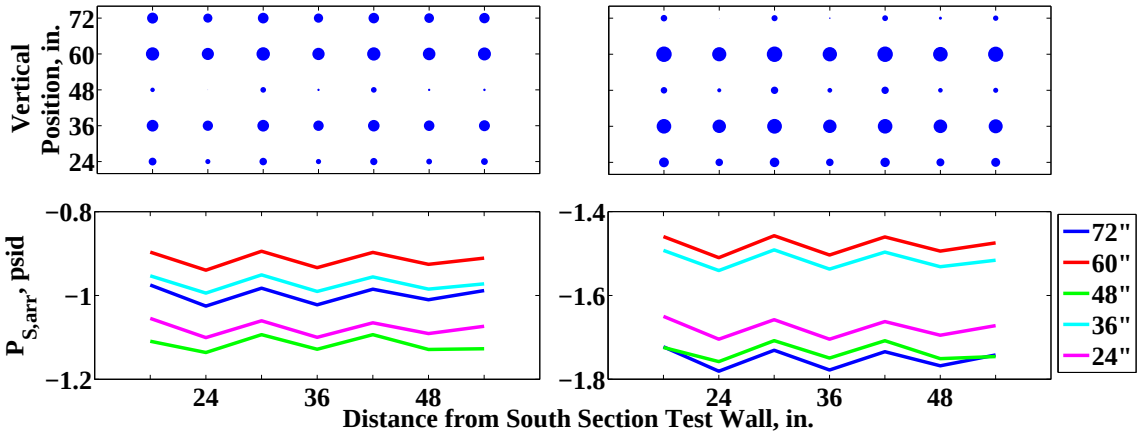

Figure J.2: Static Pressure Profile: Raw Data at Mach 0.65 (left) and Mach 0.7 (right), shown in "blob" plots (top) and line plots (bottom).

of this technique performed on measurements taken at Mach 0.8 can be seen in Figure J.3(b). The probe-type bias "W" pattern becomes more pronounced after removal of random variation effects: to remove this bias, the average of all 5-hole probes is removed from all 15 measurements, and same with the 20 Pitot-static probe measurements. Results can be seen in Figure J.3(c). Results for spatial uniformity uncertainty of array static pressure across all nominal Mach conditions using the techniques discussed to remove other uncertainty contributors can be seen in Figure J.1.

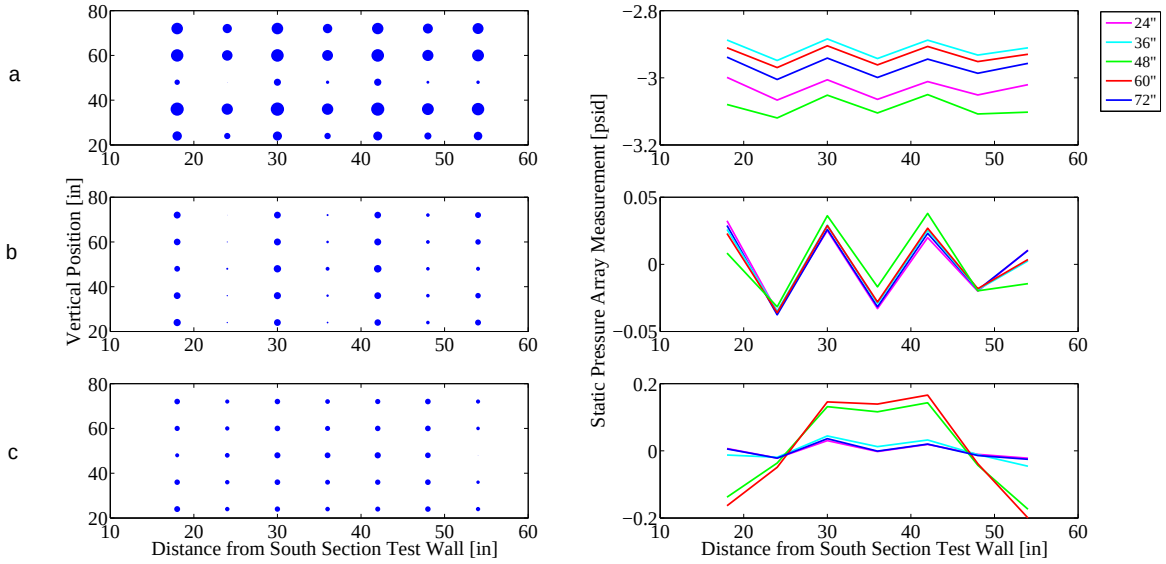

Figure J.3: Bubbles (left) showing relative magnitude of static pressure readings from the array and lines showing the same data at Mach 0.8. (a) raw data, (b) the effect of removing the rake height averages, (c) the effect of removing both the rake height and probe type biases.

A similar approach was taken with estimates for total pressure and total temperature uniformity uncertainties as they would apply to a randomly selected point in the test section. The probe-type bias was not observed for total pressure or temperature, so only the random variation effect technique was performed. Comparative results can be seen in Figures J.4 and J.5.

As stated earlier, methods and results presented in this Appendix were not used for the uncertainty analysis presented in the body of this report. They are presented only for reference and theoretical application of spatial uniformity uncertainty and flow field visualization.

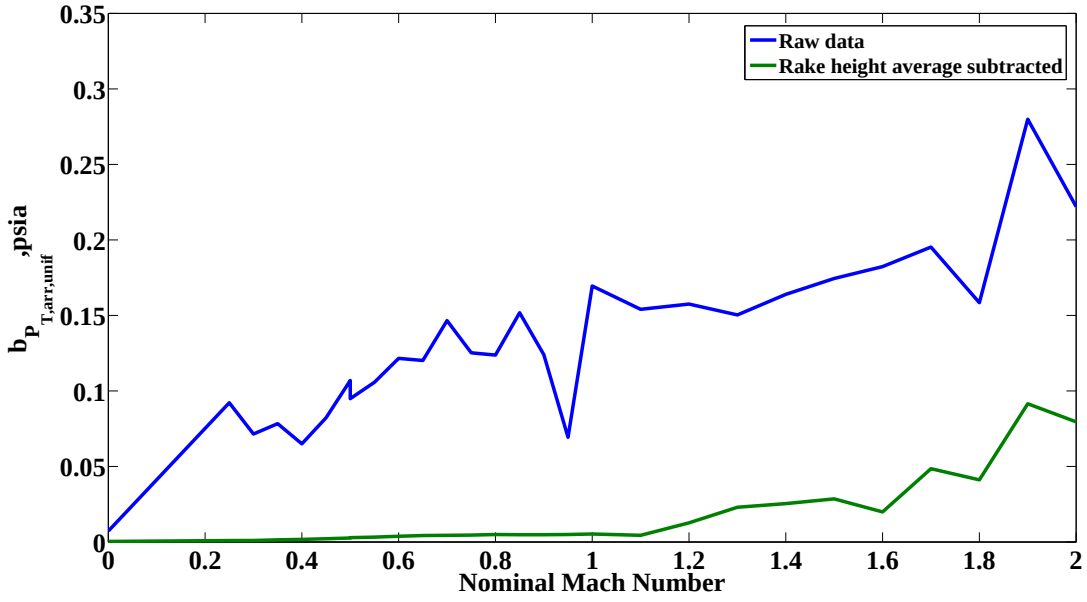

Figure J.4: Systematic Standard Uncertainty due to Total Pressure Uniformity: Technique to Isolate Uniformity Uncertainty

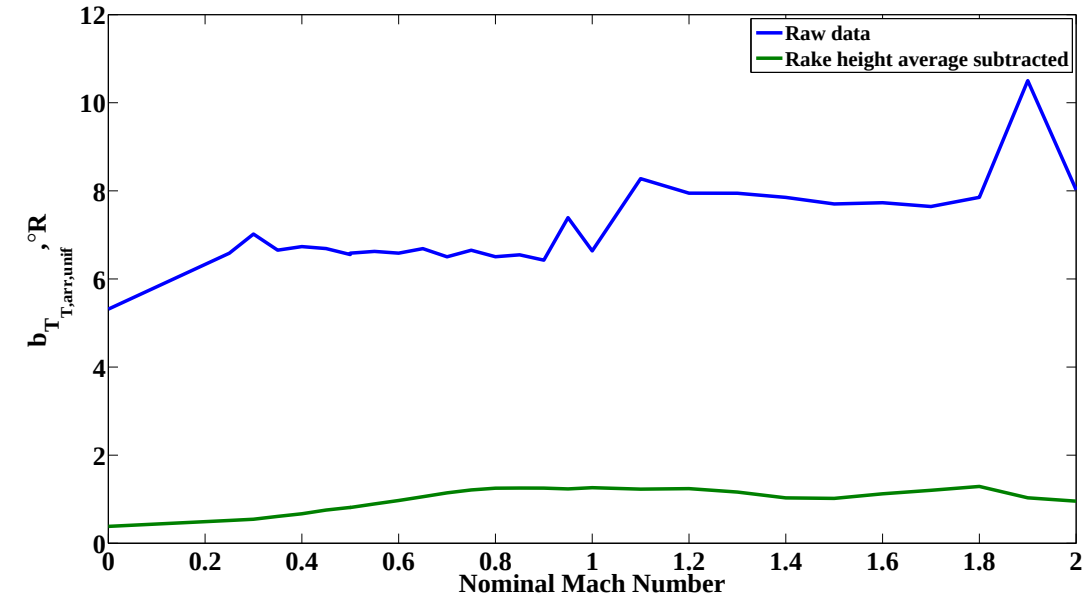

Figure J.5: Systematic Standard Uncertainty due to Total Temperature Uniformity: Technique to Isolate Uniformity Uncertainty

Appendix K: Instrumentation Uncertainty Breakdown

As described in Section 6.1.1, systematic uncertainties of the instrumentation in this analysis are acquired by MANTUS, an Excel® based tool which allows the user to break down the overall measurement into component parts, or "modules", to easily handle the analysis of multi-level instrumentation systems. A module can be configured to represent a specific function of a single component, or multiple components can be summarized into one module. The overall system is then assembled from multiple modules within MANTUS, allowing for propagation of uncertainties using the TSM to ultimately produce the final uncertainty of the measurement. This process is depicted in Figure 66. Because of the way in which uncertainties propagate through the modules in MANTUS, it is possible to determine percent contributions of the different contributors to the instrument level uncertainties.

K.1 Pressure Instrumentation System

The two instrument systems in the 8- by 6-foot SWT is are the pressure systems and thermocouple systems. The flow of instrumentation signal from measured pressure to recorded data is shown in Figure K.1. The pressure probe sends a signal through the ESP3200 Pressure scanner, to the ESP PC, to the ESCORT program where the data is recorded. A bar chart of the UPCs in this system is shown in Figure K.2. Clearly, the scanner contributes almost all of the instrument uncertainty. Numeric values are tabulated in Table K.1.

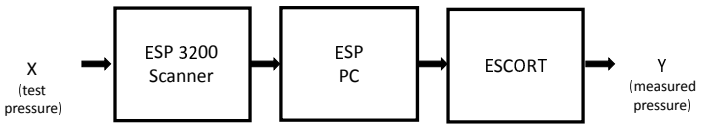

Figure K.1: Flow of pressure signal from measurement source to saved data.

K.2 Temperature Instrumentation System

The thermocouple system has five modules in the signal flow, shown in Figure K.3. A bar chart of the UPCs for this system is shown in Figure K.4. Clearly, the thermocouples contribute most heavily toward the uncertainty. Tabulated results are shown in Table K.2.

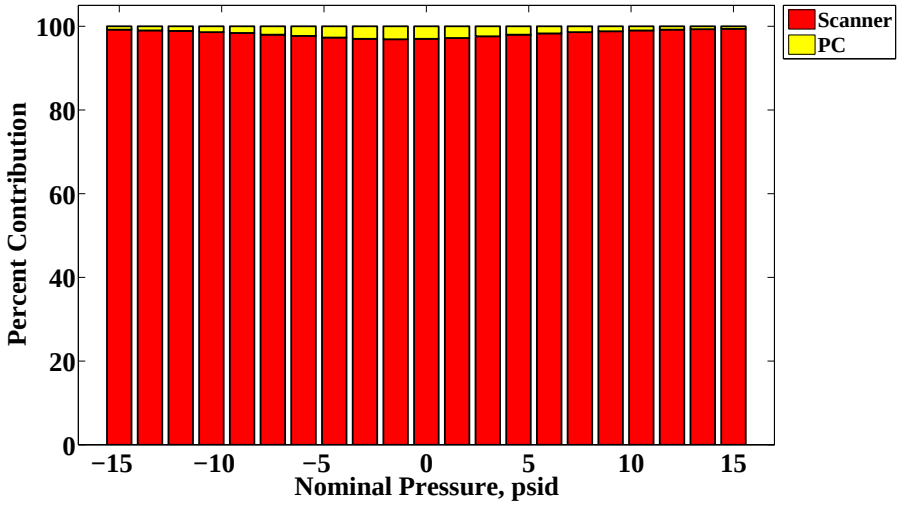

Figure K.2: Percent contributions to pressure instrumentation uncertainty.

Nominal Pressure, psid	Standard Uncertainty, psid	% due to 3200 scanner	% due to PC	% due to ESCORT
−15.00	0.0064	99.2	0.8	0.0
−13.50	0.0059	99.0	1.0	0.0
−12.00	0.0054	98.9	1.1	0.0
−10.50	0.0049	98.6	1.4	0.0
−9.00	0.0045	98.4	1.6	0.0
−7.50	0.0041	98.0	2.0	0.0
−6.00	0.0038	97.7	2.3	0.0
−4.50	0.0035	97.3	2.7	0.0
−3.00	0.0034	97.0	3.0	0.0
−1.50	0.0033	96.9	3.1	0.0
0.00	0.0033	97.0	3.0	0.0
1.50	0.0035	97.2	2.8	0.0
3.00	0.0037	97.6	2.4	0.0
4.50	0.0041	98.0	2.0	0.0
6.00	0.0044	98.3	1.7	0.0
7.50	0.0049	98.6	1.4	0.0
9.00	0.0054	98.8	1.2	0.0
10.50	0.0059	99.0	1.0	0.0
12.00	0.0065	99.2	0.7	0.0
13.50	0.0070	99.3	0.6	0.0
15.00	0.0076	99.4	0.8	0.0

Table K.1: Uncertainty due to pressure instrumentation system with percent contributions from the sources

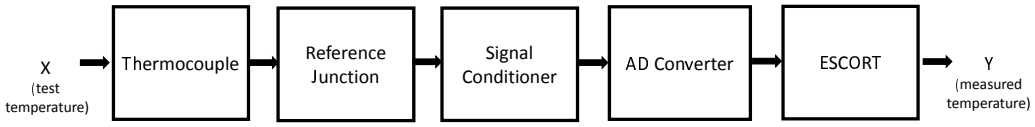

Figure K.3: Flow of temperature signal from measurement source to saved data.

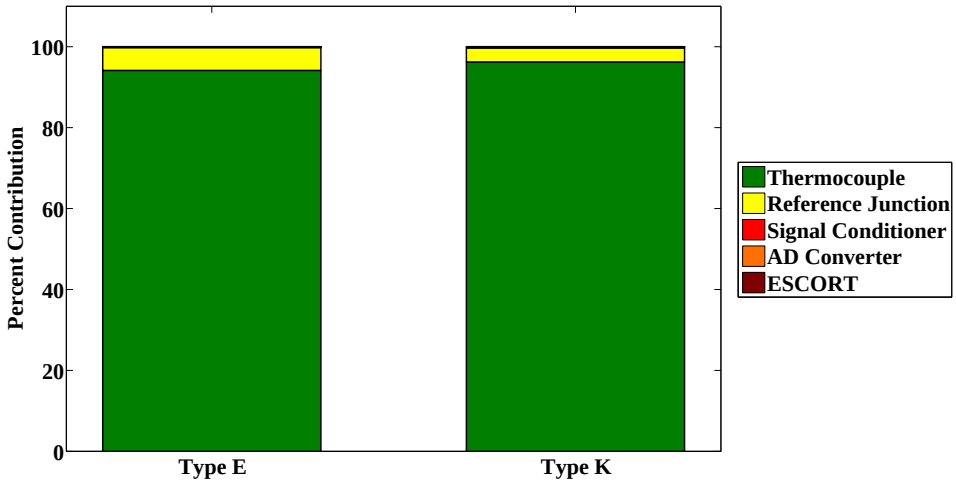

Figure K.4: Percent contributions to temperature instrumentation uncertainty; typical values for temperature range 490-670°R.

TC Type	Standard Unc., °R	% due to TC and wire	% due to Reference Junction	% due to Signal Conditioner	% due to A/D Converter	% due to ESCORT
E	2.2	94.2	5.6	0.2	0.0	0.0
K	2.9	96.2	3.5	0.3	0.0	0.0

Table K.2: Uncertainty due to thermocouple instrumentation with percent contributions from the sources; typical values for temperature range 490-670°R